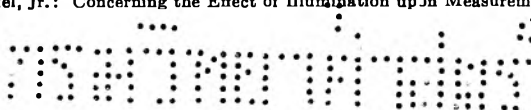


# THE JOURNAL OF PHYSICAL CHEMISTRY

(Registered in U. S. Patent Office)

## CONTENTS

Kenneth A. Wilde: Decomposition of C-Nitro Compounds. II. Further Studies on Nitroethane.....	385
A. Greenville Whittaker and Harry Williams: Burning Rate Studies. V. Effect of Acid Concentration on the Consumption Rate of Various Fuels with Nitric Acid.....	388
Shinichi Kawaguchi: Study of Nickel Oxide-Kieselguhr Catalyst. II. The Participation of Physically Adsorbed Molecules in Propylene Polymerization at 0°.....	394
James P. Hoare and Sigmund Schuldiner: Effects of Hydrogen Content on the Resistance and the Potential in the Palladium-Hydrogen-Acid System.....	399
Thomas L. O'Connor and Herbert H. Uhlig: Absolute Areas of Some Metallic Surfaces.....	402
Ryden L. Richardson and Sidney W. Benson: A Study of the Surface Acidity of Cracking Catalyst.....	405
Ulrich P. Strauss and Stanley S. Slowata: The Effect of Solubilization on the Equivalent Conductance and Reduced Viscosity of a Polysoap Derived from Poly-2-vinylpyridine.....	411
Louis F. Heckelsberg and Farrington Daniels: Thermoluminescence of Fourteen Alkali Halide Crystals.....	414
A. B. Bestul: Evidence for Mechanical Shear Degradation of High Polymers.....	418
Harold J. Moe, T. E. Bortner and G. S. Hurst: Ionization of Acetylene Mixtures and Other Mixtures by Pu <sup>239</sup> Alpha Particles.....	422
Robert Simha and Leo A. Wall: Mechanism of High Energy Radiation Effects in Polymers.....	425
J. Danon and A. A. L. Zamith: Ion-Exchange and Solvent-Extraction Studies with Polonium.....	431
Edward O. Holmes, Jr.: The Phototropy of Malachite Green Leucocyanide in Ethyl Alcohol, Cyclohexane, Ethylene Dichloride and Ethylidene Dichloride and Some Mixtures of Them.....	434
Robert L. Combs and Hilton A. Smith: Vapor Pressure Studies Involving Solutions in Light and Heavy Waters. IV. Separation Factor and Crossover Temperature for Salt Solutions of the Mixed Waters and for a Mixture of the Pure Waters from 100° to the Critical Temperature.....	441
E. H. Gleason, G. Mino and W. M. Thomas: Kinetics of the Chlorate-Sulfite Reaction.....	447
Alvin W. Baker: Solid State Anomalies in Infrared Spectroscopy.....	450
G. L. Cook and F. M. Church: Correlations of the Infrared Spectra of Some Pyridines.....	458
Edward A. Heintz and David N. Hume: Interfacial Tension and Complex Formation.....	462
L. V. Cherry, M. E. Hobbs and H. A. Strobel: Dilute Solution Measurements of Molar Kerr Constants of Some Halobenzenes, Monohalobenzotrifluorides and Benzotrifluoride.....	465
Gunnar O. Assarsson: Hydrothermal Reactions between Calcium Hydroxide and Amorphous Silica: the Reactions between 180 and 220°.....	473
Benton B. Owen and Harold L. Simons: Standard Partial Molal Compressibilities by Ultrasonics. I. Sodium Chloride and Potassium Chloride at 25°.....	479
James E. Boggs, Cullen M. Crain and James E. Whiteford: Dielectric Constant Measurements on Gases at Microwave Frequencies.....	482
Benson Ross Sundheim: Transference in Binary Molten Salt Solutions.....	485
Cheves Walling, Edgar E. Ruff and James L. Thornton, Jr.: The Adsorption of Cations by Anionic Foams.....	486
B. Zaslow and R. E. Rundle: The Crystal Structure of Tetraphenylarsonium Tetrachloroferrate(III), (C <sub>6</sub> H <sub>5</sub> ) <sub>4</sub> AsFeCl <sub>4</sub> .....	490
NOTES: S. E. S. El Wakkad and H. A. Rizk: The Polytungstates and the Colloidal Nature and the Amphoteric Character of Tungstic Acid.....	494
Elmer J. Huber, Jr., Earl L. Head and Charles E. Holley, Jr.: The Heat of Combustion of Yttrium.....	497
Roger L. Jarry: The Liquid Density, Vapor Pressure and Critical Temperature and Pressure of Perchloryl Fluoride.....	498
R. E. Kagarise: Polymorphism in Monochloroacetic Acid.....	499
Betty A. Phillips and William R. Busing: Comparison of the Infrared and Raman Spectra of Some Crystalline Hydroxides.....	502
Lohr A. Burkardt: The System 2,4,6-Trinitrotoluene-2,4,6-Trinitro- <i>m</i> -xylene.....	502
Joseph Simkin and Roger L. Jarry: The Viscosity and Surface Tension of Perchloryl Fluoride.....	503
Hans B. Jonassen, Fred W. Frey and Anneke Schaafsma: Dissociation Constants of Polyethylenamines. II. The Dissociation Constants of Tetraethylenepentamine.....	504
Meyer Melvin Markowitz: The Differential Thermal Analysis of Perchlorates.....	505
E. R. Dalbey and W. A. Gey: Studies on the Linear Crystallization of Nitrofluorene Systems.....	507
A. P. Altshuler: Thermodynamic Functions for the Isotopic Hydrogen Selenides and Hydrogen Telluride.....	509
COMMUNICATIONS TO THE EDITOR: T. Forland and J. Krogh-Moe: A Remark on Some Measurements of Transference Numbers.....	511
Arthur J. Rosenberg and Charles S. Martel, Jr.: Concerning the Effect of Illumination upon Measurements of Gas Adsorption.....	512



# THE JOURNAL OF PHYSICAL CHEMISTRY

(Registered in U. S. Patent Office)

W. ALBERT NOYES, JR., EDITOR

ALLEN D. BLISS

ASSISTANT EDITORS

ARTHUR C. BOND

## EDITORIAL BOARD

R. P. BELL

JOHN D. FERRY

S. C. LIND

R. E. CONNICK

G. D. HALSEY, JR.

H. W. MELVILLE

R. W. DODSON

J. W. KENNEDY

R. G. W. NORRISH

PAUL M. DOTY

A. R. UBBELOHDE

Published monthly by the American Chemical Society at 20th and Northampton Sts., Easton, Pa.

Entered as second-class matter at the Post Office at Easton, Pennsylvania.

The *Journal of Physical Chemistry* is devoted to the publication of selected symposia in the broad field of physical chemistry and to other contributed papers.

Manuscripts originating in the British Isles, Europe and Africa should be sent to F. C. Tompkins, The Faraday Society, 6 Gray's Inn Square, London W. C. 1, England.

Manuscripts originating elsewhere should be sent to W. Albert Noyes, Jr., Department of Chemistry, University of Rochester, Rochester 20, N. Y.

Correspondence regarding accepted copy, proofs and reprints should be directed to Assistant Editor, Allen D. Bliss, Department of Chemistry, Simmons College, 300 The Fenway, Boston 15, Mass.

Business Office: Alden H. Emery, Executive Secretary, American Chemical Society, 1155 Sixteenth St., N. W., Washington 6, D. C.

Advertising Office: Reinhold Publishing Corporation, 430 Park Avenue, New York 22, N. Y.

Articles must be submitted in duplicate, typed and double spaced. They should have at the beginning a brief Abstract, in no case exceeding 300 words. Original drawings should accompany the manuscript. Lettering at the sides of graphs (black on white or blue) may be pencilled in and will be typeset. Figures and tables should be held to a minimum consistent with adequate presentation of information. Photographs will not be printed on glossy paper except by special arrangement. All footnotes and references to the literature should be numbered consecutively and placed in the manuscript at the proper places. Initials of authors referred to in citations should be given. Nomenclature should conform to that used in *Chemical Abstracts*, mathematical characters marked for italic, Greek letters carefully made or annotated, and subscripts and superscripts clearly shown. Articles should be written as briefly as possible consistent with clarity and should avoid historical background unnecessary for specialists.

Notes describe fragmentary or less complete studies but do not otherwise differ fundamentally from articles. They are subjected to the same editorial appraisal as are Articles. In their preparation particular attention should be paid to brevity and conciseness.

Communications to the Editor are designed to afford prompt preliminary publication of observations or discoveries whose

value to science is so great that immediate publication is imperative. The appearance of related work from other laboratories is in itself not considered sufficient justification for the publication of a Communication, which must in addition meet special requirements of timeliness and significance. Their total length may in no case exceed 500 words or their equivalent. They differ from Articles and Notes in that their subject matter may be republished.

Symposium papers should be sent in all cases to Secretaries of Divisions sponsoring the symposium, who will be responsible for their transmittal to the Editor. The Secretary of the Division by agreement with the Editor will specify a time after which symposium papers cannot be accepted. The Editor reserves the right to refuse to publish symposium articles, for valid scientific reasons. Each symposium paper may not exceed four printed pages (about sixteen double spaced typewritten pages) in length except by prior arrangement with the Editor.

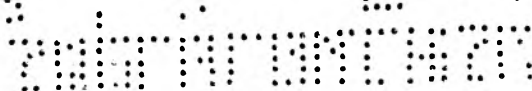
Remittances and orders for subscriptions and for single copies, notices of changes of address and new professional connections, and claims for missing numbers should be sent to the American Chemical Society, 1155 Sixteenth St., N. W., Washington 6, D. C. Changes of address for the *Journal of Physical Chemistry* must be received on or before the 30th of the preceding month.

Claims for missing numbers will not be allowed (1) if received more than sixty days from date of issue (because of delivery hazards, no claims can be honored from subscribers in Central Europe, Asia, or Pacific Islands other than Hawaii), (2) if loss was due to failure of notice of change of address to be received before the date specified in the preceding paragraph, or (3) if the reason for the claim is "missing from files."

Subscription Rates (1956): members of American Chemical Society, \$8.00 for 1 year; to non-members, \$16.00 for 1 year. Postage free to countries in the Pan American Union; Canada, \$0.40; all other countries, \$1.20. \$12.50 per volume, foreign postage \$1.20, Canadian postage \$0.40; special rates for A.C.S. members supplied on request. Single copies, current volume, \$1.35; foreign postage, \$0.15; Canadian postage \$0.05. Back issue rates (starting with Vol. 56): \$15.00 per volume, foreign postage \$1.20, Canadian, \$0.40; \$1.50 per issue, foreign postage \$0.15, Canadian postage \$0.05.

The American Chemical Society and the Editors of the *Journal of Physical Chemistry* assume no responsibility for the statements and opinions advanced by contributors to THIS JOURNAL.

The American Chemical Society also publishes *Journal of the American Chemical Society*, *Chemical Abstracts*, *Industrial and Engineering Chemistry*, *Chemical and Engineering News*, *Analytical Chemistry*, *Journal of Agricultural and Food Chemistry* and *Journal of Organic Chemistry*. Rates on request.



---

# THE JOURNAL OF PHYSICAL CHEMISTRY

(Registered in U. S. Patent Office) (© Copyright, 1957, by the American Chemical Society)

VOLUME 61

APRIL 17, 1957

NUMBER 4

---

## DECOMPOSITION OF C-NITRO COMPOUNDS. II. FURTHER STUDIES ON NITROETHANE

BY KENNETH A. WILDE

*Rohm and Haas Company, Redstone Arsenal Research Division, Huntsville, Alabama*

*Received April 23, 1956*

The rate constant for the first-order decomposition of nitroethane was found to be represented by  $k = 10^{10.83} e^{-39,700 \pm 2071/RT}$  sec.<sup>-1</sup> over the temperature range 320–440°. The equation fits data obtained in both static and flow systems, and is consistent with the postulated activated complex having a ring structure. In the range 490–535° a special fast flow system was used and the rate constant given by  $k = 10^{17.56} e^{-60,600/RT}$  sec.<sup>-1</sup>. The activation energy approximates the C–N bond strength at these temperatures and it appears that a non-chain branched mechanism with initial fission of the C–N bond can account for the results at high temperatures.

### I. Introduction

The study of the thermal decomposition of nitroethane has been extended to higher and lower temperatures than were used in the previous paper<sup>1</sup> in this series (415–460°). Rate measurements were made in a conventional static system for the range 320–360° and a special flow system for the range 490–525°. After the present work was completed the work of Gray, Yoffe and Roselaar<sup>2</sup> came to the author's attention. They also made quantitative rate measurements of nitroethane decomposition in the temperature range 430–485°, in addition to Paneth mirror and other qualitative tests at higher and lower temperatures. The positive indications of free radicals and the appearance of products such as formaldehyde and hydrogen cyanide led them to suggest that C–N bond fission is the important initial step, rather than decomposition through a low entropy cyclic activated complex as proposed by Cottrell, *et al.*,<sup>3</sup> and the author.<sup>1</sup> It is hoped that the present work will add further information for the interpretation of this important but very complex problem. A fuller discussion of the relation of the present work to that of Gray, Yoffe and Roselaar will be made after the present results have been given.

**II. Static System.**—In the previous work on nitroethane in a static system<sup>3</sup> the reaction was

(1) K. A. Wilde, *Ind. Eng. Chem.*, **48**, 769 (1956).

(2) P. Gray, A. D. Yoffe and L. Roselaar, *Trans. Faraday Soc.*, **51**, 1489 (1955).

(3) T. L. Cottrell, T. E. Graham and T. J. Reid, *ibid.*, **47**, 1089 (1951).

followed by pressure increase, and it was felt that direct analysis for nitroethane would provide more meaningful rate constants for comparison with the flow system results at higher temperatures.

A weighed amount of nitroethane was introduced into an evacuated bulb of 214 cm.<sup>3</sup> contained in the constant temperature zone of a furnace. The temperature was controlled to  $\pm 0.2^\circ$  by a Leeds and Northrop Speedomax controller. A calibrated iron-constantan thermocouple was used to measure the temperature at the reaction bulb.

After a timed interval the reaction bulb was opened to an evacuated Dry Ice trap, where the undecomposed nitroethane was condensed. Rough calculations indicated that the transfer time was equivalent to about two minutes reaction time. This was confirmed by removing the sample as soon as it was introduced. The trap contents were dissolved in 10 ml. of cyclohexane and analyzed for residual nitroethane by infrared absorption at the main C-nitro band of 6.3  $\mu$ .

Typical data obtained are shown in Fig. 1 where the partial pressure of nitroethane divided by the initial pressure is plotted *versus* reaction time (plus two minutes transfer time). The rate is first order up to about the half-time and then falls off. The rate at higher temperatures in flow systems was previously found to be first order with respect to both concentration and time.<sup>1</sup> Cottrell, *et al.*,<sup>3</sup> found the initial rate to be independent of pressure down to 30 mm. The rate constants for the initial portion of the decomposition are shown in Table I with the standard deviations of the mean,  $\sigma_k$ .

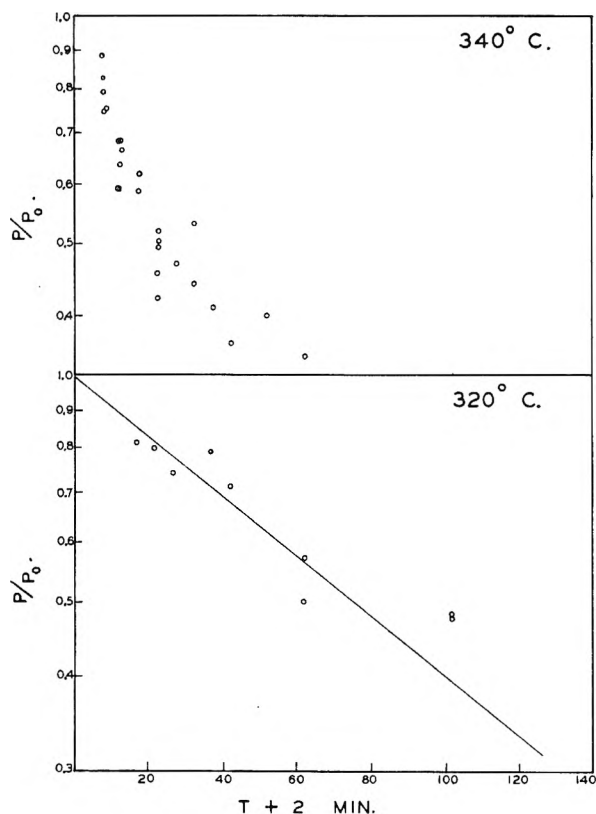


Fig. 1.

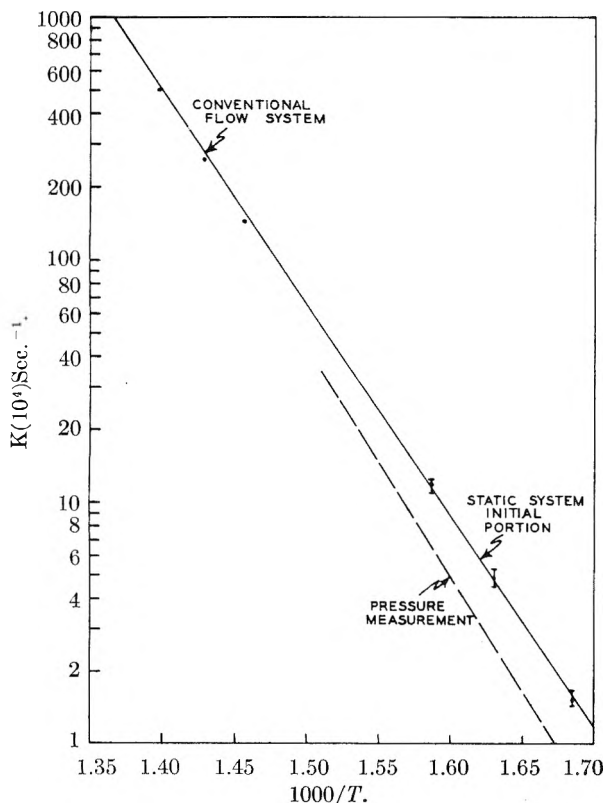


Fig. 2.—Arrhenius plot of nitroethane.

The temperature dependence of the latter half of the reaction was quite small, corresponding to an activation energy of 25–30 kcal. No tests for sur-

TABLE I  
RATE CONSTANTS FOR NITROETHANE DECOMPOSITION

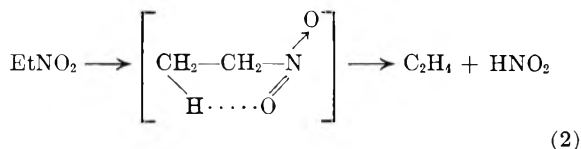
Temp., °C.	$\bar{k}$ , sec. <sup>-1</sup> × 10 <sup>4</sup>	$\sigma_k$ , sec. <sup>-1</sup> × 10 <sup>4</sup>	No. of runs
320	1.53	0.10	9
340	4.87	0.36	7
360	13.2	1.0	4

face effects were made as the decomposition has been found to be essentially homogeneous.<sup>2,3</sup>

An Arrhenius plot of the rate constants in Table I is shown in Fig. 2, together with the data for the three lowest temperatures from the conventional flow system of the previous paper.<sup>1</sup> The two sets of data, obtained under widely different conditions, agree quite well, indicating that the unimolecular decomposition mechanism is predominant below about 440°. The data obtained by pressure measurements are shown for comparison. A weighted least squares calculation<sup>4</sup> for the six points gave an Arrhenius equation as

$$k = 10^{10.83} e^{-39,700 \pm 270/RT} \text{ sec.}^{-1} \quad (1)$$

This equation covers the range 320–440° and is considerably more precise than that for either system alone. The entropy of activation is somewhat different, -11.4 e.u. versus -10.3 e.u. for the flow system results alone, but still consistent with the low entropy ring activated complex previously suggested



III. Fast Flow System.—The results at the highest temperature in the conventional flow system<sup>1</sup> are outside the limits of error of the equation through the six lower temperatures and indicate an increase in rate and activation energy at temperatures above 460°. It seemed likely that the activation energy would approach the C–N bond strength and the mechanism would change.

In order to investigate this very interesting phenomenon a system has been designed for reaction times in the range 0.10 to 1 second. The reactant stream (R) is passed through two traps to obtain a concentration of about 10% nitroethane. Only the first trap contains nitroethane, at about eight degrees higher than the second trap, which is thermostated at the required temperature (52.0°). Thus saturation is approached by condensation. The second trap was packed with glass beads to inhibit fog formation. The excellent reproducibility of the input concentration supports the assumption that the gas entering the furnace is saturated at the second bath temperature. On entering the bath the reactant stream is met by a stream (P) of 40–50 times its volume which has been preheated to the bath temperature. The temperature of the total stream drops about five degrees. Rough heat transfer calculations indicated that this temperature drop is recovered in less than 10% of the reaction length, which consists of 80 cm. of 2 mm. tubing, a

(4) W. R. McBride and D. S. Villars, *Anal. Chem.*, **76**, 901 (1954).

total volume of 2 cm.<sup>3</sup> When the reactant plus preheat stream leaves the bath, it is met by a quenching stream (Q), about one-third to one-half the volume of the main stream, which is sufficient to render the reaction rate negligible. The reaction volume, and hence reaction time, is thus sharply defined by the points of introduction of the preheat and quenching streams, avoiding a major uncertainty in flow systems. This principle could of course be used for longer reaction times.

The preheat and reaction coils are contained in a molten lead-bismuth bath, the temperature of which is controlled by a Leeds and Northrup Speedomax controller to  $\pm 1^\circ$ . The platinum resistance thermometer of the controller was used to read the temperature. Temperature explorations of the bath with a calibrated iron-constantan thermocouple showed the gradients to be less than  $1^\circ$  and also checked the reading of the platinum resistance thermometer. All flow rates were metered by conventional capillary flow meters and regulated by Nullmatic precision pressure regulators.<sup>5</sup> The helium used as a carrier gas contained less than 0.003% impurity, principally nitrogen, according to the supplier's analysis.

The concentration of reactant in the exit stream is quite low, of the order of a few tenths of a per cent., and a special method of analysis had to be developed. Gas chromatography<sup>6</sup> appeared to offer many advantages and proved to be highly satisfactory. A calibration curve of per cent. nitroethane *versus* the product of the elution peak height and width at half-height gave an excellent reproducible straight line, down to a lower concentration limit of about 0.04%. Samples were taken by passing the exit gas stream through a 500-cc. bulb, and then flushing or to the chromatographic column, which also employed a helium carrier gas. The calibration runs were made under conditions of negligible decomposition.

Since the concentrations are so low in this system, the correction for increase in number of moles flowing<sup>7</sup> is negligible and the kinetic results may be plotted as  $\epsilon$ , the fraction of reference reactant remaining, *versus* reaction time or reciprocal of total flow rate. The results obtained for nitroethane are shown in Fig. 3 for the three temperatures studied. The rate constants obtained are given in Table II.

TABLE II  
RATE CONSTANTS FOR NITROETHANE DECOMPOSITION—FAST FLOW SYSTEM

$T$ , °C.	$\bar{k}_1$ , sec. <sup>-1</sup>	$\sigma\bar{k}_1$ , sec. <sup>-1</sup>	No. of runs
490	1.59	0.07	6
505	3.51	.25	12
525	9.40	.47	10

The data are somewhat scattered but a good Arrhenius plot is obtained with the above mean values, which are represented by

$$k = 10^{17.56} e^{-60,600/RT} \text{ sec.}^{-1} \quad (3)$$

(5) Moore Products Co., Philadelphia, Pa.

(6) N. H. Ray, *J. App. Chem.*, **4**, 21 (1954).

(7) H. M. Hulbert, *Ind. Eng. Chem.*, **36**, 1012 (1944).

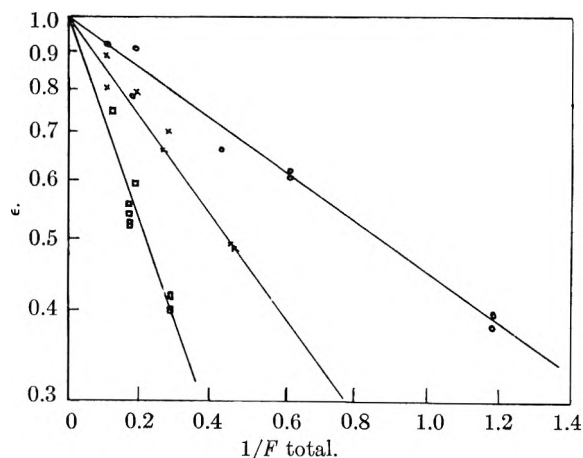
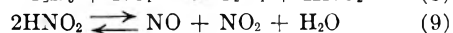
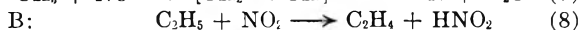
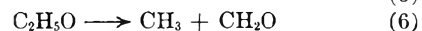
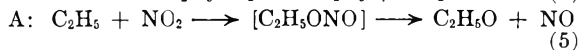
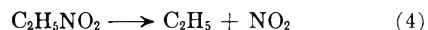


Fig. 3.—Decomposition of nitroethane fast flow system: O, 490°; X, 505°; □, 525°.

The activation energy may be in error by 5 kcal. and the frequency factor by a power of ten, but it is evident that the activation energy at these high temperatures is essentially equal to the C-N bond strength, *ca.* 57 kcal. However, this does not necessarily demonstrate that the breaking of the C-N bond is the sole initial step in the decomposition, as will be seen below. Qualitatively, the same major products were obtained as at lower temperatures: ethylene, nitric oxide and formaldehyde.

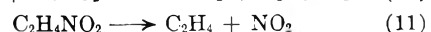
#### IV. Discussion

**A. High Temperature Range.**—Perhaps the simplest explanation of most of the experimental observations in the high temperature range is an initial C-N bond fission, followed by two possible reactions between nitrogen dioxide and ethyl radicals



The major products would be ethylene, nitric oxide, formaldehyde, etc., as observed, and the activation energy would be equal to the C-N bond strength. Gray, Yoffe and Roselaar,<sup>2</sup> and the author<sup>1</sup> as well, have emphasized the necessity of the formation of ethoxy radicals as in (A) above to explain the appearance of formaldehyde and hydrogen cyanide.

A chain reaction involving  $\text{NO}_2$  as the carrier may contribute in the high temperature range but has too high an activation energy at lower temperatures



Reaction 10 is endothermic by 21 kcal. and probably has an activation energy of the order of 30 kcal. Thus with second-order chain breaking and chain initiation by C-N bond fission ( $\sim 60$  kcal.) the over-all activation energy for such a chain reac-

tion would be<sup>8</sup>  $\sim 30 + \frac{1}{2}(60) = 60$  kcal. as observed above 460°. On examining the steps 4-9, it is seen that there is not much chance for a chain mechanism in the formation of ethoxy radical and its products, so that the activation energy must be at least the C-N bond strength. Gray and co-workers found the relative yields of formaldehyde to decrease rapidly with increasing extent of reaction. The amounts of formaldehyde and hydrogen cyanide found in the previous paper in this series were considerably less than those found by Gray and co-workers, but most of the measurements were made at about the half-time or greater.

**B. Lower Temperature Range.**—Other possible (unlikely) alternative schemes to the unimolecular step 2 below 440-460° are discussed in the previous paper.<sup>1</sup> A radical mechanism could not be found which would explain the experimental findings such as the first order with respect to time and concentration, and the ineffectiveness of nitrogen dioxide and water additives.

The induction of reaction in the low temperature range by addition of compounds which give radicals easily should not be taken as evidence that the decomposition necessarily proceeds by a radical mechanism in the absence of additives. Also, the detection of radicals in the Paneth mirror experiments of Gray and co-workers<sup>2</sup> at 500° and above does not indicate the presence or participation of radicals at lower temperatures. One might speculate that the activation energy at very low extents of reaction in the intermediate tem-

(8) A. A. Frost and R. G. Pearson, "Kinetics and Mechanism," John Wiley and Sons, Inc., New York, N. Y., 1953, p. 232.

perature range (400-460°) would approach the 60 kcal. of the initial C-N bond fission rather than the observed 40 kcal., which was largely determined by data at considerable decomposition which would emphasize the subsequent steps. In other words, at intermediate and high temperatures C-N bond fission is the only important reaction occurring before the steady state with respect to the other steps is established. Thus the products at low extent of reaction would be those of C-N bond breaking (formaldehyde, etc.), as found by Gray, *et al.*

**C. Summary.**—The decomposition of nitroethane proceeds mainly by a unimolecular mechanism up to about 440°, through a cyclic low entropy activated complex with an activation energy of about 40 kcal. Another mechanism involving initial C-N bond fission becomes noticeable at 400-420°, especially in the initial stages of reaction. Above 460° the C-N bond breaking becomes the most important initial process, the activation energy increasing from 40 kcal. to the 60 kcal. of the C-N bond. A possibility remains that a chain reaction involving abstraction of hydrogen from nitroethane by NO<sub>2</sub> is participating at high temperatures. This reaction could account for the rather high frequency factor (at least 10<sup>16</sup> sec.<sup>-1</sup>) observed at high temperatures.

**Acknowledgments.**—The author wishes to thank Dr. K. S. McCallum for the infrared analysis of nitroethane, Dr. C. B. Colburn for assistance in developing the gas chromatography analysis, and Mrs. S. M. Burns for assistance with the experimental work.

## BURNING-RATE STUDIES. PART 5. EFFECT OF ACID CONCENTRATION ON THE CONSUMPTION RATE OF VARIOUS FUELS WITH NITRIC ACID

BY A. GREENVILLE WHITTAKER AND HARRY WILLIAMS

Contribution from the Chemistry Division, Research Department, U. S. Naval Ordnance Test Station, China Lake, California

Received July 16, 1956

Consumption rate curves for the system 2-nitropropane-nitric acid were determined at four different acid concentrations ranging from 90 to 100% nitric acid. These curves indicate rather clearly the development of the "low pressure step" at high acid concentration. Other nitroparaffins were burned with nitric acid and the low pressure step was found to occur in these systems. Additional systems containing nitric acid were investigated to determine the generality of the low pressure step phenomenon. It was found that it does not always occur. By varying the combustion tube diameter it was shown that the low pressure step in the 2-nitropropane-nitric acid system is strongly dependent on the relationship between heat sources and sinks in the region of the burning surface. Also, there is some evidence that the low pressure step is sensitive to the surface temperature of the burning liquid. An hypothesis is proposed that can be used to correlate most of the observed phenomena associated with the low pressure step and can be used to qualitatively predict additional observable phenomena. As a side observation it was found that the onset of turbulent combustion had a definite relationship to nitric acid concentration and to the number of carbon atoms in the nitroparaffins.

### Introduction

Previous studies on the system 2-nitropropane-nitric acid showed that in the neighborhood of 100% nitric acid small changes in acid concentration produced large changes in the consumption rate curve.<sup>1</sup> This effect, which produces in this system the "low pressure step" phenomenon, was studied in more detail. Other nitroparaffin fuels were used with nitric acid to see if the phenomenon was of a more

general nature. In addition, several other types of fuels were burned in stoichiometric portion with nitric acid and the effect of combustion tube diameter was studied in order to get additional information that may lead to an understanding of the mechanism of the low pressure step. An hypothetical mechanism is suggested that can be used to describe most of the observed results.

**Materials.**—The compounds used were purified as follows. Pure nitric acid was prepared as described in previous work.<sup>1</sup> The 1-nitropropane and 2-nitropropane were prepared from technical grade commercial solvents material which was

(1) A. G. Whittaker, H. Williams and P. M. Rust, *THIS JOURNAL*, **60**, 904 (1956).

dried over calcium sulfate and distilled, the center fraction being retained. The indices of refraction of the fractions used were  $n_D^{25}$  1.400 and  $n_D^{25}$  1.3931, respectively. Eastman White Label nitroethane and nitromethane were used directly in these studies. Their indices of refraction were  $n_D^{25}$  1.3905 and  $n_D^{25}$  1.3809, respectively. Eastman White Label diisopropyl ether and dioxane were dried over sodium and distilled. The center fractions were retained, and they had  $n_D^{25}$  1.3676 and  $n_D^{25}$  1.4209, respectively. Eastman White Label *n*-butyric acid was dried over calcium sulfate and distilled. Again, the center fraction ( $n_D^{25}$  1.3966) was retained. Eastman White Label *m*-dinitrobenzene was dried over  $P_2O_5$  in a vacuum desiccator. The 1,5-dimethyl-tetrazole was prepared by Dr. W. G. Finnegan of this Laboratory. The material was recrystallized several times and dried in a vacuum desiccator.

**Apparatus and Procedure.**—Except for the modifications given below, the apparatus and procedure used to make the consumption rate measurements was the same as that described previously.<sup>1</sup> All the mixtures used were in stoichiometric proportions, and they were prepared by adding the calculated amount of fuel to a weighed amount of nitric acid of the proper concentration. Stoichiometric proportions are defined as a mole ratio of fuel to acid necessary to give carbon dioxide, water and nitrogen as products of complete combustion. To prepare the mixtures the nitric acid was cooled in a small flask on a block of Dry Ice before the fuel component was added. This eliminated the thermal decomposition of the nitric acid due to the local heating produced by heat of mixing.

All the consumption rate determinations given below were carried out in a pressure-controlled bomb. The pressure controller was of a Servo type and held the pressure constant to within  $\pm 1/2$  to 1 p.s.i. in the range 200 to 1000 p.s.i. and to  $\pm 2$  lb. in the range 1300 to 1700 p.s.i. Because only the smooth-burning region was of interest in this work, hand-timing was used instead of instrument-timing. Each consumption rate given in the following tables is an average of at least two independent measurements and each one of the average values has a precision of approximately  $\pm 3\%$ . There was no attempt made to carry out precise temperature control on the burning liquid. However, all measurements were made at approximately  $25 \pm 3^\circ$ .

Two of the systems were found rather difficult to ignite; namely, the butyric acid and the *m*-dinitrobenzene systems. In these cases the combustion tube was filled to within  $1/8$  in. of the top with the mixture, and the rest of the tube was filled with ethyl nitrate. The igniter was placed in the ethyl nitrate, which was easily ignited and would in turn ignite the mixture. Since this small ethyl nitrate section was well above the first fiducial mark, it did not introduce errors into the rate measurement.

### Results

The pressure range covered by the various systems given in the following tables was determined by two features. The lowest pressure reported is the lowest pressure at which ignition and sustained combustion could be obtained. The highest pressure of interest for a given system is that pressure at which the system goes into turbulent combustion. This means that only the smooth-burning portion of the consumption rate curve has been considered. Consumption rates obtained on the 2-nitropropane-nitric acid mixture at four different acid concentrations are given in Table I. Similar data on the other systems investigated are given in Tables II, III and IV.

The data in Table I show that the consumption rate increases as the acid concentration increases at all pressures. In the region of 100% nitric acid the addition of a small amount of water has a very large effect on the consumption rate over part of the pressure range. A log-log plot of these data shows that the consumption rate curves have a slight curvature concaved downward. The curva-

TABLE I  
EFFECT OF ACID CONCENTRATION OF CONSUMPTION RATE OF THE SYSTEM 2-NITROPROPANE-NITRIC ACID

Pressure, atm.	Consumption rate (cm./sec.)			
	100% HNO <sub>3</sub>	97% HNO <sub>3</sub>	95% HNO <sub>3</sub>	90% HNO <sub>3</sub>
13.9	0.132	...	...	...
14.6	.146	0.126	0.114	0.110
15.9	.163	...	...	...
16.6	.330	...	...	...
17.3	.660	...	...	...
18.0	...	...	...	0.132
21.4	.736	.175	.168	.157
28.2	.840	.280	.241	.208
31.6	...	...	...	.236
35.0	.950	.390	.330	.257
38.4	...	...	...	.278
41.8	1.08	.510	.432	.335
45.2	...	...	...	.356
48.6	1.24 <sup>a</sup>	.590	.483	.363
55.4	1.40	.625	.554	.409
62.2	2.20	.665	.597	...
69.0	3.35	.737 <sup>a</sup>	.645	.460
75.8	5.00	1.59	.737	...
82.6	6.90	2.11	.902 <sup>a</sup>	.499
89.4	...	2.59	1.05	...
96.2	...	...	1.78	...
103.0	...	4.39	2.54	.564
109.8	...	...	4.83	...
116.6	...	...	7.62	...
123.4	...	5.56	11.43	.635 <sup>a</sup>
130.2	...	...	17.78	...
137.0	...	...	25.40	1.89

<sup>a</sup> Turbulence starts.

TABLE II  
EFFECT OF ACID CONCENTRATION ON CONSUMPTION RATE OF SYSTEMS CONTAINING NITRIC ACID

Pressure, atm.	Consumption rate (cm./sec.)					
	Nitromethane + HNO <sub>3</sub>		Nitroethane + HNO <sub>3</sub>		1-Nitropropane + HNO <sub>3</sub>	
	99%	95%	99%	95%	99%	95%
11.2	...	...	...	...	0.077	...
14.6	0.086	0.071	0.076	0.109	.102	0.058
18.0	.105	...	.093	...	...	...
21.4	.141	.114	.109	.175	.166	.111
24.8	.188	...	.147	...	...	...
28.2	.215	.160	.206	.231	.238	.177
29.5	...	...	.220	...	...	...
31.6	.236	...	.379	...	...	...
35.0	.277	.198	.470	.309	.350	.234
38.4	.355	...	.518	...	...	...
41.8	.464	.246	.555	.386	.516	.315
48.6	.524	.302	.617	.434	.813	.394
55.4	.567	.353	.664	.485	1.15 <sup>b</sup>	.467
58.1	...	...	.680 <sup>a</sup>	...	...	...
59.5	...	...	.710	...	...	...
62.2	.598 <sup>a</sup>	.404	...	.516	1.45	.511
62.9	...	...	1.30 <sup>b</sup>	...	...	...
69.0	.627	.467	...	.564	...	.582
75.8	...	.518	...	.574	...	.648
82.6	...	.587	...	.622	...	.691
89.4	...	.838	...	.665	...	.610 <sup>b</sup>
96.2	...	1.897 <sup>b</sup>	...	.704	...	1.60
99.6	...	...	...	...	...	...
103.0	...	3.80	...	1.41 <sup>b</sup>	...	2.49
107.8	...	...	...	2.47	...	3.81
116.6	...	...	...	5.89	...	...

<sup>a</sup> Mild turbulence. <sup>b</sup> Violent turbulence.

TABLE III

CONSUMPTION RATE OF VARIOUS SYSTEMS CONTAINING 99% NITRIC ACID

Pressure, atm.	Consumption rate (cm./sec.)			Diisopropyl ether
	<i>m</i> -Dinitrobenzene	1,5-Dimethyl-tetrazole	Dioxane	
10.8	..	..	0.179 <sup>a</sup>	...
11.8	..	..	.329	...
13.2	..	..	.368	...
14.6	..	..	.401	0.094
18.0	..	..	.470	...
21.4	..	..	.542	...
23.4	..	..	.579	...
28.2	..	..	1.45 <sup>b</sup>	.171
35.0	..	..	2.42	...
41.8	24 <sup>b</sup>	..	5.35	.247
55.4	>24	..	...	.516
96.2	>24	23.8 <sup>b</sup>	...	...

<sup>a</sup> Flameless combustion. <sup>b</sup> Very turbulent.

TABLE IV

EFFECT OF ACID CONCENTRATION AND LUCITE ON THE CONSUMPTION RATE OF SYSTEMS CONTAINING NITRIC ACID

Pressure, atm.	Consumption rate (cm./sec.)			
	99% <i>n</i> -Butyric acid	98% <i>n</i> -Butyric acid + HNO <sub>3</sub>	95%	2-Nitropropane + 99% HNO <sub>3</sub> + 0.5% Lucite
14.6	0.231	...	...	0.120
21.4	.310	0.278	...	.175
28.2	.378	.338	...	.250
35.0	.431	.383	...	.340
41.8	.489	.422	...	.415
48.6	.538	.483	...	.485
55.4	.591	.543	...	.565
62.2	.651	.591	...	.640
69.0	.730	.644	...	2.10 <sup>a</sup>
75.8	.798	.720	...	...
82.6	1.89 <sup>a</sup>	.779	...	...
89.4	...	1.49 <sup>a</sup>	...	...
99.6	...	...	0.645	...
103.0	...	...	.679	...
109.8	...	...	.709	...
116.6	...	...	.764	...
121.0	...	...	.795	...

<sup>a</sup> Turbulent combustion.

ture increases as the concentration of the nitric acid increases and develops into the low pressure step as 100% nitric acid is approached. The data in Table II show that both nitromethane and nitroethane with 99% nitric acid show low pressure steps in their rate curves. The data also show that the onset of the step goes to lower pressure and the intensity of the step increases in the order nitromethane, nitroethane, 2-nitropropane. As with 2-nitropropane the addition of a small amount of water to the nitric acid removes the low pressure step in these systems. The nitroethane with 95% nitric acid is somewhat anomalous. In the low pressure region the mixture containing the weaker acid appears to have a higher burning rate until the low pressure step region is reached. The data on the 1-nitropropane system indicate that with 99% nitric acid there appears to be no low-pressure step, but rather the curve shows a concavity upward. The addition of water to the nitric acid makes the rate curve linear.

Table III shows data obtained with the fuels *m*-dinitrobenzene and 1,5-dimethyltetrazole. These substances are solid, but dissolve in nitric acid to give stable solutions. No smooth-burning region was observed with these fuels. Sustained combustion did not occur until the pressure was high enough to lead to turbulent combustion.

The data on dioxane-99% nitric acid in Table III show no "step" in the smooth-burning region. Although this system was stable at room temperature its combustion was different from normal liquid burning. The visible flame appeared a long distance above the liquid surface. At 13.2 atm. the bottom of the visible flame appeared about 1 in. above the liquid surface and there was evidence of NO<sub>2</sub> as a product of combustion. In spite of the fact that the flame was fairly far away from the liquid surface at all pressures the system went into turbulent combustion at a fairly low pressure. Another somewhat anomalous property of this system was observed for the single point where flameless burning occurred. This point is well below the extension of the smooth-burning part of the rate curve. In all other systems investigated flameless burning data fell either on or very slightly below it. The diisopropyl ether had a very large heat of mixing with 99% nitric acid and it reacted with the acid at room temperature. Consequently, the system contained acid decomposition and reaction products, and the composition was changing with time. Again the flame did not reach close to the liquid surface, and the surface was rather foamy. There was visible evidence of NO<sub>2</sub> in the area in between the foam and the bottom of the flame. Also, the mixture would go spontaneously into a vigorous precombustion reaction when the bomb was pressurized to 48.6 atm. or above. Combustion was not complete at all pressures since a heavy carbon deposit remained on the combustion tube. Because of all these irregularities the results given in Table III probably are not significant. Apparently this system is intermediate between the stable two-component system and the hypergolic system.

Table IV gives data on the *n*-butyric acid-99% nitric acid system which show that there is no step in the low pressure region, but the consumption rates are surprisingly high down to the very lowest pressure at which sustained combustion can be obtained. Again, the addition of water to the acid decreases the slope of the rate curve and the rate at any given pressure. The last column in Table IV shows that the addition of 0.5% Lucite to the 2-nitropropane-99% nitric acid system completely vitiates the low pressure step.

A short study of the effect of tube diameter on the low pressure step in the system 2-nitropropane-99% nitric acid was carried out. It was found that the step was present for tubes of 3 and 4-mm. inside diameter. With tubes 5, 6 and 8-mm. diameter the low pressure step was absent. Thus, for the tube sizes larger than 4-mm. diameter the rate curve in the smooth-burning region simply continued as a nearly linear extension of the lowest pressure portion of the curve until turbulent combustion was reached.

Although phenomena associated with the onset

of turbulent combustion are not the purpose of this study, there are two results which should be mentioned: (1) The pressure corresponding to the onset of turbulence appears to be a linear function of the acid concentration for the system 2-nitropropane-nitric acid. The four points indicated in Table I can be fit within the accuracy of the experiment by the equation

$$P_T = 7.5C + 797 \quad (1)$$

where  $P_T$  is the pressure in atmospheres corresponding to the onset of turbulent combustion, and  $C$  is the concentration of the nitric acid used to prepare the system in percentage units. Such a linear relation is not true for the rate at which turbulent combustion occurs; (2) there appears to be a relation between the pressure for onset of turbulence and the nitroparaffin fuel if 99% nitric acid is used. If the pressure is plotted *vs.* number of carbon atoms in the fuel, a smooth curve results, but it is probably not linear. Again, if the rate corresponding to the onset of turbulence is used, no smooth relationship results.

**An Hypothesis Describing the Low Pressure Step.**—The occurrence of the low pressure step in the system 2-nitropropane-nitric acid was known to exist since 1951.<sup>2</sup> However, it was not possible to discuss the phenomenon on the basis of a reasonable hypothesis until temperature profiles and surface temperature measurements were made.<sup>3</sup> In order to develop the hypothesis the relationships between five major factors must be considered simultaneously. These are (1) surface temperature, (2) liquid phase temperature profile, (3) chemical reactions in the preheat and gas phase zones, (4) the consumption rate curve, and (5) the heat sources and sinks and heat transfer across boundaries in the region of the preheat zone. It was shown that the surface temperature of a burning liquid is determined primarily by the rate of heat transfer to the liquid from the reacting gas above it, the heat of vaporization of the liquid, and the rate of vaporization of the liquid.<sup>3</sup> If there are reactions occurring in the liquid phase then the surface temperature is also affected by the heat absorbed per unit of the reaction and the rate of this reaction. The vaporization process is pressure dependent and allows the surface temperature to rise with the pressure, but at a slower rate than the boiling point rises with the pressure.<sup>3</sup> If an endothermic reaction takes place in the liquid, which is essentially independent of pressure, this reaction will have the effect of holding the surface temperature constant as the pressure on the system increases. The latter situation appears to hold for the system 2-nitropropane-95% nitric acid.<sup>3</sup> It will be assumed that all systems containing nitric acid will behave similarly since nitric acid decomposition is known to take place in the preheat zone of these systems. It is not assumed that the surface temperature is the same for all systems containing nitric acid, however. The absolute value of the surface temperature may vary somewhat with the fraction of nitric acid in the mixture, the vapor pressure of the fuel, etc.

(2) This phenomenon was observed early in these studies but it was not published until 1955 (see ref. 1).

(3) D. L. Hildebrand and A. Greenville Whittaker, *THIS JOURNAL*, **59**, 1024 (1955).

Figure 1 shows two temperature profiles for 2-nitropropane-95% nitric acid at different consumption rates. About 0.5% Lucite was added to the system to suppress convective mixing and thus obtain smooth profiles. In Fig. 1,  $T_1$  is the initial

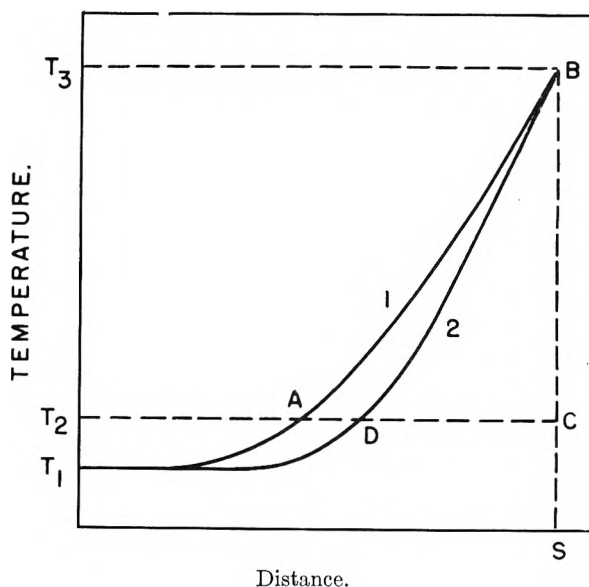


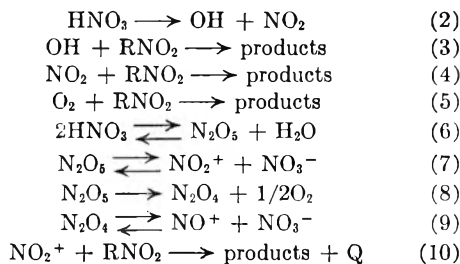
Fig. 1.—Temperature profiles at two different rates for system 2-nitropropane-95% nitric acid.

temperature of the liquid,  $T_2$  the temperature at which chemical reaction becomes significant,  $T_3$  the surface temperature (about 190°), and  $S$  is the location of the burning surface. The shape of these curves is determined almost completely by the thermal diffusivity of the liquid and the consumption rate.<sup>4</sup> Since the thermal diffusivity of the liquid systems studied do not vary a great deal, all the curves will have nearly the same characteristics at the same rate. The rate corresponding to curve 1 is less than the rate corresponding to curve 2, but the area DBC under curve 2 is less than the area ABC under curve 1. These areas are proportional to the product of the temperature and dwell time at that temperature; consequently, the amount of chemical reaction in the preheat zone varies as these areas vary. Since the area decreases as rate increases it follows that any chemical reaction in the preheat zone such as the thermal decomposition of nitric acid decreases as the rate increases. Moreover, if the effects of diffusion and convective mixing are small the concentration of any decomposition product at any given location also decreases as the rate increases. If mixing in the preheat zone is not negligible then only the average concentration of any decomposition product in the preheat zone decreases with increasing rate. If there is violent convective mixing in the preheat zone the heat transfer to the liquid is greater; hence, there is a relatively greater amount of chemical reaction. Such is the case with the 2-nitropropane-nitric acid system and this appears to be true of all nitric acid systems studied. It is also observed that the violent convective mixing decreases as the rate increases so that the profiles become quite smooth

(4) D. L. Hildebrand and W. P. Reid, unpublished.

and approach those shown in Fig. 1 even without Lucite addition. This situation causes the amount of chemical reaction in the preheat zone of these systems to decrease even more rapidly as rate increases.

Consider the following set of chemical reactions as applying to the nitroparaffin fuels with nitric acid.



Reactions 2, 3, 4 and 5 may be considered as taking place in the gas phase above the liquid. These and reactions with the products are assumed to be rapid and responsible for the exceedingly steep temperature gradient above the liquid surface.<sup>3</sup> The remaining reactions are assumed to take place in the liquid phase preheat zone. The ionization reactions

as great as in pure nitric acid. Reactions 6 and 8 represent thermal decomposition of nitric acid. Reaction 10 has been shown to produce nitro compounds for aromatic hydrocarbons<sup>5</sup> and it will be assumed to occur for aliphatic nitro compounds, although the reaction probably is not as clean. It has been shown<sup>7</sup> that nitric acid will react with 2-nitropropane in the liquid phase. It was found that there were many reaction products of which only nitric oxide and *gem*-dinitropropane have been identified to date. These products indicate that both nitration and oxidation took place. That this reaction has a fairly high activation energy is indicated qualitatively by the fact that no reaction occurred at 145° while at 160° many reaction products were produced in measurable amounts.

Figure 2 shows a smooth curve fitted to the data for 2-nitropropane-100% nitric acid. Let it be assumed that at low pressure, such as point A on this curve, the principal combustion mechanism is one of evaporation of the liquid components and their subsequent vapor phase reaction according to some scheme as shown above. These reactions establish the very steep temperature gradient above the liquid which feeds heat back to the liquid to produce a further supply of material for the vapor phase reactions. At point A nitric acid is decomposed in the liquid to give H<sub>2</sub>O, N<sub>2</sub>O<sub>4</sub> and O<sub>2</sub>. The O<sub>2</sub> escapes and reacts in a vapor phase. Much of the N<sub>2</sub>O<sub>4</sub> remains dissolved and ionized according to reaction 9. The nitrate ion thus produced tends to repress reaction 7. The water also remains in the liquid phase and tends to reverse reaction 6 which causes the N<sub>2</sub>O<sub>5</sub> concentration to decrease. This also drives reaction 7 to the left. Thus, both of these decomposition products decrease the concentration of NO<sub>2</sub><sup>+</sup>. This has the effect of slowing down reaction 10 to a negligible rate. In going from A to B the consumption rate increases; hence, liquid phase decomposition of nitric acid decreases. Since the N<sub>2</sub>O<sub>4</sub> and water concentrations are now less, reaction 7 shifts to the right and causes the NO<sub>2</sub><sup>+</sup> concentration to increase. This results in an increase in the rate of reaction 10. Thus, as a consumption rate increases there is an increase in a source of heat in the liquid phase which has the same effect on the consumption rate as an increased temperature gradient above the liquid. At some rate reaction 10 becomes appreciable and the rate increases rapidly. This is B in Fig. 2. As the rate increases the liquid phase profile becomes steeper. Hence, the time which any element of liquid spends at a given temperature grows shorter very rapidly since the rate is increasing rapidly after region B. This means that there is a limit to the extent to which reaction 10 can take place. Therefore, the whole system is self-throttling and the rate cannot increase without limit. The region where this happens is C. If the combustion continued to be controlled essentially by vapor phase reactions as in the region AB the rate would have gone along curve BE approximately. The difference in consumption rate between CD and BE at any given pressure increases as the consumption rate increases. This may indicate that reaction 10 is not completely throttled

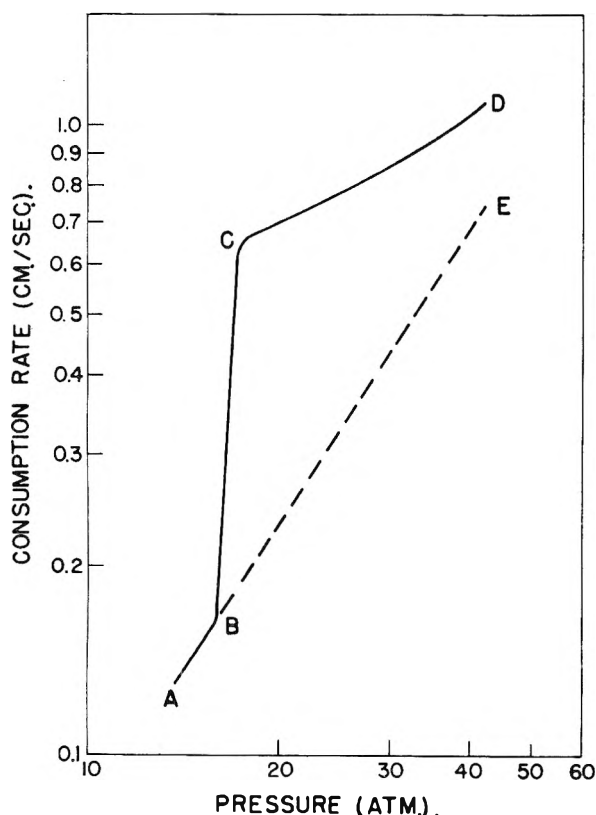


Fig. 2.—Consumption rate curves for 2-nitropropane-100% nitric acid system.

7 and 9 are assumed to be the same as those found for pure HNO<sub>3</sub>.<sup>5,6</sup> Because the dielectric constant of these mixtures is less than that of pure nitric acid the ionization of N<sub>2</sub>O<sub>5</sub> and N<sub>2</sub>O<sub>4</sub> probably is not

(5) E. D. Hughes, C. K. Ingold and R. I. Reed, *J. Chem. Soc.*, 2400 (1950).

(6) R. J. Gellespie, E. D. Hughes and C. K. Ingold, *ibid.*, 2552 (1950).

(7) C. M. Steese and A. G. Whittaker, unpublished results.

C, but continues to increase slightly in extent at least until turbulent combustion sets in. This completes the essential basic features of the hypothesis. It suggests that the liquid phase reactions are essential to the low pressure step. However, it must be emphasized that the temperature profile studies<sup>4</sup> showed that the amount of reaction in the liquid phase is quite small compared to the vapor phase reaction, but it is a basic assumption of this hypothesis that these minor liquid phase reactions can modulate the major reactions markedly and thereby produce large effects in the total consumption rate.

### Discussion of Results

Reactions 6 and 7 show that addition of water decreases the  $\text{NO}_2^+$  concentration. It has been shown that this decrease in  $\text{NO}_2^+$  concentration is sharp with the addition of the first few per cent. of water to pure nitric acid,<sup>5</sup> and it occurs in very small concentrations after about 5% water is added. It follows, then, that reaction 10 will be strongly affected by small additions of water to the nitric acid. This is consistent with the fact that the low pressure step sets in sharply in going from 97 to 99% acid in the 2-nitropropane system. At the concentration of 97% acid the effects of reaction 10 start to show up, but the  $\text{NO}_2^+$  concentration is reduced so that the effect of reaction 10 takes hold more gradually and never becomes very great. The result is the concave downward shape of the rate curve. This is also shown in the curves of the weaker acids, but to a lesser extent as would be expected. The other nitroparaffin systems were not investigated in as much detail, but it appears that water addition had the same effect on them. Although the hypothesis does not deal with the decrease in total consumption rate by the addition of water, it is probable that this comes about by the fact that water acts as a diluent for the vapor phase reactions which in turn decreases the temperature gradient above the liquid. It is also possible that water can act as a direct inhibitor to these reactions.

If the above hypothesis were valid, it would be reasonable to expect that the effects of increasing reaction 10 would show up gradually in the rate curve. A log rate *vs.* log pressure plot of the data for the systems containing nitromethane and nitroethane shows that the step does set in gradually as the rate increases. That is, the transition from region AB to CD is not as abrupt as shown in Fig. 2. The nitroethane system shows the more gradual transition. It might be expected that 1-nitropropane would behave much like nitroethane. This turns out to be the case. The transition is very gradual and occurs at higher pressure. Unfortunately, the system goes into turbulent combustion before the low pressure step is complete. This results in a rate curve that is concaved upward in the smooth burning region. As would be expected from the hypothesis the addition of 5% water to this system straightens out this portion of the rate curve.

The rather sudden appearance of the low pressure step at point B in the 2-nitropropane system is difficult to understand. It may be associated with the greater activity of the secondary hydrogen in

2-nitropropane as compared to the hydrogens in the other nitroparaffins. Indeed, it was noted that the intensity of the low pressure step was in the order nitromethane, nitroethane, 2-nitropropane. If the hypothesis were correct it follows that this is the order of reactivity of the nitroparaffins with  $\text{NO}_2^+$  (or  $\text{HNO}_3$ ). This, then, is a predicted result that can be verified by independent experiment.

The observation that the low pressure step disappears as combustion tube diameter increases is compatible with the hypothesis. If relative heat loss in the region of the liquid surface is defined as the ratio of the quantity of heat lost to the combustion tube walls per second to the quantity of heat produced by the combustion per second, then it follows that the relative heat loss decreases as tube diameter increases. This is due to the fact that the heat capacity of the tube increases approximately linearly with the tube radius whereas the quantity of heat produced increases as the radius squared. This means that a larger fraction of the heat goes into the liquid as tube size increases. Some of this additional heat can be absorbed by decomposing a somewhat larger amount of nitric acid. This produces more of the inhibitors for reaction 10. Therefore, reaction 10 never becomes significant and the low-pressure step never develops when the combustion tube is equal to or greater than a certain critical size.

It was found that 0.5% Lucite also caused the low pressure step to disappear. Temperature profile studies showed that the surface temperature is increased about 40° when 0.5% Lucite is added.<sup>8</sup> This means that  $T_3$  in Fig. 1 moves up and since the thermal diffusivity and consumption rate do not change appreciably the entire profile will be raised somewhat. This increases the area under the curve which indicates that more nitric acid can decompose in the preheat zone. Hence, reaction 10 is suppressed and the low pressure step does not develop.

Since reactions 2 through 10 do not depend on any specific property of the nitroparaffins any substance can be substituted for  $\text{RNO}_2$  as long as it can react with nitric acid and its decomposition and ionization products. Therefore, the low pressure step phenomenon should be fairly general for systems containing nitric acid. That the phenomenon may be actually difficult to find is indicated by the tube diameter effect and the effect of added Lucite. These results show that the low pressure step is very sensitive to the liquid phase profile and how it is affected by heat sources and sinks and surface temperature. There are many other conditions that must be satisfied also. For example, the substance must be miscible with nitric acid and form a stable system, combustion must have a smooth-burning region in the proper pressure range, etc. All these additional requirements combine to make the low pressure step observable in only a few systems rather than in most of the systems containing nitric acid.

Nevertheless, an effort was made to find the low pressure step in additional systems. Two general types of compounds were sought (1) compounds

(8) D. L. Hildenbrand and A. G. Whittaker, unpublished results.

that are very difficult to nitrate with nitric acid (thus a system in which reaction 10 would not be expected to be significant), (2) compounds that would show the low pressure step, but did not contain an  $\text{NO}_2$  group. So far this search has not been very fruitful, but it is continuing. Compounds falling in the first class are *m*-dinitrobenzene and 1,5-dimethyltetrazole.

The results show that these systems had no smooth-burning region; hence, they gave no information on the low pressure step. It appears that the vapor pressure of these substances at the surface temperature was so low that an adequate supply of fuel for the vapor phase reactions could not be maintained. Sustained combustion could occur only in the turbulent region where particles of fuel were entrained in the vapor phase.

Dioxane probably does not react with  $\text{NO}_2^+$  readily. It is more likely that the opening of the ring is a more important but slow reaction with nitric acid. Since this does not involve  $\text{NO}_2^+$  it is reasonable to expect no low pressure step in this system. The fact that this system had an abnormally large dark zone indicates that even the vapor phase reactions probably were rather slow.

Compounds falling in the second class were diisopropyl ether and *n*-butyric acid. Unfortunately, the diisopropyl ether was too reactive with nitric acid and this system gave no useful information. The results obtained with normal butyric acid were very interesting. With 99% acid the slope of the smooth-burning region was very close to that of the upper part of the step for the corresponding 2-nitropropane system. It may be inferred from this that *n*-butyric acid reacts with  $\text{NO}_2^+$  readily and reaction 10 is significant down to the lowest rate. It is also possible that this system has a lower surface temperature than the 2-nitropropane system because it has a higher fraction of nitric acid. Lower

surface temperature would favor reaction 10. The addition of water should repress reaction 10, and should, in correct amount, cause the low pressure step to develop. Although water had the expected effect of decreasing the rate and slope of the curve, it also rapidly moved the minimum pressure for sustained combustion to higher pressure. Consequently, it was not possible to observe the region of interest of the rate curve. Therefore, it was not possible to tell whether the addition of water affected this system in accordance with the hypothesis.

It is clear that with the aid of the hypothesis outlined above, general predictions can be made about the variation of the liquid phase temperature profile and surface temperature with respect to the low pressure step. Also, some specific predictions can be made about the effect on the low pressure step of adding small amounts of such things as nitrogen tetroxide and potassium nitrate. Finally, it is to be emphasized that, although the present results favor the ionic reactions 2 through 10, they are by no means unique. It is possible to write a chain free-radical mechanism that has the same properties as the reactions given. Consequently, the hypothesis is introduced as being suggestive and not conclusive. Its chief virtue lies in the fact that it indicates many ways of getting new significant information. As such, it is a good working hypothesis even though it may ultimately be shown to be completely incorrect.

**Acknowledgments.**—The authors wish to thank Professor H. S. Johnston of Stanford University for helpful discussions on the reactions of nitric acid. Also, Drs. W. G. Finnegan, R. Boschan, R. Reed and W. P. Norris of the Organic Branch, Chemistry Division, U. S. Naval Ordnance Test Station gave helpful information on the chemical properties of the organic compounds considered for this research.

## STUDY OF NICKEL OXIDE-KIESELGUHR CATALYST. II. THE PARTICIPATION OF PHYSICALLY ADSORBED MOLECULES IN PROPYLENE POLYMERIZATION AT 0°

BY SHINICHI KAWAGUCHI

*Institute of Polytechnics, Osaka City University, Osaka, Japan*

*Received July 18, 1956*

The catalytic polymerization of propylene over a series of nickel oxide-kieselguhr catalysts was studied with various initial pressures mainly at 0°, and the so-called Zeldowitch equation was found to fit the course of the reaction. By extrapolating the linear plot of this rate equation, the initial rate of reaction and the amount of initial adsorption were determined; the latter consists at least mainly of physical adsorption. The adsorption isotherm of propylene satisfies the B.E.T. equation, and plotting the initial rate vs. the amount of initial adsorption gives a straight line which intercepts the abscissa, indicating that the initial rate is first-order with respect to the *effective* amount of adsorption, that is,  $R_0 = k(v - v_0)$ . This result was considered to give quantitative evidence that reactant molecules participate in the reaction *via* a van der Waals layer, but not directly from the gas phase.

The course of the catalytic polymerization of gaseous olefins on a nickel oxide-kieselguhr catalyst was extensively studied by Koizumi, who presented two rate laws<sup>1</sup>

$$-V \frac{dP}{dt} = \frac{kP}{a + b(P_0 - P)V} \quad (1)$$

$$-V \frac{dP}{dt} = \frac{kP}{a' + b'(P_0 - P)V} \times \frac{1}{\sqrt{t}} \quad (2)$$

where  $V$  is the volume of the reaction vessel,  $P_0$

(1) M. Koizumi, *J. Chem. Soc. Japan*, **64**, 794 (1943); *J. Inst. Polytech., Osaka City Univ.*, **4C**, 1 (1953).

is the initial pressure, and  $k$ ,  $a$ ,  $b$ ,  $a'$ ,  $b'$  are constants. These equations are rather empirical, but eq. 1 was derived on the assumption that the reaction rate is controlled by the first-order surface migration of monomer molecules to active centers, which is retarded by the product. This law was reported to fit the observed data in the earlier stage of reaction, *i.e.*, up to several ten minute periods. Equation 2, which holds for the later part of the reaction course, *i.e.*, for several ten-hour periods, was derived on the assumption that the diffusion process of monomer through the polymer layer is rate determining. Tamele<sup>2</sup> also reported that the catalytic polymerization of propylene on silica-alumina catalyst at 200° could be expressed as a first-order reaction which was retarded by the product. Thus, the rate law employed is the same as eq. 1

$$\frac{dx}{dt} = \frac{k(a-x)}{1+bx} \quad (3)$$

where  $a$  is the initial pressure of propylene,  $x$  is the pressure drop at time  $t$ , and  $k$  and  $b$  are constants. The linear representation of this equation was given recently by Johnson<sup>3</sup>

$$\frac{x}{t} = \left(a + \frac{1}{b}\right) \frac{1}{t} \ln \frac{a}{a-x} - \frac{k}{b} \quad (4)$$

It is well known that in surface-catalyzed reactions, the kinetics obtained do not always represent the initial rates for various initial concentrations of reactant. This paper reports the rate law which refers to the initial rate of catalytic polymerization of propylene on nickel oxide-kieselguhr catalysts.

When propylene is brought into contact with a catalyst in a given volume at a low temperature, van der Waals adsorption proceeds and a rapid pressure drop is observed during the first few minutes. For nickel oxide or kieselguhr alone, neither of which has any catalytic activity, van der Waals adsorption practically attains equilibrium in several minutes. Thus, the pressure drop after a few minutes can be considered to be due solely to the "chemical" reaction, although during the first few minutes this is concealed by the predominant physical adsorption. Therefore, if the pressure-time curve is extrapolated to time zero, both the amount of physical adsorption and the initial rate of the "chemical" reaction can be obtained. In the previous paper<sup>4</sup> this extrapolation was performed by a rather inaccurate graphical method. Recently Taylor and Thon<sup>5</sup> showed that the Zeldowitch equation 5 can reproduce many published data of chemisorption and catalysis.

$$\frac{dq}{dt} = ae^{-\alpha q} \quad (5)$$

where  $q$  is the amount or fraction of reaction, and  $a$  and  $\alpha$  are constants. This equation proved to fit our data for propylene polymerization and was adopted as the extrapolation method.

(2) M. W. Tamele, *Faraday Soc. Disc.*, **8**, 270 (1950).

(3) O. Johnson, *THIS JOURNAL*, **59**, 827 (1955).

(4) S. Kawaguchi and H. Kihara, *J. Chem. Soc. Japan, Pure Chem. Sec.*, **75**, 15 (1954); *J. Inst. Polytech., Osaka City Univ.*, **4C**, 202 (1953).

(5) H. A. Taylor and N. Thon, *J. Am. Chem. Soc.*, **74**, 4169 (1952).

## Experimental Results

The experimental procedures, including the apparatus and material preparations, were previously described.<sup>4</sup> The composition and the specific volume of a series of catalysts are listed in Table II. The reaction was studied mainly at 0° and at various initial pressures of propylene.

The integrated form of the Zeldowitch equation 5 is written as follows for the present case

$$P = P_0' + \frac{2.3}{\alpha} \log t_0 - \frac{2.3}{\alpha} \log (t + t_0) \quad (6)$$

where  $P$  is pressure at time  $t$ ,  $P_0'$  the initial pressure for the reaction, and  $t_0 = 1/a\alpha$ . The observed  $P$  values were plotted against  $\log(t + t_0)$  and the constant  $t_0$  which gives the best straight line was determined. From the  $t_0$  and  $\alpha$  which is given by the slope of the straight line, the initial rate  $a$  was obtained. Furthermore, by extrapolating the straight line to  $t = 0$ ,  $P_0'$ , the initial pressure for the reaction was defined. Then  $(P_0 - P_0')$  corresponds to the initial adsorption, where  $P_0$  is the initial pressure before adsorption, which can be calculated with dead space data.

**Results at 0°.**—At 0° eq. 6 satisfactorily covers the reaction period (usually about four hours). As an example some results obtained on catalyst no. 2 (NiO 18%) are summarized in Table I, where the amount of initial adsorption and the initial rate of polymerization are presented in cc. (STP)/g. and cc. (STP)/min. g., respectively, and  $\alpha$  in g./cc. The adsorption isotherms of

TABLE I  
AMOUNT OF INITIAL ADSORPTION AND INITIAL RATE OF POLYMERIZATION OF PROPYLENE ON NICKEL OXIDE-KIESELGUHR CATALYST (NiO 18%) AT 0°

Initial pressure, <sup>a</sup> $P_0$	$P_0'$ mm.	Zeldowitch constant $\alpha$ , g./cc.	Amount of initial adsorpn. $v$ , cc. (STP)/g.	Initial rate of polymn. $R_0 \times 10^2$ , cc. (STP)/ min. g.
65.3	37.0	7.40	3.90	3.38
161.5	126.3	0.31	5.68	8.06
259.3	214.2	.27	6.59	9.17
333.5	284.8	.22	7.28	11.59
416.9	367.2	.20	7.53	12.72
515.8	462.1	.16	8.36	15.35
783.5	720.2	.13	10.01	18.75

<sup>a</sup>  $P_0$  is the initial pressure corrected for the dead space expansion, and  $P_0'$  is the initial pressure for the chemical reaction determined by Zeldowitch extrapolation.

propylene on catalysts of various composition are plotted in Fig. 1. These data follow the B.E.T. equation and the values of constants,  $v_m$ , and  $c$ , are listed in Table II. The pressure dependence

TABLE II  
B.E.T. CONSTANTS OF ISOTHERMS AND CONSTANTS OF EQUATION 8 FOR PROPYLENE POLYMERIZATION AT 0°

Cat. no.	0	1	2	4	6	8	10
NiO, %	0	8.6	18.1	38.0	57.0	80.8	100
B.E.T. constants $v_m$ , cc. (STP)/g.	2.2	6.9	9.4	14.9	18.8	20.6	13.8
$c$	58	128	36	53	53	53	58
Constants in eq. 8							
$k \times 10^2$ , min. <sup>-1</sup>	...	2.6	2.5	1.4	0.49	0.15	...
$v_0$ , cc. (STP)/ g.	...	1.9	2.6	6.8	8.2	11.7	...

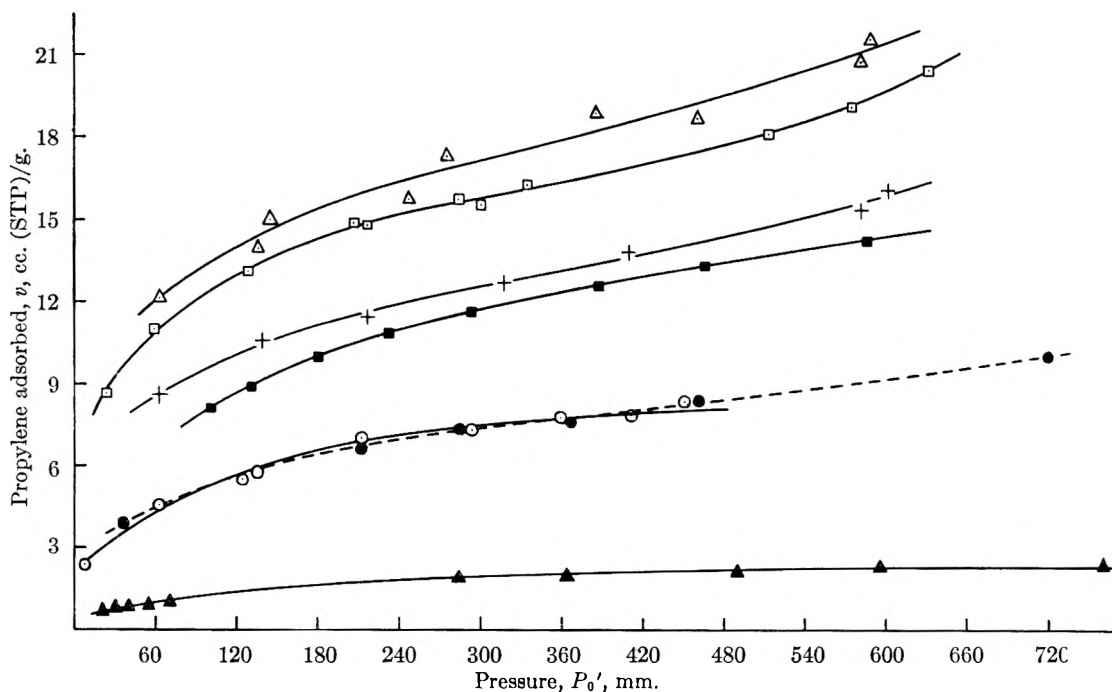


Fig. 1.—Adsorption isotherms of propylene at 0° on nickel oxide-kieselguhr catalysts: ▲, no. 0; ○, no. 1; ●, no. 2; +, no. 4; □, no. 6; △, no. 8; ■, no. 10.

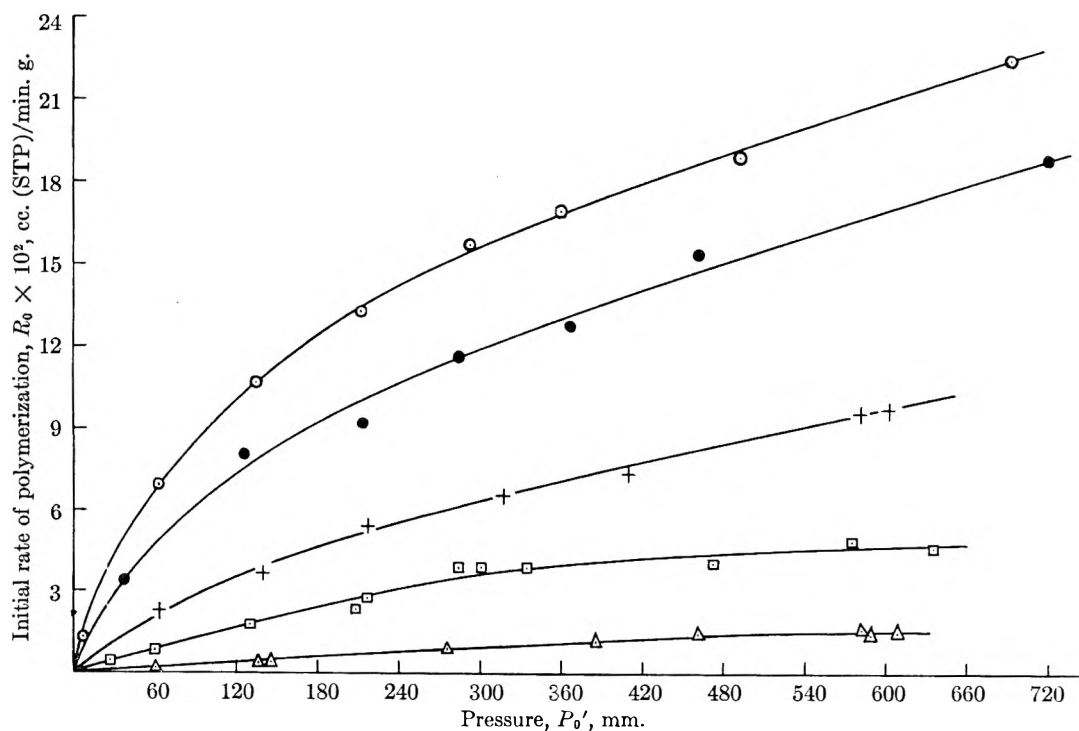


Fig. 2.—Initial rates of propylene polymerization at 0° over nickel oxide-kieselguhr catalysts: ○, no. 1; ●, no. 2; +, no. 4; □, no. 6; △, no. 8.

of the initial rate of polymerization is shown in Fig. 2.  $\log R_0$  vs.  $\log P_0'$  gave straight lines (when a few low pressure points were excluded in each case) and the pressure exponents were found to be as follows

$$R_0 = kP^x \quad (7)$$

$x = 0.49$  for cat. no. 1  
 $0.60$  for cat. no. 2  
 $0.64$  for cat. no. 4  
 $0.75$  for cat. no. 6  
 $1.0$  for cat. no. 8 (to ca. 500 mm.)

Thus, the initial rate is not proportional to the monomer gas pressure except for catalyst no. 8; this invalidates the assumption used for the time-course rate equation 1.

Furthermore, if the initial rate  $R_0$  is plotted directly against the amount of adsorption  $v$ , a straight line which intercepts the abscissa is drawn (Fig. 3), indicating that the rate law can be formulated as

$$R_0 = k(v - v_0) \quad (8)$$

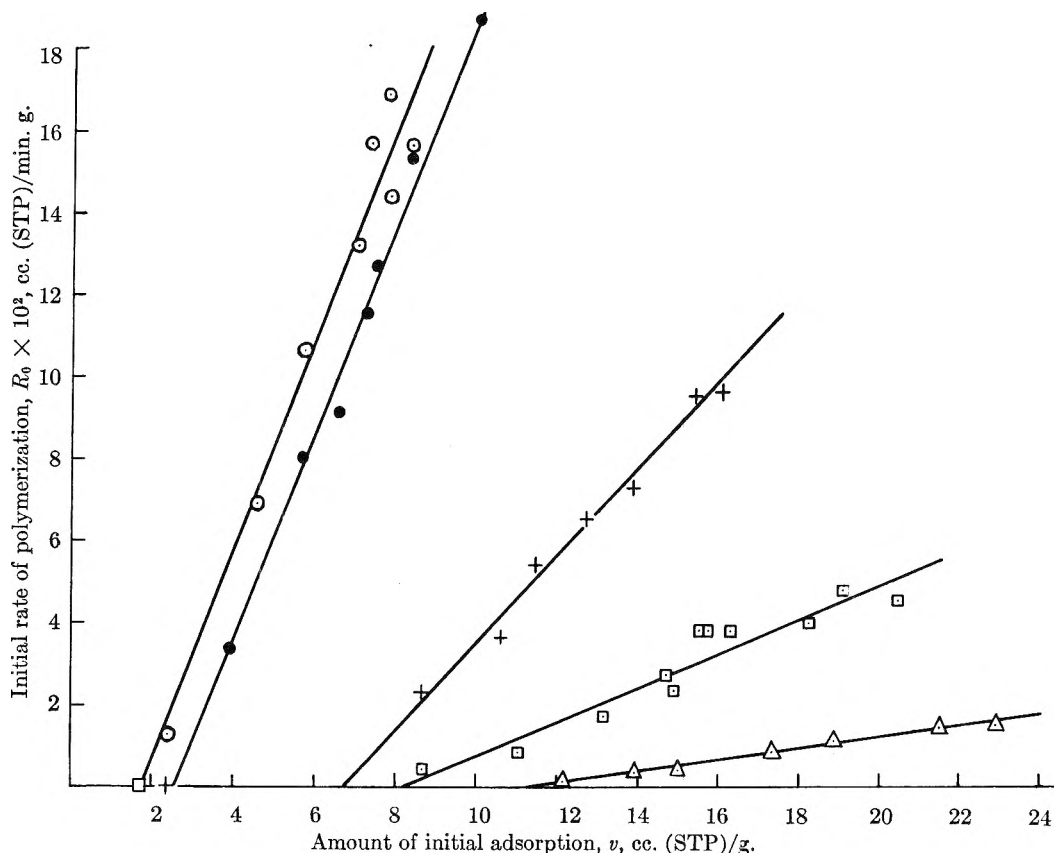


Fig. 3.—Initial rates of propylene polymerization as functions of amounts of initial adsorption at 0° on nickel oxide-kieselguhr catalysts: O, no. 1; ●, no. 2; +, no. 4; □, no. 6; △, no. 8.

where  $k$  and  $v_0$  are constants. This equation shows that some part of the adsorbed molecules cannot contribute to the reaction, and the initial rate of the reaction is proportional to the *effective* amount of adsorption. The ineffective amount,  $v_0$ , of the propylene adsorption increases linearly with the nickel oxide content of the catalysts as shown in Table II and Fig. 4. This straight line nearly coincides with the linear sum of  $v_m$  values for the two components (dotted line in Fig. 4). The dotted line gives the  $v_m$  values which catalysts of various composition should have if there were no interaction between the two components. The actual  $v_m$  values are much larger, revealing the surface area enhancing effect of the dual system. The apparent first-order rate constant  $k$  in eq. 8 increases as the nickel oxide content decreases (Table II). It is not certain so far whether or not the rate constant  $k$  reaches a maximum at any composition below 20% nickel oxide, and further investigation on catalysts of lower nickel oxide content is desirable.

**Temperature Effect.**—To find the activation energy for this reaction and the isosteric heat of adsorption, another series of experiments was performed at various temperatures. In Table III are summarized the results of several preliminary experiments on catalyst no. 2 at lower temperatures.

Table I shows the normal pressure dependence of the Zeldowitch constant,  $\alpha$ , but Table III reveals some anomalous temperature dependence. The Arrhenius plot of the initial rate of poly-

TABLE III  
INITIAL ADSORPTION AND INITIAL RATES OF POLYMERIZATION OF PROPYLENE ON THE NICKEL OXIDE-KIESELGUHR CATALYST (NiO 18%) AT LOWER TEMPERATURES

Temp., °C.	Initial pressure, mm. $P_0$	Zeldowitch const. $\alpha$ , g./cc. $P_0'$	Initial adsorption, $v$ , cc. (STP)/g.	Initial rate of polymn. $R_0 \times 10^3$ cc. (STP)/min. g.	
-11.7	503.1	440.4	0.214	9.65	7.20
-7.2	491.4	435.0	.210	8.48	8.64
20.0	507.4	456.4	.182	6.93	27.5
20.0	494.5	449.1	.190	6.65	27.6
35.4	377.8	348.7	.262	4.89	47.7

merization,  $R_0$ , is illustrated for each catalyst in Fig. 5; the apparent activation energies calculated are 7.1, 6.5, 5.9, 5.9 and 6.1 kcal./mole for catalysts no. 1, 2, 4, 6 and 8, respectively.

Preliminary experiments at higher temperatures gave Arrhenius plots of different slope resulting in lower activation energies. A detailed study of this problem is in progress.

**Analysis of the Initial Adsorption.**—To detect how much chemisorption is included in the amount of initial adsorption, the evacuation and re-adsorption method was applied. At 0° a sample of catalyst was kept in contact with propylene of 160 mm. for three minutes and then evacuated at the same temperature for one hour. Re-adsorption at the same pressure and evacuation were repeated alternately. The amount of adsorption in each three minutes diminished successively: 3.04, 2.84, 2.67, 2.55, 2.45 cc., the irreversible sorption being

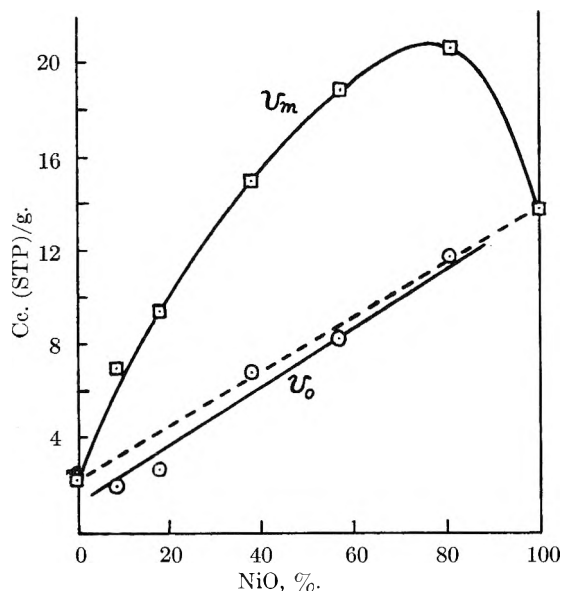


Fig. 4.—Monolayer volume ( $v_m$ ) and ineffective amount of adsorption ( $v_0$ ) of propylene at  $0^\circ$  as functions of composition of the nickel oxide-kieselguhr catalyst.

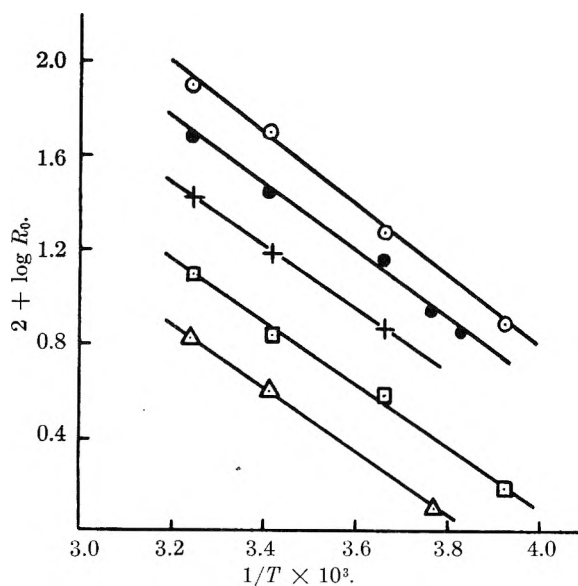


Fig. 5.—Arrhenius plots of the initial rates ( $R_0$ ) of propylene polymerization over nickel oxide-kieselguhr catalysts: O, no. 1; ●, no. 2; +, no. 4; □, no. 6; Δ, no. 8.

piled up stepwise as: 0.20, 0.37, 0.49, 0.59 cc. The catalyst was then evacuated at  $100^\circ$  for two hours, and the usual time-course of pressure decrease was measured. The analysis of this data gave the initial rate of 0.21 cc./min., and the pressure reading at three minutes corresponded to 3.24 cc. sorption. The latter value is a little larger than the 3.04 cc. recorded above on the fresh catalyst, indicating the complete regeneration of the catalyst. The irreversible sorption of 0.20 cc. during the first three minutes is much smaller than  $3 \times 0.21$  cc., the monomer loss, which should be observed if the over-all reaction started without any time lag; hence the former should be considered as a part of the observed time-course and not the rapid initial chemisorption. However, the possibility cannot be excluded that easily desorbable chemisorp-

tion might be included in the observed amount of initial adsorption.

### Discussion

It is important to decide which step of the over-all process is measured as the initial rate in the present experiments. At the temperatures investigated, van der Waals adsorption is largely responsible for the initial pressure drop. Since the rate of physical adsorption is rapid, the physical adsorption can be assumed to have reached equilibrium in advance of the rate process, and the initial rate (calculated by the Zeldowitch extrapolation of data obtained after the first ten minutes) hardly includes the physical adsorption term.

Of the elementary processes involved in the over-all reaction, only the chemisorption of monomer



and the addition processes



need to be considered.  $M_a$  denotes physically adsorbed monomer, S the bare active site and SM chemically adsorbed monomer.

It may not be strictly accurate to exclude chemisorption from the initial adsorption, but certainly the physical adsorption is predominant. If the chemisorption is as rapid as the physical adsorption, the addition processes, particularly ( $b_1$ ), would be rate determining and the initial rate would be written as

$$R_0 = k_{b_1}[M_a^*]_0[SM]_0$$

The subscript zero refers to time zero and  $[M_a^*]$  denotes the effective monomer concentration. If SM becomes constant at lower pressures and is independent of pressure in the range examined, the initial rate becomes first order with respect to the effective monomer concentration. The exponential decay of the rate which satisfied the Zeldowitch equation might be explained by the assumption that the rate constants of the addition steps decrease as monomer units of the surface complexes increase. The catalytic polymerization of olefins proceeds stepwise on the present catalyst as evidenced by the product analysis.<sup>1</sup>

On the other hand, if the chemisorption is of measurable speed and the addition steps are much slower, the initial rate will correspond to the chemisorption ( $a_1$ ) and the following rate law will hold.

$$R_0 = k_{a_1}[M_a^*]_0[S]_0 = k[M_a^*]_0$$

Physical interpretations of the empirical Zeldowitch equation have been given by a number of workers.<sup>6</sup>

The evidence does not warrant a choice between these two mechanisms. However, the exponential decay of the rate suggests that the main process occurring in the reaction period studied is chemisorption. The former explanation, that a sharp

(6) M. A. Cook and A. G. Oblad, *Ind. Eng. Chem.*, **45**, 1456 (1953); H. J. Engel and K. Hauße, *Z. Elektrochem.*, **57**, 726 (1953); J. E. Germain, *Compt. rend.*, **238**, 345 (1954); A. S. Porter and F. C. Tompkins, *Proc. Roy. Soc. (London)*, **A217**, 529 (1953); P. T. Landsberg, *J. Chem. Phys.*, **23**, 1079 (1955); I. Higuchi, T. Ree and H. Eyring, *J. Am. Chem. Soc.*, **77**, 4969 (1955).

decrease in addition rate constants gives rise to the logarithmic rate law, seems improbable.

It should be emphasized that the monomer molecule which reacts with substrate comes from the van der Waals layer and not directly from the gas phase, since the initial rate is proportional to the fractional power of the propylene pressure and, furthermore, to the effective amount of physical adsorption (Fig. 3 and eq. 8). These results, we believe, furnish quantitative evidence for the participation of physically adsorbed molecules in a chemical reaction. A number of authors<sup>7</sup> have made such a suggestion, but without evidence of a quantitative nature. Sadek and Taylor<sup>7g</sup> obtained results suggesting that the rate of chemisorption might be determined by the concentration of hy-

drogen gas bound by van der Waals forces on the surface of the nickel-kieselguhr catalyst. Recently Ehrlich<sup>7h</sup> derived theoretically a rate equation of chemisorption of gas *via* the physically adsorbed state.

Our experiments show that at low temperatures the apparent activation energy of the initial rate process and the heat of physical adsorption<sup>8</sup> (and therefore the true activation energy) do not vary appreciably with catalyst composition. Hence, the nature of the rate processes and that of the active centers on these catalysts are the same irrespective of catalyst composition. The change of *k* values with the composition of the catalyst (Table II) can be largely attributed to the change in the density of the active centers.

**Acknowledgment.**—This work is an extension of Prof. M. Koizumi's previous investigation. The author is grateful to him for his interest throughout this study.

(8) The energy factor *c* (Table II) is practically constant except for catalyst no. 1.

(7) (a) E. K. Rideal, *Proc. Camb. Phil. Soc.*, **35**, 130 (1939); (b) R. C. Hansford and P. H. Emmett, *J. Am. Chem. Soc.*, **60**, 1185 (1938); (c) J. Sheridan, *J. Chem. Soc.*, 133 (1945); (d) G. C. Bond and J. Sheridan, *Trans. Faraday Soc.*, **48**, 651 (1952); (e) *ibid.*, **48**, 658 (1952); (f) G. C. Bond, J. Sheridan and D. H. Whiffen, *ibid.*, **48**, 715 (1953); (g) H. Sadek and H. S. Taylor, *J. Am. Chem. Soc.*, **72**, 1168 (1950); (h) G. Ehrlich, *THIS JOURNAL*, **59**, 473 (1955).

## EFFECTS OF HYDROGEN CONTENT ON THE RESISTANCE AND THE POTENTIAL IN THE PALLADIUM-HYDROGEN-ACID SYSTEM

BY JAMES P. HOARE AND SIGMUND SCHULDINER

*Naval Research Laboratory, Washington, D. C.*

*Received July 25, 1956*

The amount of hydrogen dissolved in palladium was determined by relative resistance measurements, coulometric determinations and by reduction with ceric ion. Open-circuit potentials were determined against a Pt/H<sub>2</sub> reference electrode in the same hydrogen-saturated sulfuric acid solutions. It was found that the potential of an  $\alpha$ -palladium-hydrogen alloy (H/Pd atomic ratio = 0.025  $\pm$  0.005) was equal to 0.0495  $\pm$  0.0005 volt; and the potential of a  $\beta$ -palladium-hydrogen alloy (H/Pd  $\sim$  0.6) was equal to zero volt. The results also showed that from H/Pd = 0.025 to 0.36 the potential was 0.050 volt. Relative resistance measurements on increasing the hydrogen content of palladium gave valid quantitative results but when the hydrogen content of the metal was decreased this was not necessarily true. Pure hydrogen-free palladium when placed in a hydrogen-saturated acid solution spontaneously absorbed hydrogen until a H/Pd ratio of 0.025 was reached. Palladium-hydrogen alloys of H/Pd content greater than 0.36 spontaneously lost hydrogen in solution without a decrease in the relative resistance.

### Introduction

It was shown by Fischer<sup>1</sup> that there is a nearly linear relationship between the resistance of palladium-hydrogen alloys and the hydrogen content. This relationship is

$$R = R_0(1.0292 + 0.000668V)$$

where *R* is the measured resistance, *R*<sub>0</sub> is the resistance of pure, hydrogen-free palladium, and *V* is the concentration of hydrogen dissolved in the palladium in relative volumes. This relationship holds for a range of hydrogen volumes from about 30 to 925 relative volumes which corresponds to a H/Pd atomic ratio of about 0.025 to 0.73. This work was confirmed by other investigators.<sup>2</sup>

Stout<sup>3</sup> showed that the potential of a Pd/H<sub>2</sub> electrode was a function of the H/Pd atomic ratio. Previous work at this Laboratory<sup>4</sup> has shown that

when the atomic ratio of H/Pd  $\sim$  0.6 ( $\beta$ -phase) the potential of this electrode immediately after opening the circuit against a Pt/H<sub>2</sub> electrode in the same hydrogen-saturated solution is zero volt. However, under open-circuit conditions (no external current flow) the potential rose to 0.050 volt where it remained independent of time. It was thought that this corresponded to the hydrogen-poor palladium-hydrogen alloy ( $\alpha$ -phase). In order to determine quantitatively the amount of hydrogen dissolved in the palladium and the effects of the H/Pd atomic ratio on the potential for these two cases, this investigation was undertaken.

### Experimental Method

The palladium electrodes studied consisted of palladium wires 0.038 cm. in diameter and from 10 to 13 cm. in length wound in the form of a toroid or in the form used by Coehn and Jurgens.<sup>6</sup> No glass was used in the system; the cell was the same Teflon cell used in previous work.<sup>4</sup> The frames which held the palladium wire were made of virgin polyethylene. Each end of the palladium wire was welded to a platinum wire. The weld area and all platinum inside the cell was imbedded in polyethylene which prevented solution

(1) F. Fischer, *Ann. Physik*, [4] **20**, 503 (1906).

(2) For example: F. Krüger and G. Gehm, *Ann. Physik*, [5] **16**, 174 (1933); A. Coehn and H. Jürgens, *Z. Physik*, **71**, 179 (1931).

(3) H. P. Stout, *Disc. Faraday Soc.*, **1**, 107 (1947).

(4) J. P. Hoare and S. Schuldiner, *J. Electrochem. Soc.*, **102**, 485 (1955); S. Schuldiner and J. P. Hoare, *J. Chem. Phys.*, **23**, 1551 (1955).

(5) Ref. 2, Fig. 16, p. 195.

contact with the platinum leads. The solution used in all experiments was highly purified, pre-electrolyzed 2 *N* sulfuric acid stirred with highly purified hydrogen, helium or oxygen at atmospheric pressure. The temperature was  $26 \pm 1^\circ$ .

All potentials were measured against a Pt/H<sub>2</sub> electrode in the same solution. The resistance values were determined with a General Radio Resistance Limit Bridge, Type 1652 A. It was found that measuring the resistance of the palladium wire in air, distilled water or immediately after immersion in acid solution gave virtually the same results. Because of this all resistance measurements were made while the wire was immersed in solution.

The palladium wire was cleaned initially in concentrated nitric acid and then heated to white heat. The resistance of the palladium wire in conductivity water plus platinum and copper leads was then measured. After subtracting the resistance of the leads (which included the weld), the remaining resistance was that of the pure, hydrogen-free palladium wire,  $R_0$  (1 mΩ/mm.). The electrode was then placed in the cell and the change in resistance,  $R$ , was determined during the course of an experiment. A check on  $R_0$  was made at the end of a run by heating the wire white hot and redetermining the resistance.

The amount of hydrogen dissolved in the palladium wire was determined by several methods. These consisted of relative resistance ( $R/R_0$ ) measurements, coulometric methods and the reduction of ceric ion. The relative resistance measurements were converted to H/Pd atomic ratios by using the data of Fischer.<sup>1</sup> In the coulometric methods the hydrogen dissolved in the palladium was removed by anodic polarization. The loss of hydrogen was followed either by changes in the relative resistance or by changes in the potential of the wire. The analysis with ceric ion consisted of stopping the flow of hydrogen and removing the sulfuric acid solution from the cell and then adding a known amount of about 0.12 *N* ceric sulfate in 1 *N* sulfuric acid solution to the cell. This solution was then either stirred with helium or sealed from the atmosphere without stirring by any gas. Small samples of the solution were periodically removed with a hypodermic syringe and titrated against a standard solution of ferrous ammonium sulfate with a Gilmont Ultramicroburet which could be read to 0.001 ml. In this way the amount of hydrogen dissolved in the palladium could be determined<sup>2</sup> at any time and the rate of removal of hydrogen from the palladium could be followed.

### Results and Discussion

A typical run relating the change of relative resistance,  $R/R_0$ , and the change in potential with time is shown in Fig. 1. For the first part of these

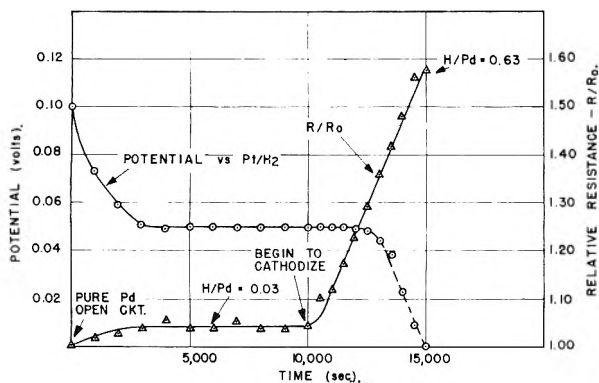


Fig. 1.—Variation of relative resistance and potential of palladium with time before and after cathodic polarization.

curves the initially pure, hydrogen-free palladium wire was allowed to remain in the hydrogen saturated sulfuric acid solution on open-circuit. As hydrogen dissolved in the metal, the relative resistance increased until a H/Pd atomic ratio = 0.03 was

reached. This ratio remained constant and independent of time. In this and other runs the steady-state H/Pd ratio under open-circuit conditions was equal to  $0.025 \pm 0.005$ . This plateau was found to be independent of time for periods as long as 48 hours. These atomic ratios show that the palladium wire was in the  $\alpha$ -phase.<sup>1,2,7</sup>

The open-circuit potential values initially show that owing to the low hydrogen content of the palladium and probably also to the presence of a small amount of oxide on the wire surface, the potentials were appreciably more noble than 0.050 volt. In time, the hydrogen content became constant, any possible trace of oxide was removed, and a steady-state potential of 0.0495 volt was reached. These results show that under open-circuit conditions, in hydrogen-stirred sulfuric acid solution, the  $\alpha$ -phase of definite H/Pd composition is formed and its steady-state potential against a Pt/H<sub>2</sub> electrode in the same solution is  $0.0495 \pm 0.0005$  volt.

In the second part of the curves shown in Fig. 1, the effects of electrolytically filling the palladium wire with hydrogen by cathodic polarization at a current strength of 0.040 ampere for a series of 1000 second intervals are shown. The relative resistance and the potential were measured simultaneously after opening the circuit and allowing the potential to reach a steady value. After the palladium electrode was polarized beyond 0.0495 volt, the open-circuit potentials were not steady-state values but were taken at a reading for which the change in potential with time was small ( $K < 10^{-4}$  v./min.). This is shown in the section of the potential curve with a dash line. When the potential reached zero, it corresponded to a relative resistance value which in turn corresponded to a H/Pd atomic ratio of 0.63. At this atomic ratio the palladium is in the  $\beta$ -phase<sup>8</sup> and its potential against a Pt/H<sub>2</sub> electrode in the same solution is zero volt. The experiment shown in Fig. 1 was repeated four times giving virtually the same results.

A continuation of the experiments above is shown in Fig. 2. Here, once the  $\beta$ -phase was reached by cathodic polarization the circuit was opened and the relative resistance and the potential changes with time were determined while still maintaining a constant flow of hydrogen. As also shown in previous work,<sup>4</sup> the potential spontaneously changed from zero to about 0.050 volt. The relative resistance, however, increased slightly and then remained constant. The potential indicated a loss of hydrogen, but the relative resistance values did not. Therefore in another series of similar experiments the palladium wire was allowed to remain on open-circuit in the hydrogen-stirred sulfuric acid solution for as long as seven days. The hydrogen flow was then stopped and the solution was replaced with a known amount of ceric sulfate solution. The hydrogen dissolved in the palladium wire quantitatively reduced ceric ion to cerous and by titrating the remaining ceric ion with ferrous ion, the total amount of hydrogen was determined. This value corresponded to an atomic ratio of H/Pd

(7) K. A. Moon, *J. Phys. Chem.*, **60**, 502 (1956).

(6) F. A. Lewis and A. R. Ubbelohde, *J. Chem. Soc.*, 1710 (1954); S. Schuldiner and J. P. Hoare, *J. Electrochem. Soc.*, **103**, 178 (1956).

(8) D. P. Smith, "Hydrogen in Metals," University of Chicago Press, Chicago, Ill., 1948, pp. 84-119.

equal to  $0.36 \pm 0.02$ . This result plus the above relative resistance results prove that hydrogen did leave the metal spontaneously without a decrease in the relative resistance. This means that the changes of resistance were primarily due to deformation of the palladium lattice rather than to the presence of hydrogen in the lattice. The results shown in Fig. 1, however, indicate that on filling the palladium with hydrogen the relative resistance does give an accurate measurement of the hydrogen content because here the lattice deformation is directly proportional to the amount of hydrogen added. Under the conditions of these experiments, the expanded palladium lattice does not appear to collapse with the loss of hydrogen.

The results shown in Fig. 2 demonstrate that even at  $H/Pd = 0.36$ , the potential is about 0.050 volt. This atomic ratio indicates that the  $\alpha$ - and  $\beta$ -phases coexist. The potential must then be a mixed potential of the  $\alpha$ - and  $\beta$ -phases with the  $\alpha$ -phase being the potential determining phase. This is also shown in Fig. 1 where the potential did not change appreciably from 0.050 volt until after a 0.36  $H/Pd$  ratio was exceeded.

In the experiment shown in Fig. 3, a palladium wire of known weight was cathodized to a  $H/Pd$  ratio of about 0.8. This gave a relative resistance of about 1.75. The circuit was then opened and when the potential reached a value of zero volt, the sulfuric acid solution was replaced with a known amount of standard ceric sulfate solution and the flow of hydrogen was changed to a flow of helium. This point corresponded to zero time in Fig. 3. At 2000 second intervals, samples of ceric sulfate solution were removed and analyzed for the equivalent amount of hydrogen removed by oxidation from the palladium wire. At the same time relative resistance measurements were taken.

When the relative resistance came to the value of unity, the total number of gram-equivalents of hydrogen removed from the palladium corresponded to a  $H/Pd$  ratio of 0.607. This again confirmed our findings that the zero potential corresponded to a  $\beta$ -phase palladium-hydrogen alloy. In Fig. 3 the total change in relative resistance does not correspond to an atomic ratio of 0.6 because as previously shown in Fig. 2, hydrogen may escape from the alloy down to as low as  $H/Pd = 0.36$  without changing  $R/R_0$ . These results show that relative resistance measurements can be used reliably to determine hydrogen content in palladium-hydrogen alloys only when filling the metal with hydrogen.

It is interesting to note that the collapse of the expanded palladium lattice does follow the removal of hydrogen when an oxidizing agent is present. This is further confirmed by the results shown in Fig. 4. In these experiments a comparison of the rate of hydrogen removal from palladium and the effect of an oxidizing reaction in collapsing the expanded lattice is demonstrated. In the case of the experiment in which hydrogen flow in the acid solution was replaced with helium flow, the relative resistance showed virtually no change after 19 hours, but when the helium flow was replaced with hydrogen a potential of 0.050 volt against  $Pt/H_2$  was

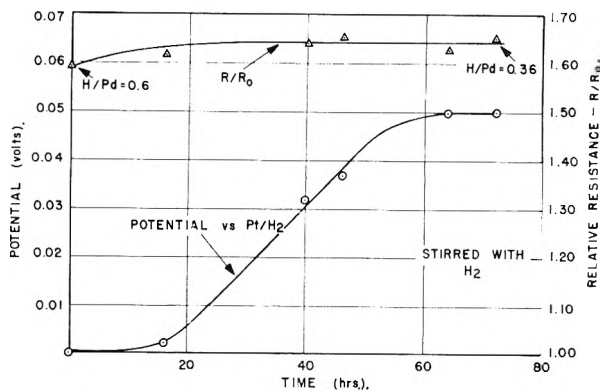


Fig. 2.—Variation of relative resistance and potential of palladium with time on open-circuit after cathodic polarization.

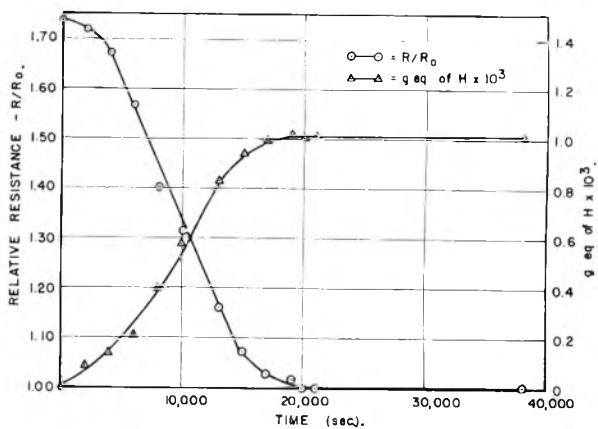


Fig. 3.—Quantitative removal of hydrogen from palladium by ceric sulfate with corresponding changes in relative resistance.

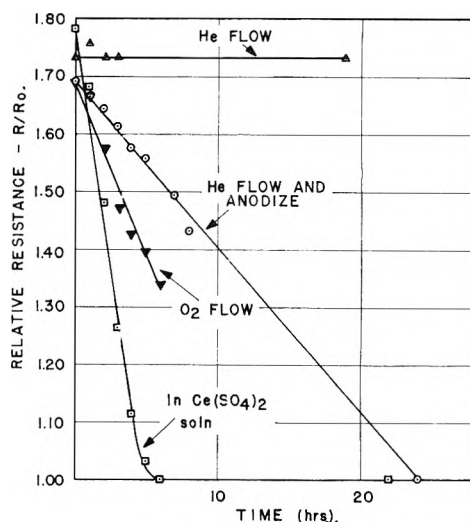


Fig. 4.—Effective of various processes for the removal of hydrogen from palladium on the change of relative resistance with time.

found. This confirmed the results shown in Fig. 2 that when an oxidizing agent is not present, the expanded lattice does not collapse even though the hydrogen content is considerably reduced.

In the experiment shown in Fig. 4 where the hydrogen was removed by anodic polarization, the

current used was 0.00105 ampere. It required 86,400 seconds to remove all the hydrogen from the palladium. This meant that there was 90.7 coulombs/96,500 =  $0.940 \times 10^{-3}$  gram-equivalent of hydrogen removed. Since there was  $1.66 \times 10^{-3}$  gram-equivalent of palladium in the wire,  $0.940/1.66 = 0.57$ , which was the atomic ratio of H/Pd. This result corresponded to a value within the experimental error to a  $\beta$ -palladium-hydrogen alloy.

### Conclusions

1. The potential of  $\alpha$ -palladium (H/Pd =  $0.025 \pm 0.005$ ) against a Pt/H<sub>2</sub> reference electrode in the same solution is  $0.0495 \pm 0.0005$  volt.

2. The potential of  $\beta$ -palladium (H/Pd  $\sim 0.6$ ) is zero volt.

3. From H/Pd = 0.025 to 0.36, the potential is 0.050 volt because the simultaneous existence of  $\alpha$ - and  $\beta$ -phases give a mixed potential which is dominated by the potential of the  $\alpha$ -phase in this region.

4. Pure hydrogen-free palladium when placed in hydrogen-saturated acid solution spontaneously absorbed hydrogen until a H/Pd ratio of 0.025 was reached.

5. Palladium-hydrogen alloys of H/Pd content greater than 0.36 spontaneously lost hydrogen in solutions free of oxidizing agents without a decrease in the relative resistance.

6. Relative resistance measurements on increasing the hydrogen content of palladium gave valid quantitative results, but when the hydrogen content of the metal was decreased this was not necessarily true. It was concluded that this was so because the relative resistance was primarily a measure of lattice deformation and that this process was not necessarily reversible when the hydrogen content was diminished.

7. Collapse of the expanded palladium lattice did follow the loss of hydrogen when the hydrogen was removed by an oxidative process.

## ABSOLUTE AREAS OF SOME METALLIC SURFACES

BY THOMAS L. O'CONNOR AND HERBERT H. UHLIG

*Corrosion Laboratory, Department of Metallurgy, Massachusetts Institute of Technology, Cambridge, Massachusetts*

*Received July 31, 1956*

Using the BET method, with ethane as adsorbate at  $-183^\circ$ , roughness factors were calculated for various metal surfaces. Abraded iron foil or 18-8 stainless steel sheet has a roughness factor of 3.1 to 3.4, in fair agreement with Erbacher's value of 2.5 employing adsorbed monolayers of polonium or of bismuth containing Th-C indicator. Hydrogen-reduced iron foil was found to have smaller area, the roughness factors averaging 1.2. Pickled 18-8 stainless steel acquired a factor of 4.1 when HCl-H<sub>2</sub>SO<sub>4</sub> was used, but of only 1.4 after immersion in HNO<sub>3</sub>-HF. Electropolishing of stainless steel produced a relatively smooth surface, the roughness factor being 1.1. Evaporated iron films had factors of 5 to 10 depending on thickness of the final film when the evaporation source *in vacuo* was iron wire heated electrically to 1000-1100°. However, if the temperature was raised to 1300°, the roughness factors averaged 1.8. It is thought that the higher temperature of the condensed film in the latter instance produced some sintering of iron crystals with reduction in over-all area. Polarization capacitance determinations did not lead to reproducible surface area values. Because of the several errors that can enter such measurements, it is believed that areas obtained from gas adsorption are more nearly correct.

Knowledge of the absolute surface area is important to the interpretation of many measurements dealing with metal properties. This factor concerns, for example, studies of catalysis, adsorption, overvoltage and reaction rates, including measurements of high temperature oxidation and corrosion. Common neglect of this factor does not mean it is of small consequence, or that it can be justifiably neglected. The presently reported results show, confirming limited information by other investigators, that surface preparation of bulk metals by one means or another may change the ratio of absolute to apparent area (roughness factor) by either a small percentage or by several hundred per cent. Brown and Uhlig<sup>1</sup> showed that when deep fissures result from pickling a metal like electrodeposited chromium, this ratio may increase to a value as high as 50.

**Method of Measurement.**—The method used for presently reported values was the well known BET method of gas adsorption<sup>2,3</sup> which is concerned essentially with the volume of gas  $v_m$  necessary to form a monolayer on the surface. We chose ethane as adsorbate at liquid oxygen temperatures ( $-183^\circ$ ) in accord with similar use of this gas previously.<sup>1</sup> Ethane has a low vapor pressure at  $-183^\circ$ ,

thereby permitting area measurements for a total surface no larger than 100 cm.<sup>2</sup> or even less. The cross sectional area of the ethane molecule computed from X-ray data of solid ethane is equal to  $20.5 \times 10^{-16}$  cm.<sup>2</sup>. This value is in satisfactory accord with the area computed from adsorption of the gas on fused quartz beads,<sup>1</sup> or on glass beads, as shown by the present data, assuming that quartz or glass are supercooled liquids having absolute surface areas identical with apparent areas. Research grade ethane obtained from the Phillips Petroleum Company was fractionated, the middle portion was dried with P<sub>2</sub>O<sub>5</sub> and then stored in a five-liter glass flask. Tank helium was purified by passing it through a glass bead-packed liquid N<sub>2</sub> trap at  $-196^\circ$  and through activated charcoal also at liquid N<sub>2</sub> temperature, and was then stored in a glass flask.

The procedure was to seal the metal specimen in a glass adsorption cell (dead space = 16 cc.), evacuate and surround the cell with liquid oxygen. Helium, at a few millimeters of pressure, was introduced into the cell to accelerate cooling of the metal specimen to liquid O<sub>2</sub> temperature. Helium was then pumped out and ethane adsorbed at successively higher pressures, values for which were measured using a McLeod gage. Helium, which does not adsorb at liquid oxygen temperature, was employed in the usual manner to calibrate the volume of the system. A glass U bend cold trap surrounded by solid CO<sub>2</sub>-acetone mixture prevented condensation of mercury into the cell at  $-183^\circ$ . Separate measurements showed that ethane was not adsorbed in this trap.

The maximum pressures of ethane employed were sufficiently low (max. =  $8 \times 10^{-3}$  mm.) to make deviations from the perfect gas law negligible. However, all pressure measurements involving a temperature gradient were corrected

(1) C. Brown and H. H. Uhlig, *J. Am. Chem. Soc.*, **69**, 462 (1947).  
 (2) S. Brunauer, P. Emmett and E. Teller, *ibid.*, **60**, 309 (1938).  
 (3) L. Wooten and C. Brown, *ibid.*, **65**, 113 (1943).

for thermal diffusion using the empirical equations outlined by Liang.<sup>4</sup> In accord with his method, the ratio of true to observed pressure  $R$  is given by

$$\frac{\alpha \left(\frac{x}{f_1}\right)^2 + \beta \left(\frac{x}{f_1}\right) + R_m}{\alpha \left(\frac{x}{f_1}\right)^2 + \beta \left(\frac{x}{f_1}\right) + 1}$$

where  $\alpha$  and  $\beta$  are temperature dependent constants equal to 27.6 and 11.0, respectively, at  $-183^\circ$ ;  $x$  is the product of observed pressure (in mm.) and of tube diameter in mm. (in the present instance 4 mm.);  $R_m = \sqrt{T_1/T_2}$  where  $T_1$  equals absolute temperature of gas in the adsorption cell and  $T_2$  is room temperature, hence,  $R_m = \sqrt{90/298} = 0.55$ ; and  $f_1$  is a function of the collision diameters for ethane (5.30 Å.) and nitrogen (3.75 Å.) equal to 0.382. Values of  $R$  so calculated are plotted as a function of observed pressure in Fig. 1. For example, the vapor pressure of ethane ( $p_0$ ) at  $-183^\circ$  as measured by the McLeod gage was 9.0  $\mu$ , but taking into account thermal diffusion ( $R = 0.80$ ), the corrected vapor pressure became 7.2  $\mu$ . In general, the thermal diffusion corrections increase the BET area by about 10% over that calculated without applying the correction. This correction is less than the apparent variation of area as determined through the use of various gases as adsorbates.<sup>6</sup>

**Area of Iron and Stainless Steel Specimens.**—Areas were determined for rolled Armco iron sheets 0.003-inch thick, measuring 200 cm.<sup>2</sup> geometric area and formed into spirals. Some of these were treated in a stream of purified dry hydrogen for 1/2 hour at  $1000^\circ$  and cooled in hydrogen. They were then sealed individually in the adsorption cell which was cooled during glass-blowing operations so as to avoid surface oxidation. The specimens within the cell were finally reduced in hydrogen at  $400^\circ$  for 1/2 hour, followed by a two-hour baking *in vacuo* at  $400^\circ$ .

Stainless steel sheet specimens (18-8 Type 304) were abraded, finished with 2/0 emery paper and coiled into spirals. They were degreased with benzene, pickled, washed and then immersed successively into acetone and distilled benzene. Either of two pickles was employed, resulting in different surface areas. The first consisted of 25 vol. % concentrated HCl, 25 vol. % concentrated H<sub>2</sub>SO<sub>4</sub> at  $35^\circ$  for 10 minutes (producing the larger surface), and the second consisted of 15 vol. % concentrated HNO<sub>3</sub>, 10 vol. % concentrated HF at  $90^\circ$  for 10 minutes.

One stainless steel and one Armco iron specimen, both abraded, were also measured. They were degreased in benzene before sealing within the adsorption cell.

Electropolished stainless steel specimens were prepared from rolled sheet using the glycerol-phosphoric acid electrolyte as described by Uhlig.<sup>7</sup> Electropolishing was carried out at about  $100^\circ$  at a current density of 0.3 amp./cm.<sup>2</sup> for 60 minutes. The specimens were then washed, and immersed successively into acetone and benzene.

Areas determined from the amount of adsorbed ethane are listed in Table I. Order of reproducibility of the area determination itself can be estimated from single specimens whose areas were determined twice in succession. Maximum deviation is  $\pm 1.5\%$  of the determined area. Various specimens of pickled 18-8 steel show this same order of reproducibility, indicating that surface area preparation by pickling can be repeated within close limits. Three hydrogen-reduced specimens show a maximum deviation of 4% from the average area.

Glass beads were also run in order to check the cross-sectional area of the ethane molecule used for calculation of absolute area. The beads were new, not having been used for any purpose previously, and were cleaned with a synthetic detergent, washed in water and dried. After sealing into the adsorption cell, they were baked out at  $400^\circ$  for several hours. Their average diameter, as determined with a micrometer, was 0.407 cm. and their absolute area was within 4% of the apparent area.

(4) S. Chu Liang, *J. Applied Phys.*, **22**, 148 (1951); *THIS JOURNAL*, **56**, 660 (1952).

(5) S. Chu Liang, private communication.

(6) R. Davis, T. DeWitt and P. Emmett, *THIS JOURNAL*, **51**, 1232 (1947).

(7) H. H. Uhlig, *Trans. Electrochem. Soc.*, **78**, 265 (1940).

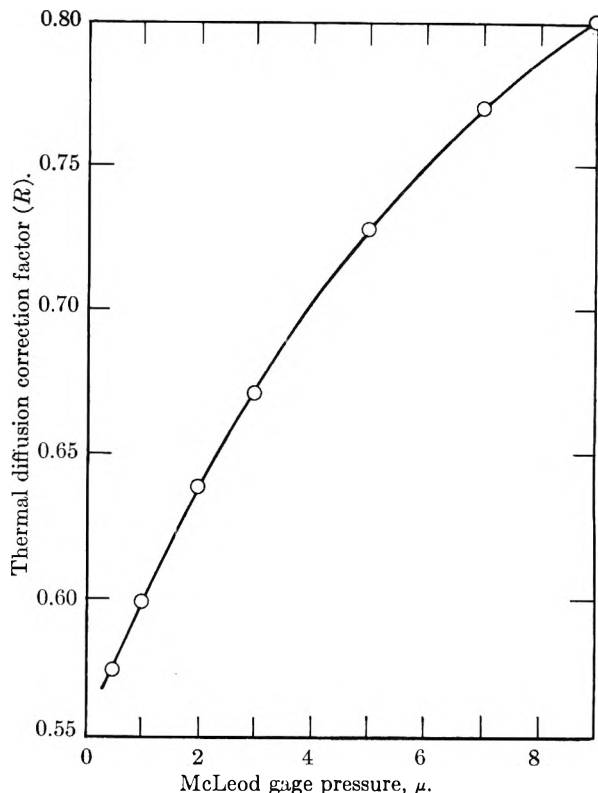


Fig. 1.—Thermal diffusion correction factor for ethane.

**Area of Evaporated Iron Films.**—Iron was evaporated *in vacuo* (less than  $10^{-6}$  mm.) onto glass tubes measuring approximately 3.5 cm. long by 0.4 cm. in diameter. The source of iron was either electrically heated "Puron" wire 0.04-inch diameter, or high purity Bureau of Standards wire 0.010-inch diameter wrapped around electrically heated tungsten wires of 0.025 inch diameter located at the center of an evacuated glass bulb. The procedure of evaporation has been described previously by Gatos and Uhlig<sup>8</sup> who used similar iron films in their studies of passivity. Eight glass tubes, each of which contained an iron wire sealed inside, were confined to a rotary track *in vacuo* by eight magnets moving slowly on a circular platform outside a 500-ml. glass bulb. The glass tubes in this way acquired a uniform layer of iron from the evaporation source over a period of several minutes to one hour. The iron-coated tubes were then transferred through a larger size evacuated glass tube connecting to the gas adsorption cell. Accordingly the surface areas could be measured uncontaminated by previous contact with air and without correction for the metal filaments used as source of evaporated iron. The two sources of iron vapor differed in that the iron wires were electrically heated to only  $1000$ – $1100^\circ$  as determined by an optical pyrometer, whereas iron-wrapped tungsten wires were heated to about  $1300^\circ$ . This difference produced a marked change in surface area as described later. The iron wires in both cases were previously cleaned by pickling in HCl, and were then reduced in purified dry H<sub>2</sub> at  $1000^\circ$  for 1/2 hour. Thickness of the evaporated films was estimated by their dissolution in HCl and determination of total iron colorimetrically by the *o*-phenanthroline method. In the calculation of thickness, the density of iron was assumed equal to that of bulk iron, namely, 7.86. Absolute areas are listed in Table II.

### Discussion of Results

Evaporation of iron from electrically heated wires at  $1000$ – $1100^\circ$  produces films having 3 to 6 times the area of films formed by evaporating iron on tungsten at  $1300^\circ$ . This difference is thought to result primarily from differences in temperature of the condensed film during evaporation, the lower

(8) H. Gatos and H. H. Uhlig, *J. Electrochem. Soc.*, **99**, 250 (1952).

TABLE I  
ABSOLUTE AREAS OF IRON AND STAINLESS STEEL SURFACES

Spec.	Specimen	Surface prep.	Area (cm. <sup>2</sup> )		Roughness factor
			Geometric	Absolute	
1a	Armco Iron Sheet	H <sub>2</sub> -reduced 1000°	200	244	1.22
b	Armco Iron Sheet (check on same spec.)		200	244	1.22
2	Armco Iron Steel	H <sub>2</sub> -reduced 1000°	200	257	1.29
3a	18-8 Stainless Steel	Pickled 25 vol. % HCl-25 vol. % H <sub>2</sub> SO <sub>4</sub> , 35°, 10 min.	40.5	164	4.05
b	18-8 Stainless Steel (check on same spec.)	Pickled 25 vol. % HCl-25 vol. % H <sub>2</sub> SO <sub>4</sub> , 35°, 10 min.	40.5	169	4.17
c	18-8 Stainless Steel	Pickled 25 vol. % HCl-25 vol. % H <sub>2</sub> SO <sub>4</sub> , 35°, 20 min.	40.5	165	4.1
d	(check on same spec.)	Pickled 25 vol. % HCl-25 vol. % H <sub>2</sub> SO <sub>4</sub> , 35°, 50 min.	40.5	149	3.7
4	18-8 Stainless Steel	Pickled 25 vol. % HCl-25 vol. % H <sub>2</sub> SO <sub>4</sub> , 35°, 10 min.	40.5	166	4.10
5	18-8 Stainless Steel	Pickled 25 vol. % HCl-25 vol. % H <sub>2</sub> SO <sub>4</sub> , 35°, 10 min.	69.6	292	4.20
6	18-8 Stainless Steel	Pickled 25 vol. % HCl-25 vol. % H <sub>2</sub> SO <sub>4</sub> , 35°, 10 min.	64.0	260	4.06
7	18-8 Stainless Steel	Pickled 15 vol. % HNO <sub>3</sub> , 10 vol. % HF 90°, 10 min.	40.5	55	1.36
8	18-8 Stainless Steel	Abraded 2/0 emery, degreased in benzene	40.5	124	3.06
9	Armco Iron Sheet	Abraded 2/0 emery, degreased in benzene	41.1	138	3.4
10	18-8 Stainless Steel	Electropolished	115	129	1.12
11	Glass beads	Washed, baked 400°	137	142	1.04

TABLE II  
ABSOLUTE AREAS OF EVAPORATED IRON FILMS

Spec.	Evap. temp., °C.	Source of evaporated iron	Thickness of film, Å.	Area (cm. <sup>2</sup> )		Roughness factor
				Geometric	Absolute	
1	1000-1100	Westinghouse "Puron" <sup>a</sup> Wire	840	34.0	167	4.9
2	1000-1100	Westinghouse "Puron" Wire	1720	29.6	312	10.5
3	1000-1100	Westinghouse "Puron" Wire	1860	34.0	317	9.3
4	1000-1100	Westinghouse "Puron" Wire	2000	17.3	186	10.7
5	1000-1100	Westinghouse "Puron" Wire	3250	17.2	164	9.5
6	1000-1100	Westinghouse "Puron" Wire	4150	16.5	144	8.7
7	1300	Bureau Std. Wire <sup>b</sup> (wrapped on tungsten wire)	1500	17.7	31.6	1.79
8	1300	Bureau Std. Wire (wrapped on tungsten wire)	1730	16.8	29.7	1.77
9	1300	Westinghouse "Puron" (wrapped on tungsten wire)	1660	34.0	59.0	1.74

<sup>a</sup> 0.005% C, 0.003% S, < 0.001% P, < 0.001% Si, 0.001% Cu (proximate analysis by supplier). <sup>b</sup> 0.001% C, 0.001% S, 0.0005% P, 0.001% Si, 0.002% Cu (analysis supplied through courtesy of H. E. Cleaves, National Bureau of Standards).

evaporation temperatures favoring growth of a porous film made up perhaps of individual crystals, whereas at higher evaporation temperatures the condensed film is heated sufficiently by radiation to sinter it to a pore-free layer.<sup>9</sup> The effect presumably depends on the metal as well as temperature because Beeck, *et al.*,<sup>10</sup> reported that evaporated copper films characteristically sinter rapidly to a film having no measurable internal surface in contrast to nickel films which in their experiments were found to be porous. Trapnell's<sup>11</sup> results on evaporated Ni, Fe, Rh, Mo, Ta and W films showed greater adsorption on films deposited on glass at -183° in contrast to films on glass maintained at 0° during evaporation. This corresponds, as in our case, to greater surface area the lower the temperature of the film during condensation. Porter and Tompkins<sup>12</sup> also report that available area for adsorption of H<sub>2</sub> on evaporated iron films decreases with increasing temperature used to presinter the film *in vacuo*.

When the films are porous, but probably not otherwise, the observed roughness factor depends on film

(9) Thermocouples cemented to the outside glass surface gave readings of about 60 and 80° for the two conditions of evaporation. The actual condensation temperatures are not known.

(10) O. Beeck, A. Smith and A. Wheeler, *Proc. Roy. Soc. (London)*, **A177**, 62 (1940).

(11) B. Trapnell, *Trans. Faraday Soc.*, **51**, 368 (1955).

(12) A. Porter and F. Tompkins, *Proc. Roy. Soc. (London)*, **A217**, 529 (1953).

thickness, increasing from 4.9 for a film 840 Å. thick to about 10 for films 1800 Å. or more thick. Beeck, *et al.*, also found that the available surface of nickel films increased with thickness, as did Rideal and Trapnell<sup>13</sup> for evaporated tungsten films, and Porter and Tompkins<sup>14</sup> for iron films.

Roughness factors for abraded stainless steel and for iron equal to 3.1 and 3.4, respectively, agree reasonably well with the value 3.8 for abraded Armco iron reported by Powers and Hackerman<sup>15</sup> using the BET method with krypton for adsorbate. Burstein, Shumilova and Golbert<sup>16</sup> report a value of 2 for rolled iron using a method based on chemisorption of oxygen. Erbacher<sup>17</sup> determined surface areas of metals by adsorption of radioactive monolayers of bismuth containing Th-C indicator, or of polonium, from their aqueous salt solutions. He and his co-workers also employed Pb(NO<sub>3</sub>)<sub>2</sub> containing Th-B in methanol or pyridine.<sup>18</sup> Roughness factors were reported of 1.7 for polished surfaces of Ni, and 2.5 for abraded surfaces of Ni, Au and Ag

(13) E. Rideal and B. Trapnell, *ibid.*, **A205**, 409 (1951).

(14) A. Porter and F. Tompkins, *ibid.*, **A217**, 544 (1953).

(15) R. Powers and N. Hackerman, *J. Electrochem. Soc.*, **100**, 314 (1953).

(16) R. Burstein, N. Shumilova and K. Golbert, *Acta Physicochim.*, **21**, 785 (1946).

(17) O. Erbacher, *Z. physik. Chem.*, **163**, 215 (1933); *Chem. Z.*, **62**, 601 (1938).

(18) O. Erbacher, G. Jensen-Hellmann and A. Mellin, *Z. Metallkunde*, **40**, 249 (1949).

using either fine or coarse emery paper. Erbacher's value of 2.5 for abraded metals is in reasonable agreement with the values listed in Table I. Davis, Dewitt and Emmett<sup>6</sup> using krypton, butane and "Freon" for adsorbates reported roughness factors of 1.10 to 1.37 for silver foil and 1.07 to 1.64 for Monel foil depending on the gas used. No direct comparison can be made with values listed in Table I because the authors did not state surface preparation, but it would appear reasonable that the surfaces were probably those resulting from rolling and would therefore be essentially smooth.

Electropolished stainless steel is relatively smooth, having a roughness factor of only 1.12. In comparison, Rhodin<sup>19</sup> reported that abraded and electropolished copper had a roughness factor of about unity.

Polarization capacity measurements have been used for surface area measurements,<sup>20,21</sup> but the results appear to be much higher than those reported above. Hackerman and Powers,<sup>15</sup> using this method, report a roughness factor of 20 for

(19) T. N. Rhodin, *J. Am. Chem. Soc.*, **72**, 4343 (1950).

(20) F. Bowden and E. Rideal, *Proc. Roy. Soc. (London)*, **120A**, 59 (1928).

(21) F. Bowden and E. O'Connor *ibid.*, **128A**, 317 (1930).

abraded iron. Impurities have been indicated as one source of error, causing as much as a threefold change in measured surface capacitance.<sup>22</sup> Other possible sources of error are discussed by Wiebe and Winkler.<sup>23</sup> Surface area measurements in this Laboratory using the current-time integral for a given change of potential, with the aid of a ballistic galvanometer, confirm that this method, without further refinements, does not lead to reproducible results, and that the values obtained of absolute areas are not in accord with values derived from gas adsorption. The fair correspondence of metal areas reported by several investigators, values of which were obtained by gas adsorption using more than one gas, and with radioactive ion deposition measurements by Erbacher, *et al.*, suggests that the presently reported roughness factors are reliable and are of the correct order of magnitude.

**Acknowledgment.**—This research was supported by the Office of Naval Research on Contract No. N5-ori-78 NR 036-007 T.O. 15 to whom the authors express their appreciation.

(22) F. Bowden and K. Grew, *Disc. Faraday Soc.*, No. 1, 91 (1947).

(23) A. Wiebe and C. Winkler, *Canadian J. Chem.*, **31**, 306, 665, 1118 (1953).

## A STUDY OF THE SURFACE ACIDITY OF CRACKING CATALYST

By RYDEN L. RICHARDSON<sup>1</sup> AND SIDNEY W. BENSON

*Chemistry Department, University of Southern California, Los Angeles 7, California*

*Received August 10, 1956*

The surface acidities of several fresh synthetic silica-alumina cracking catalysts were estimated from the quantities of "permanently" bound basic gas adsorbed at temperatures ranging between 20–300°. Both pyridine and trimethylamine were used as adsorbates and kinetic measurements were made with a high temperature adsorption balance containing a quartz helix. It was found that the adsorbed gas consists of two fractions: the first fraction desorbs rapidly and the second desorbs very much more slowly. This second fraction, which may be designated as "permanently" or firmly bound, is considered a measure of the surface acidity. First-order plots permit extrapolations to zero time, *i.e.*, start of desorption. The acidity measurements also were affected by (1) particle size, (2) trace water in catalyst and (3) slightly by temperature. Desorption appeared to be effusion-controlled after the initial stages. Other kinetic aspects, calorimetric measurements and trend of Cat A conversion with acidity are reported.

### Introduction

Catalytic cracking plays an important role in petroleum technology. A detailed account appearing early in the literature cites the increased yields of high octane gasoline obtained by the large scale application of cracking catalysts.<sup>2</sup> Cumulative research on cracking catalysts reveals that these highly porous solids possess acidic surfaces, stable at high temperatures and capable of cracking hydrocarbons by an ionic mechanism rather than the free radical mechanism characteristic of thermal cracking. The catalytic process can be initiated at temperatures considerably lower than that required by non-catalytic or thermal cracking. For example, Frost<sup>3</sup> has found that thermal cracking at 450° leads to only 2% yield of decomposition products but this yield may be increased to 36% by introduction of catalyst. With increasing tem-

perature, the rates of the two processes approach each other, due to the higher activation energy of the non-catalytic process. More precisely, Sachanen<sup>4</sup> reports activation energies of 20 kcal. for catalytic cracking, 58 kcal. for non-catalytic cracking.

Greensfelder<sup>5</sup> has made careful studies of the cracking of pure hydrocarbons over silica-zirconia-alumina catalyst and found that product distribution is in harmony with the carbonium ion mechanism. Rearrangement of carbonium ions to the more stable tertiary form leads to relatively high yields of C<sub>4</sub>'s and extensive isomerization.

Early work on catalyst acidity by Thomas<sup>6a</sup> and Grenall<sup>6b</sup> involved back titration of powdered catalysts at room temperature, using 0.1 *N* aqueous solutions of potassium hydroxide and hydrochloric

(4) A. N. Sachanen, "Conversion of Petroleum," Second Ed., Reinhold Publ. Corp., New York, N. Y., 1948, p. 324.

(5) B. S. Greensfelder, H. H. Voge and G. M. Wood, *Ind. Eng. Chem.*, **41**, 2573 (1949).

(6) (a) C. L. Thomas, *ibid.*, **41**, 2564 (1949); (b) A. Grenall, *ibid.*, **41**, 1485 (1949).

(1) Union Oil Company of California, Brea Research Center, Brea, California.

(2) E. Houdry, W. F. Burt, A. E. Pew and W. A. Peters, *Refiner Natural Gasoline Mfr.*, **17**, 574 (1938).

(3) A. V. Frost, *J. Phys. Chem. (Russ.)*, **14**, 1313 (1940).

acid. Their data established a definite trend of increasing catalytic activity with increasing acidity.

Turning to the question of acid strength, Walling<sup>7</sup> conducted experiments on powdered catalyst dispersed in isoöctane. The presence of carbonium ion in catalytic cracking necessitates a catalyst of considerable acid strength, able to force a proton onto olefin or abstract hydride ion from a hydrocarbon. Many acidic sites measured by a strong base like OH<sup>-</sup> may be far too weak for the production of carbonium ions. Also, an attempt to distinguish differences in acid strengths of the various sites would be limited in aqueous systems because water would level the stronger species to the strength of H<sub>3</sub>O<sup>+</sup>. Hence, Walling's technique involved an assortment of organic indicators of *pK* values between 0.4 and 3.3, dissolved in isoöctane. After shaking a small amount of powdered catalyst in a given indicator solution, the color of the catalyst surface was observed. The acid strength of a surface was considered in terms of "the ability of the surface to convert an adsorbed neutral base to its conjugate acid." In comparison with other solid substances examined by this technique, it is stated that the silica-alumina surfaces of cracking catalysts are "apparently strong surface acids." Recent work by Mapes and Eischens<sup>8</sup> probes more carefully the question whether acidic sites fall under the Brönsted or Lewis definition of an acid. Upon studying the infrared spectra of ammonia chemisorbed on cracking catalysts, they find characteristic absorption bands for both NH<sub>3</sub> and NH<sub>4</sub><sup>+</sup>. Trambouze and co-workers<sup>9</sup> report that at normal cracking temperatures most of the acid sites of SiO<sub>2</sub>-Al<sub>2</sub>O<sub>3</sub> gels are of the Lewis type.

Returning to quantitative determinations of acidity, Tamele<sup>10</sup> made careful titrations in a non-aqueous system, titrating the surface of the catalyst (suspended in benzene as a fine powder) with *n*-butylamine. The indicator was *p*-dimethylaminoazobenzene. This method also was recently employed in a study<sup>11</sup> showing the rate dependence of propylene polymerization on the acidity of alumina-silica catalysts. Another quantitative approach, the high temperature adsorption of a basic gas, was applied by Mills, Oblad and Boedeker.<sup>12</sup> Nitrogen was employed as a sweep gas or carrier for relatively non-volatile substances, such as quinoline. Surface acidity was measured by the millimoles of a basic gas chemisorbed per gram of catalyst at elevated temperatures. Such a technique permits exploration of the temperature effect, variation in base strength of the adsorbate, and eliminates liquid solvent interferences. But such a method requires an accurate distinction between physical adsorption and chemisorption.

The present research has focused attention on this problem, *i.e.*, the experimental distinction between loosely and firmly held adsorbates. Rate data for

the desorption process have been obtained with a modified adsorption balance and a sweep gas, such as nitrogen, has been eliminated. Other aspects of the general problem such as (1) temperature effect, (2) base strength of adsorbate, (3) trace water in catalyst, and (4) particle size of the catalyst have been briefly considered.

## II. Experimental

A. Reagents were purified carefully with the aid of a high vacuum line. Pyridine was dried with barium oxide, triple distilled and pumped several times after freezing. The trimethylamine was a heart-cut obtained from batch-wise distillations, followed by thorough degassing.

B. Weighing tube experiments represented preliminary work on the effect of temperature and trace water on catalyst acidity. The Pyrex weighing tube and the simple heating block assembly are shown in insert of Fig. 1. The weighing tube was charged with 2-3 g. of Davison DA-1 fluid cracking catalyst, immobilized with a small plug of Pyrex wool. Then the sample was degassed at 300°. During final stages of degassing, pressures as low as 10<sup>-4</sup>-10<sup>-5</sup> mm. were obtained with the heating block in place. Then the tube was removed, allowed to cool and reweighed to the nearest milligram. This pumping-weighing cycle was repeated until constant weight was attained. A loss in weight always occurred during this process, mainly due to the desorption of water. The reported values for the per cent. volatile matter lost upon calcination at 1700°F. (hereafter abbreviated as V.M.) apply to the catalyst sample after this degassing step.

Then the tube was again attached to the high vacuum line, exposed to pyridine vapor and pumped down to 10<sup>-4</sup>-10<sup>-5</sup> mm. The sample temperature varied within ±5° during these operations. Finally the weighing tube was allowed to cool, detached from the line and weighed. As in the case of degassing, the pumping-weighing cycle was repeated to the point of constant weight. Increase in weight was attributed to chemisorbed pyridine on the acidic sites of the catalyst. This weight of pyridine, expressed in millimoles per gram of degassed sample, was identified as the acidity of the catalyst surface.

C. The high temperature adsorption balance used in rate and acidity measurements is schematically presented in Fig. 1. Useful references on this type of instrument appear elsewhere.<sup>13</sup> A sensitive quartz helix, Q, supported an aluminum foil sample bucket at end of a Pyrex thread. The all-Pyrex casing had a  $\mathbb{F}$  joint at J to facilitate loading and a  $\mathbb{J}$  joint at J' for lateral adjustment of the helix and sample. Seals were made with Shawinigan resin. Catalyst sample S was held within ±0.5° by brass pipe U, heated by a trimming circuit controlled by mercury regulator R. Insulation was furnished by blanket M of powdered magnesia and layer W of Pyrex wool. Temperatures were checked by thermocouple T.

Helix elongations E were measured by a Gaertner Cathetometer having a 67 cm. scale, giving measurements within 0.005 cm. The catalyst samples ranged between 300-500 mg. and could be weighed to ±0.2 mg. (helix sensitivity = 22.6 mg. per cm.). Both trimethylamine and pyridine were used at temperatures between 20-300° to measure the acidity of fresh Davison DA-1 fluid cracking catalyst having a Cat-A activity<sup>14</sup> of 44. This powdered synthetic catalyst was pressed into 3/16" pills to prevent sample loss upon degassing. Usually the sample charge amounted to 3 or 4 pills plus 1/2-1/4 pill fragment to adjust sample weight within desired limits.

Catalyst samples were uniformly degassed at 300° for approximately 20 hours to a final pressure of 10<sup>-5</sup> mm. This permitted the attainment of constant weight. Then the sample was exposed to one of the basic gases, either Me<sub>3</sub>N at 100-200 mm. for ~20 minutes, or pyridine at 10 mm. for ~60 minutes. Finally, the desorption process was begun by shutting off the adsorbate supply and quickly opening system to the pumps. Helix elongation was measured at various times after start of the desorption process and the net elongation gave a proportional measure of the apparent surface acidity.

(7) C. Walling, *J. Am. Chem. Soc.*, **72**, 1164 (1950).

(8) J. E. Mapes and R. P. Eischens, *THIS JOURNAL*, **58**, 1059 (1954).

(9) Y. Trambouze, L. de Mourgues and M. Perrin, *J. chim. phys.*, **51**, 723 (1954).

(10) M. W. Tamele, *Disc. Faraday Soc.*, **8**, 270 (1950).

(11) O. Johnson, *THIS JOURNAL*, **59**, 827 (1955).

(12) G. A. Mills, E. R. Boedeker and A. G. Oblad, *J. Am. Chem. Soc.*, **72**, 1559 (1950).

(13) (a) J. W. McBain and A. M. Bakr, *ibid.*, **48**, 690 (1926);

(b) S. L. Madorsky, *Rev. Sci. Inst.*, **21**, 393 (1950).

(14) J. Alexander, *Proc. Am. Petr. Inst.*, **27**, (3) 51 (1947).

D. The adiabatic calorimeter consisted of a very thin-walled small test tube made from drawn Pyrex tubing. The test-tube was carefully wrapped with Pyrex wool and placed in a casing similar to that used in the high temperature balance, permitting effective thermostating. The fluid catalyst samples were thoroughly degassed at 300° before making the calorimetric measurements. A small thermocouple bead of iron and Constantan wires (30 and 50 B & S gage, respectively) was buried half way into the bed of fluid catalyst. The sample size normally amounted to 1-2 g. Since the thermocouple bead was exposed, a blank run was made at 300° to be sure that no heat effects were caused by a reaction of the bead with  $\text{Me}_3\text{N}$ .

### III. Data and Discussion

A. Weighing Tube Experiments.—These measurements were of a preliminary nature and concerned the effect of temperature and trace water on catalyst activity. Table I presents some data for pyridine on fresh Davison fluid cracking catalyst which was degassed for 17 hours at 300°. Note that the acidity is but slightly temperature-dependent, decreasing from 0.18 mmole per g. at 24° to 0.14 mmole per g. at 300°. This small effect occurs mainly in the range between 24 and 100°.

TABLE I

## WEIGHING TUBE EXPERIMENTS

Adsorbent = Davison DA-1, fluid, Calc. at 850°F., Cat A = 44, adsorbate = pyridine.

Contact no.	Temp. (°C.)	Pyridine pressure (mm.)	Contact period (hr.)	Pumping period (hr.)	Final pressure (mm.)	Amount chemisorbed (mmole/g.)
Run I: degassed 17 hr., 300°, final press. = $10^{-6}$ mm., V.M. = 0.3 wt. %						
1	300	10	1.5	25	$10^{-3}$	0.14
2	200	10	0.8	1.4	$10^{-5}$	.14
3	100	10	0.6	1.5	$10^{-4}$	.15
4	24	10	17	25	$10^{-6}$	.18
Run II: degassed 24 hr., 20°, final press. = $10^{-5}$ mm., V.M. = 2.6 wt. %						
1	20	10	20	46	$10^{-4}$	0.89

As to imposed variations in the pyridine contact period or desorption period, the measured acidity does not appear to be noticeably responsive. Hence, it is believed that the sample becomes saturated within a contact period of one hour and can be desorbed of all but the chemisorbed material in  $\leq 24$  hours.

Another portion of the same fresh catalyst was charged and degassed for 24 hours at room temperature instead of 300°. The milder degassing produced a sample of higher V.M. (2.6 versus 0.3 weight per cent.), which presumably contained a larger proportion of residual water. This catalyst was subsequently exposed to pyridine at room temperature and pumped for a period of 46 hours, leading to a final pressure of  $10^{-4}$  mm. The resulting acidity was higher, amounting to 0.89 mmole per g. as compared to the 0.18 mmole per g. of the sample degassed under more severe conditions.

These fragmentary data strongly suggest a definite relation between catalyst acidity and trace water content, assuming the volatile matter to be water. Hansford's study<sup>15</sup> of the cracking of normal butane by silica-alumina catalyst disclosed that dehydration decreases catalyst activity. Hans-

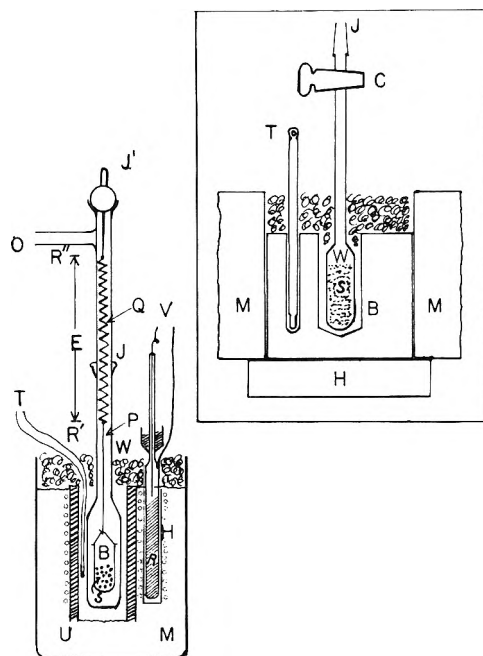


Fig. 1.—Insert schematically presents weighing tube apparatus with the following parts: § joint J, stopcock C, weighing tube W, powder sample S, heating block B, mercury thermometer T, magnesia lagging M and heater H. Main figure shows high temperature adsorption balance involving following parts: ball joint J', outlet O, quartz helix Q, § joint J, Pyrex suspension thread P, aluminum foil sample bucket B, pelleted sample S, mercury regulator R, relay lead V, trimming heater H, brass pipe U, magnesia-insulation M, thermocouple T, Pyrex wool layer W. The upper cathetometer reading, lower cathetometer reading and helix elongation are represented by  $R'$ ,  $R''$  and E, respectively.

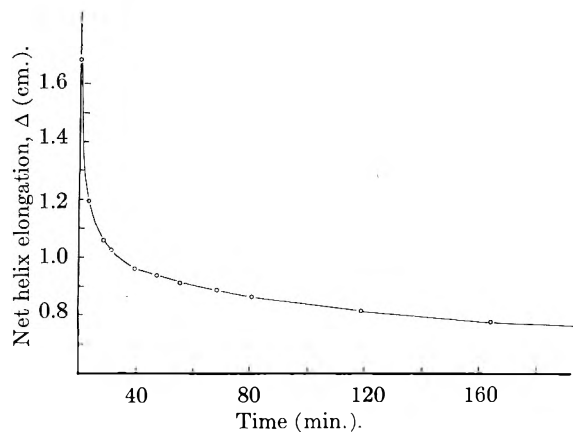


Fig. 2.—Desorption rate curve for trimethylamine at 20°. Plot of net helix elongation ( $\Delta$ ) vs. time. (The surface acidity in mmole/g. =  $1.099 \Delta = 1.099 (E - E_0)$ . See Fig. 1 for definition of E). Adsorbent = Davison DA-1 cracking catalyst, Cat A = 44, calcined at 850°F., degassed at 300°.

ford and co-workers<sup>16</sup> as well as Hindin, Mills and Oblad<sup>17</sup> observed a similar effect in the deuterium exchange between catalyst and hydrocarbon. The latter reported an optimum value of approximately 0.8 weight %  $\text{D}_2\text{O}$ .

(16) R. C. Hansford, P. G. Waldo, L. C. Drake and R. E. Honig, *ibid.*, **44**, 1108 (1952).

(17) S. G. Hindin, G. A. Mills and A. G. Oblad, *J. Am. Chem. Soc.*, **73**, 280 (1951).

(15) R. C. Hansford, *Ind. Eng. Chem.*, **39**, 849 (1947).

As a whole, these observations suggest that a cracking catalyst has Lewis acid sites on its surface which, upon addition of small amounts of water, are at least partially converted to Brönsted type acids—these being able to donate protons and thereby give rise to carbonium ions. If too much water is added, the excess water can act as a base, in competition with unsaturated hydrocarbons, and thereby reduce catalyst activity.

**B. Rate Measurements with Adsorption Balance.**—Experiments with the high temperature adsorption balance gave both the rate and related acidity measurements of this research. As earlier mentioned, one of the main goals of this study was to distinguish between loosely and firmly bound adsorbate on an empirical basis.

Consider the desorption rate curve for trimethylamine on Davison DA-1 at 20° shown in Fig. 2. The initial pumping proceeds at a very fast rate of desorption which drops off appreciably in 10–20 minutes and after half an hour approaches—but does not reach—a constant rate of desorption. The sample does not reach constant weight even after two hours of pumping. Approximately half of the initially adsorbed trimethylamine is removed during this period. It will become evident that an acidity measurement on the basis of the raw data shown in Fig. 2 has its complications.

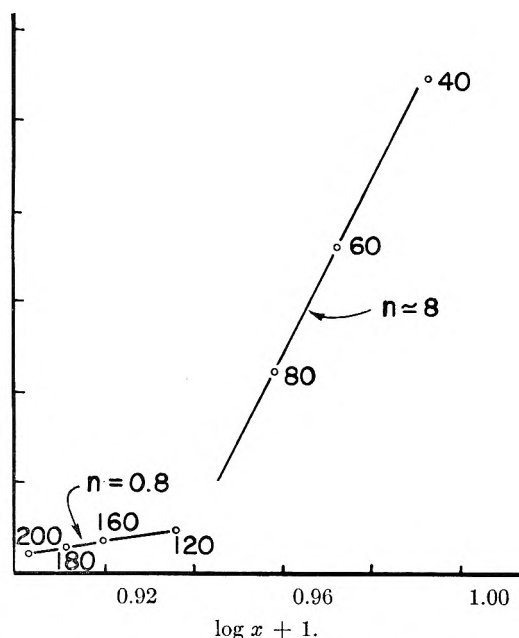


Fig. 3.—Test for order of rate data: desorption of trimethylamine from Davison DA-1 catalyst at 20°. (Raw data in Fig. 2).

A conventional test for order, involving the logarithmic form of the general rate equation

$$\log \left( \frac{dx}{dt} \right) = \log k + n \log x$$

was subsequently applied to the data. Using  $x$  = mmole of adsorbate/g., the results of this test appear in Fig. 3. The instantaneous rates,  $dx/dt$ , were measured from a large scale plot of acidity versus time using a Brown and Sharpe tangent meter. Numbers adjacent to each point in Fig. 3

represent the time in minutes after start of desorption.

A steep slope corresponding to  $n \sim 8$  apparently applies to those points taken during the early phase of desorption. After pumping approximately two hours,  $n$  approaches a value close to unity. This pointed to the possible utility of first-order plots.

First-order plots for trimethylamine at 20°, as well as pyridine at 25 and 200°, are shown in sections of Fig. 4. The same catalyst (fresh Davison type DA-1, cat A = 44) and degassing procedure apply to all of the data. All plots show a fair adherence to linearity after initial desorption. This adherence appears earlier at the higher temperatures. Note that the higher temperature also gives a smaller intercept (lower acidity at zero time).

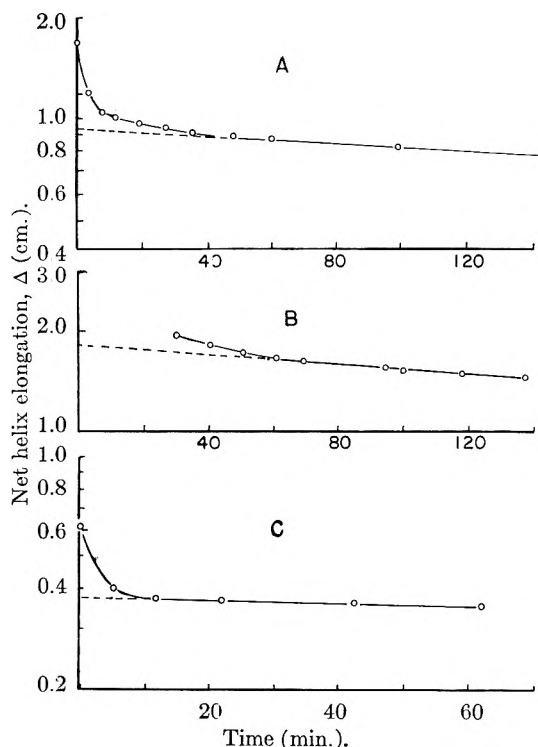


Fig. 4.—Semi-logarithmic plots of net helix elongation,  $\Delta$  vs. time. Adsorbent = Davison DA-1 cracking catalyst, Cat A = 44, calcined at 850°F., degassed at 300°. Curve A, trimethylamine at 20°; curve B, pyridine at 25°; curve C, pyridine at 200°.

The possibility of pyridine decomposing or polymerizing while being adsorbed to constant weight was examined at 300°. First the pyridine was allowed to contact the catalyst sample at the usual pressure for 55 minutes and then desorbed. After about 70 minutes the desorption was stopped. Again the pyridine was allowed to contact the catalyst as before, but this time for a prolonged period of 136 minutes. Upon subsequent desorption, there resulted a definite displacement in the plot of acidity versus time. This displacement amounted to 0.08 mmole per gram. For this reason, subsequent runs with pyridine at 300° were made with a contact time of only ten minutes.

First-order plots for trimethylamine at 20, 200 and 300° appear in Fig. 5 and features typical of the pyridine runs are noted.

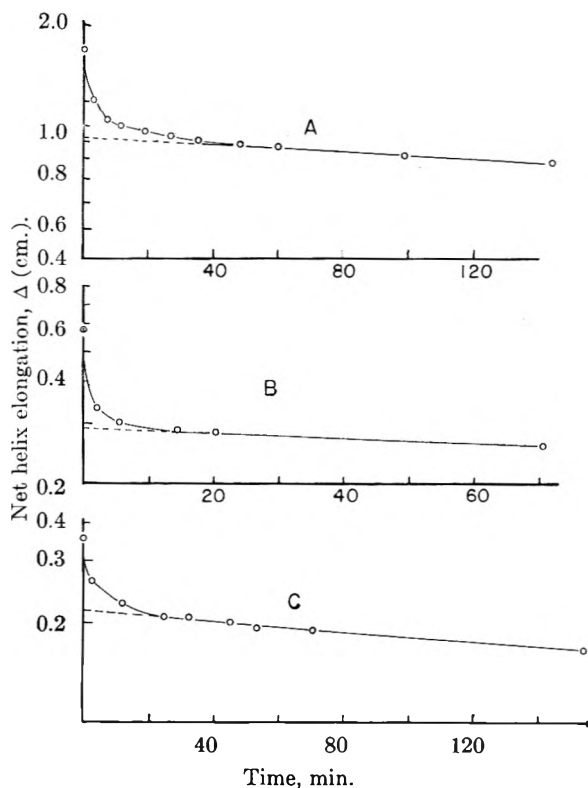


Fig. 5.—Semi-logarithmic plots of net helix elongation,  $\Delta$  vs. time. Adsorbent = Davison DA-1 cracking catalyst, Cat A = 44, calcined at 850°F., degassed at 300°. Curve A, trimethylamine at 20°; curve B, trimethylamine at 200°; curve C, trimethylamine at 300°.

Estimates on the activation energy for the desorption process were made from the pyridine data plotted in Fig. 6. The slope of the solid line corresponds to an activation energy of 3 kcal./mole and an uncertainty of  $\pm 1$  kcal./mole pertains to limiting slopes indicated by the dotted lines. Such a low value for the activation energy certainly does not correspond to desorption of a chemisorbed species. Rather, it suggests that effusion is the rate-controlling step.

**C. Calorimetric Measurements.**—In order to further examine the energetics of the adsorption process, the  $\Delta H$  of adsorption for trimethylamine on two different catalyst samples was measured at 300° with a crude adiabatic calorimeter. Both measurements indicated very fast reactions. Maximum e.m.f. values were reached in about 0.5 minutes (plot of thermocouple e.m.f. vs. time).

Using samples degassed at 300°, the following results were obtained. The adsorption of trimethylamine on Davison DA-1, Cat A = 33, fresh fluid catalyst gave a  $\Delta H = -38 \pm 6$  kcal./mole. Another run, measuring the heat of adsorption of trimethylamine on Davison DA-1, Cat A = 44, fresh fluid catalyst gave a  $\Delta H = -33 \pm 6$  kcal./mole. These values indicate strong acid-base interactions. It is interesting to compare, for example, the above  $\Delta H$  values with those of the following acid-base systems<sup>18</sup>

(18) "Selected Values of Chemical Thermodynamic Properties," Circular of the Bureau of Standards, #500, U. S. Government Printing Office, Washington, D. C., February 1, 1952.

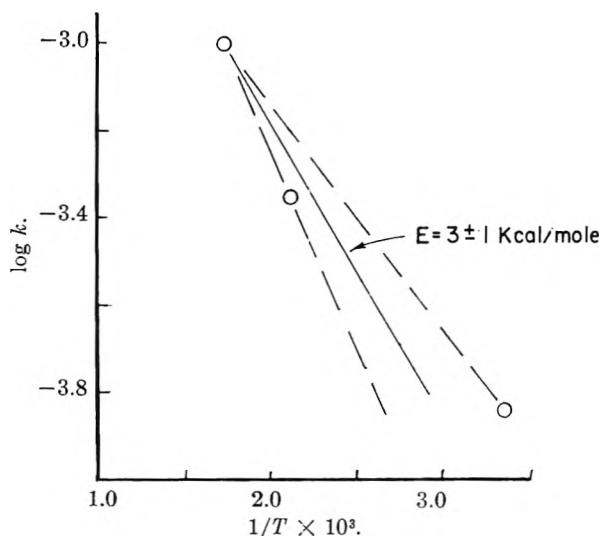


Fig. 6.—Activation energy for desorption of pyridine between 25 and 300°. Adsorbent = Davison DA-1 cracking catalyst, Cat A = 44, calcined at 850°F., degassed at 300°.

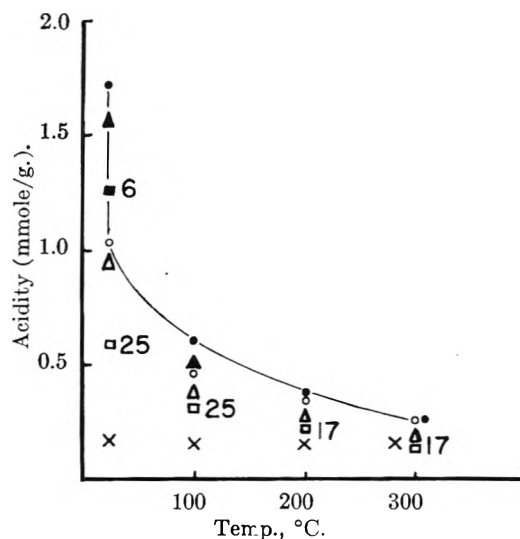
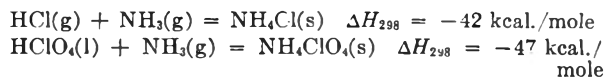


Fig. 7.—Plot of acidity vs. temperature. Trimethylamine and pyridine on Davison DA-1 cracking catalyst, Cat A = 44, calcined at 850°F., degassed at 300°. Legend: (1) acidity extrapolated to zero time on first-order plots,  $\circ$ ; trimethylamine and  $\bullet$ , pyridine. (2) acidity after 1 hour of pumping,  $\Delta$ , trimethylamine and  $\blacktriangle$ , pyridine. (3) acidity after indicated hours of pumping =  $\square$ , trimethylamine and  $\blacksquare$ , pyridine. (4) Weighing tube method with fluid sample =  $\times$ .



Comparable values have been obtained by Eley and co-workers<sup>19</sup> for the bond energy  $\text{RN} \rightarrow \text{AlC}_{-3}$  for a series of nitrogen bases.

**D. Acidity as a Function of Base Strength and Catalyst Particle Size.**—Acidity versus temperature data for  $\text{Me}_3\text{N}$  and pyridine on Davison DA-1 Cat A = 44 appear in Fig. 7. The lowest points (crosses) have a very slight temperature dependence and apply to fluid catalysts.<sup>20</sup> These points were obtained by the weighing tube technique using

(19) D. D. Eley, M. H. Dilk and M. G. Sheppard, *Trans. Faraday Soc.*, **46**, 261 (1950).

(20) Particles not over 200  $\mu$  in diameter.

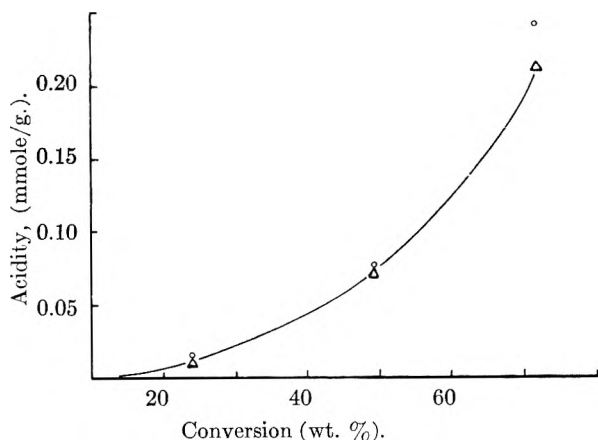


Fig. 8.—Acidity *vs.* weight per cent. conversion (Cat A Test). Data apply to several catalyst samples exposed to trimethylamine at 300°. Legend: (1) acidity extrapolated to zero time on first-order plot = O. (2) acidity after 1 hour of pumping = Δ.

pyridine as the adsorbate. The higher points pertain to pelleted fluid samples and appear to be considerably more temperature-dependent. These data were obtained with the high temperature absorption balance using either trimethylamine or pyridine as the adsorbate.

Apparently the gross particle size of the catalyst, *i.e.*, fluid *versus* pelleted fluid, has an important bearing on the observed acidity. Regarding effusion as rate-controlling, the finely divided fluid catalyst should empty faster (smaller mean distance of escape) than the large aggregates of pelleted catalyst.

All data show a spread in acidity, depending on the time of absorption involved. This spread becomes smaller at higher temperatures. Again, effusion presents a partial basis for this effect. Since its rate increases either exponentially with  $T$  or as  $T^{1/2}$  in the initial stages, the amount of time required to empty a given pore system decreases with increasing temperature. Another factor enters the picture: the proportion of loosely held adsorbate is smaller at the higher temperature. Therefore, higher diffusion rates and smaller amount of removable adsorbate both contribute to the clustering of points at the higher temperatures. Note particularly the good agreement obtained at 300°, irrespective of catalyst particle size, time of pumping or adsorbate used.

It seems strange at first glance that the weaker base, pyridine, should give larger acidity values than the stronger base,<sup>21</sup> trimethylamine. The pyridine points are consistently higher than trimethylamine points. Energetically, a strong base should donate bond to weaker acidic sites as well as the stronger ones. But the weaker base should bond only to the stronger sites. The anomaly can be resolved if effusion is considered rate-controlling. Pyridine (mol. wt. = 79) will effuse more slowly than trimethylamine (mol. wt. = 59), giving higher values for the acidity.

(21) Relative base strengths estimated from values of  $K_b$  in aqueous solution, which admittedly ignores steric and electronic effects. For non-aqueous systems see D. D. Eley and H. Watts, *J. Chem. Soc.*, 1319 (1954), and H. C. Brown, *J. Am. Chem. Soc.*, 69, 1137 (1947).

Pertinent discussions<sup>22,23</sup> on the effects of diffusion in porous catalyst systems consider factors such as pore diameter, particle size, molecular weight and pressure.

**E. Acidity *versus* Catalyst Activity.**—In this final section it merely will be stated that the acidities of several different catalyst samples were measured with trimethylamine at 300°. The Cat A activities of these samples were spaced at 13, 36 and 44. A plot of acidity *versus* Cat A activity was not linear as obtained by other workers,<sup>24</sup> but showed the same trend of increasing activity with increasing acidity.

A more general measure of cracking activity, expressed in the Cat A weight per cent. conversion, also gave a non-linear increase when plotted against increasing acidity. The data appear in Fig. 8. It is felt that such a plot is a more general measure of cracking activity of the catalyst and the selective nature of the Cat A value (volume per cent. gasoline in the cracked product) is premature in view of the complexities of this testing method. The dealkylation of cumene would have been more desirable, clean-cut cracking reaction.

#### IV. Conclusions

The picture obtained from this and other studies is that silica-alumina cracking catalysts are highly porous solids whose surfaces have the properties of very strong acids. The acidic sites apparently are partially of a Brønsted nature because they respond to trace amounts of water. Also, they are of great strength, giving heats of reaction with bases which are consistent with strong acid-base interaction.

The acidic sites tightly bind basic molecules at high temperatures, even after considerable pumping. The variation of acidity with temperature is not serious and measurements at room temperature should be of practical value. Acidities do not exceed a few tenths milliequivalent per gram of catalyst and probably cover no more than a few per cent. of the total surface (estimate based on 400 m.<sup>2</sup>/gram, 0.1 milliequivalent/gram, and ~10 Å.<sup>2</sup> per pyridine molecule). The magnitude of the acidity values herein reported is comparable to the proportion of alkali metal ions that Danforth<sup>25</sup> used in poisoning studies with similar catalyst.

Due to small pore diameter and large mean free paths encountered during evacuation, the effusion rate of gaseous basic molecules becomes very low and the acidity measurements become sensitive to particle size of the adsorbent, molecular weight of adsorbate, temperature and duration of evacuation. Approximately first-order kinetics apply to desorption process and the activation energy is very small.

Although the high temperature sorption balance is a useful tool for detailed study of the problem, it appears that a simple weighing tube technique using

(22) R. W. Blue, *et al.*, *Ind. Eng. Chem.*, 44, 2710 (1952).

(23) A. Wheeler, "Advances in Catalysis," Vol. III, Academic Press, Inc., New York, New York, 1951, p. 286.

(24) T. H. Milliken, Jr., G. H. Mills and A. G. Oblad, *Disc. Faraday Soc.*, 8, 230 (1950).

(25) J. D. Danforth and D. F. Martin, Paper Presented Before the Division of Petroleum Chemistry of the American Chemical Society, Sept. 12-15, 1955, Minneapolis, Minn., No. 34, page 195.

finely powdered adsorbents and a stable, basic gas such as trimethylamine gives reliable measurements with relatively little time and effort.

Acidities measured by either method are in accord with other data which relate the increase in

cracking activity with increasing concentration of acidic sites.

**Acknowledgments.**—The authors wish to thank C. S. Copeland, R. C. Hansford and G. A. Mickelson for their helpful comments.

## THE EFFECT OF SOLUBILIZATION ON THE EQUIVALENT CONDUCTANCE AND REDUCED VISCOSITY OF A POLYSOAP DERIVED FROM POLY-2-VINYLPYRIDINE<sup>1</sup>

BY ULRICH P. STRAUSS AND STANLEY S. SLOWATA

*School of Chemistry, Rutgers, The State University, New Brunswick, New Jersey*

*Received August 13, 1956*

The effects of solubilized *n*-decane, benzene and 1-octanol on aqueous solutions of a polysoap, prepared by partial quaternization of poly-2-vinylpyridine with *n*-dodecyl bromide, were explored by electrical conductivity and viscosity studies. The results indicate that, in general, changes in the molecular dimensions of the polysoap molecules are paralleled by changes in the equivalent conductance. With decane which is solubilized in the lipophilic regions of the polysoap molecule, the conductance change was very small. However, benzene and octanol, which are at least partly solubilized near the ionic groups, produced large conductance depressions at high polysoap concentration. With the gradual addition of benzene or octanol to a 2% polysoap solution, the equivalent conductance decreased continuously over the range where the reduced viscosity went through a maximum, thus indicating the absence of a causal relationship between the electrical charge and the forces which produce the viscosity maximum. On the other hand, in the range where octanol produced a viscosity minimum there appeared a conductance minimum, also. Beyond saturation, addition of more solubilize caused no further change in the equivalent conductance. The findings, obtained with several polysoaps, that the viscosity minimum usually occurs when about one, and saturation when about two long-chain alcohol molecules have been solubilized per dodecyl group suggest the possible existence of stoichiometric relationships between the dodecyl groups and the solubilized alcohol molecules.

### Introduction

It has been shown that polysoaps derived from poly-2- and poly-4-vinylpyridine solubilize many compounds which are normally insoluble or only very slightly soluble in water.<sup>2-4</sup> Depending on the nature of the additive, various effects on the reduced viscosity of the polysoap have been observed. Aliphatic hydrocarbons uniformly depress the reduced viscosity<sup>2b-7</sup>; with the stepwise addition of aromatic hydrocarbons the reduced viscosity usually passes through a maximum,<sup>2b,4,7</sup> while with long-chain alcohols the viscosity usually passes through both a maximum and a minimum.<sup>4</sup> The viscosity maxima increase sharply with increasing polysoap concentration and disappear at very low polysoap concentrations; therefore, they have been ascribed to interactions between polysoap molecules. The other viscosity effects which are much less concentration-dependent are assumed to be caused, at least partly, by changes in the molecular dimensions of the polysoap molecules.

In view of these findings it seemed desirable to determine the effect of additives on the electrical conductivity of polysoap solutions. It was hoped that such a study would provide valuable informa-

tion concerning several points of interest: first, what effect changes in the molecular dimensions and interactions would have on the apparent degree of ionization of the polysoap; second, whether the viscosity maxima and minima are caused by electrical charge effects; and third, whether the locus of solubilization of the additive inside the polysoap molecule affects the conductivity.

The results of such exploratory conductance and viscosity studies are presented in this paper. As representative solubilizes we used *n*-decane, benzene and 1-octanol. The polysoap was obtained by the quaternization of poly-2-vinylpyridine with *n*-dodecyl bromide.

### Experimental

**Materials.**—Polysoap No. SS-4282 was prepared by partial quaternization of poly-2-vinylpyridine (our sample No. L13) with *n*-dodecyl bromide using a method previously described,<sup>2a</sup> except that a 1:1 nitromethane-nitroethane mixture was used in place of the nitroethane solvent.

Most of the HBr was removed from the polysoap by raising the pH of a 5.15% aqueous solution from 2.93 to 5.63 with an anion-exchange resin, Ionac A300, in the hydroxide form. The polysoap was recovered by freeze-drying. Potentiometric titration of the polysoap with silver nitrate solution gave 1.790 and 1.787 milliequivalents of bromide ion per gram of polysoap. Nitrogen was 7.54%. (The nitrogen analysis was performed by W. Manser, Mikrolabor der E. T. H., Zurich, Switzerland.) From these analytical data it follows that 33.2% of the nitrogen was quaternized with *n*-dodecyl bromide.

The solubilizes, *n*-decane, benzene (thiophene-free) and 1-octanol, all Eastman Kodak White Label products, were redistilled before use.

**Procedure.**—Viscosities were measured at 25.00° in a Bingham viscometer.<sup>8</sup> Corrections were made on the observed *pt*-products for both drainage and kinetic energy.<sup>9</sup> The calibration was based on water and a series of sucrose

(1) This investigation was supported by research grants from the Rutgers Research Council and from the Office of Naval Research. Reproduction in whole or in part is permitted for any purpose of the United States Government.

(2) (a) U. P. Strauss and E. G. Jackson, *J. Polymer Sci.*, **6**, 649 (1951); (b) L. H. Layton, E. G. Jackson and U. P. Strauss, *ibid.*, **9**, 295 (1952).

(3) U. P. Strauss, S. J. Assony, E. G. Jackson and L. H. Layton, *ibid.*, **9**, 509 (1952).

(4) U. P. Strauss and N. L. Gershfeld, *THIS JOURNAL*, **58**, 747 (1954).

(5) E. G. Jackson and U. P. Strauss, *J. Polymer Sci.*, **7**, 473 (1951).

(6) L. H. Layton and U. P. Strauss, *J. Colloid Sci.*, **9**, 149 (1954).

(7) U. P. Strauss and L. H. Layton, *THIS JOURNAL*, **57**, 352 (1953).

(8) E. C. Bingham, "Fluidity and Plasticity," McGraw-Hill Book Co., Inc., New York, N. Y., 1922.

(9) R. M. Fuoss and G. I. Cathers, *J. Polymer Sci.*, **4**, 97 (1949).

solutions of known viscosities<sup>10</sup> giving the constants  $(\rho t)_0 = 9947 \text{ g. sec./cm.}^2$  for water, and  $\lambda/\rho = 1.562 \times 10^4 - 1.89 \times 10^{-5} (\rho t/\rho)^2$ , in the notation of Fuoss and Cathers.<sup>9</sup>

Alternating-current conductance measurements were made at 25.00° with a Shedlovsky type bridge.<sup>11,12</sup> The cell contained bright platinum electrodes and had a cell constant of  $0.905 \pm 0.001$ .<sup>13</sup> The distilled water used in preparing the solutions had a specific conductance of  $1.2 \times 10^{-6}$  reciprocal ohm per centimeter. The accuracy of the method was tested by measuring the equivalent conductances of several KCl solutions and comparing the results with published values.<sup>14</sup>

Previously described methods were used for preparing and equilibrating the polysoap solutions.<sup>6,7</sup> After the desired amount of solubilize had been added, the sealed tubes were tumbled end-over-end for two days at 45° and for at least one more day at 25° before the conductivity and viscosity measurements were made.

### Results and Discussion

The effects of solubilized decane, benzene and octanol on the reduced viscosity, and on the equivalent conductance, of a 1.99% aqueous polysoap solution are illustrated in Fig. 1. The abscissa for both the upper and lower diagrams is  $K$ , the concentration of solubilize expressed in grams per 100 ml. of solution. In the upper diagram the ordinate (on a logarithmic scale) is the reduced viscosity,  $\eta_{sp}/C$ , where  $\eta_{sp} = (\eta - \eta_0)/\eta_0$ ,  $\eta$  and  $\eta_0$  being the viscosity values of the solution and solvent, respectively, and  $C$  is the polysoap concentration in grams per 100 ml. of solution. In the lower dia-

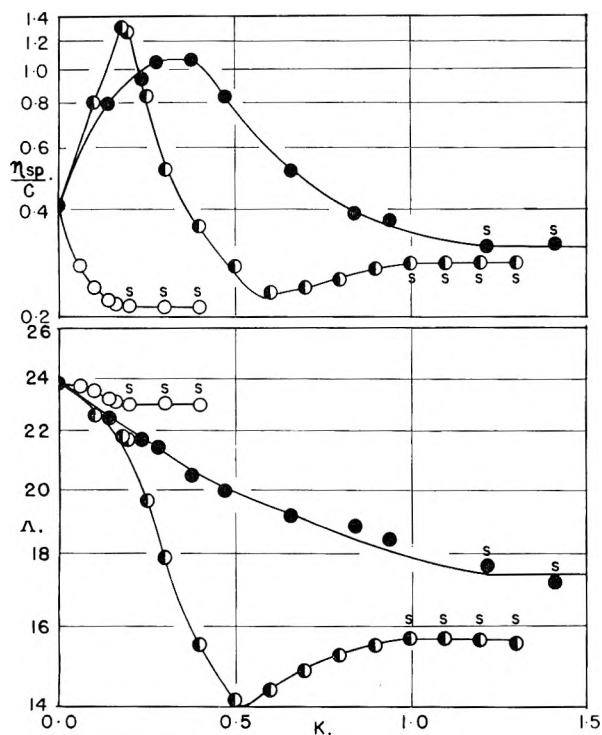


Fig. 1.—Effects of solubilizes on the reduced viscosity (upper diagram) and equivalent conductance (lower diagram) of a 1.99% polysoap solution:  $\circ$ , *n*-decane;  $\bullet$ , benzene;  $\bullet$ , 1-octanol.

(10) F. J. Bates, *et al.*, "Polarimetry, Saccharimetry and the Sugars," Circular C440, National Bureau of Standards, Washington, D. C., 1942, p. 673.

(11) T. Shedlovsky, *J. Am. Chem. Soc.*, **52**, 1793 (1930).

(12) D. Edelson and R. M. Fuoss, *J. Chem. Ed.*, **27**, 610 (1950).

(13) G. Jones and B. C. Bradshaw, *J. Am. Chem. Soc.*, **55**, 1780 (1933).

(14) T. Shedlovsky, *ibid.*, **54**, 1411 (1932).

gram the ordinate is  $\Lambda$ , the equivalent conductance of the polysoap, based on its bromide ion content.

Among the three solubilizes decane, which is represented by the open circles, exhibits the simplest behavior. The familiar drop in the reduced viscosity is accompanied by a similar, but considerably smaller drop in the equivalent conductance. Addition of decane beyond its solubilization limit causes no further changes in the reduced viscosity and the equivalent conductance. Points corresponding to solutions containing a visible excess of solubilize are marked with the symbol S in Fig. 1.

The maximum which occurs in the reduced viscosity on the solubilization of benzene has been ascribed to aggregation of polysoap molecules, caused by changes in the hydrocarbon content of their surfaces.<sup>2,4</sup> The equivalent conductance is seen to decrease uniformly in the region of the viscosity maximum. This result leads to two conclusions. First, it eliminates the possibility that the viscosity maximum is caused directly by electrical charge effects. Second, if we accept the above hypothesis for the explanation of the viscosity maximum, then it follows that aggregate formation has no noticeable effect on the equivalent conductance.

With octanol the conductance behavior in the region of the viscosity maximum is similar to that observed for benzene. Whether the small change in the slope of the  $\Lambda$ -curve near the position of the viscosity maximum has any significance is difficult to decide at this time. On the other hand, it is clear that the viscosity minimum is accompanied by a minimum in the conductance curve. The viscosity minimum has previously been ascribed to changes in molecular dimensions.<sup>4</sup> It appears that the equivalent conductance goes up and down with the molecular dimensions. However, results obtained at only one polysoap concentration do not indicate conclusively the respective effects of molecular dimensions and interactions on the reduced viscosity. This matter will be pursued further below, in connection with results obtained at several polysoap concentrations.

Just as in the case of decane, the equivalent conductance becomes constant when the benzene and the octanol reach their respective solubilization limits. Therefore, conductivity may be used as a new method for determining solubilization limits in polysoap solutions. The values of the solubility,  $K_s$ , of decane, benzene and octanol in the 1.99% polysoap solution are 0.17, 1.20 and 0.97 g./100 ml., respectively. After subtracting the water solubilities of these compounds (0.00,<sup>15</sup> 0.18,<sup>16</sup> and 0.06<sup>15</sup> g./100 ml., respectively), this amounts to 0.085, 0.51 and 0.47 g. of the respective compounds solubilized per gram of polysoap. From these figures we can calculate that for each dodecyl group there are solubilized 0.33 molecule of decane, 3.6 molecules of benzene and 2.0 molecules of octanol. The last value is very close to the values obtained in another study for the solubilization of 1-heptanol by several polysoaps prepared from poly-4-vinylpyridine and containing varying amounts of dodecyl

(15) J. W. McBain and P. H. Richards, *Ind. Eng. Chem.*, **38**, 642 (1946).

(16) R. L. Bohon and W. F. Clausen, *J. Am. Chem. Soc.*, **73**, 1571 (1951).

groups.<sup>4</sup> With one exception, the number of heptanol molecules solubilized per dodecyl group was near two, while in the case of decane and benzene the number fell off rapidly with decreasing dodecyl content of the polysoap. These results suggest that there may be some stoichiometric relationship between the solubilized long-chain-alcohol molecules and the dodecyl groups. The suggestion is strengthened by the observation that in practically all cases where a viscosity minimum has been noted, this minimum occurs when about half the amount of alcohol needed for saturation has been added; *i.e.*, when approximately one alcohol molecule has been solubilized per dodecyl group. Possibly two-dimensional ordered arrangements of pyridinium and alcohol groups of different configuration exist on the surface of the polysoap molecules at the viscosity minimum and at saturation. However, we feel that further data are needed before more definite conclusions can be drawn concerning this phenomenon.

As has already been mentioned the conductance appears to parallel the molecular dimensions. In order to interpret this result, we shall discuss briefly the expected dependence of the conductivity on the relevant molecular properties. Quantitative theories concerning polyelectrolyte conductivity and electrophoresis have recently been developed by several authors.<sup>17-20</sup> However, these theories apply only when the conductivity is measured in the presence of simple electrolyte. No rigorous quantitative theory is available for our results which were obtained in the absence of simple electrolyte. The procedure which has been employed in such cases for both polyelectrolytes<sup>21,22</sup> and soap micelles<sup>23</sup> is to consider part of the counter ions bound to and travelling with the macro-ion while the remainder of the counter ions is considered completely free. Relaxation and electrophoretic interference phenomena are not explicitly evaluated. If the fraction of free counter ions is denoted by the symbol  $\alpha$ , the equivalent conductance is given by the equation

$$\Lambda = \alpha(\mathcal{F}u + \lambda_{Br^-}) \quad (1)$$

where  $\mathcal{F}$  is the faraday,  $u$  the mobility of the macro-ion and  $\lambda_{Br^-}$  the equivalent conductance of the bromide ion. The mobility of the macro-ion should be proportional to the charge and may be expressed by the relation

$$u = \alpha g(R) \quad (2)$$

The function  $g(R)$  lumps together the effects of the molecular dimensions. This function is predominantly governed by the friction coefficient of the macro-ion and should, in general, vary inversely with  $R$ , the radius of the equivalent sphere of the polyion.<sup>24</sup> It is clear then that our observa-

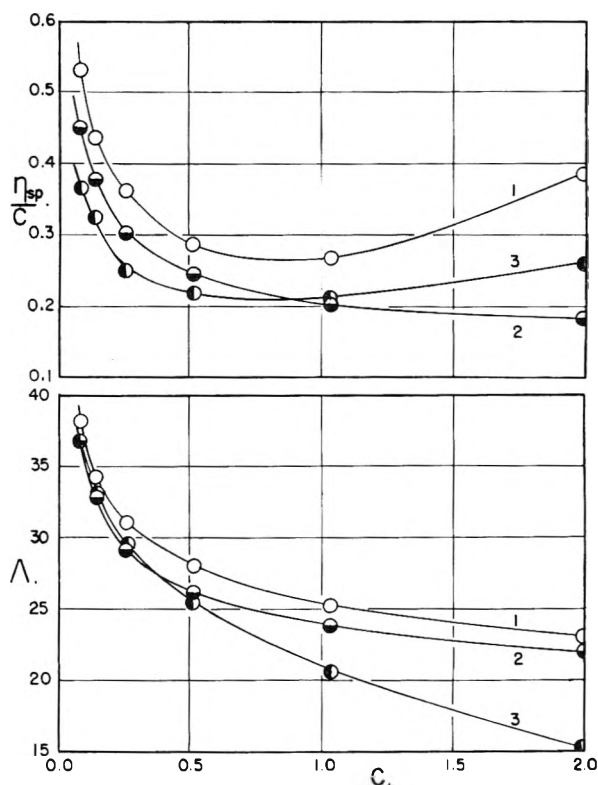


Fig. 2.—The effect of saturation with solubilizates on the reduced viscosity (upper diagram) and equivalent conductance (lower diagram) as a function of the polysoap concentration. Additive is: 1, none; 2, *n*-decane; 3, 1-octanol.

tion that  $\Lambda$  moves in the same direction as  $R$  cannot be explained in terms of  $g(R)$ , but must be understood in terms of  $\alpha$ . A decrease in the effective degree of ionization as the polysoap molecule contracts seems reasonable, since bringing together the ionic groups of the polyion should increase their electrostatic attraction for counter ions.

In order to examine this problem further, we have studied the effects on the reduced viscosity and equivalent conductance when polysoap solutions of various concentrations are saturated with decane and with octanol.<sup>25</sup> The results are presented graphically in Fig. 2, the viscosity behavior in the upper and the conductivity behavior in the lower diagram. The curves denoted by 1 illustrate the polysoap behavior in the absence of an additive. The shape of the conductivity curve is familiar from previous work with polyelectrolytes and has been ascribed to increasing counter-ion association with increasing polyelectrolyte concentration.<sup>21</sup> This decrease in the extent of ionization also reduces the intramolecular repulsion and hence causes

$g(R)$  to be almost constant. With increasing impenetrability of the polyion, the inverse dependence of  $g(R)$  on  $R$  becomes stronger. Because of their compactness, polysoap ions should be quite impermeable. For our qualitative discussion, a knowledge of the exact dependence of  $g(R)$  on  $R$  is unnecessary, and our general conclusions depend only on the consideration that  $g(R)$  does not increase with increasing  $R$ .

(25) The extent of solubilization at saturation was not determined except in the 2% polysoap solution. However, in other studies with polysoaps it has been found that, at saturation, the ratio of solubilizate to polysoap is independent of the polysoap concentration.<sup>3,4,5</sup>

(17) J. J. Hermans and H. Fujita, *Proc. Akad. Amsterdam*, **B58**, 182 (1955).

(18) H. Fujita and J. J. Hermans, *ibid.*, **B58**, 188 (1955).

(19) J. J. Hermans, *J. Polymer Sci.*, **18**, 527 (1955).

(20) J. Th. G. Overbeek and D. Stigter, *Rec. trav. chim.*, **75**, 543 (1956).

(21) R. M. Fuoss and U. P. Strauss, *J. Polymer Sci.*, **3**, 246 (1948).

(22) U. Schindewolf, *Z. physik. Chem.*, **1**, 134 (1954).

(23) P. Van Ryselberghe, *This Journal*, **43**, 1049 (1939).

(24) The nature of  $g(R)$  depends on the permeability of the polymer molecule to the solvent. If there is free drainage, one would expect

the polysoap molecule to contract. The contraction is the primary cause for the initial decrease of the reduced viscosity.<sup>2a,21</sup> As the polysoap concentration increases further, the reduced viscosity increases again, presumably because of intermolecular interactions between different polysoap molecules.

The curves denoted by 2 illustrate the behavior of the polysoap when it is saturated with decane. Over the polysoap concentration range from 0.08 to 0.51 g./100 ml. the decane uniformly depresses the reduced viscosity by about 15%. Because of the independence of the polysoap concentration, this depression is ascribed to a change in the molecular dimensions. In the 1 and 2% polysoap solutions, the depressions of the reduced viscosity amount to 26 and 50%. This increase in the reduced viscosity depression over the depression found at the lower polysoap concentrations indicates that the decane here also reduces the interactions between different polysoap molecules. The effect of decane on the equivalent conductance is a depression which amounts to 3.5% at  $C = 0.08$  then increases slowly to 6.5% at  $C = 0.5$  and decreases again to 4.4% at  $C = 2.0$ . Probably the most significant aspect of this result is the relative smallness of the decrease in the equivalent conductance compared to the change in the molecular dimensions. Apparently the opposing effects of decreasing ionization and decreasing friction coef-

ficient on the equivalent conductance partly cancel each other.

The curves corresponding to octanol saturation are denoted by 3. The reduced viscosity is depressed fairly uniformly over the whole concentration range. Therefore most of the depression is probably due to a decrease in the molecular dimensions. This decrease which ranges from about 22 to 33% is larger than that due to decane. Nevertheless, in the dilute polysoap solutions the effects of octanol and decane on the equivalent conductance are about the same. On the other hand, in the more concentrated polysoap solutions octanol causes a strikingly large drop in the equivalent conductance. This behavior may be connected with the fact that octanol is solubilized near the charged groups in the polysoap molecule and can therefore exert a direct effect on their extent of ionization. The solubilized octanol molecules may lower the local dielectric constant in the neighborhood of the ionic groups. Such a dielectric constant lowering would be expected to be more pronounced at the higher polysoap concentrations where the polysoap molecules are more compact and the solubilized alcohol molecules consequently closer together. It may be significant that benzene which, too, is believed to be solubilized partly in the polar region of the polysoap molecule<sup>2</sup> also produces a large depression in the conductance of the 2% polysoap solution (see Fig. 1).

## THERMOLUMINESCENCE OF FOURTEEN ALKALI HALIDE CRYSTALS<sup>1</sup>

BY LOUIS F. HECKELSBERG AND FARRINGTON DANIELS

Chemistry Department, University of Wisconsin, Madison, Wisconsin

Received August 30, 1956

In this investigation the thermoluminescence glow curves of fourteen alkali halides from liquid air temperature to red heat were measured after exposure of the crystals to X-ray or  $\gamma$ -radiation. The effects produced by various amounts of radiation were studied using crystals of LiF and NaCl. The thermoluminescence of mixed crystals containing various alkali halides was also studied.

The alkali halides were chosen for study because they all emit light when heated after previous exposure to  $\gamma$ -rays and because they have simple crystalline structures.

### Experimental

**Materials.**—Large fused crystals of LiF, NaCl, KCl and KBr were obtained from the Harshaw Chemical Company. Crystals of LiCl, LiBr, NaF, NaBr, NaI, KF, KI, RbCl, RbBr and RbI were grown by either the Kyropolus<sup>2</sup> method or by the slow cooling of liquid salts in platinum crucibles. In several cases, they were further purified by recrystallization.

Eight crystals containing various mole percentages of NaCl and NaBr were grown. These crystals were grown by first mixing the salts at room temperature and then melting them. The melts were held in a liquid state for 24 hours before the crystallization process was started to ensure uniform distribution of the halogen ions. Six NaCl crystals containing one mole per cent. of a foreign alkali or halogen ion were also grown by this method.

**Apparatus.**—For the determination of the glow curves a modification of the apparatus described by Boyd<sup>3,4</sup> was used

for the temperature range of 25 to 500°. For the low temperature range of -186 to 50° the apparatus shown in Fig. 1

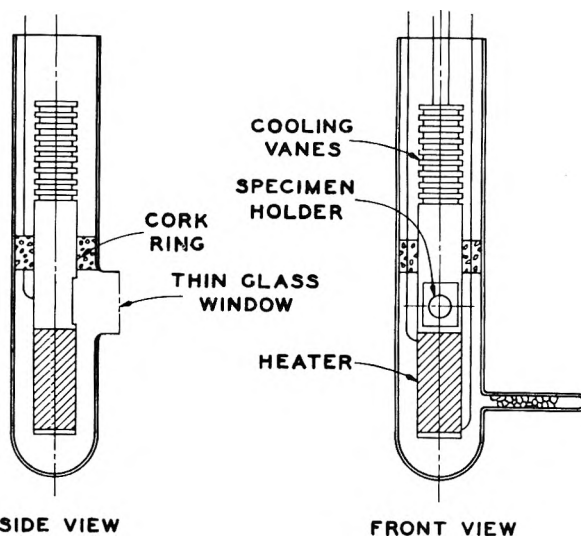


Fig. 1.—Apparatus for X-ray exposure at low temperatures.

(1) From the Ph.D. thesis of L. F. Heckelsberg, University of Wisconsin, 1951.

(2) S. Kyropolus, *Anorg. Chem.*, **154**, 308 (1926).

(3) C. A. Boyd, Ph.D. Thesis, University of Wisconsin, 1948.

(4) C. A. Boyd, *J. Chem. Phys.*, **17**, 1221 (1949).

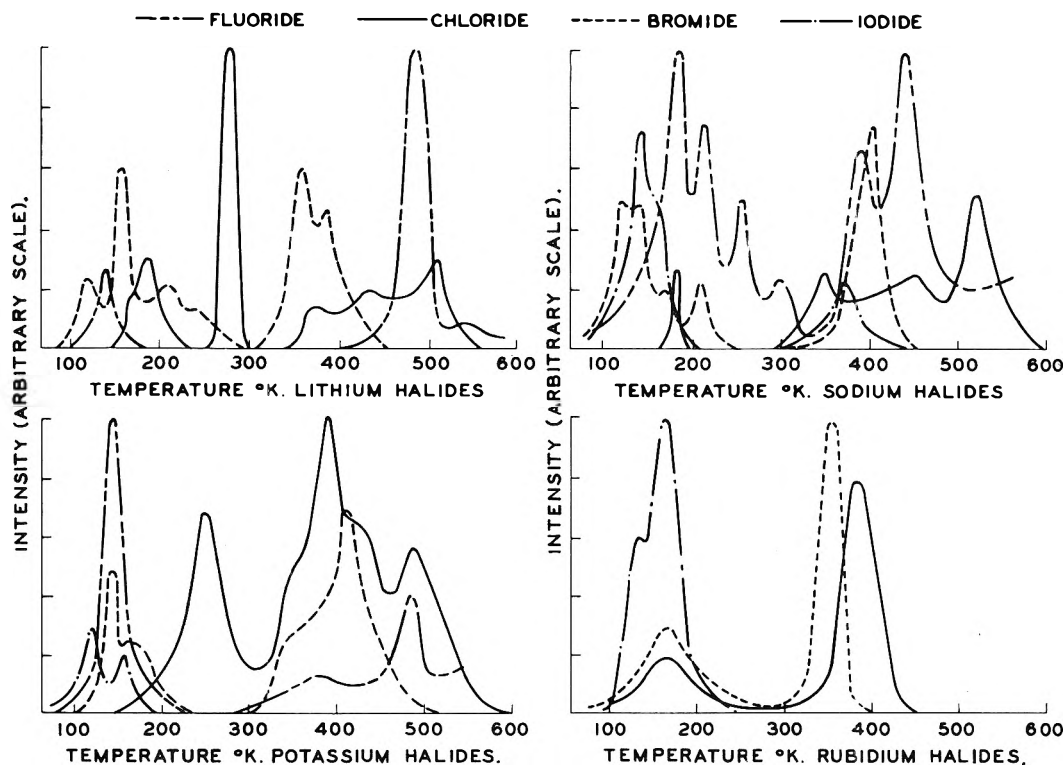


Fig. 2.—Thermoluminescent "glow curves" of the alkali halides (see Table I).

was used. This apparatus consisted essentially of a 1.2 cm. diameter brass bar mounted in a one-inch diameter Pyrex test-tube. Six feet of No. 22 Nichrome wire was wrapped around one end of the bar while cooling fins were machined on the other end. The thin glass window was obtained by blowing a bubble and then passing a long hot flame across the bubble. The tube was evacuated, by means of a side arm, to prevent condensation on the cold metal. The resulting apparatus was insulated with ground asbestos cement. Liquid air was placed around the brass rod in the upper compartment while the apparatus was mounted vertically and the crystal was exposed to an X-ray beam. After exposure the liquid air was poured off, the apparatus was mounted horizontally and the crystal was heated electrically at a rate of approximately  $0.8^\circ$  per second. The heating rate for the furnace used in the high temperature range was about  $1^\circ$  per second. The light evolved was measured with a photomultiplier tube, RCA 1P21 and the electrical current amplified and recorded with a Brown recorder.

Two different sources of radiation were used. For the low temperature range a copper target X-ray tube operating at 37 kv. and 18 ma. was used. The remaining radiation dosages were obtained from a hollow cylindrical  $\text{Co}^{60}$  source. The radiation intensity inside the source, where the crystals were placed, was found by three different methods to be approximately 6,500 Roentgen units per hour.

### Results and Discussions

**Glow Curves.**—The thermoluminescence glow curves of fourteen alkali halides, all having the simple NaCl type lattice, were obtained during this investigation. The cesium halides and RbF were not studied because they have a different lattice type. RbCl and RbBr have lattice transition points from the CsCl to the NaCl type lattice below  $25^\circ$ . No attempt was made to grow a LiI crystal because of its low melting point and its extremely hygroscopic nature.

The glow curves which cover a temperature range from 100 to  $600^\circ\text{K}$ . are combinations of two separate measurements: a low temperature glow

curve from  $100^\circ\text{K}$ . to about  $325^\circ\text{K}$ ., activated by X-rays, and a high temperature glow curve from about 300 to  $600^\circ\text{K}$ ., activated by  $\gamma$ -rays. Experimental difficulties made it impossible to extend a single glow curve from 100 to  $600^\circ\text{K}$ . in a single experiment. In several cases, such as with RbBr, the range of the low temperature glow curve was extended in order to obtain a peak occurring around  $350^\circ\text{K}$ .

While the temperature corresponding to maximum light emission is always the same, the height of the peak and the area under it depends on the amount of radiation the crystal receives. Some crystals are more sensitive to radiation than others. For example, in the high temperature peaks of LiF and LiCl, LiCl requires about 300 times more radiation than LiF to emit the same amount of light. Whether this difference in sensitivity is an intrinsic property of the crystal or whether it is due to impurities or to some factor in the process of crystallization is not known. It was also found that the glow curves become more complicated with increasing amounts of radiation. Therefore, to obtain a glow curve characteristic of a crystal the least amount of radiation necessary to activate it was used.

Because of these difficulties some method had to be found to present the glow curves in a manner that will allow comparison between them. The method used here presents the data in the form of relative, composite curves with a supplementary table. The shape of the glow curves can be seen in Fig. 2, and the relative peak heights are given in Table I. The relative peak heights given in this table are calculated roughly by dividing the heights of the peaks by the amount of radiation.

The peak heights in Fig. 2 have no absolute significance because the amount of exposure to radiation was different for the different crystals and for the high and low temperatures. The calculations are only approximate but they are based on a considerable amount of data. For the transparent crystals used in this investigation, the amount of light emitted was found to be proportional to the weight of the crystal, at least, for crystals weighing several grams or less. Experiments with long periods of radiation indicate that the height of a peak is roughly proportional to the amount of radiation received, in the initial phase of exposure. It must be kept in mind, however, that peaks slightly above room temperature will be affected by the thermal draining of the traps.

TABLE I  
EXPERIMENTAL DATA FOR THERMOLUMINESCENCE GLOW CURVES

Salt	Range above room temp.		Range below room temp.	
	Relative height <sup>a</sup>	$\gamma$ -Radiation, R.	Relative height <sup>b</sup>	X-Ray radiation, min.
LiF	712,000	500	1,000	1.5
LiCl	1,800	70,000	91,000	0.08
LiBr	80,000	9,250	3,700	2.5
NaF	5,500	2,000	650	4.0
NaCl	158	5,000	400	2.0
NaBr	1,540	5,000	11,600	2.0
NaI	3	45,000	24,600	1.0
KF	2	96,000	4,800	0.75
KCl	3,700	5,000	550	5.0
KBr	7	17,000	210	10.0
KI	.....	.....	710	5.0
RbCl	2,040	9,000	15	20.0
RbBr	910	13,500	25	20.0
RbI	.....	.....	500	3.0

<sup>a</sup> Height of peak divided by gamma radiation dosage in Roentgens. <sup>b</sup> Height of peak divided by X-ray dosage in minutes.

Recently Sharma<sup>5</sup> published glow curves for LiCl, NaF, NaI, KBr and KI which were irradiated with low energy electrons. Although he used a faster rate of heating his results are in general agreement with the results of this investigation. His conclusions that the thermoluminescence peaks are related to color centers were borne out during this investigation. This relationship has been observed earlier by Pringsheim<sup>6</sup> and Dutton and Maurer.<sup>7</sup> It was found during this investigation that the coloration produced by the  $\gamma$ -radiation at room temperature faded out at temperatures corresponding to the major high temperature peaks. KI and RbI have no coloration at room temperature and have no high temperature peaks. Sharma, in an earlier note,<sup>8</sup> found that KI radiated at  $-185^\circ$  has a peak at  $235^\circ$  K. which was not observed during this investigation. He found that the coloration produced by the radiation at low temperatures faded at this peak temperature.  $\gamma$ -Radiation at room temperature will not activate at  $235^\circ$  K. peak because of

thermal deactivation; and the X-ray radiation used at  $-185^\circ$  in the present investigation was probably too weak to give this peak.

From results of the present investigation the low temperature peaks appear to be far more sensitive to radiation than the peaks which occur at temperatures above  $25^\circ$ .

In addition to the fading of the F-centers with thermoluminescence a relationship was found between the major high temperature peaks and the absorption spectra of the F-centers. Ivey<sup>9</sup> has shown that the absorption spectrum shifts to longer wave lengths, or lower energy values, as the size of the ions and lattice constants increase. Results of this investigation show a marked tendency for the major high temperature peaks in the thermoluminescence glow curves to shift to lower temperatures, or smaller trapping energies, with increasing lattice constants. While it is possible to correlate the major high temperature peaks with F-centers, or missing halogen ions, adequate explanations cannot be offered now for the other peaks which come in at the lower temperatures.

The glow curves of RbCl and RbI are of interest because of a phase change below room temperature from a CsCl to a NaCl type lattice. The low temperature peaks of these salts are very broad compared to the usual narrow peaks found in the low temperature region. Also these crystals required larger amounts of radiation than other crystals.

**Effects of Extended Radiation.**—The heights of the peaks of a glow curve depend upon the amount of radiation that a crystal receives. The high temperature peaks of LiF and NaCl were found to be ideal for studying this relation. These peaks are initially simple, symmetrical peaks and are thermally stable, that is, the temperature at which the maximum emission of light occurs is high enough to prevent thermal draining of the traps at room temperature.

The effects of exposure to X-rays on the low temperature peak of NaCl were also studied. This low temperature peak appears to reach saturation, or its maximum height, with one to 1.5 minute exposure to X-rays (37 kv. and 18 ma.). Peaks which occur close to the irradiation temperatures should become saturated quickly.

High energy radiation not only affects the heights of the peaks but it also causes considerable alteration in the shapes of the glow curves. The changes in the shape of the glow curves caused by increasing amounts of radiation are shown in Fig. 3. These glow curves are composites obtained during the study of the effects of varying amounts of radiation on the thermoluminescence behavior of LiF. Very similar effects were found with NaCl.

The saturation curves were obtained by exposing a large number of crystals to varying amounts of radiation and then obtaining their glow curves. No crystal was used more than once.

The glow curve labeled 1 (Fig. 3) is the initial curve obtained using a freshly prepared crystal and a small amount of radiation. In the case of LiF a beautifully symmetrical peak could be obtained

(5) J. Sharma, *Phys. Rev.*, **101**, 1295 (1956).

(6) P. Pringsheim and P. Yuster, *ibid.*, **78**, 293 (1950).

(7) D. Dutton and R. Maurer, *ibid.*, **90**, 126 (1953).

(8) J. Sharma, *ibid.*, **85**, 692 (1952).

(9) H. F. Ivey, *ibid.*, **72**, 341 (1947).

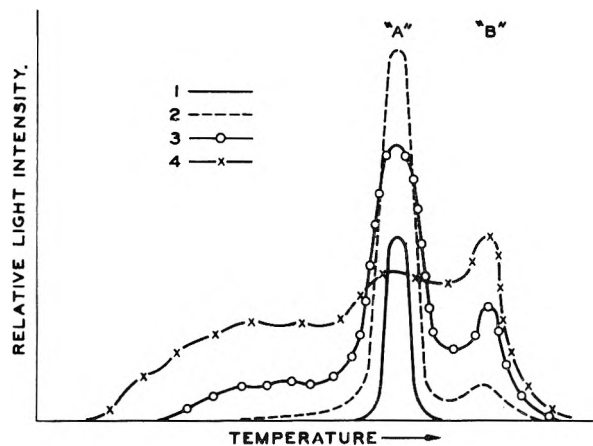


Fig. 3.—Typical "glow curves" showing effects of various amounts of radiation on lithium fluoride.

with radiation dosages as small as ten Roentgen units. Experience gained during this study indicates that the smallest possible amount of radiation should be used in order to obtain a glow curve in which the shape is not influenced by continued radiation.

Glow curve 2 shows the shape obtained at the maximum height of the peak labeled "A." For LiF this maximum is reached at values of 10,000 to 20,000 Roentgen units depending on the origin of the crystals used. In the case of NaCl this maximum was reached with dosages of about 15,000 Roentgen units for the one series of crystals studied. Of interest in this glow curve is the formation of a new peak (labeled "B") on the high temperature side of peak "A."

Glow curve 3 shows the formation of a number of small peaks on the low temperature side of peak "A." These peaks are numerous and are irregular in their locations. Glow curve 4 shows the shape obtained in the crystals which received the largest amount of radiation. In the case of LiF this value was about 100,000 Roentgen units while for NaCl it was about 400,000 Roentgen units. Peak "B" is now the predominant peak. In the case of NaCl, peak "A" completely disappeared in crystals receiving 40,000 Roentgen units. In this glow curve over twenty-five small peaks were observed. These results on NaCl have been confirmed and extended by the recent work of Hill and Schwed.<sup>10</sup>

**Mixed Crystals.**—Eight crystals containing different mole fractions of NaCl and NaBr were prepared. The abilities of these crystals to thermoluminesce are shown in Fig. 4. The log of the relative light intensity was used so as to be able to plot all the points on one graph. Each of these crystals received a radiation dosage of 70,000 Roentgen units of  $\text{Co}^{60}$  radiation. One experimental difficulty encountered in the mixed crystals was the formation of a white opaque coating on exposure of the crystals to the moisture in the air. This coating, which also appears on pure NaBr, was scraped off the crystal before its glow curve was determined.

Boyd,<sup>3,4</sup> who did some preliminary work on this system, found on X-ray examination a decided variation in the lattice constants at approximately

(10) J. L. Hill and P. Schwed, *J. Chem. Phys.*, **23**, 652 (1955).

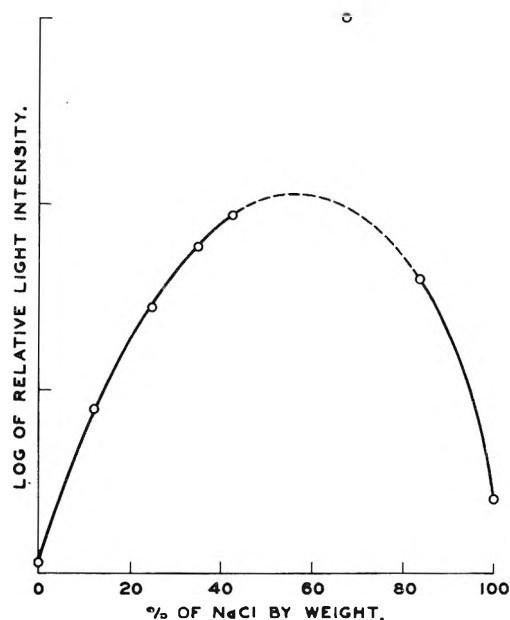


Fig. 4.—Relative intensity of light emitted by the NaCl-NaBr system.

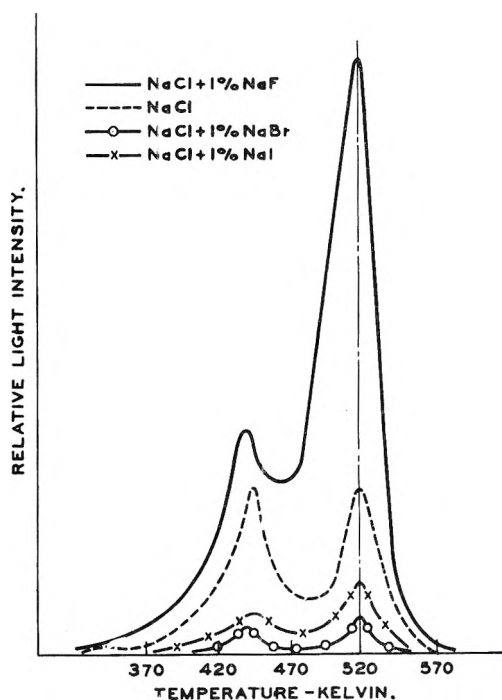


Fig. 5.—"Glow curves" of NaCl containing 1 mole % of foreign halogen ions.

75 mole % NaCl (63% by weight). The peak in Fig. 4 occurs at approximately the same composition indicating some relation between lattice spacing and thermoluminescence.

Glow curves of NaCl containing one mole % of various halogen ions are shown in Fig. 5. These crystals received a dosage of 10,000 Roentgen units in the  $\text{Co}^{60}$  source. The degree of coloration caused by  $\gamma$ -radiation (orange) varied from crystal to crystal. The color of light emitted on heating was always blue.

It will be observed that, within experimental error, no variation appears in the temperature

where maximum light emission occurs. Adding a smaller size halogen ion increases the crystal's ability to thermoluminesce while adding a larger halogen ion decreases it. This same behavior of ion size was observed for NaCl containing one mole per cent. of various alkali ions.

### Summary

It is well established that F-centers are due to missing halogen ions and since it has been found that the coloration of the crystal disappears when the major high temperature peak disappears, it is felt that this peak in the glow curves is related to missing halogen ions. In support of this relationship, it is known that the absorption spectrum of F-centers shifts to longer wave lengths as the lattice constants increase, in the same manner as the temperature of the major high temperature peak drops to lower temperatures as the lattice constants increase. No adequate explanation can be offered now for the other peaks.

Saturation experiments show that the height and the shape of glow curves depend upon the

amount of radiation which the crystals receive. For a study of the influence of the crystal on the thermoluminescence the minimum amount of radiation should be used in activating the crystal so as to obtain a characteristic glow curve uninfluenced by the radiation itself.

The thermoluminescence of sodium chloride induced by intense X-rays has been studied by Hill and Schwed,<sup>10</sup> and the thermoluminescence of lithium fluoride, potassium chloride and potassium bromide induced by intense  $\gamma$ -radiation has been studied by Ghormley and Levy.<sup>11</sup>

Mixed crystal experiments showed that adding foreign alkali or halogen ions to NaCl varied its ability to thermoluminesce but did not affect the temperatures of the peaks. Therefore, the minor peaks in the alkali halides, if related to impurities, are due to impurities other than those of the alkali or halogen family.

The authors are glad to acknowledge support of this research by the Atomic Energy Commission.

(11) J. A. Ghormley and H. A. Levy, *THIS JOURNAL*, **56**, 548 (1952)

## EVIDENCE FOR MECHANICAL SHEAR DEGRADATION OF HIGH POLYMERS<sup>1-3</sup>

BY A. B. BESTUL

*National Bureau of Standards, Washington, D. C.*

*Received September 7, 1966*

The author has previously reported the decrease in molecular weight of high molecular weight polyisobutenes during the flow of their concentrated solutions through capillaries at high rates of shear at moderate temperatures. The present paper reports the results of several experiments which support the conclusion that this molecular weight decrease results from mechanical shear degradation. The existence, rate and extent of degradation is uniquely dependent on the severity of shearing, since the results are unaffected by interruption of shearing at any stage of the degradation process, and the degradation remains characteristic of rate of shear when solutions are subjected successively to different rates of shear in varied orders. The observed phenomenon is in fact degradation, and not an artifact of solution non-equilibrium, since there is no recurrence during the shearing of a solution of polymer precipitated and dried after previous degradation. The degradation is not a pyrolytic one energized by the adiabatic collapse of cavities of any kind, since it is not promoted by the presence of a highly volatile compound in solution. The degradation occurs for the higher molecular weight fractions from a previously degraded polymer, and unfractionated polymers will suffer the degradation at lower average molecular weights than will fractions. Therefore the degradation ruptures only the higher molecular weight individual molecules and occurs only above a minimum concentration of these. The degradation appears to occur with the same general mechanism in polymers of several different chemical compositions, since generally similar results are obtained with polystyrene and polymethyl methacrylate as well as polyisobutene.

### 1. Introduction

In earlier papers<sup>4-6</sup> the author has reported measurements on the degradation of high molecular weight polyisobutene molecules during the flow of their concentrated solutions through capillaries at high rates of shear. It is the purpose of the present paper to assemble the results of several previously unpublished experiments which further indicate that the process concerned is in fact mechanical shear degradation.

(1) Extracted partly from a thesis submitted to the Graduate School of the University of Maryland in partial fulfillment of the requirements for the degree of Doctor of Philosophy.

(2) This work was performed as part of a research project last sponsored by the National Science Foundation in connection with the Government Synthetic Rubber Program.

(3) Presented before the sessions of the Division of Polymer Chemistry at the 128th National Meeting of the American Chemical Society in Minneapolis, Minnesota, on September 11-16, 1955.

(4) A. B. Bestul, *J. Appl. Phys.*, **22**, 1069 (1954).

(5) P. Goodman and A. B. Bestul, *J. Polymer Sci.*, **18**, 235 (1955).

(6) A. B. Bestul, *J. Chem. Phys.*, **24**, 1196 (1956).

### 2. Experimental Procedures and Results

The experimental techniques and the calculations used in obtaining the results reported here were similar in all cases to those stated in reference 4. Polymer solutions were sheared by being repeatedly forced through a capillary shearing tube in the McKee Consistometer.<sup>7,8</sup> The shear load, which is proportional to the pressure drop established along the capillary when the solution is forced through it, was observed every other passage of the solution through the capillary. The effect of shearing on the molecular weight of the polymer is followed by intrinsic viscosity determinations before and after a shearing run or at any stage of the run where it is desired to know the molecular weight. If an intrinsic viscosity determination is to be made during the course of a run it is necessary to sacrifice the run at that point.

**2.1 Successive Shearing at Different Shear Rates.**—In two companion runs solutions of 9.4 wt. % Vistanex B-100 polyisobutene ( $\bar{M}_v$ , viscosity average molecular weight = 1,740,000) in *n*-hexadecane were sheared initially at rates of shear of 66,000 and 33,000 sec.<sup>-1</sup>, respectively, and sub-

(7) E. A. McKee and H. S. White, *ASTM Bull. No. 153*, 90 (1948).

(8) E. A. McKee and H. S. White, *J. Research Natl. Bur. Standards*, **46**, 18 (1951).

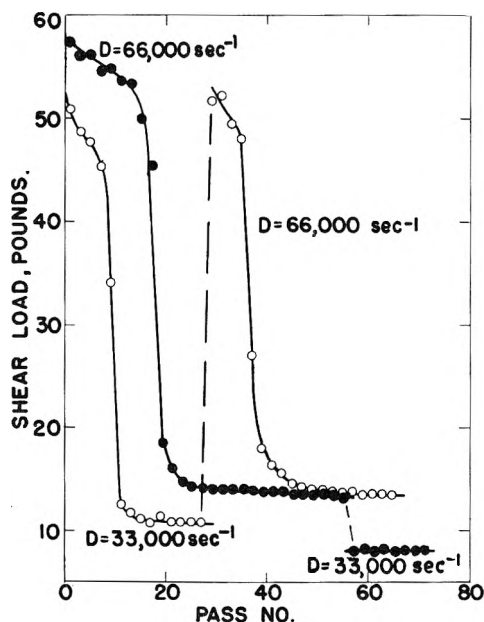


Fig. 1.—Shear load decreases for 9.4 wt. % Vistanex B-100 polyisobutene in *n*-hexadecane at 40°. Filled circles represent shearing first at  $D$  (nominal rate of shear) equal 66,000  $\text{sec}^{-1}$  and subsequently at 33,000  $\text{sec}^{-1}$ . Open circles represent shearing first at 33,000  $\text{sec}^{-1}$  and subsequently at 66,000  $\text{sec}^{-1}$ .

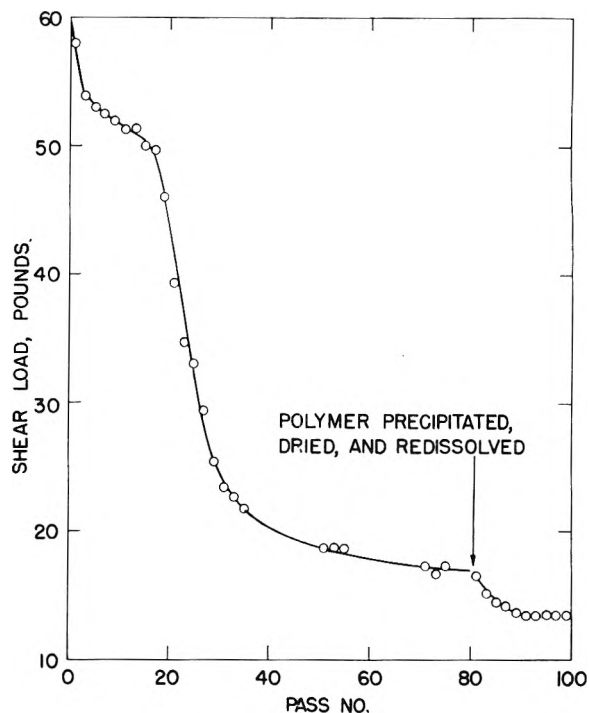


Fig. 3.—Attempted degradation after recovery and redissolution of polymer.

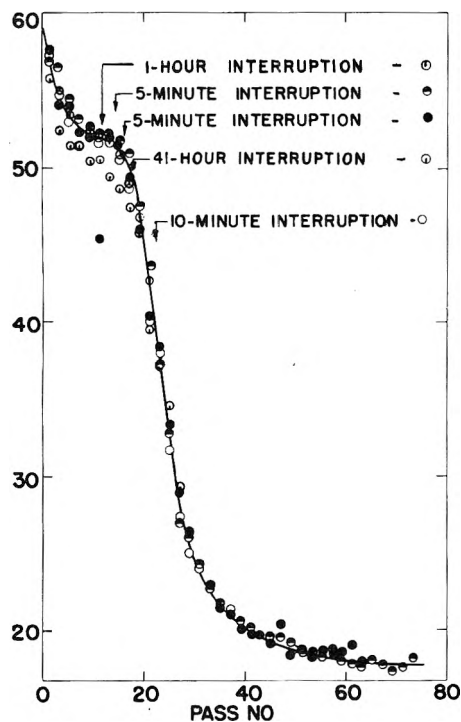


Fig. 2.—Shear load decrease plots for runs with interruptions (10 wt. % Vistanex B-100 polyisobutene in *n*-hexadecane at 40° and  $D = 66,000 \text{ sec}^{-1}$ ).

sequently at interchanged rates. For these two runs Fig. 1 shows the shear load observed during the successive passes of the solution through the capillary. Shearing at 66,000  $\text{sec}^{-1}$  before or after shearing at 33,000  $\text{sec}^{-1}$  reduced  $\bar{M}_v$  to 1,150,000. Shearing at 33,000  $\text{sec}^{-1}$  before shearing at 66,000  $\text{sec}^{-1}$  reduced  $\bar{M}_v$  to 1,420,000. After shearing at 66,000  $\text{sec}^{-1}$  subsequent shearing at 33,000  $\text{sec}^{-1}$  effected no further  $\bar{M}_v$  reduction.

As discussed in reference 4 almost all of the molecular weight decrease occurs while the shear load maintains its

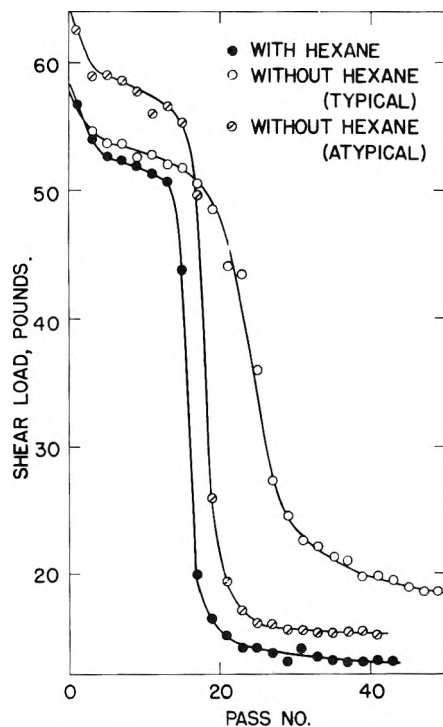


Fig. 4.—Runs with and without hexane in solution.

relatively high value during the earlier passes at a given rate of shear. The runs represented in Fig. 1 are atypical in that the decrease of shear load following the early relatively high values is more rapid than usually observed. A more typical, slower decrease of shear load is illustrated in Fig. 2. The difference is not related to the concentration difference between 9.4 and 10%. The over-all molecular weight decrease is quantitatively the same whether the shear load decrease is unusually rapid, as in Fig. 1, or slower as in Fig. 2. Therefore, the difference in the rate of shear load decrease following the relatively high early values is immaterial as regards the extent of molecular weight decrease.

**2.2 Interruption of Shear Degradation Process.**—Five runs on 10 wt. % solutions of Vistanex B-100 polyisobutene at 66,000 sec.<sup>-1</sup> were interrupted for various intervals of time at various stages of the shearing process and then resumed. The shear load as a function of the number of passes for these runs is shown in Fig. 2, which also shows the position and duration of the interruptions. The behavior of the shear load and the extent of molecular weight reduction in these cases is the same as in uninterrupted runs made under the same conditions otherwise.

**2.3 Shearing of Solution of Recovered Degraded Polymer.**—A solution of 10 wt. % Vistanex B-100 polyisobutene in *n*-hexadecane was sheared at 40° and 66,000 sec.<sup>-1</sup> until the shear load became nearly constant for successive passes. The polymer was then recovered by dilution with toluene, precipitation with methanol and vacuum drying to constant weight. It was then again dissolved at 10 wt. % concentration in *n*-hexadecane and again sheared under the previously stated conditions. The shear load during successive passes throughout this procedure is shown in Fig. 3.

During the 80 passes before recovery of the polymer,  $\bar{M}_v$  decreased from 1.74 million to 1.13 million. There was no further decrease in  $\bar{M}_v$  on subsequent shearing after recovery and redissolution. Correspondingly there was no large decrease of shear load with number of passes during shearing after recovery and redissolution. The small shear load decrease with shearing after recovery and redissolution is commonly observed during the initial passes for a solution in cases where there is no decrease of  $\bar{M}_v$  and is probably a slight thixotropic effect. It is not pertinent to the present consideration. The difference in final shear loads before and after recovery and redissolution may be the result of solution non-equilibrium before recovery.

**2.4 Degradation in Presence of Highly Volatile Compound.**—A solution of 10 wt. % Vistanex B-100 polyisobutene, 5% hexane and 85% *n*-hexadecane was sheared at 40° and 66,000 sec.<sup>-1</sup>. The shear load for successive passes is shown in Fig. 4.  $\bar{M}_v$  decreased from 1.74 million to 1.13 million just as it does in degradation under identical shearing conditions in a solution identical except with the hexane replaced by *n*-hexadecane.

The shear load curve for the solution with hexane lies generally about 10% below the curve for an atypical run

without hexane represented by the barred circles in Fig. 4. The shift between the two is probably the direct result of replacing 5% of the hexadecane with hexane. The atypical shape of the shear load curve seems to be reproducible for the solutions with hexane, though it is not so for solutions without hexane. For solutions without hexane the atypical shape of curve is obtained only very seldom and as a rule the typical shape of curve shown by the open circles in Fig. 4 is obtained.

**2.5 Shearing of Fractions from Degraded Polymer.**—A sample of Vistanex B-100 polyisobutene shear degraded from  $\bar{M}_v$  1.74 million to 1.13 million was fractionated by dilution with toluene and fractional precipitation with methanol. The two highest molecular weight fractions were each about 20% of the unfractionated polymer and had  $\bar{M}_v$  values of 1,550,000 and 1,320,000, respectively. These fractions, dissolved at 10 wt. % concentration in *n*-hexadecane, were sheared at 40° and 66,000 sec.<sup>-1</sup>. The resulting shear load curves are shown in Fig. 5. The  $\bar{M}_v$  values after this shearing were 1,500,000 and 1,320,000, respectively. The limits of uncertainty of the intrinsic viscosity determinations are about  $\pm 1\%$ .

Although the measured  $\bar{M}_v$  of the 1.32 million  $\bar{M}_v$  fraction is not reduced after shearing, the sharp drop of shear load after the first pass for this fraction indicates that a small amount of shear degradation, within the limits of uncertainty of the intrinsic viscosity determinations, may have occurred during the shearing of the fraction. Any such degradation could not have amounted to more than one bond rupture per 100 polymer molecules.

**2.6 Degradation of Polymer Fractions.**—A sample of Vistanex B-100 polyisobutene was fractionated. Three of the fractions obtained represented 20–30, 40–50 and 60–65% precipitation. They had  $\bar{M}_v$  values of 3.05, 1.80 and 0.90 million, respectively. These fractions were dissolved at 10 wt. % concentration in *n*-hexadecane. The solutions were sheared at 40° and 66,000 sec.<sup>-1</sup>, after which the  $\bar{M}_v$  values were 1.57, 1.64 and 0.90 million, respectively.

**2.7 Degradation of Polystyrene and Polymethyl Methacrylate.**—A 10 wt. % solution of polystyrene and a 5 wt. % solution of polymethyl methacrylate, both in  $\alpha$ -methylnaphthalene, were sheared at 40° and 66,000 sec.<sup>-1</sup>. The polystyrene was an unfractionated material of about 3 million  $\bar{M}_v$ . The polymethyl methacrylate was a top fraction of about 10% from an unfractionated sample of about 5 million  $\bar{M}_v$ . Both of these polymers were supplied by Dr. L. A. Wall of the Polymer Structure Section of the National Bureau of Standards.

The shear load curves for the shear degradation of these polymers are shown in Fig. 6. The shearing reduced the intrinsic viscosity,  $[\eta]$  in  $\alpha$ -methylnaphthalene at 30° from 4.64 to 4.28 dl./g. for the polystyrene and from 6.88 to 4.03 for the polymethyl methacrylate. These intrinsic viscosity values are not converted to molecular weights since the necessary constants are not established for the polymers in this solvent. The solvent was used because of its low vapor pressure since the viscometer used for degradation cannot be used with solvents having high vapor pressures.

The scatter in the shear load curve for the polystyrene is reproducible as shown by comparing the two runs represented, but its cause is not known. The scatter during the early passes for the polymethyl methacrylate is often observed for especially high molecular weight polymers, and is probably associated with the nature of the degradation process for such polymers.

### 3. Discussion

The unique dependence of the existence and extent of the observed degradation process on the occurrence and severity of shearing is demonstrated by the results of the runs with successive shearing at different rates of shear and those with interruptions in the shearing process (see Figs. 1 and 2). That the observed degradation is not an artifact based on alteration of the solution condition during shearing is demonstrated by the absence of degradation effects during the shearing of the recovered, previously degraded polymer (see Fig. 3).

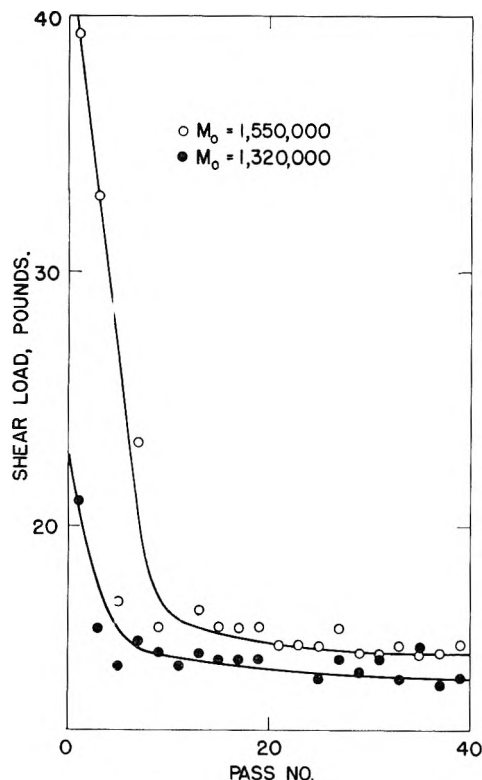


Fig. 5.—Degradation of fractions from degraded polydisperse polymer: ( $M_0$  = molecular weight before shearing).

The insensitivity of the degradation process to the presence of hexane (see Fig. 4) shows that it is not caused by heating from adiabatic collapse of cavities from turbulence or any other source. Because of its relatively high vapor pressure, hexane in solution would increase any such heating. If the observed degradation were pyrolytic and dependent on the above type of heating, rather than mechanical, the presence of hexane would increase the severity of degradation. No cavitation is expected in the shearing reported and these results confirm its absence or lack of influence here.

The degradation results on fractions from degraded samples (Fig. 5) and on fractions from undegraded polymer demonstrates that it is the higher molecular weight individual molecules which are ruptured and that a minimum concentration of such molecules is necessary to produce rupture in any. Apparently the fractionation of the degraded unfractionated polymer concentrated enough molecules of high individual molecular weight into the fractions so that they degraded further on subsequent shearing, although before fractionation their concentration was too low to support further degradation. For the fractions of undegraded polymer the molecular weight below which shear degradation does not occur under the reported conditions is apparently not far below two million. This limit previously was found to be somewhat below one million for the unfractionated, undegraded polymer itself.<sup>4</sup>

The generally similar results for polystyrene and polymethyl methacrylate (Fig. 6) suggest that the degradation observed for the three different chemical compositions occurs by a common general mechanism. The concept of rupturing chemical bonds by concentrating the requisite activation energy into a single bond with the aid of entanglements between individual molecules is consistent with these results.

#### 4. Conclusions

The above discussed indications are all consistent with the proposed mechanical degradation process. No other type of degradation yet proposed is consistent with all the observations reported in this and earlier papers on the process. This is especially true of: (1) the unique dependence of the existence, rate and extent of the process on the severity of shearing, (2) the fact that a critical molecular weight exists, dependent on the

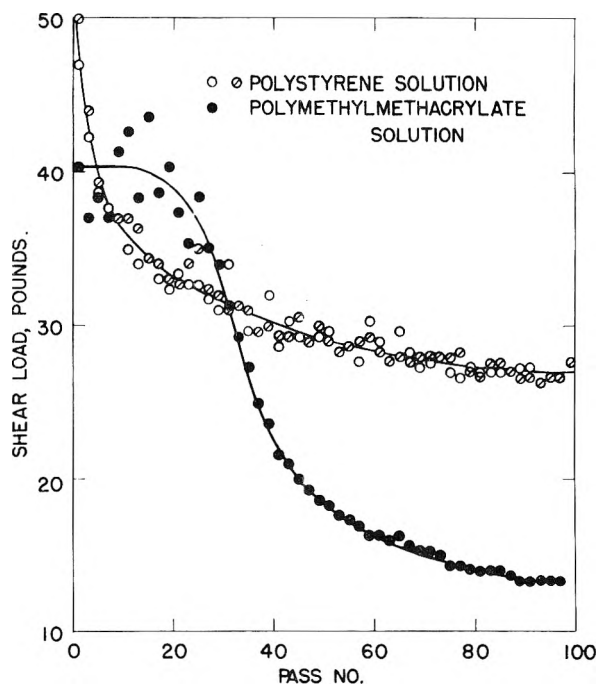


Fig. 6.—Degradation of polystyrene and polymethyl methacrylate solutions.

severity of shearing, above which individual molecules in sufficient concentration suffer this degradation and below which they do not and (3) the fact that the presence of a highly volatile component in solution does not promote the degradation. Little doubt can remain that we are dealing here with mechanical shear degradation.

**Acknowledgments.**—The assistance of Miss H. V. Belcher and of Maria Bestul in some of the experimental work and in the preparation of figures is gratefully acknowledged. The author expresses his appreciation to Dr. George M. Brown of the University of Maryland, who was in charge of the thesis from which parts of this paper were extracted. Thanks are offered to the Enjay Company, Inc., and to Dr. L. A. Wall of the National Bureau of Standards Polymer Structure Section for supplying the polymer samples investigated. Some of the experiments reported were suggested by colleagues. Dr. Philip Goodman, now at the Corning Glass Works, Research Laboratory, Corning, New York, initiated one of the experiments.

# IONIZATION OF ACETYLENE MIXTURES AND OTHER MIXTURES BY $\text{Pu}^{239}$ $\alpha$ -PARTICLES

BY HAROLD J. MOE,<sup>1</sup> T. E. BORTNER AND G. S. HURST

Health Physics Division, Oak Ridge National Laboratory, Oak Ridge, Tennessee

Received September 17, 1956

The ionization produced when  $\text{Pu}^{239}$   $\alpha$ -particles were completely absorbed in binary gas mixtures having acetylene as one of the components was measured. The  $W$  value (electron volts per ion pair) was computed from the known energy and the indirectly measured ionization for various percentages of the two gases in the mixture. The  $W$  values for varying proportions of a binary gaseous mixture were then compared to  $W_m$  as determined by the equation  $1/W_m = (1/W_1 - 1/W_2)Z + 1/W_2$  where  $Z = P_1/(P_1 + \alpha P_2)$  and  $W_m$  is the  $W$  value for a mixture of two gases having partial pressures  $P_1$  and  $P_2$  and  $W$  values  $W_1$  and  $W_2$ , respectively. Good agreement was found when the following values were used for the empirical constant " $\alpha$ ":  $\text{N}_2\text{-C}_2\text{H}_2$ , 0.265;  $\text{CO}_2\text{-C}_2\text{H}_2$ , 0.927;  $\text{CH}_4\text{-C}_2\text{H}_2$ , 0.386;  $\text{N}_2\text{-CH}_4$ , 0.617;  $\text{He-C}_2\text{H}_2$ , 0.058;  $\text{C}_2\text{H}_2\text{-A}$ , 3.42;  $\text{C}_6\text{H}_6\text{-A}$ , 5.376;  $\text{CH}_4\text{-A}$ , 2.00. The  $W$  values for mixtures of neon with acetylene would not yield to this interpretation.

## Introduction

In radiation chemistry ionization appears to play a dominant role in the course of radiation induced reactions. Lind<sup>2</sup> shows, for example, that for every ion pair produced by the action of  $\alpha$ -particles on acetylene, twenty  $\text{C}_2\text{H}_2$  molecules are polymerized to form a solid material. Furthermore, Lind shows that reactions of this type may proceed at a faster rate if certain other gases are present. Clearly then, the amount of ionization produced by  $\alpha$ -particles in gas mixtures is of great importance. Because of current interest<sup>3</sup> in the radiolysis of acetylene, this work consists primarily of a study of the amount of ionization produced in acetylene when mixed with various other gases. These quantities will be expressed in terms of  $W$ , *i.e.*, the total  $\alpha$ -particle energy divided by the total number of ion pairs. Huber, *et al.*,<sup>4</sup> assumed that, in the case of a mixture,  $\alpha$ -particles lose a fraction of their energy to each gas component and that after this allocation of energy no further energy transfers took place. With this assumption the  $W_m$  for the mixture was given by

$$\frac{1}{W_m} = \left( \frac{1}{W_1} - \frac{1}{W_2} \right) Z' + \frac{1}{W_2} \quad (1)$$

where  $Z' = (S_1 P_1)/(S_1 P_1 + S_2 P_2)$  and  $W_1$  and  $W_2$  are the  $W$  values for the two gas components having molecular stopping powers  $S_1$  and  $S_2$  and pressures  $P_1$  and  $P_2$ . In radiation chemistry the assumption has been made that the amount of ionization produced in a binary mixture is simply the sum of the ionization that would have been produced in the individual gases. This essentially amounts to eq. 1. The error introduced by this assumption can be seen from what follows.

If the measured values of  $1/W_m$  are plotted as a function of  $Z'$ , the curve would be a straight line if eq. 1 held. However, in many cases of the application of the equation to experimental data, large deviations occurred. Haerberli, *et al.*,<sup>5</sup> attempted an

explanation using the assumption that a portion of the  $\alpha$ -particle energy is used to form  $\delta$ -rays and that this energy is divided between the gas components in proportion to their stopping powers for  $\delta$ -rays. This assumption led to a modified form of the original equation. Bortner and Hurst<sup>6</sup> showed that the same modified form could be obtained by an assumption that the "effective" stopping power ratio is not determined from the stopping powers reported in the literature. They further showed that the more complex equation could be reduced to eq. 1 if the requirements on  $Z'$  be relaxed, *i.e.*

$$\frac{1}{W_m} = \left( \frac{1}{W_1} - \frac{1}{W_2} \right) Z + \frac{1}{W_2} \quad (2)$$

where  $Z = P_1/(P_1 + \alpha P_2)$  in which " $\alpha$ " is an empirically determined constant for a particular mixture and reduces to  $S_2/S_1$  in cases where eq. 1 holds.

Equation 2 is found to be a good empirical representation of a vast amount of data. In a few cases the data cannot be represented by eq. 2 but even in these cases, this equation is useful in separating sudden changes in  $1/W_m$  as a function of  $Z$  from the more gradual ones.

**Apparatus and Method.**—The apparatus<sup>6</sup> consists of a large parallel-plate ionization chamber enclosed in a vacuum system. An uncollimated  $\text{Pu}^{239}$   $\alpha$ -source is placed at the center of the lower plate. The rate of ionization is measured by collecting the ions with an electric field and observing the rate of change of voltage on a capacitor. This rate of change is calibrated by using  $\text{N}_2$ , a gas in which the  $W$  value is well known. The best available grades of the gases were used and these were further purified by fractional distillation with a liquid nitrogen cold trap.

## Results

The results are shown in Figs. 1–10. In all cases the data are first compared to eq. 1, using literature values for the stopping powers of the component gases. The values for the atomic stopping power of all the gases except neon are quoted from von Trautenberg.<sup>7</sup> These are normalized with oxygen, *i.e.*,  $S_0 = 1.00$ . Attention should be directed to this fact since most tables give molecular stopping powers relative to air. Normalization to oxygen is the most convenient scale, for then the molecular stopping power may be obtained by simply adding<sup>8</sup> the values for all the atoms in the molecule.

(6) T. E. Bortner and G. S. Hurst, *Phys. Rev.*, **93**, No. 6, 1236 (1954).

(7) H. R. von Trautenberg, *Z. Phys.*, **5**, 396 (1921).

(8) L. H. Gray, *Proc. Camb. Phil. Soc.*, **40**, 72 (1944).

(1) A.E.C. Radiological Fellow.

(2) S. C. Lind, "The Chemical Effects of Alpha Particles and Electrons," The Chemical Catalog Company, Inc., Reinhold Publ. Corp., New York, N. Y., 1928.

(3) See, for example, L. M. Dorfman and F. J. Shipko, *J. Am. Chem. Soc.*, **77**, 4723 (1955); S. C. Lind, *THIS JOURNAL*, **56**, 920 (1952); **58**, 800 (1954).

(4) P. Huber, E. Baldinger and W. Haerberli, *Helv. Phys. Acta*, **23**, Suppl. III (1949).

(5) W. Haerberli, P. E. Huber and E. Baldinger, *ibid.*, **26**, 145 (1953).

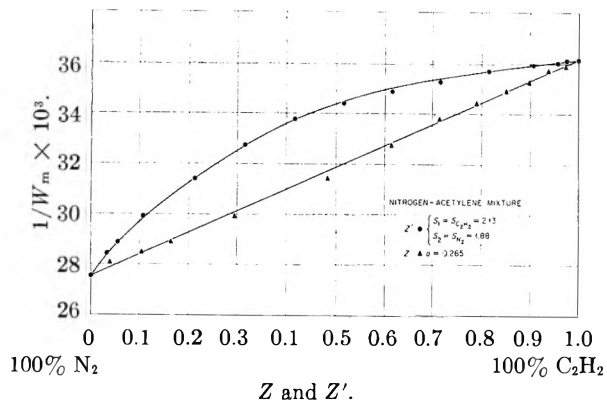


Fig. 1.—Nitrogen-acetylene mixture:  $Z'$  (●),  $S_1 = S_{C_2H_2} = 2.13$ ,  $S_2 = S_{N_2} = 1.88$ ;  $Z$  (▲),  $a = 0.265$ .

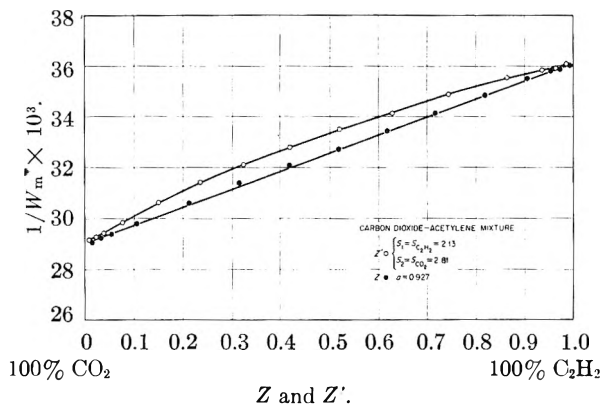


Fig. 2.—Carbon dioxide-acetylene mixture:  $Z'$  (○),  $S_1 = S_{C_2H_2} = 2.13$ ,  $S_2 = S_{CO_2} = 2.81$ ;  $Z$  (●),  $a = 0.927$ .

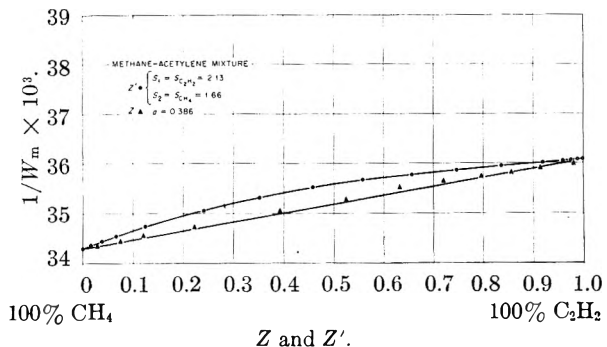


Fig. 3.—Methane-acetylene mixture:  $Z'$  (●),  $S_1 = S_{C_2H_2} = 2.13$ ,  $S_2 = S_{CH_4} = 1.66$ ;  $Z$  (▲),  $a = 0.386$ .

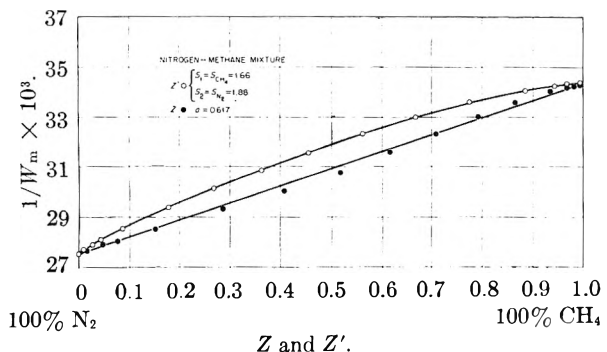


Fig. 4.—Nitrogen-methane mixture:  $Z'$  (○),  $S_1 = S_{CH_4} = 1.66$ ,  $S_2 = S_{N_2} = 1.88$ ;  $Z$  (●),  $a = 0.617$ .

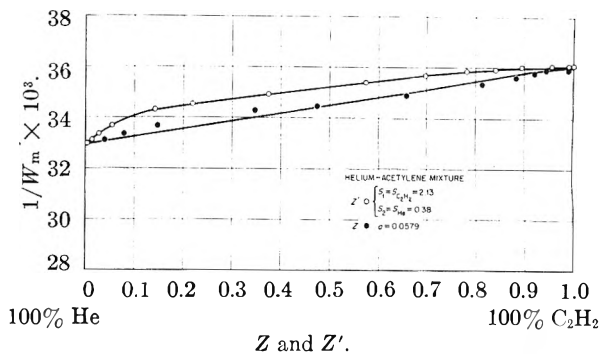


Fig. 5.—Helium-acetylene mixture:  $Z'$  (○),  $S_1 = S_{C_2H_2} = 2.13$ ,  $S_2 = S_{He} = 0.38$ ;  $Z$  (●),  $a = 0.0579$ .

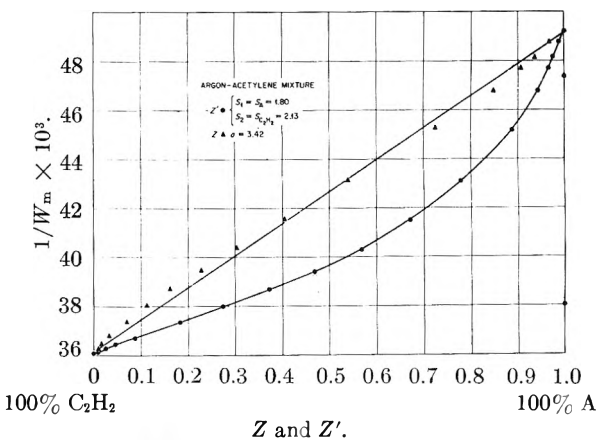


Fig. 6.—Argon-acetylene mixture:  $Z'$  (●),  $S_1 = S_A = 1.80$ ,  $S_2 = S_{C_2H_2} = 2.13$ ;  $Z$  (▲),  $a = 3.42$ .

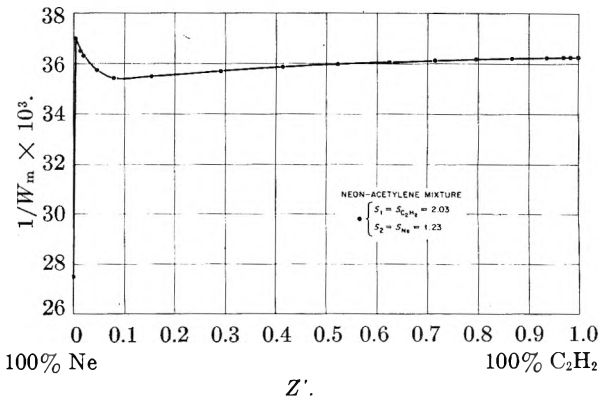


Fig. 7.—Neon-acetylene mixture: ●,  $S_1 = S_{C_2H_2} = 2.03$ ;  $S_2 = S_{Ne} = 1.23$ .

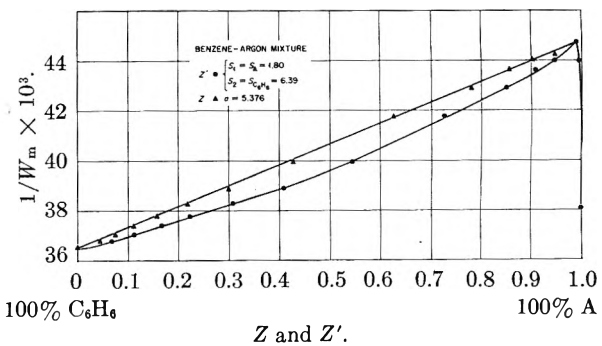


Fig. 8.—Benzene-argon mixture:  $Z'$  (●)  $S_1 = S_A = 1.80$ ,  $S_2 = S_{C_6H_6} = 6.39$ ;  $Z$  (▲),  $a = 5.376$ .

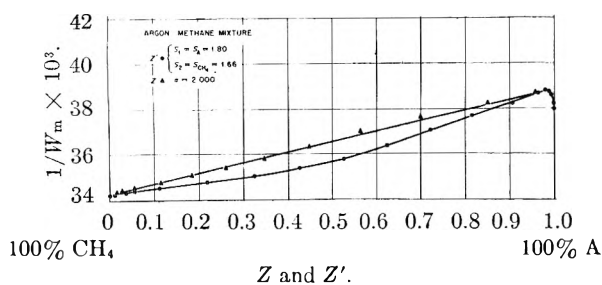


Fig. 9.—Argon-methane mixture:  $Z'$ (●),  $S_1 = S_A = 1.80$ ,  $S_2 = S_{CH_4} = 1.66$ ;  $Z$ (▲),  $a = 2.000$ .

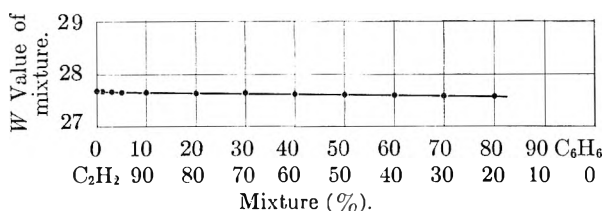


Fig. 10.—Graph of  $W$  value for acetylene-benzene mixture vs. % mixture.

The atomic stopping power for neon is quoted from Mano<sup>9</sup> and this value is relative to air. In general, the data do not fall on a straight line when plotting  $1/W_m$  against  $Z'$ . When the best value for "a" is found, eq. 2 fits the data very well. Comparison of "a" with  $S_2/S_1$  for the mixtures are shown in Table I.

TABLE I

Gas mixture	$S_2/S_1$	"a"	Fig. no.
$N_2-C_2H_2$	0.883	0.265	1
$CO_2-C_2H_2$	1.34	.927	2
$CH_4-C_2H_2$	0.779	.386	3
$N_2-CH_4$	1.13	.617	4
$He-C_2H_2$	0.178	.058	5
$C_2H_2-A$	1.18	3.42	6
$Ne-C_2H_2$	0.577	..	7
$C_6H_6-A$	3.55	5.38	8
$CH_4-A$	0.922	2.00	9
$C_2H_2-C_6H_6$			10

The most pronounced departure from the unmodified  $Z'$  plot (*i.e.*, using eq. 1) is found in the  $N_2-C_2H_2$  mixture (Fig. 1). In the cases in which small percentages of the second component greatly increase the ionization of the mixture (*i.e.*,  $He-C_2H_2$ ,  $A-C_2H_2$ , etc.), the minimum  $W$  value obtained is used in eq. 2 for the determination of "a."

Figure 5 is the curve obtained for helium and acetylene. In the case of helium, the addition of very small percentages of a second gas produces a very rapid increase in ionization. Jesse<sup>10,11</sup> has made a thorough study of the effect of impurities added to helium, and he attributes the sudden increase in ionization to the metastable state in helium. In the present study, when the mixture is 0.13% acetylene in helium,  $W$  has a value of 30.3 plus or minus 0.3 e.v./ip.<sup>12</sup> The subsequent increase in ionization is due to the greater rate of ionization with the addition of larger percentages of acetylene.

The  $W$  value 30.3 was used as  $W_{He}$  to determine the value for "a."

The curve for acetylene and argon is shown in Fig. 6. Much has been written<sup>13-15</sup> on the effect of the argon metastable state on the ionization produced in a mixture. The maximum ionization in this mixture occurred at 0.5% acetylene in argon. The  $W$  value at this percentage mixture was 20.3 plus or minus 0.2 e.v./ip. This curve shows the importance of eq. 2 in separating the sudden change in ionization due to the metastable state from the more gradual one.

The  $W$  value for the mixture of neon with acetylene, Fig. 7, cannot be expressed by eq. 2. The effect for very small percentages of acetylene is similar to that in argon, with the maximum ionization occurring at a mixture of 0.33% acetylene in neon. However, the ionization then decreases reaching a minimum which is below the ionization in acetylene. A possible explanation for this effect is that with increasing amounts of acetylene, metastable states are lost through three-body collisions in which the energy is shared by the two acetylene molecules; thus neither of the molecules would be ionized. However, the cross-section for this reaction is not likely to be large enough to account for the magnitude of the decrease in current. Another possible reaction is the one in which a  $C_2H_2$  molecule collides with the metastable Ne atom giving the latter enough energy to raise the state of excitation from a metastable one to a radiative one.

Figure 8 shows the extrapolated curve for benzene mixed with argon. The curve could not be run to 100% benzene because there were no facilities to keep the chamber at a high temperature to prevent the benzene vapor from condensing at the higher partial pressure mixtures. The maximum ionization is reached at 0.5% benzene in argon. The  $W$  value of the mixture at this point is 23.3 plus or minus 0.2 e.v./ip. Here again the effect of the argon metastable state on the ionization can be seen.

The curve of methane in argon (Fig. 9) shows an effect which has led to the belief<sup>15</sup> of an excited state in argon at about 15 e.v. Since the ionization potential of methane is 13.1 e.v., it is impossible to explain the increase in ionization as due to the argon metastable state which is 11.5 e.v. Since the curve is similar to those found for argon mixtures which can be explained on the basis of the metastable state, it is possible that there exists in argon an excited state which can explain the increase in ionization. Because the effect is not as great as in those gases whose ionization potentials are below 11.5 e.v., and because it does not reach a maximum until a greater amount of the second component is present (*i.e.*, 3% methane), it is believed that the effect is due to an excited state having a life time longer than that of most excited states but less than a metastable life time. The maximum amount of ionization occurs with 3% methane and the  $W$  value for the mixture at that point is 25.8 plus or minus 0.3 e.v./ip.

The last curve shown (Fig. 10) is simply a plot of

(9) G. Mano, *Ann. Phys.*, **1**, 407 (1934).

(10) W. P. Jesse, ANL-4944, 2 (1952).

(11) W. P. Jesse, *Phys. Rev.*, **100**, No. 6, 1755 (1955).

(12) The absolute accuracy claimed for  $W$  is plus or minus 1%.

(13) W. P. Jesse, ANL-4828, 5 (1952).

(14) J. Sharpe, *Proc. Phys. Soc. (London)*, **A65**, 859 (1952).

(15) C. E. Melton, G. S. Hurst and T. E. Bortner, *Phys. Rev.*, **96**, 643 (1954).

the  $W$  value for percentage mixtures of acetylene with benzene as a function of the percentage mixture. The curve appears to be a straight line which extrapolates to a value of 27.5 plus or minus 0.3 e.v./ip. for the  $W$  value of benzene.

#### Discussion

In all mixtures studied, except Ne-C<sub>2</sub>H<sub>2</sub>, it is found that eq. 2 accurately represents the  $W$  values for  $\alpha$ -particles losing their entire energy in the gas mixture. Table I shows that appreciable errors would be made by assuming eq. 1. It is fur-

ther emphasized that the constant " $a$ " appearing in eq. 2 has, to this date, no correlation with other physical constants of the gases comprising the mixture.

**Acknowledgments.**—The authors wish to express their thanks to Dr. Robert L. Platzman of Purdue University for his interest in and suggestion of these mixtures. We also wish to thank Dr. S. C. Lind and Dr. P. S. Rudolph of the Chemistry Division, Oak Ridge National Laboratory, for stimulating discussions on the subject.

## MECHANISM OF HIGH ENERGY RADIATION EFFECTS IN POLYMERS

BY ROBERT SIMHA AND LEO A. WALL

*Department of Chemical Engineering, New York University, New York, N. Y.*

*Polymer Structure Section, National Bureau of Standards, Washington, D. C.*

*Received September 19, 1956*

A series of elementary processes for cross-linking and scission reactions based on free radical intermediates in a homogeneous system are proposed. The kinetic evaluation under several approximations leads to expressions for the amounts of volatiles, unsaturation, cross-links and scissions as functions of time and intensity of radiation. The dependence of the rates on intensity is linear only in special cases. Isotopic substitution with deuterium should decrease the production of unsaturation. Hydrogen yield, on the other hand, can remain constant if certain conditions are fulfilled. The observed isotopic differences in polystyrene may indicate an additional step for the capture of atoms. This is suggested to occur through the phenyl ring. Qualitative considerations that seem to favor free radical over ion intermediates in polymers are mentioned.

#### Introduction

A number of investigations of the effects of atomic radiation on solid polymers have been reported during recent years.<sup>1-3</sup> The most obvious changes are either predominant cross-linking or predominant scission. These are accompanied by an evolution of volatiles such as hydrogen and the formation of double bonds. The results are not only sensitive to the structure of the repeating unit but also depend on the method of sample preparation.

Formulation of possible mechanisms and their kinetic evaluation are necessary for a quantitative description of the observed over-all effects and for a comprehension of the basic processes. Most efforts in this direction have dealt with gross over-all effects.<sup>4,5</sup> Recently a series of elementary mechanisms have been postulated and the ensuing kinetics developed by Okamoto and Ishihara.<sup>6</sup> Some of the steps to be proposed here are similar to theirs. Others, however, are significantly different and hence the over-all results are different.

One may think of the development of a theory which gives, in terms of elementary processes, over-all rates as well as information about changes in molecular weight and molecular weight distribution, similar to that which has been done<sup>7,8</sup> for free

radical thermal depolymerization. This is more difficult, particularly when simultaneous build-up and breakdown processes are to be considered. Moreover, basic knowledge of the steps is much more limited and hence we are by necessity, here, more speculative. We shall therefore deal only with rates of production of double bonds, volatiles, unstable species such as H atoms, radical "sites" along a chain, cross-links and scissions.

A number of fundamental assumptions will be made. First, ionic processes will be entirely disregarded and only certain selected free radical processes considered. Second, the kinetics considered will be that appropriate to a homogeneous system, such that spatial coordinates do not appear in the rate equations and diffusion rates do not enter the picture. Third, actual integrations are performed under steady-state conditions with respect to atomic species and all types of radicals. Since the processes take place in the solid state, this can be a questionable assumption as we know from free radical polymerization. It will nevertheless be used in this first attempt, to facilitate the mathematical operations.

For the same reason several further simplifying approximations will appear in the treatment. Some of these can be justified on a chemical basis; others may well have to be revised. In any instance, where a term has been discarded, only the zero approximation with respect to this term has been pursued. However, we believe that the elementary processes proposed here will have to appear in any kinetic treatment of radiation effects on polymers, provided the first two assumptions are reasonable.

(1) K. H. Sun, *Modern Plastics*, **32**, 141 (1954).

(2) Leo A. Wall, Conference on Effects of Radiation on Dielectric Materials, Naval Research Laboratory, Washington, D. C., Dec. 14-15, 1954, ONR Symposium Report ACR-2, page 139.

(3) R. Simha and L. A. Wall, Chapter to appear in "Catalysis Series," edited by P. H. Emmett.

(4) A. Charlesby, *Proc. Roy. Soc. (London)*, **222A**, 60 (1954).

(5) A. R. Schultz, Nuclear Engineering and Science Congress, Dec. 12-16, 1955 (Cleveland, Ohio).

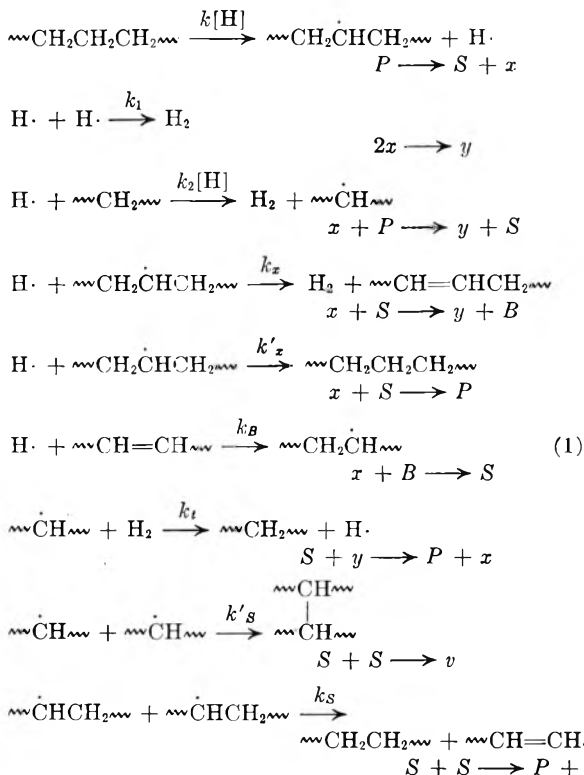
(6) H. Okamoto and A. Ishihara, *J. Polymer Sci.*, **20**, 115 (1956).

(7) R. Simha, L. A. Wall and P. J. Blatz, *ibid.*, **5**, 615 (1950).

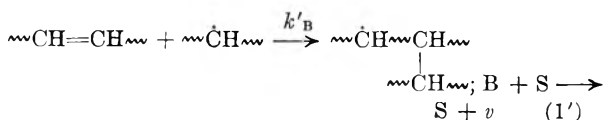
(8) R. Simha and L. A. Wall, *THIS JOURNAL*, **56**, 707 (1952).

## Kinetics without Main Chain Scission

For simplicity we consider first the cross-linking process in the prototype vinyl polymer, polymethylene or linear polyethylene. The following postulated reactions are expressed both chemically and symbolically.



An additional reaction of double bonds leading to crosslink formation, *viz.*



will be disregarded until later, since it merely modifies somewhat the final results.

From (1) we derive the set

$$\begin{aligned} dx/dt &= k[\text{H}] - 2k_1x^2 - [k_2[\text{H}] + (k_x + k'_x)S + k_B B]x + k_t yS \\ dS/dt &= k[\text{H}] + k_2[\text{H}]x - (k_x + k'_x)Sx + k_B Bx - k_t yS - (k_s + k'_s)S^2 \\ dB/dt &= k_x Sx - k_B Bx + (k_s/2)S^2 \\ dy/dt &= k_1x^2 + [k_2[\text{H}] + k_x S]x - k_t yS \\ dv/dt &= (k'_s/2)S^2 \end{aligned} \quad (2)$$

No equation for C-H bonds has been written and their number is assumed to remain constant during the irradiation, which is reasonable enough. Thus  $k[\text{H}]$  and  $k_2[\text{H}]$  may be regarded as constants, the former being moreover proportional to the intensity  $I$  of radiation.

From (2) one has

$$dy/dt = dE/dt + dv/dt + 1/2(dS/dt - dx/dt) \quad (3)$$

where the parenthesis vanishes under the assumption of a steady state with respect to  $S$  and  $x$ . This condition yields

$$x \{k_2[\text{H}] + k_B B - (k_x + k'_x)S\} = (k_s + k'_s)S^2 + k_t yS - k[\text{H}]$$

On substitution into

$$k_1x^2 + (k_2[\text{H}] + k_B B)x = k_t yS + [(k_s + k'_s)/2]S^2$$

a quartic in  $S$  results. Manageable relations are obtained by making the following alternative approximations

$$\begin{aligned} (k_2[\text{H}] + k_B B)x &\leq k_1x^2 & (a), (a') \\ 2k_t yS &\leq (k_s + k'_s)S^2 & (b), (b') \\ (k_x + k'_x)Sx &\ll (k_2[\text{H}] + k_B B)x & (c) \end{aligned}$$

We shall find that alternatives (a) and (a'), that is, essentially, abstraction of H by H· preferred over combination of two H, or *vice versa*, do not lead to fundamentally different results. However, the consequences of (b) and (b'), respectively, are very different. This can already be concluded from the fact that  $k_t yS$  is the only negative term in  $dy/dt$ , eq. 2. Considering the difference in bond energies of H-H and C-H, (b) seems more reasonable. Condition (c) means essentially preferred abstraction of H from any C-H bond rather than from loci adjacent to radical sites  $S$  or addition to sites. This is justifiable only as a concentration effect under usual irradiation conditions and by assuming that H atoms or other mobile active species can diffuse rapidly enough. In any case, (c) is required only in conjunction with (a) and (b) which otherwise still result in a cubic for  $S$ , but not with (a', b).

We now have

$$S = \{2k[\text{H}]/(k_s + k'_s)\}^{1/2}; \quad x = k[\text{H}]/(k_2[\text{H}] + k_B B); \\ dB/dt = (K_2 - K_1 B)/(k_2[\text{H}] + k_B B)$$

with

$$\begin{aligned} K_1 &= k[\text{H}] k'_s k_B / (k_s + k'_s); & (4a, b, c) \\ K_2 &= 2^{1/2} k[\text{H}] (k_s + k'_s)^{-1/2} \{k_x (k[\text{H}])^{-1/2} + k_s k_2 [\text{H}] / [2(k_s + k'_s)]^{1/2}\} \end{aligned}$$

and the integral

$$-K_1 t = k_B B + (k_2[\text{H}] + k_B B_\infty) \ln(1 - B/B_\infty)$$

where  $B_\infty = K_2/K_1$  represents the saturation value of double bonds  $B$ . Finally, the rate of production of  $\text{H}_2$  gas is

$$dy/dt = k[\text{H}]k'_s/(k_s + k'_s) + dB/dt = (dy/dt)_{t \rightarrow \infty} + dB/dt$$

and

$$dv/dt = k[\text{H}]k'_s/(k_s + k'_s)$$

Thus  $dy/dt$  decreases with increasing  $t$  and approaches a limiting value (see Fig. 1). This is valid as long as variations in the number of C-H bonds are negligible and, in addition, condition (b) is not violated. The rate of cross-linking is constant since  $S$  is constant;  $x$  decreases to a constant value as  $B$  increases from zero to  $B_\infty$ .

Conditions (a', b) yield the results

$$S = \{k[\text{H}]/(k_s + k'_s)\}^{1/2} / \{1 + (k_x + k'_x) / [2k_1(k_s + k'_s)]^{1/2}\}^{1/2} \\ x = \{(k_s + k'_s)/2k_1\}^{1/2} S \quad (4a', b')$$

$$dB/dt = C_2 - C_1 B$$

with

$$\begin{aligned} C_1 &= k_B \{(k_s + k'_s)/2k_1\}^{1/2} S \\ C_2 &= \{k_x [(k_s + k'_s)/2k_1]^{1/2} + k_s/2\} S^2 \end{aligned}$$

the integral:  $B = B_\infty (1 - e^{-C_1 t})$ ;  $B_\infty = C_2/C_1$ ;

and  $dy/dt = dB/dt + k'_S/2 S^2$ ;  $dv/dt = (k'_S/2)S^2$ . Thus the two results (4) are of similar form (see Fig. 1 dashed lines).

It is of interest to examine the dependence on radiation intensity. According to (4a, b, c),  $B_\infty$  is a linear function of the square root  $I^{1/2}$ . However, if  $k_S$  is of the order of  $k'_S$  or larger, the variable term is eliminated by virtue of condition (c) and the final amount of unsaturation in the polymer is independent of intensity. The rate of attainment of this value is governed by  $K_2$  and thus depends on  $I$  as the first power or stronger, if the  $k_x$ -term is not negligible. The rate of cross-linking and the limiting rate  $(dy/dt)_\infty$  are proportional to  $I$ . From (4a',b) on the other hand,  $B_\infty$  is proportional to  $S$  and, hence, to  $I^{1/2}$ . The initial rate  $dB/dt$  varies as  $I$ ;  $(dy/dt)_\infty$  and  $dv/dt$  are proportional to  $I$ . Thus one may be able to distinguish between the two cases of rapid and slow combination of H atoms by means of the difference in  $B_\infty$  as a function of  $I$ .

Finally we consider the effect of isotope substitution. With  $J > 1$ , denoting the isotopic ratio of respective rate constants, we have

$$\begin{aligned} k_2[\text{H}]/k_2[\text{D}] &= k_x^{\text{H}}/k_x^{\text{D}} = k_S^{\text{H}}/k_S^{\text{D}} = J \\ k_t^{\text{H}}/k_t^{\text{D}} &= J' > J \end{aligned}$$

assuming that the diverse abstraction processes are all governed by the same factor  $J$ , and that the remaining constants are not affected. Now in (4a, b, c),  $B_\infty \propto \text{constant} \cdot k_x(k_S + k'_S)^{1/2} + \text{constant} (k_S k_2[\text{H}])$ . Hence a sharp reduction in  $B_\infty$  occurs by a factor of the order of  $J^2 \approx 6-9$ . The rate  $dB/dt$  is less diminished, particularly if the  $k_x$ -term is not negligible.

We can express the dependence of  $y$  on  $J$  by means of the equation, following from (4a, b, c).

$$k_B(dy/dt) = K_1(k_2[\text{H}] + k_B B_\infty)/(k_2[\text{H}] + k_B B)$$

Whence, for  $k'_S \ll k_S$

$$(dy/dt)_0 = \text{constant} (k_2[\text{H}]J) + \frac{\text{constant} (k_x k_S^{1/2} J^{1/2})}{\text{constant} (k_2[\text{H}]k_S)}$$

$$(dy/dt)_\infty = \text{constant} (J)$$

and for  $k'_S \gg k_S$

$$(dy/dt)_0 = \text{constant} (k_2[\text{H}]) + \frac{\text{constant} (k'_S^{1/2} k_x)}{\text{constant} (k_S k_2[\text{H}]/J)}$$

$$(dy/dt)_\infty = \text{constant}$$

Also

$$dv/dt = (dy/dt)_\infty = \text{constant} (k'_S/(k'_S + k_S/J))$$

In (4a',b),  $S$  is increased for the D-isotope, provided the abstraction rates  $k_x$  and  $k_S$  are not small in comparison with the corresponding addition steps  $k'_x, k'_S$ .  $B_\infty$  is reduced in any case but by the lesser factor  $1/J$  or weaker, since, by assumption, the recombination of atoms is not changed. The rate  $dB/dt$  is decreased.

Equation 4a'b yields

$$dy/dt = (k'_S/2)S^2 + C_2(1 - B/B_\infty)$$

Thus for  $k'_S \ll k_S, k'_x \ll k_x$

$$(dy/dt)_0 = \text{const. } J/(1 + \text{const. } J^{-1/2}) + \text{const. } J^{-3/2} + \text{const. } J^{-1}$$

$$(dy/dt)_\infty = \text{const. } J/(1 + \text{const. } J^{-1/2})$$

and for  $k'_S \gg k_S, k'_x \gg k_x$

$$(dy/dt)_0 = \text{const.} + \text{const.}/J$$

$$(dy/dt)_\infty = \text{const.}$$

Thus  $(dy/dt)_\infty$  and the rate of cross-linking increase for the heavier isotope when addition steps involving radicals  $S$  are less important than abstraction steps. In the opposite instance they remain constant. The initial rate  $(dy/dt)_0$  also increases in the first instance, even from (4a',b), since the first term ought to predominate. In the opposite case,  $(dy/dt)_0$  is smaller for the heavier isotope.

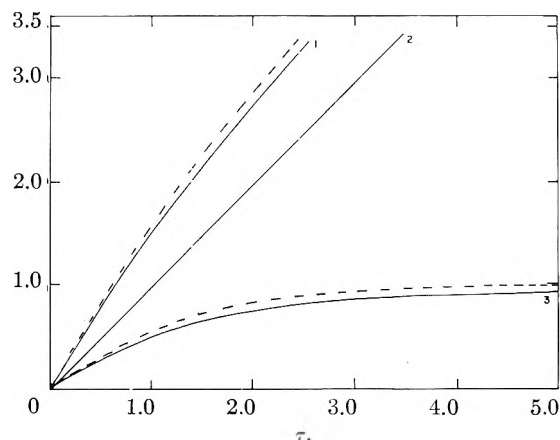


Fig. 1.—Product concentrations as function of time in reduced variables; Equations 4a, b, c, for  $k_2[\text{H}]/k_B B_\infty = 1$ : 1, hydrogen,  $y/B_\infty$ ; 2, cross-links,  $v/B_\infty$ ; 3, double bonds,  $B/B_\infty$ . Dashed lines correspond to 1 and 3, for eq. 4a', b, with  $k'_S S^2/(2C_2) = 1$ ; curve 2 is unchanged in this special case.

Wall and Brown<sup>9</sup> found that the gas evolution from  $\gamma$ -irradiated polyethylene remains practically unchanged on complete deuteration of the polymer. In polystyrene, on the other hand, deuteration reduces the gas evolution by a factor of approximately 2.5. To interpret both results on the basis of the processes (1) and the approximations made requires for the former polymer the assumption that the addition steps  $k'_S$  and  $k'_x$  are more important than  $k_S$  and  $k_x$  in  $(dy/dt)_\infty$ . Under the same assumption only  $(dy/dt)_0$  can be reconciled with the experimental result for polystyrene. An experimental analysis of the isotope effect in double bond formation is very desirable.

The approximations used thus far lead to a limiting finite rate  $(dy/dt)_\infty$  and an asymptotic approach to a maximum value  $B_\infty$ , provided, of course, that volatiles remain in the reaction mixture. The behavior of  $dy/dt$  arises from the elimination of the only step in (1), viz.,  $k_2 y S$ , which consumes  $y$ -molecules. Under certain conditions the set (2) will lead to a maximum value of  $B$  at an intermediate time, whereas  $y$  itself approaches asymptotically a steady state. This is, for example, the case under conditions (a,b'). If, moreover,  $k_2[\text{H}] \gg k_B B, S$  turns out to be proportional to  $y^{-1/2}$ . Hence the cross-linking rate decreases monotonically. Also  $y$  is found to approach a steady value, as one might expect, and  $B$  to reach a maximum. We do not think at this stage that a more detailed description of these results is necessary.

(9) Leo A. Wall and D. W. Brown, THIS JOURNAL, 61, 129 (1957).

It remains to consider the influence of eq. 1', which results in the additional terms

$$(dv/dt)_{\text{add}} = -(dB/dt)_{\text{add}} = k'_B SB$$

We find now in place of (4a,b,c)

$$dB/dt = B_\infty(1 - B/B_\infty)[K'_1 + K_3(B_\infty + B)]/(k_2[H] + k_B B)$$

with

$$\begin{aligned} 2K_3 B_\infty &= \sqrt{K'_1{}^2 + 4K_2 K_3} - K'_1 \\ K'_1 &= K_1 + k_2[H]K_3/k_B \\ K_3 &= k'_B k_B [2k[H]/(k_S + k'_S)]^{1/2} \end{aligned}$$

which is readily integrated, leading once more to an essentially exponential solution, and where  $dy/dt$  again approaches a limiting value equal to

$$(dy/dt)_\infty = (k'_S/2)S^2 + k'_B SB_\infty = (dv/dt)_\infty$$

There is now a delayed approach to the limiting rate of cross-linking. However,  $dy/dt$  continues to decrease monotonically, since the quantity  $dB/dt - k'_B S(B_\infty - B)$  is positive for  $B < B_\infty$ . These results somewhat modify the dependence of the cross-linking rate on intensity  $I$ .

Conditions (a',b) yield similar results. The parameter  $C_1$  in eq. 4a,b is replaced by  $C + k'_B S$ ,  $B_\infty$  remains proportional to  $I^{1/2}$ , and  $(dv/dt)_\infty$  and  $(dv/dt)_0$  remain proportional to  $I$ .

Figure 1 shows the reaction products as functions of time at a given intensity  $I$  according to eq. 4,a,b,c and 4a,b, respectively. These can be written in the reduced forms

$$\begin{aligned} -\tau &= B/B_\infty + [1 + k_2[H]/k_B B_\infty] \ln(1 - B/B_\infty) \\ y/B_\infty &= \tau + B/B_\infty \\ v/B_\infty &= y/B_\infty - B/B_\infty \end{aligned}$$

with

$$\tau = K_1 t / (k_B B_\infty)$$

and

$$\begin{aligned} B/B_\infty &= 1 - e^{-\tau} \\ y/B_\infty &= k'_S S^2 / (2C_2) \tau + B/B_\infty \end{aligned}$$

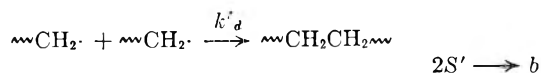
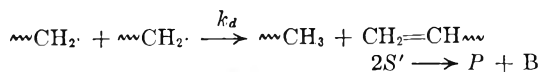
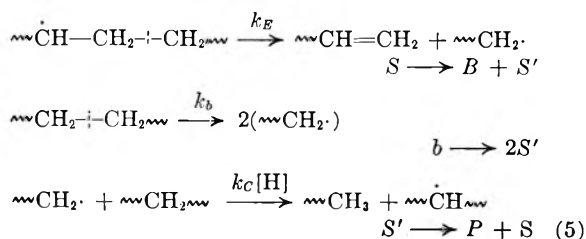
with

$$\tau = C_1 t$$

Thus, as pointed out previously, only  $B$  reaches saturation under the approximations (a,b,c) or (a',b). The reason for this, as stated before, is the assumed constancy of the (C-H)-concentration, which restricts the treatment to moderate intensities and conversions. However, in both situations the rates of hydrogen and double bond formation decrease continuously while the rate of cross-link formation is constant. Because of our choice of constants for Fig. 1, the latter quantity is identical for both cases.

### Kinetics with Main Chain Scission

We now superimpose on eq. 1 the processes



An additional step, the combination of  $S$  and  $S'$  sites to form a branched structure, will again be disregarded for the present. Equation 5 yields the additional terms

$$\begin{aligned} (dS/dt)_{\text{add}} &= -k_E S + k_C[H]S' \\ (dB/dt)_{\text{add}} &= k_E S + k_d S'^2 \\ dS'/dt &= k_E S - k_C[H]S' - 2(k_d + k'_d)S'^2 + 2k_b b \quad (6) \\ db/dt &= -k_b b + k'_d S'^2 - k_E S \end{aligned}$$

Equation 3 now becomes

$$dy/dt = dB/dt + (k'_S S^2/2) + 1/2(dS/dt - dx/dt) + 1/2dS'/dt + db/dt \quad (3')$$

In evaluating  $S'$  for a steady state we assume at once

$$k_C[H] \cdot S' \gg 2(k_d + k'_d)S'^2 \quad (D)$$

which becomes equivalent to

$$(k_d + k'_d)(k_E S + 2k_b b) \ll (k_C[H])^2$$

The preferred abstraction of an H by a site  $S'$  rather than mutual interaction is justifiable on the basis of concentration. However, a cage effect may vitiate condition (D). Equation 6 then yields

$$k_C[H]S' = k_E S + 2k_b b; \quad (dS/dt)_{\text{degr}} = 2k_b b$$

Hence  $(dS/dt)_{\text{total}}$  can be written as previously, provided  $k[H]$  is replaced by  $k[H] + 2k_b b$ , which is again proportional to  $I$ . Referring to the case (a,b,c), the expressions for  $S$  and  $x$  in (4a,b,c) are correspondingly modified. They show that the build-up and breakdown contribution are, in general, strongly coupled. To simplify matters we assume

$$\begin{aligned} k_E S &\gg k_d(k_E S + 2k_b b)^2 / (k_C[H])^2 \quad (E) \\ k[H] &\gg 2k_b b \quad (F) \end{aligned}$$

Condition (E) means that disproportionation of  $S'$  is not important for double bond formation in comparison with splits next to a site  $S$ . It requires essentially again a large value of the abstraction step  $k_C[H]$ . Condition (F) is less satisfactory and can hardly be justified by the ratio 2:1 of C-H and C-C bonds. At least, terms of the order  $k_b b/k[H]$  ought to be included in the expression for  $S$  and  $x$  during the first stages of the reaction when  $b$  is still large. Nevertheless we shall adhere here to the approximation (F). Then  $S$  and  $x$  retain their values, as determined in the absence of degradation, and the two series of equations are only loosely coupled. As a consequence, eq. 4a,b,c for  $dB/dt$  retains its form with

$$K_1 = K_1 \text{ previous} (1 - 2k_E/k'_S S)$$

In  $K_2$ ,  $k_S S$  in the second term is replaced by  $k_S (1 + 2k_E/k'_S S)$ , whereas  $(k_S + k'_S)$  is not changed. In the present approximation, changes in double bond formation are due entirely to the competition between the disappearance of sites  $S$  through adjacent C-C splits and their mutual interactions to form double bonds or cross-links. It will be noted

that inverse terms in  $I^{1/2}$  now appear in  $B_\infty = K_2/K_1$ . This quantity is also larger than previously.

Equation 6 together with approximations (D-F) yields for the rate of backbone scission

$$db/dt = Ab^2 - k_b b - k_E S \quad (7)$$

with

$$A(k_C[H])^2 = 4k_b^2 k'_d$$

We note immediately a defect in (7). The rate does not level out but approaches a constant negative value when  $b \rightarrow 0$ . This is merely an expression of the fact that our approximations can be valid only for moderate degrees of degradation. Otherwise  $S$  cannot remain constant, but must decrease, and with it the probability of the first step in (5). For  $b \approx b_0$ , the initial value, the solution

$$(k_b b + k_E S)/(Ab - k_b) = (k_b b_0 + k_E S)e^{-k_b t}/(Ab_0 - k_b)$$

may be used and substituted into familiar expressions appropriate for molecular weight changes in random depolymerizations. Of course, the rate of cross-linking also must be taken into consideration. In eq. 7,  $db/dt$  depends on  $I$  through  $k_b$ .

Equation 3' reduces in the steady-state approximation to

$$dy/dt = k'_s S^2/2 + dB/dt + db/dt$$

The rate of gas evolution tends, as previously, to a limiting value, which is not affected by the degradation, in our approximation, since  $(db/dt)_\infty$  must go to zero. Prior to this stage, however, there arises the possibility of a maximum, if  $dB/dt + db/dt = 0$  for  $B \pm B_\infty$ . For example, if  $k_b b$  predominates,  $db/dt \approx -k_b b$ . The initial value of  $dB/dt = K_2/k_2[H]$ , defined in (4a,b,c). As long as  $k_S/(k_S + k'_s)$  is of the order of unity, the former ratio is of the order of  $k[H]$  and the above condition is not realized at an early stage due to condition (F). Later on, however, this could become possible, although our approximations may be inadequate for a quantitative description. We are not aware of any pertinent experimental evidence. Moreover, in a degrading polymer such as polymethyl methacrylate, abstraction reactions would be less favored than in unsubstituted vinyl polymers, and some of the conditions advocated here may well require revision.

Similar conclusions are reached for the case (a'b). In the expression for  $dB/dt$ ,  $(k_S + k'_s)$  and hence  $C_1$ , eq. 4a',b remain uncharged. The second term in  $C_2$  is modified by the factor  $1 + 2k_E/k_S S$ , yielding once more an increase in  $B_\infty$ , and a term proportional to  $I^{-1/2}$ . From eq. 7,  $db/dt$  is determined, with  $S$  given by (4a',b). The last equation for  $dy/dt$  also remains intact in terms of the appropriate  $S$ -value. The condition for a maximum in  $dy/dt$  becomes, if  $k_b$ -scission predominates

$$C_2 e^{-C_1 t} = k_b b_0 e^{-k_b t}$$

the outcome depending on the relative values of  $C_1$  and  $k_b$ .

The rate of cross-linking,  $dv/dt$ , remains unchanged, since to our approximation, cross-linking and bond breaking take place independently. In general, however,  $dv/dt$  is increased by a factor,  $1 + 2k_b b/k[H]$ , arising from  $S$ . That is,  $S'$ -radicals produce additional sites  $S$  for cross-linking. The ratio,  $dv/db$ , then will determine whether a gel

point can be reached in competition with breakdown processes.

Since simultaneous degradation probably occurs even in cross-linking polymers such as polyethylene, it is pertinent to consider the effect of isotopic substitution on the relations just developed. We have

$$k_C[H]/k_C[D] = k_a^H/k_a^D = J > 1$$

disregarding any influence on the bond breaking processes.  $S$  is increased for the heavier isotope, as we saw previously. From (7) we conclude that the recombination step is increased as  $J^2$  in the heavier isotope, which is therefore less vulnerable to degradation, as long as the recombination constant,  $k'_d$ , is sufficiently important. The last term in (7) varies at best as  $J^{1/2}$ . A weak increase in  $B_\infty$  and  $dB/dt$  for the heavier isotope also results. ( $dy/dt$ ) is at best affected by the first term in (7), since the contribution  $k_E S$  cancels out in  $dB/dt + db/dt$ .

The inclusion of cross combination  $k'_d S S'$  does not introduce anything particularly new within our approximations. Condition (F) ensures that  $S$  remains as before. Hence  $dB/dt$  and  $db/dt$  are also not affected.

To recapitulate, our essential approximation was the uncoupling of the breakdown and build-up relations, which is valid only for moderate extents of degradation. Otherwise the parallel decrease in the number of C-H linkages must be taken into consideration.

### Discussion

We are not satisfied with the interpretation of the isotope effect on  $dy/dt$  in polystyrene, where a decrease is observed for the deuterated polymer.<sup>9</sup> On the other hand, the constant yield found in polyethylene<sup>9</sup> can be accounted for. Only for the initial rate  $(dy/dt)_0$  could a decrease be derived. The inclusion of chain scission, furthermore, does not contribute significantly. Whether removal of some rather severe approximations made here changes our results in the direction suggested by experiment remains to be seen. As a possible alternative, we wish to suggest the possibility of capture of H-atoms by the phenyl ring competing with the recombination and abstraction processes. Clearly, in order to obtain an isotope effect, the competition with the latter must be considered. That is, we revert to our previous condition (a). To illustrate the effect of this "capture" factor, it is sufficient to consider instead of a modified eq. 2 the simpler set

$$\begin{aligned} dx/dt &= k[H] - 2k_1 x^2 - (k_2[H] + k_3[R])x = 0 \\ dy/dt &= k_1 x^2 + k_2[H]x \end{aligned}$$

where  $k_3[R]$  is the capture constant of the ring. A comparison with (2) shows that the R-reaction essentially replaces the previous terms  $(k'_d S + k_E B)x$ , that is, atom capture by radical sites and double bonds. The essential difference now is the approximately constant supply of "sinks." Condition (a) leads to

$$dy/dt = k[H]/(1 + r)$$

with

$$r = k_3[R]/k_2[H]$$

The rate for the deuterated polymer is reduced by the factor  $(1 + r)/(1 + Jr)$ . The observed value

of 0.4<sup>9</sup> requires, with  $J = 3$ , that  $r = 3$  and  $r_3^D = 9$ . Condition (a') on the other hand, yields

$$dy/dt = k_1k[H]/(k_3[R])^2$$

which can, at best, result in a weaker isotope effect than previously.

Dorfman<sup>10</sup> has irradiated with electrons mixtures of deuterated and non-deuterated paraffinic waxes. In these experiments the gas contained hydrogen and deuterium in the ratio of about 2.2 to 1. This apparently contradicts the results of Wall and Brown<sup>9</sup> where the separately irradiated substances gave equal amounts of gas. However, the two results are not necessarily incompatible with each other, for in a mixture the abstraction steps of H or D atoms will have a selective effect. Dorfman's results do not contradict a free-radical mechanism in which abstraction processes by atoms play an important part.

In the experiments<sup>10</sup> on mixtures, evidence for molecular detachment of hydrogen molecules is found. It is estimated that 20% of the hydrogen is produced in this manner, which is considerably less than the 50% found for ethane in the gas phase.<sup>11</sup> In order to take account of this mechanism a simple modification of the scheme presented in this paper would be required.

At the moment it is a rather open question as to what role ionic processes play in the high energy irradiation of solid polymers. Recently reported studies<sup>12,13</sup> of ionic reactions in the gas phase have led to the suggestion that they may be responsible for the changes in irradiated polymers. Such reactions as



were observed. Incidentally, when deuterated species were used, a negligible isotope effect of 1.03 was found. This type of reaction is of interest here because it synthesizes a cross-link, *i.e.*, a C-C bond, and produces a molecule of hydrogen. The rate of such reactions, one would anticipate, would be proportional to the extent of ionization and, hence, to the irradiation dose unless the concomitant structural changes affected the efficiency of ionization. Other types of ionic steps have been suggested<sup>10</sup> as possible mechanisms.

(10) Leon M. Dorfman, paper presented at the 30th Colloid Symposium, June 18-22, 1956, Madison, Wis.

(11) Leon M. Dorfman, *THIS JOURNAL*, **60**, 826 (1956).

(12) D. P. Stevenson and D. O. Schissler, *J. Chem. Phys.*, **23**, 1353 (1955).

(13) D. O. Schissler and D. P. Stevenson, *ibid.*, **24**, 926 (1955).

However, certain theoretical considerations<sup>14</sup> as well as the abundant<sup>15,16</sup> evidence for free radicals in irradiated systems indicate that the precursors of the observed products and structures are atomic or radical species.

The above mentioned theoretical considerations lead to a recombination time, of the order of 10<sup>-13</sup> sec.<sup>14</sup>, in an aqueous system for ion-electron pairs. For hydrocarbon substances the time would be expected to be of the same order or somewhat smaller.

It is clear then that in the solid phase ionic processes will be very short-lived and hence contribute less to the over-all results than they do in gas phase systems. Another fact which appears to argue against the ion mechanisms is that polydienes<sup>17</sup> are more difficult to cross-link with ionizing radiation than polyethylene. Unsaturated substances have lower ionization potentials and therefore the number of ions formed in such materials should be as great or greater than in saturated compounds. On the other hand, the low response of polydienes to radiation is explainable by a free radical mechanism because it is known<sup>18</sup> that such substances produce fewer radicals on irradiation and it is likely that radical chain mechanisms operating through the double bonds will require appreciable activation energy and have steric restrictions.

There are some discrepancies in the literature as to the behavior of polyethylene during irradiation. Earlier workers<sup>19,20</sup> report a linear increase with dose in hydrogen production and double bond formation. More recent results<sup>9,21,22</sup> show that the rates of production of both products decrease with increasing extent of irradiation. These different observations may be the result of differences in total dosages, experimental techniques and type of radiation used. It will be noted that the theoretical curves 1 and 3 in Fig. 1 start out linearly and subsequently deviate in a direction that is in qualitative accord with experiment.

(14) A. H. Samuel and J. L. Magee, *ibid.*, **21**, 1080 (1953).

(15) E. E. Schneider, *Disc. Faraday Soc.*, **19**, 158 (1955).

(16) L. A. Wall and D. W. Brown, *J. Research Natl. Bur. Standards*, **57**, 131 (1956).

(17) L. A. Wall, National Bureau of Standards, unpublished work.

(18) A. Prévot-Bernas, A. Chapiro, C. Cousin, Y. Landler and M. Magat, *Disc. Faraday Soc.*, **12**, 98 (1952).

(19) M. Dole and C. D. Keeling, *J. Am. Chem. Soc.*, **75**, 6082 (1953).

(20) M. Dole, C. D. Keeling and D. G. Rose, *ibid.*, **76**, 4304 (1954).

(21) E. J. Lawton, P. D. Zemany and J. S. Balwit, *ibid.*, **76**, 3437 (1954).

(22) A. A. Miller, E. J. Lawton and J. S. Balwit, *THIS JOURNAL*, **60**, 599 (1956).

## ION-EXCHANGE AND SOLVENT-EXTRACTION STUDIES WITH POLONIUM

BY J. DANON AND A. A. L. ZAMITH

*Escola Nacional de Quimica, Rio de Janeiro, Brazil**Received September 21, 1956*

An investigation has been made of the ion-exchange and solvent-extraction behavior of polonium in hydrochloric and nitric acid media. Adsorption by an anion-exchange resin, Dowex-1, from nitric acid solutions is unusually slow. Reducing agents, which had no effect on anion exchange and solvent extraction in hydrochloric acid solutions, exerted a marked influence on these processes in nitric acid media. The tendency of polonium to form complexes and its oxidation-reduction reactions are discussed.

Until recently our knowledge of polonium chemistry was obtained from investigations with trace-amounts of the element.<sup>1</sup> Research with weighable quantities of  $^{210}\text{Po}$ , which has now been produced by the irradiation of bismuth has clarified many important aspects of the chemistry of this element.<sup>2</sup>

Useful information about the complex ions of an element can be derived from its ion-exchange behavior. The study of the complex ions of polonium is important for an understanding of its solution chemistry since, as was recognized more than twenty years ago, this element has a marked tendency to form complexes with all the anions investigated.<sup>3</sup> The present paper describes some studies on the adsorption of polonium by cation and anion-exchange resins and extraction by organic solvents from hydrochloric and nitric acid media.

### Experimental

Polonium was separated from a RaD + RaE + Po source by chloroform extraction of the dithizone complex.<sup>4</sup> To eliminate any trace of dithizone, the extracted polonium was separated from the solution by spontaneous deposition on silver and then dissolved in nitric acid. This solution was electrolyzed with gold electrodes and the anodic deposit of polonium was used in our experiments.<sup>1</sup> The solutions were prepared in twice-distilled water in quartz apparatus with analytical grade reagents. The radiochemical purity of our source was controlled by radiation absorption measurements; the  $\alpha$ -particle range in nuclear photographic plates showed that the polonium was essentially free from other  $\alpha$ -emitters.

Amberlite IR-120 was the cation-exchange resin employed in this study. The sodium form, 20-40 mesh, was washed with 4 *M* HCl to remove impurities; the regenerated sodium form was converted to the acid form with 1 *M* HCl, washed with water, and dried at 60°. The anion-exchange studies were carried out with Dowex-1 (8% DVB, 50-100 mesh), Amberlite IRA-410 and Dowex-2. These strong-base resins were washed with 4 *M* HCl, converted to the chlorides or nitrates and dried at 60°.

Measured amounts of the resin and the polonium solution were mechanically agitated at room temperature ( $25 \pm 3^\circ$ ) until equilibrium was attained. An aliquot was then centrifuged, and the  $\alpha$ -activity of the solution measured with a thin-window G.M. counter. The polonium adsorbed is the difference between the initial and equilibrium activity of the solution.

For the extraction experiments, equal volumes (10 ml.) of the solution and the solvent were agitated for 15 minutes; the two phases were separated, evaporated and the activity in each determined.

### Results

**Cation Exchange.**—The absorption of polonium by the cation-exchange resin was investigated for

- (1) M. Haissinsky, "Le Polonium," Hermann et Cie, Paris, 1937.
- (2) K. W. Bagnall, "Some Aspects of Polonium Chemistry," Proceedings of the International Conference on the Peaceful Uses of Atomic Energy, Vol. 7, p. 386, United Nations, 1956.
- (3) M. Haissinsky, *Compt. rend.*, **195**, 131 (1932).
- (4) G. Boussières and C. Ferradini, *Anal. Chim. Acta*, **4**, 610 (1950).

hydrochloric acid concentrations of 0.05–2.5 *M* and nitric acid concentrations of 0.1–5.0 *M*. The initial concentration of polonium was approximately  $2 \times 10^{-10}$  *M* in each experiment.

The following distribution coefficients *D* (amount of Po in counts per minute per gram of dry resin divided by the amount of Po in counts per minute per ml. of solution) were obtained in hydrochloric acid solutions: 150 at 0.05 *M* HCl, 10 at 0.1 *M* HCl, 1.3 at 0.2 *M* HCl and <1 at higher acidities. The comparable results for adsorption in nitric acid solutions are plotted in Fig. 1. Of particular interest is the finding that while adsorption of polonium is negligible at concentrations of hydrochloric acid greater than 0.2 *M*, it is appreciable at the highest concentration of nitric acid used (5 *M*).

When oxalate ion was added to a 1 *M*  $\text{HNO}_3$  solution of polonium, the following values of *D* were found: 26.7 in the absence of oxalic acid, 6.7 for 0.01 *M* oxalic acid, and <1 for oxalic acid solutions stronger than 0.05 *M*.

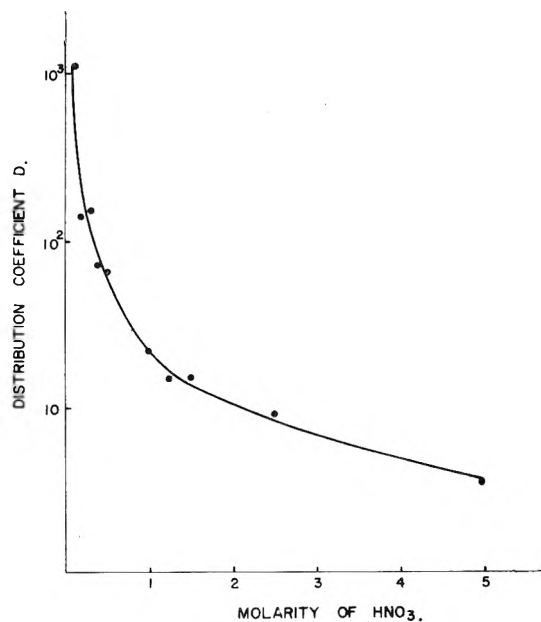


Fig. 1.

In all these experiments the adsorption equilibrium was attained in 3–4 hours. The results show that the adsorption of polonium by the resin decreases with the acid molarity and that the shape of the adsorption curve is markedly dependent on the nature of the anion in the solution. This indicates that polonium forms positively charged ions in the three media and that its tendency to

ward complex formation is different for each of the anions studied: oxalate > hydrochloride > nitrate. These results are in agreement with those obtained by electromigration studies with polonium.<sup>1</sup>

**Anion Exchange. Hydrochloric Acid Solution.**—Polonium was markedly adsorbed by the strong-base resins at all the hydrochloric acid concentrations investigated (0.05–12 *M*). The results obtained with Dowex-1 are shown in Fig. 2.

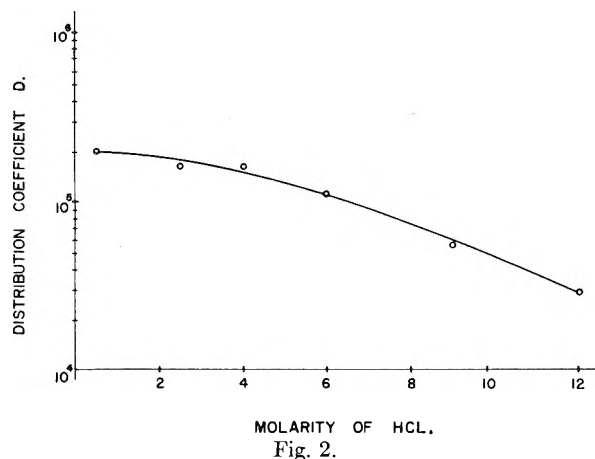


Fig. 2.

Very high values of *D* were observed at low hydrochloric acid concentrations ( $D \approx 1.5 \times 10^2$  at 0.05 *M* HCl), but these data showed poor reproducibility.

The polonium was probably in its usual +4 oxidation state, but to avoid possible reduction by the resin or by impurities, chlorine was added to the more concentrated hydrochloric acid solutions (>4 *M*); the chlorine addition did not influence the *D* values.

Studies with both micro<sup>1</sup> and macro-quantities<sup>5</sup> of polonium indicate that hydrazine reduces polonium (+4) to a lower oxidation state. We found that reducing agents have practically no influence on the adsorption of polonium from hydrochloric acid, although at low hydrochloric acid concentrations, hydrazine caused a slight increase in the *D* values observed with Dowex-1.

The adsorption equilibrium was attained both in the oxidized and reduced state in approximately 24–48 hours. When some experiments were repeated with the polonium initially in the resin phase, the value of *D* for a given HCl concentration was found to be independent of the initial conditions; this indicates the reversibility of the adsorption process.

Although correlations between adsorption by anion-exchange resins and extraction by organic solvents (particularly diethyl ether) have been reported,<sup>6</sup> with ether we found only a slight extraction of polonium (3.4%) from 6 *M* hydrochloric acid; in the presence of hydrazine the extraction by ether was negligible.

**Nitric Acid Solutions.**—The following values of *D* were obtained with Dowex-1 in the nitrate form:

(5) K. W. Bagnall, R. W. M. D'Eye and J. H. Freeman, *J. Chem. Soc.*, 2320 (1955).

(6) K. A. Kraus, F. Nelson and G. W. Smith, *THIS JOURNAL*, **58**, 11 (1954).

123 at 0.8 *M* HNO<sub>3</sub>, 110 at 2 *M* HNO<sub>3</sub>, 97 at 3.5 *M* HNO<sub>3</sub>, and 90 at 5 *M* HNO<sub>3</sub>. The most striking aspect of the adsorption of polonium from this media is the slowness with which the process occurs. The equilibrium is reached after several days, in some cases after a week. This is true also for adsorption by Amberlite IRA-410.

It was previously found that Po(+4) is not extracted by ether and other organic solvents from nitric acid solutions.<sup>7</sup> However, when the solution contains a small amount of a reducing agent some polonium passes into the organic phase. Figure 3 illustrates the effect of increasing HNO<sub>3</sub> molarity on the percentage of polonium extracted by ether for the various reducing agents used.

As was observed in the solvent-extraction studies, the adsorption of polonium by the resin is altered in the presence of a reducing agent. Our results are shown in Fig. 4. Adsorption equilibrium was attained in 24–48 hours.

It can be seen from this figure that the values of *D* obtained in the presence of hydrogen peroxide, sulfur dioxide and hydroxylamine fall approximately on the same adsorption curve, whereas with hydrazine much higher values were observed. The lower curve is similar to that obtained by Nelson and Kraus for the adsorption of bismuth (III) and lead(II) by the same resin from HNO<sub>3</sub> media.<sup>8</sup>

## Discussion

The ion-migration experiments mentioned before<sup>1</sup> and coprecipitation studies<sup>9</sup> have furnished evidence for the existence of complex polonium chlorides, probably as compounds of the type M<sub>2</sub>PoCl<sub>6</sub> (M = NH<sub>4</sub>, Cs); this has been confirmed by recent research with weighable quantities of the element.<sup>5</sup>

The adsorption of polonium by Dowex-1 is qualitatively similar to that of gold(III),<sup>10</sup> platinum(IV)<sup>6</sup> and other elements which show a general decrease in adsorption with increasing hydrochloric acid concentration. On the basis of the interpretation given by Kraus for the adsorption of elements by anion-exchange resins,<sup>6,10,11</sup> one would conclude that at trace concentrations the negatively charged complexes of polonium are essentially completely formed at low hydrochloric acid molarities (<0.5 *M*).<sup>12</sup> This conclusion is supported by absorption spectrum studies of polonium in hydrochloric acid solutions,<sup>13</sup> which show that at least two complexes, Po(OH)Cl<sub>5</sub> and PoCl<sub>2+b</sub>, exist in hydrochloric acid solution. At HCl concentrations near 1 *M* the equilibrium be-

(7) J. Danon and A. A. L. Zamith, *Nature*, **177**, 746 (1956).

(8) F. Nelson and K. A. Kraus, *J. Am. Chem. Soc.*, **76**, 5916 (1954).

(9) M. Guillot, *J. chim. phys.*, **28**, 92 (1931).

(10) K. A. Kraus and F. Nelson, *J. Am. Chem. Soc.*, **76**, 984 (1954).

(11) K. A. Kraus and F. Nelson, "Anion-Exchange Studies of the Fission Products," Proceedings of the International Conference on the Peaceful Uses of Atomic Energy, Vol. 7, p. 113, United Nations, 1956.

(12) However, the interpretation of the adsorption of elements by anion-exchange resins is not in a satisfactory state.<sup>11</sup> See also C. D. Coryell and Y. Marcus, *Bull. Research Council Israel*, **3**, 500 (1954); M.I.T. Progress Report, November, 1954; and R. A. Horne, M.I.T. Progress Report, February 1956, p. 14.

(13) D. J. Hunt, "Absorbance Studies of Polonium Complexes in Chloride Solutions," Information Report MLM-979, Mound Laboratory, 1954.

tween these two forms is shifted toward the complete formation of  $\text{PoCl}_{2+b}$ . Since under these conditions the adsorption by the cation-exchange resin is negligible and essentially all polonium migrates in the electric field to the anode,  $\text{PoCl}_{2+b}$  is probably a negatively charged complex, possibly  $\text{PoCl}_6^{-2}$ .

At all the hydrochloric acid concentrations the adsorption of polonium by Dowex-1 is higher than that of the other M(IV) elements studied.<sup>14</sup> A comparison with the adsorption of tellurium(IV)<sup>15</sup> and selenium(IV)<sup>11</sup> suggests that the order in which these elements tend to form negatively charged complexes in hydrochloric acid is: polonium > tellurium > selenium.

Although hydrazine did not influence the anion-exchange behavior of polonium in hydrochloric acid it has been shown that under these conditions polonium is reduced to a low oxidation state.<sup>5</sup> Since under this form polonium is strongly adsorbed by the anion-exchange resins at all the hydrochloric acid concentrations investigated, it is plausible to assume that the low oxidation state is also strongly complexed in this acid.

The adsorption of Po(IV) by Dowex-1 in nitric acid solution was much slower than that which has been reported for other elements, in nitric acid and hydrochloric acid media. Only a few elements, *viz.*, molybdenum(VI), tungsten(VI)<sup>16</sup> and less markedly protactinium(V),<sup>17</sup> behave similarly. As these elements have a strong tendency to hydrolyze under such conditions, the slow adsorption may be related to the presence of hydrolytic polymers in the aqueous phase.<sup>16</sup> Apparently polonium(IV) nitrate, like tellurium(IV) nitrate, forms hydrolyzed species even at high nitric acid concentrations, as was suggested before by F. Joliot.<sup>18</sup>

On the basis of the solubility data of polonium nitrate,<sup>19</sup> it was concluded that  $\text{PoO}(\text{NO}_3)_3^{-1}$  ions are formed below 1 M  $\text{HNO}_3$ ,<sup>20</sup> and  $\text{Po}(\text{NO}_3)_5^{-1}$  are formed at higher concentrations of this acid. However, the results from ion-migration and cation-exchange studies show that positively charged ions of polonium are present until at least 5 M  $\text{HNO}_3$ , indicating that the negatively charged complexes are not completely formed at these concentrations. It seems that a fraction of these positively charged species are hydrolytic polymers of polonium.

In the cation-exchange experiments the equilibrium was attained, as usually, in a few hours. Presumably the slow step in the anion-exchange process is not the adsorption but the depolymerization of polonium polymers with the formation of negatively charged complexes. Slow depoly-

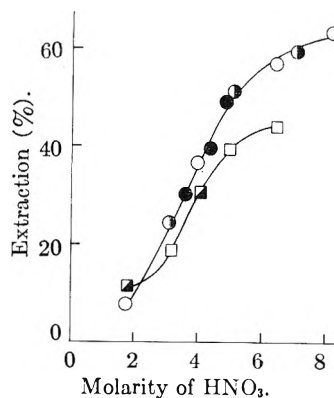


Fig. 3.—○, organic peroxide; ●, sulfur dioxide; ◐, hydrogen peroxide; □, hydrazine; ◑, hydroxylamine.

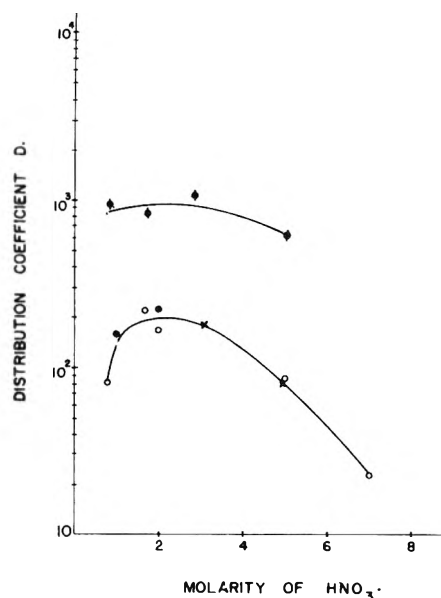


Fig. 4.—●, hydrazine, 0.05M; ○, hydrogen peroxide, 0.1M; ●, sulfur dioxide, 0.05M; ×, hydroxylamine, 0.05 M.

merization was observed with plutonium polymers in  $\text{HNO}_3$  media.<sup>21</sup>

The oxidation-reduction behavior of polonium appears to be influenced by the amount of polonium, by the medium and by the reducing agent. In agreement with electrochemical studies with trace amounts of polonium in sulfuric and acetic acid media,<sup>22</sup> our solvent-extraction and anion-exchange data suggest that hydrazine, sulfur dioxide, hydrogen peroxide and hydroxylamine reduce polonium(+4) to a lower oxidation state. With macro-amounts of the element in hydrochloric acid solutions, it was found that hydrazine and sulfur dioxide reduce polonium(+4); hydroxylamine has no effect on solutions of polonium chlorides, but it reduces polonium(+4) in sulfuric acid solution,<sup>23</sup> and hydrogen peroxide oxidizes polonium(+2) to the +4 state. Nitric acid or its radiolysis products appears to oxidize macro-amounts of reduced polonium to its normal +4 state.<sup>23</sup>

(21) K. A. Kraus and F. Nelson, "Hydrolytic Behavior of Heavy Elements," Proceedings of the International Conference on Peaceful Uses of Atomic Energy, Vol. 7, p. 245, United Nations, 1956.

(22) M. Guillot and M. Haisinsky, *Bull. soc. chim.*, 239 (1935).

(23) K. W. Bagnall, personal communication.

(14) K. A. Kraus, G. E. Moore and F. Nelson, *J. Am. Chem. Soc.*, **78**, 2692 (1956).

(15) U. Schindewolf and C. D. Coryell, M.I.T. Progress Report, November 1955, p. 16 and February 1956, p. 16.

(16) K. A. Kraus, F. Nelson and G. E. Moore, *J. Am. Chem. Soc.*, **77**, 3972 (1955).

(17) K. A. Kraus and G. E. Moore, *ibid.*, **72**, 4293 (1950).

(18) F. Joliot, *J. chim. phys.*, **27**, 119 (1930).

(19) E. Orban, "The Solubility of Polonium Nitrate in Nitric Acid Media," Information Report MLM-973, Mound Laboratory, 1954.

(20) The existence of polonyl ions  $\text{PoO}^{+2}$  in  $\text{HNO}_3$  media was previously suggested by F. Joliot.<sup>18</sup>

The failure of hydroxylamine to reduce polonium in hydrochloric acid solution probably is due to the stability of the complex polonium(IV) chlorides. However, the reactions of polonium with hydrogen peroxide seem to be a function of the concentration of the element, since in all media investigated hydrogen peroxide oxidizes macro-amounts of polonium(+2) and apparently reduces trace-amounts of polonium(+4). For plutonium (IV) also the reactions with hydrogen peroxide in nitric acid media are different for trace and macro-quantities of the element.<sup>24</sup>

Little can be said about the numerical value of the lower oxidation state of trace-amounts of

(24) G. T. Seaborg and J. J. Katz, "The Actinide Elements," National Nuclear Energy Series, Vol. 14-A, McGraw-Hill Book Co., New York, N. Y., 1954, p. 279.

polonium in nitric acid. Although recent research with weighable quantities of the element showed that the reduction of polonium(+4) in hydrochloric and sulfuric acid gives a +2 oxidation state, there is evidence for a +3 state in hydrochloric acid.<sup>6</sup> The tendency of reduced polonium to form negatively charged complexes in nitric acid and its extraction by ether under these conditions are properties similar to those of +3 elements such as gold, bismuth and thallium.

**Acknowledgments.**—The authors wish to thank Dr. K. W. Bagnall, Professor Charles D. Coryell, Dr. Ralph A. Horne for helpful discussions and for making available polonium and tellurium data prior to publication, and Dr. Ugo Camerini for his continued interest and support.

## THE PHOTOTROPY OF MALACHITE GREEN LEUCOCYANIDE IN ETHYL ALCOHOL, CYCLOHEXANE, ETHYLENE DICHLORIDE AND ETHYLIDENE DICHLORIDE, AND SOME MIXTURES OF THEM

By EDWARD O. HOLMES, JR.

*Contribution from the Chemical Laboratory of Boston University, Boston, Mass.*

*Received September 24, 1956*

The phototropy of malachite green leucocyanide dissolved in alcohol is shown to yield three reverse (dark) reaction products, the original leucocyanide, the carbinol, and (or) the ethyl ether depending on conditions. A mechanism is offered that can explain the formation of these products. The phototropy of this solute dissolved in cyclohexane, ethylene dichloride or ethylidene dichloride and some mixtures of these solvents shows that (1) in pure cyclohexane no carbonium ion (MG)<sup>+</sup> is formed but that polymerization occurs, (2) that more (MG)<sup>+</sup> ion is formed on irradiation when ethylene dichloride is used as the solvent than when ethylidene dichloride is used, (3) that in a solvent composed of mixtures of the above with cyclohexane, that as the proportion of the halogenated hydrocarbon is increased more (MG)<sup>+</sup> is formed, and (4) that this begins suddenly when the dielectric constant of the solvent is about 4.5 and rises rapidly. Mechanisms are proposed by which the above and other results may be interpreted.

### Part A. Solutions of Malachite Green Leucocyanide (I) in Ethyl Alcohol

The phototropy of malachite green leucocyanide (I) has been investigated in dry alcohol and also in mixtures of alcohol and water by a number of authors.<sup>1-7</sup> The results show that, on irradiation, malachite green leucocyanide (I) dissolved in alcohol is photo-ionized to yield the carbonium ion (MG)<sup>+</sup> and the cyanide ion, and that the quantum efficiency of the process is very close to unity.

When the source of light is removed, the color of the solution fades with greater or less velocity depending on conditions to a product(s) of unknown composition. This product will yield the brilliantly colored carbonium ion (MG)<sup>+</sup> on the addition of an acid such as hydrochloric, whereas the original leucocyanide (I) will not. Several mechanisms have been proposed but none is completely satisfactory.

In order to elucidate more completely the true mechanism involved in the above changes, the au-

thor examined the absorption spectra of the products of the dark reaction formed under various conditions and compared them with those of the leucocyanide (I), the carbinol (II) and the ethyl ether (III).

The results, tabulated in Table I, indicate that the composition of the dark reaction (thermal) product is a mixture of the carbinol (II) and the ethyl ether (III), or the leucocyanide (I) itself depending on conditions.

TABLE I

$\lambda_{\max}$ of pure malachite green, Å.	$\lambda_{\max}$ dark reaction products, Å.
1. Leucocyanide (I), 2720	HCN(g) added, <sup>a</sup> 2725
2. Carbinol (II), 2650	Dry ethyl alc., 2640-2660
3. Ethyl ether (III), 2670	OH <sup>-</sup> , CN <sup>-</sup> or H <sub>2</sub> O, 2650-2660

<sup>a</sup> Product will not form (MG)<sup>+</sup> on addition of acid.

If a very small amount of KOH or KCN or water was added to the alcoholic solution of the leucocyanide (I), before irradiation, the dark reaction product was a mixture of the carbinol (II) and the ether (III) with the carbinol (II) present in larger amount, whereas when dry alcohol alone was used as the solvent, the proportion of the ether (III) was larger. On the other hand, when any of the above solutions were saturated with HCN gas, either before or after irradiation, the leucocyanide (I) was

(1) J. Lifschitz, *Ber.*, **52**, 1919 (1919).

(2) J. Lifschitz and C. L. Joffe, *ibid.*, **97**, 426 (1921).

(3) Edith Weyde and W. Frankenburger, *Trans. Faraday Soc.*, **27**, 561 (1931).

(4) Edith Weyde, W. Frankenburger and W. Zimmerman, *Z. physik. Chem.*, **B17**, 276 (1932).

(5) L. Harris and J. Kaminsky, *J. Am. Chem. Soc.*, **57**, 1151, 1154 (1935).

(6) F. E. E. Germann and C. L. Gibson, *ibid.*, **62**, 110 (1940).

(7) J. G. Calvert and H. E. Rechen, *ibid.*, **74**, 2101 (1952).



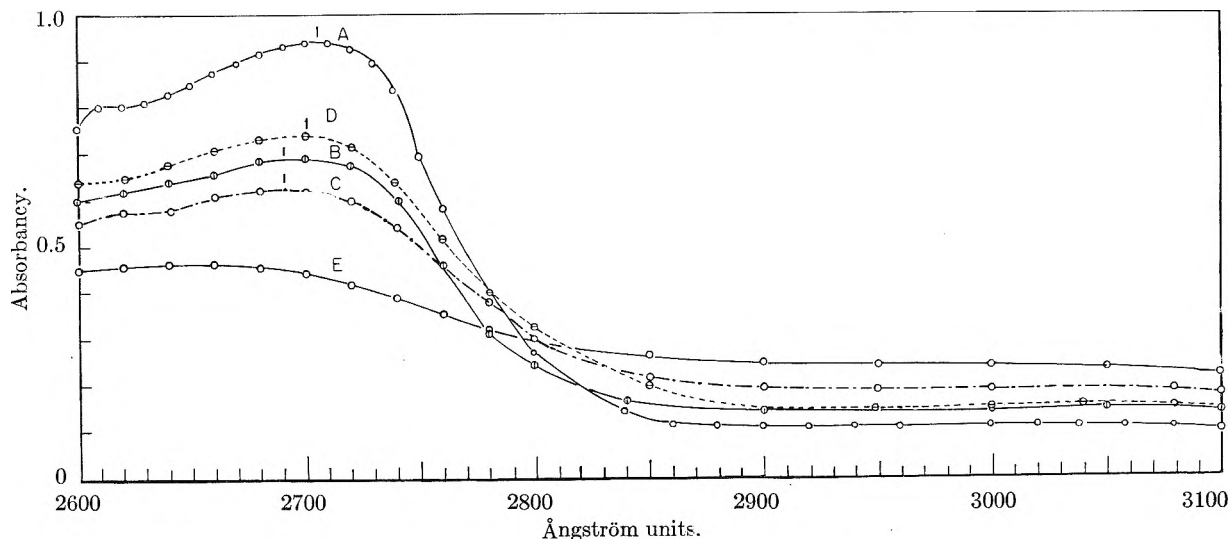


Fig. 1.—Absorption spectra of malachite green leucocyanide (I) dissolved in pure cyclohexane: A, original solution; B, irradiated 4 minutes in Pyrex flask; C, irradiated 4 minutes more in Pyrex flask; D, after standing 15 days; E, irradiated 1 minute in quartz flask.

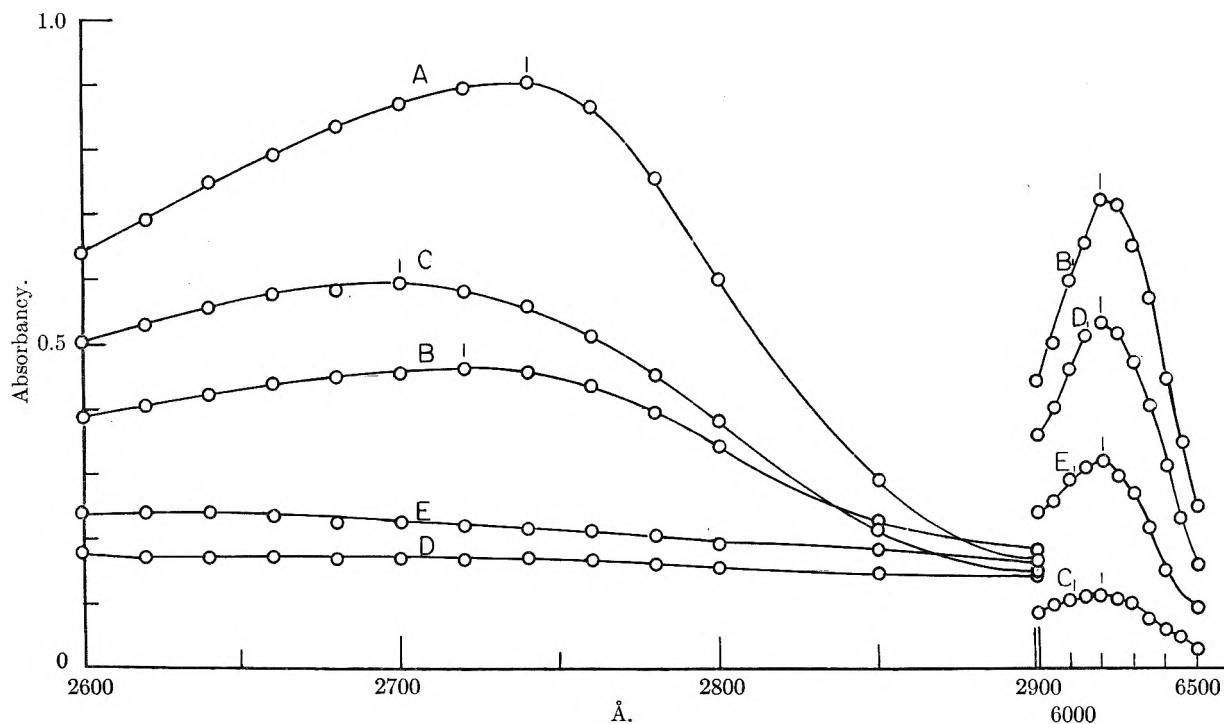


Fig. 2.—Absorption spectra of malachite green leucocyanide (I) dissolved in a mixture of cyclohexane and ethylene dichloride (mole fraction = 0.5763): A, original solution; B, irradiated 4 minutes in Pyrex flask; C, after standing 4 days; D, irradiated 1 minute in quartz flask; E, after standing 1 day.

**Absorption Measurements.**—All the following absorption curves were made with a Beckman D.U. instrument by hand scanning methods. Many curves (87 in all) were recorded but only a relatively few essential examples are included in this paper.

### Results

**Part I. Malachite Green Leucocyanide (I) Dissolved in Pure Cyclohexane** (concn. =  $2.17 \times 10^{-5}$  moles/l.).—The absorption curves obtained are reproduced in Fig. 1. No carbonium ion (MG)<sup>+</sup> was produced by irradiation in either Pyrex or quartz flasks under any conditions. However, the curves do indicate that a photoreaction did occur. This is revealed by the flattening out of the

original absorptior curve and the appearance of a long level portion in the region 2850–3100 Å., where absorbancy has increased about in proportion to the decrease in that of the original leucocyanide (I). As no increase in absorbancy in any other region could be located, the product formed must be responsible for this low flat region. Had the leucocyanide (I) molecule been broken into fragments, surely the benzene molecule would have been among them and been recognized by its characteristic absorption spectrum. As this proved not to be the case, one is forced to conclude that the photo-product must be polymer-like with its various parts

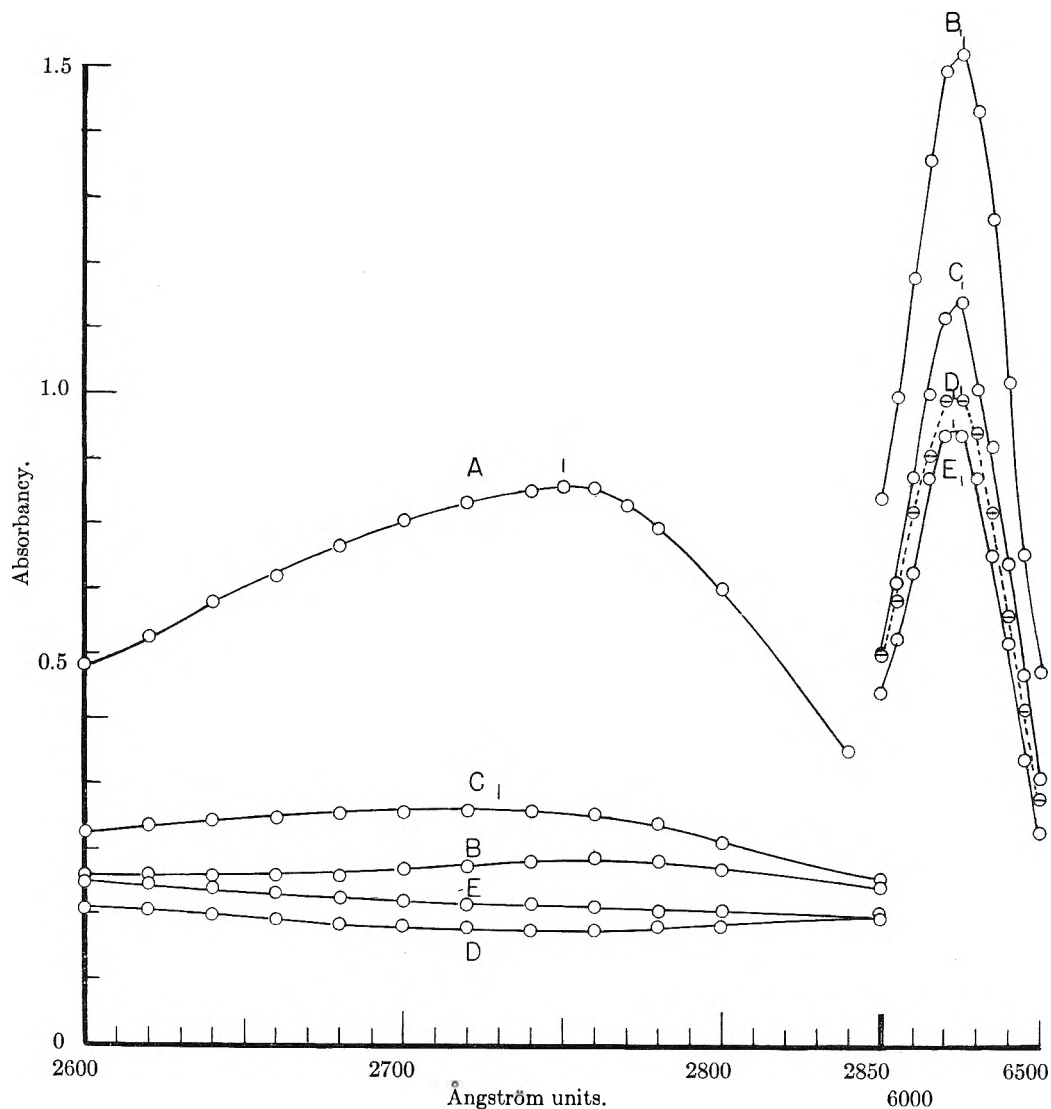


Fig. 3.—Absorption spectra of malachite green leucocyanide (I) dissolved in pure ethylene dichloride: A, original solution; B, irradiated 4 minutes in Pyrex flask; C, after standing 3 days; D, irradiated 1 minute in quartz flask; E, after standing 2 days.

so hooked together as to absorb feebly over a wide (2850–3100 Å.) region.

**Part II. Solute—Malachite Green Leucocyanide:** (I) Solvent Cyclohexane–Ethylene Dichloride (mole fraction of ethylene dichloride = 0.5763, concn. =  $2.17 \times 10^{-5}$  mole/l.).—This particular mixture was selected as a typical case. Its solvent ratio by volume was one-to-one and the phenomena that occurred are typical of those in the mixtures containing a larger ratio of ethylene dichloride but are less pronounced. Figure 2, showing the absorption curves obtained, consists of two sections: the left hand covers the range 2600–2900 Å.—showing the changes that occur in the original leucocyanide (I), and the right-hand section covering the range 6000–6500 Å. includes the strongest maximum of the carbonium ion (MG)<sup>+</sup>, whose  $\lambda_{\max}$  remains very close to 6200 Å. in all solvents and mixtures.

Curve A is that of the original unirradiated solution. Curve B is that of the above after four-minutes irradiation in a Pyrex flask, and B<sub>1</sub> the corre-

sponding portion in the region 6000–6500 Å. It is evident that considerable carbonium ion (MG)<sup>+</sup> has been produced by this initial irradiation. After allowing the solution to remain in the dark for four days, the absorption spectrum was recorded and is represented by curve C in the ultraviolet region and the corresponding curve C<sub>1</sub> in the visible for the carbonium ion (MG)<sup>+</sup>. Comparing this pair of curves with those recorded previously, B and B<sub>1</sub>, it will be observed that curve C runs above curve B and has a maximum slightly to the left, whereas curve C<sub>1</sub> is much below B<sub>1</sub>, with the position of its  $\lambda_{\max}$  unchanged. Hence considerable of the (MG)<sup>+</sup> ion has been converted into leucocyanide (I) and also into another product whose  $\lambda_{\max}$  is further toward the short wave region of the ultraviolet.

On one minute more irradiation in which the above solution was contained in a thin-walled quartz flask held about one inch from the quartz burner and constantly shaken, the absorption curve of the leucocyanide (I), curve D, had dropped

almost to the abscissa while that of the carbonium ion (MG)<sup>+</sup> had risen to a high value curve D<sub>1</sub> but not as high as on the former irradiation. The inference to be drawn is that considerable of the original leucocyanide (I) must have been converted either by the first or second irradiation into a new product that is not decomposed into the carbonium ion (MG)<sup>+</sup>. The absorption spectra in our available range did not indicate the nature of this new photo-product.

After one day standing in the dark, the absorption spectrum of the leucocyanide (E) had risen a small amount whereas that of the carbonium ion (MG)<sup>+</sup> ( $\lambda_{\max}$  6200 Å.) had fallen to one-half of its former value, indicating regeneration of the leucocyanide. No further work was performed on this mixture.

**Part III. Malachite Green Leucocyanide Dissolved in Pure Ethylene Dichloride** (concn. =  $2.17 \times 10^{-5}$  mole/l.).—Curve A in Fig. 3 is the absorption spectrum of the original unirradiated leucocyanide (I) having an absorbancy of 0.86 at a  $\lambda_{\max}$  of 2750 Å. After the usual four-minute irradiation in a Pyrex flask, the spectrum is represented by curve B which has a hardly perceptible  $\lambda_{\max}$  at 2760 Å. and an absorbancy of 0.28. The corresponding curve B<sub>1</sub> for the carbonium ion (MG)<sup>+</sup> has a  $\lambda_{\max}$  at 6250 Å. and an absorbancy of 1.53. After standing for three days, it is observed a small change only has occurred in the ultraviolet region as the points of curve C are only slightly above those on curve B. On the other hand, a considerable change has occurred in the absorption spectrum of the carbonium ion (MG)<sup>+</sup> curve C<sub>1</sub>.

On further irradiation (one minute in a quartz flask), curve D is obtained for the leucocyanide and curve D<sub>1</sub> for the (MG)<sup>+</sup> ion. Allowing the solution to stand for two days, curve E was obtained for the absorption spectrum in the ultraviolet region and curve E<sub>1</sub> for that of the (MG)<sup>+</sup> ion.

An inspection of the above curves shows that the initial radiation of the solution in the Pyrex flask converted a relatively large quantity of the malachite green leucocyanide (I) into the carbonium ion (MG)<sup>+</sup>. The fraction converted cannot be calculated with any degree of certainty as there are undoubtedly other photolysis products formed.

By dividing the value of  $\lambda_{\max}$  for curve B<sub>1</sub> by that for C<sub>1</sub> one obtains the ratio 1.33 and performing the same operation on  $\lambda_{\max}$  for curves B and C, a value of 1.28 is obtained—disregarding the slight shift in the position of  $\lambda_{\max}$  in the later case. As those figures are approximately equal they show a nearly complete reversion of (MG)<sup>+</sup> back into the leucocyanide (I).

However, on further irradiation of the solution in a quartz flask, a new photochemical process must occur as curve D is much below curve C and curve D<sub>1</sub> is below C<sub>1</sub>. As no characteristic absorption spectrum could be found for this new product, it was assumed that the original leucocyanide (I) and also some of the carbonium ion (MG)<sup>+</sup> had been photolyzed into small aliphatic fragments whose ultraviolet absorption spectrum could not be detected with the solvent used.

Two days later, the corresponding absorption

spectra, represented by curves E and E<sub>1</sub>, indicate a slight reversion of the carbonium ion (MG)<sup>+</sup> into the leucocyanide (I).

It is well known that the carbonium ion (MG)<sup>+</sup> has additional maxima both in the long-wave ultraviolet region and the short-wave visible. In ethylene dichloride, the ratio of  $\lambda_{\max}$  3200 Å. to that at  $\lambda_{\max}$  6250 Å. is 0.20 ( $\pm 0.01$ ) and that of  $\lambda_{\max}$  4360 Å. to the same peak at  $\lambda_{\max}$  6240 Å. is 0.18 ( $\pm$ ) showing that these two maxima are of about the same intensity, which has been shown to be the case in alcohol by Perekalin and others<sup>8</sup> where the values are 0.24 and 0.25, respectively.

**Part IV. Malachite Green Leucocyanide Dissolved in Pure Ethylene Dichloride** (concn. =  $2.17 \times 10^{-5}$  mole/l.).—Figure 4 shows the absorption spectrum curve A obtained when pure ethylene dichloride was used as a solvent. This solvent was chosen because its dipole moment (2.07 Debye units)<sup>9</sup> is greater than that of ethylene dichloride (1.89 Debye units),<sup>9</sup> whereas their dielectric constants are about the same, that of the former being 10.23 at 25° and the latter 9.90 at the same temperature.<sup>10</sup>

The absorption spectra obtained were essentially similar to those obtained when ethylene dichloride was used as the solvent except in degree. Curve A is that of the original unexposed solution having  $\lambda_{\max}$  at 2745 Å. with a corresponding absorbancy of 0.86. Curves B ( $\lambda_{\max}$  2630 Å.) and B<sub>1</sub> ( $\lambda_{\max}$  6200 Å.) are those obtained after four-minute irradiation in a Pyrex flask. Curves C and C<sub>1</sub> were obtained two days later. Curves D and D<sub>1</sub> represent the results of a one-minute exposure of the same solution in the quartz flask. Curves E and E<sub>1</sub> are the final values obtained one day later.

A study of the above series of absorption curves reveals that photo-ionization does not occur to such a large extent as in the case of ethylene dichloride, and also that the reverse (dark) reactions, while still slow, are nevertheless more rapid than those when ethylene dichloride was used as the solvent. In fact on examination of the solution 90 days later there remained no color at all in the ethylene dichloride solution whereas the corresponding ethylene dichloride solution was still highly colored.

Moreover, a comparison of the ratios the values of  $\lambda_{\max}$  for the other peaks (at 4300 and 3160 Å.) of the absorption spectrum of the carbonium ions (MG)<sup>+</sup> are of interest. The ratio of  $\lambda_{\max}$  4300 Å. to  $\lambda_{\max}$  6200 Å. was 2.0 and of  $\lambda_{\max}$  3160 Å. is 2.0 also: showing that the two ratios are the same in both solvents. It is further evident from an examination of the curves that considerable of the original leucocyanide (I) was photo-ionized to the carbonium ion (MG)<sup>+</sup> which reverted on standing into a small amount of the original leucocyanide (I) whereas a much larger amount transforms itself into some compound that has a long flat absorption spectrum in the region 2500–2800 Å. as represented by curve E.

(8) V. V. Perekalin, M. V. Savost Yanova and R. I. Morozova, *Zhur. Obshchei Khim. J. Gen. Chem. U.S.S.R.*, **22**, 321 (1952).

(9) A. A. Maryott, M. M. Hobbs and P. M. Gross, *J. Am. Chem. Soc.*, **63**, 659 (1941).

(10) J. T. Denison and J. B. Ramsey, *ibid.*, **77**, 2615 (1955).

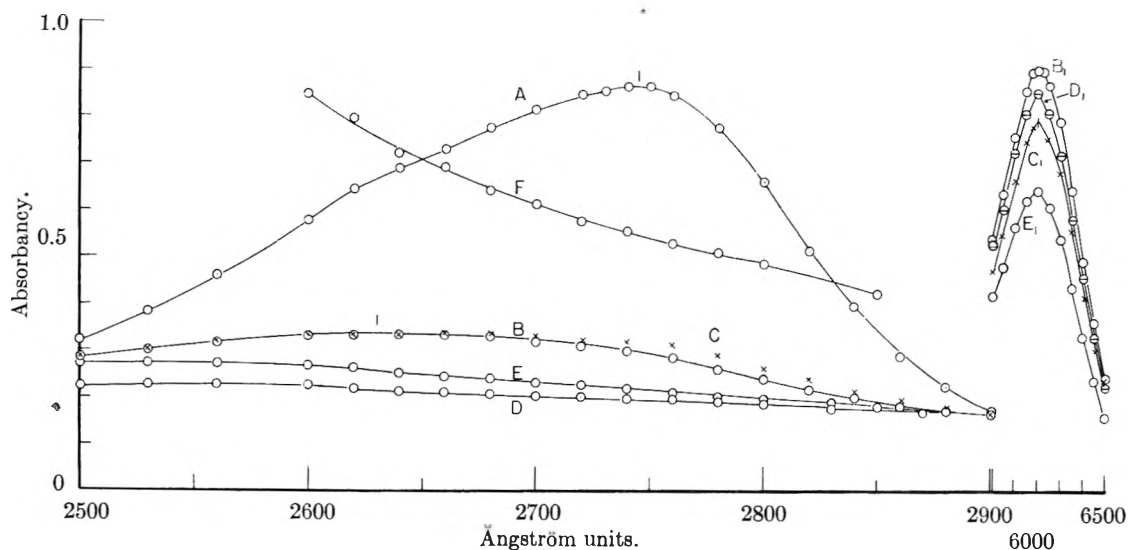


Fig. 4.—Absorption spectra of malachite green (I) dissolved in pure ethylidene dichloride; A, original solution; B, irradiated 4 minutes in Pyrex flask; C, after standing 2 days (curve omitted but represented by points  $\times \times \times$ , etc.); D, irradiated 1 minute in quartz flask; E, after standing 1 day.

Curve F, obtained after 91 days standing, during which the solution became colorless in the visible region, proves that considerable of the new compound has formed. It was unfortunate that this spectrum could not be followed further into the ultraviolet where a maximum is indicated but the solvent was too opaque to permit further measurements in that region.

**Part V.**—Figure 5 shows some of the data of cyclohexane and ethylene dichloride for the various mixtures plotted against mole fraction as abscissa. Although the uniformity of the data is not very good in some cases, due to the difficulty of producing uniform irradiation in each run with the equipment at our disposal, the trends are clear, thus making it worthwhile to present the following curves.

Curve L shows that the position of  $\lambda_{\max}$  increased from 2700 Å. in pure cyclohexane solution along a smooth curve to 2745 Å. in ethylene dichloride.

Curve A represents the absorbancy of the solute (I) in the pure solvents and various of their mixtures. The irregularity of the curve was rather unexpected but repeated checks convinced the author that this was not due to experimental error (estimated to be 0.02). It is known<sup>11</sup> that this mixture of solvents does give abnormal boiling point curves.

Curve B<sub>1</sub> represents the values of the absorbancies of the carbonium ion (MG)<sup>+</sup> whose peak value occurs about 6200 Å. after four minutes of irradiation of the solution in a Pyrex flask. It appears to consist of a portion where little or no photo-ionization occurs then a sudden break and a rather steep straight section rounding off as the concentration of the ethylene dichloride approaches 100%.

The corresponding curve B for the absorbancy of the leucocyanide (I) shows a steady decline. The scatter of the points is rather large but may be due to the fact that the position of  $\lambda_{\max}$  in each

case is different and one is not comparing exactly the same thing. The general tendency of a downward sloping curve is clear and warrants its inclusion.

Curve C represents the values of  $\lambda_{\max}$  for the solute I in the various solutions after reversal times of from one to five days. The scatter of the points here is undoubtedly accentuated by this large difference in reversal times. However, the trend is clear in this case as with B below and hence the curve is included.

Curve D represents the values of the absorbancies for the solute I on final irradiation (one minute duration on a quartz flask) and covers the range 2640–2740 Å. It is much below B and hence represent a more nearly complete photolysis of the solute.

This series of curves summarizes the behavior of solutions composed of the pure solvents and mixtures thereof as far as summarization can successfully be carried. A similar summarization for the case in which the leucocyanide (I) is dissolved in cyclohexane, ethylidene dichloride and mixtures of these two is reproduced in Fig. 6. This series of absorbancy curves has the same general character as the former, differing largely in degree.

**Part VI. Solutions of Malachite Green Leucocyanide (I) in a Mixture of Cyclohexane and Ethylidene Dichloride** (concn. =  $2.17 \times 10^{-5}$  mole/l.).—The absorption spectra of three solutions of malachite green leucocyanide (I) dissolved in a mixture of cyclohexane and ethylidene dichloride in which the mole fractions of the latter were 0.355, 0.563 and 0.750, respectively, were obtained for the usual conditions of irradiation, and reversal times.

In general, they were similar to those in which cyclohexane and ethylene dichloride were used as a solvent but in this case the changes were not so pronounced. The degree of photo-ionization increased with increasing mole fraction of the dichloride and the reverse (dark) reactions showed considerable formation of a component having a flat maximum in the region 2660 Å. Reversal rates were com-

(11) C. R. Fordyce and D. R. Simonsen, *Ind. Eng. Chem.*, **41**, 104 (1941); also "Tables of Azeotropes," The Dow Company (Horsley), Midland, Michigan, refs. 2403 and 2404.

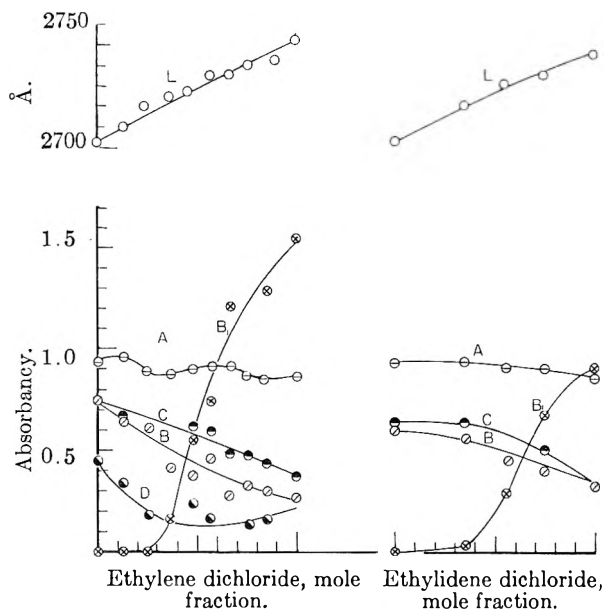


Fig. 5.—Summarized data for solution of malachite green leucocyanide (I) in cyclohexane and ethylene dichloride and their mixtures: L, position of  $\lambda_{max}$  in Å.; A, absorbancies of original solutions; B, absorbancies after 4 minutes irradiation in Pyrex flask; B<sub>1</sub>, absorbancies of (MG)<sup>+</sup> corresponding to those of curve B; C, absorbancies after standing various numbers of days; D, absorbancies after irradiation in quartz flask.

Fig. 6.—Summarized data for solutions of malachite green leucocyanide (I) in cyclohexane and ethylidene dichloride and their mixtures: L, position of  $\lambda_{max}$  in Å.; A, absorbancies of original solutions; B, absorbancies after 4 minutes irradiation in Pyrex flask; B<sub>1</sub>, absorbancies of (MG)<sup>+</sup> corresponding to those of curve B; C, absorbancies after standing various numbers of days.

paratively rapid in the mixture containing 0.563 as the mole fraction of ethylidene dichloride, thus making the reading of the spectrophotometer somewhat uncertain.

**General Observations.**—From an examination of the various absorbancy curves for the solutions of malachite green leucocyanide (I) of the same

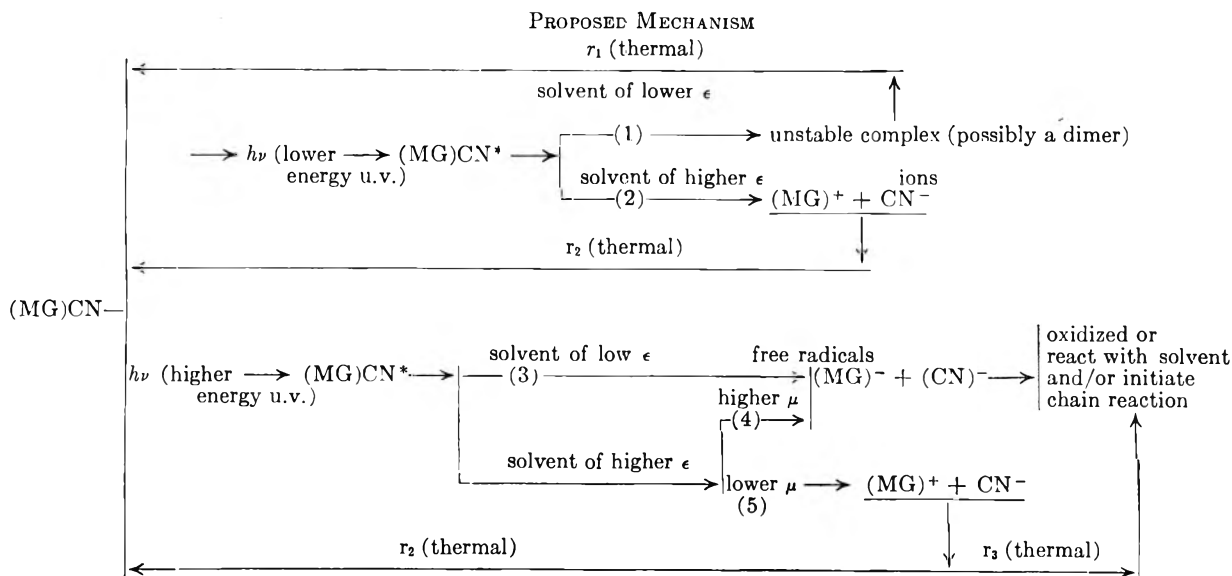
concentration and treated under like conditions as represented in Fig. 1–6, one can draw certain definite conclusions. In the first place, photo-ionization proceeds to a greater extent in solutions in which ethylene dichloride is mixed with cyclohexane than in those where ethylidene dichloride is used in its place. It is believed that this result is not due to the very small difference in dielectric constant but more likely to the larger difference in the dipole moment of the ethylidene dichloride.

Also, it is observed that irradiation with light that traverses the wall of the quartz flask causes the reformation of less carbonium ion (MG)<sup>+</sup> than did the original irradiation in a Pyrex flask, and therefore must cause the formation of still more compounds of unknown nature.

The sharp break in curve C in Fig. 5 at mole fraction 0.25 and the corresponding one, curve C in Fig. 6, can be interpreted as indicating that photo-ionization starts to occur in the region where the dielectric constant is about 4.5 (assuming a linear relationship in both cases). After this break occurs, a region in which the photo-ionization is roughly proportional to the mole fraction of either one of the dichlorides. Keeping in mind that longer exposure does not produce additional (MG)<sup>+</sup> and that there is no dark reverse reaction with appreciable velocity this is rather puzzling. The best interpretation is represented by the mechanism proposed below.

In Part B-I where cyclohexane only is the solvent mechanisms (1) and (3) predominate but in Part B-III where ethylene dichloride is the solvent, mechanisms (2), (4) and (5) predominate. In Part B-II, represented in particular in Fig. 2 and in general in Fig. 5, there is a gradual shift with the increasing dielectric of the medium from mechanisms (1) and (3) to (2), (4) and (5).

In Part B-IV in which ethylidene dichloride only is the solvent, mechanisms (2), (4) and (5) predominate with (2) suppressed in comparison with the case in which ethylene dichloride (Part B-III) is the solvent. As above, in the intermediate mix-



where  $\epsilon$  = dielectric constant,  $\mu$  = dipole moment, and (MG)CN\* = activated molecule.

tures represented in Fig. 6, there is a gradual shift from mechanisms (1) and (3) to (2), (4) and (5) with increasing dielectric constant and dipole moment.

The suppression of mechanism (2) may be attributed to the higher dipole moment of ethylidene dichloride as the dielectric constants of the two dichlorides are so nearly the same.

Reactions  $r_1$  and  $r_2$  are slow thermal reactions requiring days for completion. As  $r_2$  is so much more rapid in pure ethyl alcohol, where  $\Phi$  is almost unity and  $\epsilon$  is 23.2 debyes, than in media of lower dielec-

tric constants, the rate must depend largely on this constant and the mechanism be almost exclusively (2). Reaction  $r_3$  is a thermal reaction that is more rapid than  $r_2$  in solutions of higher dielectric constant and polarity.

The above mechanisms allow one to conclude that as the dielectric constant of the solvent increases the photo-ionization process requires less energy than the free radical process as the former predominates when lower energy quanta are absorbed by the solute.

## VAPOR PRESSURE STUDIES INVOLVING SOLUTIONS IN LIGHT AND HEAVY WATERS. IV. SEPARATION FACTOR AND CROSSOVER TEMPERATURE FOR SALT SOLUTIONS OF THE MIXED WATERS AND FOR A MIXTURE OF THE PURE WATERS FROM 100° TO THE CRITICAL TEMPERATURE

BY ROBERT L. COMBS AND HILTON A. SMITH

*Chemistry Department, University of Tennessee, Knoxville, Tennessee*

*Received October 6, 1956*

An investigation has been made of the separation factor of the isotopes of hydrogen in salt solutions of heavy and light water with particular emphasis on the crossover temperature at which point the separation factor becomes one. The separation factor for a mixture of the pure waters is presented and compared to the square root of the ratio of the vapor pressures of pure light water to pure heavy water. The agreement between these functions is rather good, though there is some deviation at the extremes of temperature. The addition of a salt to the mixed waters was found to lower the separation factor and the crossover temperature indicating that both properties are a function of the structure of the liquid phase. The lowering of the crossover temperature was found to be related to other functions which are indication of order or disorder of water in solutions. It was found that anions had the most influence in lowering the separation factor and the crossover temperature, with larger anions giving the greatest effect. Results determined by an independent method, Rayleigh distillation, were found to agree with direct measurements to at least 4 parts in 1000. The lowest separation factor (0.966) obtained in this research indicates that it might be possible to produce heavy water above the crossover temperature by a process of extractive distillation using either lithium iodide or potassium orthophosphate as the "solvent."

This investigation was undertaken to explore a possible method for the separation of light and heavy water and to gather fundamental information on the structure of aqueous solutions at high temperatures. The most important factor by which a separation process can be judged is the separation factor,  $\alpha$ , defined for distillation work with heavy and light water by

$$\alpha = \frac{(H/D)_{\text{gas}}}{(H/D)_{\text{liquid}}} \quad (1)$$

where (H/D) is the molar ratio of hydrogen to deuterium in the gas or liquid phase as is indicated by the subscript. Benedict<sup>1</sup> and Weaver<sup>2</sup> have shown that the separation factor is substantially independent of the original composition and of the extent to which the process has proceeded. Those processes with an  $\alpha$  greatly removed from one give large separation in a single stage. At room temperature  $\alpha$  for water vaporization is greater than one but approaches one with a rise in temperature.<sup>3</sup> Miles and Menzies<sup>4</sup> and Riesenfeld and Chang<sup>5</sup> have shown that the vapor pressures of

light and heavy water are equal at about 225° and that the vapor pressure of deuterium oxide becomes larger than that of protium oxide above this temperature. Thus one would expect  $\alpha$  to become one at about 225° and to be less than one above this temperature. The temperature at which the separation factor is equal to one, but above or below which  $\alpha$  is below or above one, is called the crossover temperature. Googin and Smith<sup>6</sup> have investigated the possibility of using extractive distillation<sup>7,8</sup> at room temperature and have found that there is essentially no possibility of improving the separation by the addition of salts. In fact, there is a lowering of  $\alpha$  and a decrease in separation with solutes present. If this lowering continues above the crossover temperature the separation will then be increased. Here the separation factors of solutions from 100° to the critical temperature were determined directly by analysis of both phases. Few, if any, direct measurements of  $\alpha$  have been made in this range. Most investigators estimate  $\alpha$  from the vapor pressure of the pure waters by using questionable assumptions.<sup>9</sup>

(1) M. Benedict, *Chem. Eng. Progr.*, **43**, 41 (1947).

(2) B. Weaver, *Anal. Chem.*, **26**, 474 (1954).

(3) R. L. Combs, J. M. Googin and H. A. Smith, *THIS JOURNAL*, **58**, 1000 (1954).

(4) F. T. Miles and A. W. C. Menzies, *J. Am. Chem. Soc.*, **58**, 1067 (1936).

(5) E. H. Riesenfeld and T. L. Chang, *Z. physik. Chem.*, **B33**, 120 (1936).

(6) J. M. Googin and H. A. Smith, *THIS JOURNAL*, **61**, 345 (1957).

(7) M. Benedict and L. C. Rubin, *Trans. Am. Inst. Chem. Engrs.*, **41**, 353 (1945).

(8) A. Weissberger, "Technique of Organic Chemistry," Vol. 4, Interscience Publishers, Inc., New York, N. Y., 1951, pp. 317-356.

If they occur, changes in the crossover temperature and  $\alpha$  caused by the addition of salts to the mixed waters should be related in some manner to the differences in structure between salt solutions and the pure waters at high temperatures. Water is a complex and variable mixture whose individual molecules are more or less associated.<sup>10-12</sup> Of the many theories on the structure of water, some<sup>13-16</sup> have been proposed based on crystalline character similar to ice, while others<sup>17-19</sup> have been based on structures which are loose and very transient. If each water molecule in the ice crystal were oriented in a definite way,<sup>14</sup> permitting the assignment of a unique configuration to the crystal, one would expect the residual entropy at very low temperatures to vanish. It is found experimentally that ordinary ice has a residual entropy of 0.82 cal. per mole<sup>20,21</sup> while heavy ice has a residual entropy of 0.77 cal. per mole.<sup>22</sup> Pauling<sup>23-26</sup> (taking into account the tetrahedral molecule of water<sup>26</sup> and assuming that each water molecule is so oriented that its two hydrogen atoms are directed approximately toward two of the four surrounding oxygen atoms, that only one hydrogen atom lies along each oxygen-oxygen line, and that under ordinary conditions the interaction of non-adjacent molecules is such as not to stabilize appreciably any one of the many configurations satisfying these conditions with reference to the others) calculated the residual entropy of ice to be 0.806 cal. per mole. This agreement and neutron diffraction studies<sup>27</sup> provide strong support for the postulated structure of ice. Pauling, also, feels that the structure of water is in part similar to that of ice and in part based upon closest packing. As the temperature increases, the structure should collapse and the density increase except when thermal motion becomes appreciable and requires more space. The point of balance between these two effects will be the temperature of maximum density. Comparison of the properties<sup>4,5,28-34</sup> of light and heavy water indicates

that heavy water is more associated than light water at room temperatures, while at higher temperatures heavy water is less associated (referring to critical temperature and vapor pressure for the higher temperatures). Thus a crossover temperature, where the two waters have the same amount of association, will be expected to occur between room temperature and the critical temperature for any property of the mixed waters which depends on the association. There have been a number of papers<sup>18,19,30,35,36</sup> written about the temperature effect on the structure and properties of light water but only a few<sup>4,5</sup> about heavy or the mixed water.

The problem of the influence of a dissolved salt on the structure of water has been studied by many investigators using dielectric properties of solutions,<sup>37-39</sup> X-ray diffraction patterns,<sup>14,40</sup> infrared absorption spectra,<sup>41</sup> Raman spectra,<sup>14,42</sup> calculated hydration energies,<sup>43</sup> viscosity data,<sup>14,44</sup> and molar volumes.<sup>14</sup> It was generally found that a rise in temperature was quite similar to dissolving an electrolyte in water and that a salt always lowers the temperature of maximum density. Because of the partial charges on the water molecule, there will be interaction between the oxygen-part of the water molecule and the cation and between the hydrogen-part and the anion. Thus anions should show the greater difference in their influence on the structure of light or heavy water as they directly interact with the positive part (where the protium or deuterium atom is located) of the water molecule. Furthermore, a large anion would fit less well into the structure of water and would cause a larger effect than would a small anion. In contrast, the cation would influence the fractionation of oxygen isotopes as Feder and Taube<sup>45</sup> have shown in the case of carbon dioxide. The critical temperatures of salt solutions could predict the association in the liquid phase at high temperatures. In this connection, only alkali halides<sup>46,47</sup> have been studied, and, since the solute increases the critical temperature, these data indicate more association in the salt solutions.

(9) G. N. Lewis and R. E. Cornish, *J. Am. Chem. Soc.*, **55**, 2616 (1933).

(10) H. M. Chadwell, *Chem. Revs.*, **4**, 375 (1927).

(11) N. E. Dorsey, "Properties of Ordinary Water-Substance," Reinhold Publ. Corp., New York, N. Y., 1940, pp. 161-178.

(12) J. R. Partington, "An Advanced Treatise on Physical Chemistry," Vol. 2, Longmans, Green, and Co., New York, N. Y., 1951, pp. 41-43.

(13) W. C. Röntgen, *Ann. physik. Chem.*, [3] **45**, 91 (1892).

(14) J. D. Bernal and R. H. Fowler, *J. Chem. Phys.*, **1**, 515 (1933).

(15) R. H. Fowler and J. D. Bernal, *Trans. Faraday Soc.*, **29**, 1049 (1933).

(16) J. D. Bernal, *ibid.*, **33**, 27 (1937).

(17) B. E. Warren, *J. Appl. Phys.*, **8**, 645 (1937).

(18) J. Morgan and B. E. Warren, *J. Chem. Phys.*, **6**, 666 (1938).

(19) S. Katzoff, *ibid.*, **2**, 841 (1934).

(20) W. F. Giaque and M. F. Ashley, *Phys. Rev.*, [2] **43**, 81 (1933).

(21) W. F. Giaque and J. W. Stout, *J. Am. Chem. Soc.*, **58**, 1144 (1936).

(22) E. A. Long and J. D. Kemp, *ibid.*, **58**, 1829 (1936).

(23) L. Pauling, *ibid.*, **57**, 2680 (1935).

(24) Cf. K. S. Pitzer and J. Polissar, *THIS JOURNAL*, **60**, 1140 (1956).

(25) L. Pauling, "The Nature of the Chemical Bond," 2nd ed., Cornell University Press, Ithaca, N. Y., 1948, pp. 301-306.

(26) C. P. Smyth, *Phil. Mag.*, [6] **47**, 530 (1924).

(27) E. O. Wollan, W. L. Davidson and C. G. Shull, *Phys. Rev.*, [2] **75**, 1348 (1949).

(28) I. Kirshenbaum, "Physical Properties and Analysis of Heavy Water," McGraw-Hill Book Co., Inc., New York, N. Y., 1951, pp. 1-68, 416.

(29) R. T. Lagemann, L. W. Gilley and E. G. McLeroy, *J. Chem. Phys.*, **21**, 819 (1953).

(30) P. C. Cross, J. Burnham and P. A. Leighton, *J. Am. Chem. Soc.*, **59**, 1134 (1937).

(31) K. Wirtz, *Angew. Chem.*, **A69**, 138 (1947).

(32) G. W. Stewart, *J. Chem. Phys.*, **2**, 558 (1934).

(33) J. W. Ellis and B. W. Sorge, *ibid.*, **2**, 559 (1934).

(34) J. S. Rowlinson, *Physica*, **19**, 303 (1953).

(35) J. A. Pople, *Proc. Roy. Soc. (London)*, **A205**, 163 (1951).

(36) M. A. Azim, S. S. Bhatnagar and R. N. Mathur, *Phil. Mag.*, [7] **16**, 580 (1933).

(37) C. H. Collie, J. B. Hasted and D. M. Ritson, *Proc. Phys. Soc. (London)*, **60**, 71, 145 (1948).

(38) G. H. Haggis, J. B. Hasted and T. J. Buchanan, *J. Chem. Phys.*, **20**, 1452 (1952).

(39) J. B. Hasted and S. H. M. El Sabeh, *Trans. Faraday Soc.*, **49**, 1003 (1953).

(40) G. W. Stewart, *J. Chem. Phys.*, **7**, 869 (1939); **11**, 72 (1943).

(41) E. Ganz, *Ann. Physik.*, [5] **28**, 445 (1937); *Z. physik. Chem.*, **B35**, 1 (1937).

(42) T. H. Kujumzelis, *Z. Physik*, **110**, 742 (1938).

(43) E. J. W. Verwey, *Rec. trav. chim.*, **60**, 887 (1941); **61**, 127 (1942).

(44) R. W. Gurney, "Ionic Processes in Solution," McGraw-Hill Book Co., Inc., New York, N. Y., 1953, pp. 159-185.

(45) H. M. Feder and H. Taube, *J. Chem. Phys.*, **20**, 1335 (1952).

(46) E. Schroer, *Z. physik. Chem.*, **129**, 79 (1927).

(47) C. H. Secoy, *THIS JOURNAL*, **54**, 1337 (1950).

The solubility of a solute and the structure of the solvent are related. At room temperature, heavy water is a poorer solvent for most salts than is light water.<sup>48,49</sup> Some lithium salts<sup>50</sup> at room temperature, strontium chlorides<sup>51</sup> and sodium iodide<sup>52</sup> above 60° are the only salts which were found to be more soluble in heavy water. The difference in solubility decreases with temperature for all salts studied except sodium sulfate.<sup>52,53</sup>

The measurement of the distillation separation factor for the isotopes of hydrogen from 100° to the critical temperature of the pure waters and their salt solutions should give information on the structure of water and its solutions at high temperatures where little previous work has been done. This aspect will be considered here as well as the practical problem of production of heavy water.

### Experimental

In this investigation the separation factor was determined directly by analyzing samples of the gas and of the liquid phase which had been in equilibrium and substituting the composition values in equation 1. The pressure vessel used for securing the equilibrium was constructed from cold-rolled steel and tested to 4100 p.s.i.g. at 290°. Two valves were in the head of the vessel so that the liquid and the gas phase could be sampled separately. The liquid-sampling tube, extending into the solutions, was fashioned from chrome-molybdenum steel tubing supplied by Aminco.<sup>64</sup> The valve packing was graphite-impregnated (no oil) asbestos thread of 1/8 inch diameter. The gasket for the head was constructed out of 1/16 inch copper sheet. The liner found to be most satisfactory for neutral and basic solutions was a stainless steel cup which fitted tightly into the vessel. The capacity of the vessel with this liner in place was approximately 100 ml. For acidic solutions, a Pyrex glass liner was used. A heater (1600 watts at 120 volts) covered the bottom section up to the trap connections. The head of the vessel was not heated or insulated, but its large heat capacity together with the consistency of the results obtained indicated that insulation was unnecessary. A shaker which made 47 complete cycles per minute kept the heater and the vessel oscillating within a 25-degree angle of vertical while equilibrium was being established. There were eight regular sample traps used and two Rayleigh distillation traps. There was no difference in construction between the liquid sample traps and the gas sample traps. Each trap was numbered and had different connections at each end. One side of each trap had a 12/30 standard-taper male joint so that it could be connected to the purification train or capped when necessary, while the other side had an Aminco<sup>64</sup> superpressure fitting so that it could be connected to the pressure vessel or capped when necessary. The regular sample traps were used for the sampling of both phases during ordinary distillation and had a total capacity of less than 20 ml. With these traps, the 12/30 joint was made from Pyrex glass with a Kovar to Pyrex glass seal<sup>65</sup> immediately underneath so that the remainder of the trap could be constructed of metal (copper and steel). This glass joint was necessary to prevent leakage when the trap was heated on the purification train to remove water from hygroscopic salts. The Rayleigh traps were constructed entirely of metal with the standard-taper joint being of brass.

Each had the same fittings as the regular traps but had a total capacity of over 100 ml.

The purification train was a modification of the apparatus used by Googin and Smith.<sup>6</sup> Only one other trap was employed besides the sample holder as this apparatus was used only to remove and purify the water collected in the metal traps and to test the metal traps for leaks. The metal traps were leak-tested by evacuating and allowing them to stand for one hour; if a McLeod gage showed a constant reading over this period the traps were considered gas-tight. Before initial use and after each run in which the salt was difficult to dehydrate, a special cleaning procedure was used. Each trap was consecutively cleaned with cleaning solution, washed with distilled water, steamed for over one hour, washed with acetone, dried in a current of air, and tested for moisture residue. The joints and stopcocks of the purification train were lubricated with Apiezon M grease which had been shown to give no exchange or contamination with heavy water.<sup>6</sup> There were two sample holders used so that a sample could be analyzed while another sample was being purified as this operation often required several hours. The falling drop method was used to analyze the samples for the mole per cent. of deuterium oxide. The method and apparatus have been described previously in detail.<sup>3</sup> During the distillation the isotopes of oxygen would be fractionated, but under the conditions<sup>6</sup> used here the change in the separation factor due to this should be less than 0.001.

The chemicals used were reagent grade as commercially supplied whenever possible. The deuterium oxide<sup>66</sup> was 99.8%. The lithium iodide was used in two forms. Lithium iodide with three molecules of water of crystallization was obtained in the form of plates from Mallinckrodt Chemical Works. Before this material was obtained, lithium iodide was prepared from Merck reagent grade hydriodic acid for methoxyl determination and Fisher Scientific Company C.P. grade lithium hydroxide. After some of the water had been evaporated from a slightly acidic solution of the above compounds, the solution was placed in a pressure vessel and heated above 200°. A white crystalline material was obtained by filtering the solution. This was in contrast to the yellow amorphous material obtained by heating the lithium iodide solution to dryness in air or in a vacuum furnace. The crystalline material obtained from the vessel was placed in a vacuum desiccator over magnesium perchlorate, repeatedly ground up and evacuated until a fine white hygroscopic powder was obtained. It was estimated from the change in deuterium concentration for a solution of this material in mixed waters that less than one molecule of water remained with each lithium iodide molecule after this treatment. Silver fluoride was prepared by Mellor's procedure<sup>67</sup> from Eimer and Amend C.P. grade silver nitrate, Merck anhydrous reagent grade potassium carbonate, and Baker reagent grade hydrofluoric acid. The silver fluoride was dried in darkness in a platinum dish placed in a vacuum desiccator over anhydrous magnesium perchlorate. The resulting material was brown in color and completely soluble in water; it decomposed to a slight extent when exposed to moisture and light.

The procedure generally followed for an ordinary distillation was to load the vessel with the charge (50 ml. of approximately 50 mole % D<sub>2</sub>O plus a 0.1 mole fraction of the salt) and to test for leaks by submerging the vessel under water after nitrogen at 4.2 kg. cm.<sup>-2</sup> had been placed in the vessel. If no bubbles appeared during five minutes, the vessel was considered gas-tight. After this testing the vessel was placed in the heater and shaker ensemble and was brought to the desired temperature where it was shaken for six to ten hours for the attainment of equilibrium. The shaking was then stopped, and the temperature read with a copper-constantan thermocouple and a Wheelco potentiometer. Approximately 0.5 ml. was bled into the atmosphere from the liquid-sampling tube to make sure that only solution was in the tube. Next, the sample traps were connected to the vessel and placed in a Dry Ice-acetone bath. Usually less than 1 g. of sample was collected in each trap. The liquid sample was always collected first since the pres-

(48) T. Chang and Y. Hsieh, *Sci. Repts. Natl. Tsing Hua Univ.*, **A6**, 252 (1948) (*C. A.*, **43**, 6492c (1949)); *J. Chinese Chem. Soc.*, [16], **10**, 65 (1949) (*C. A.*, **43**, 8821g (1949); *ibid.*, **44**, 28f (1950)).

(49) E. C. Noonan, *J. Am. Chem. Soc.*, **70**, 2915 (1948).

(50) E. Lange, *Z. Elektrochem.*, **44**, 1 (1938).

(51) F. T. Miles, R. W. Shearman and A. W. C. Menzies, *Nature*, **138**, 121 (1936).

(52) R. D. Eddy and A. W. C. Menzies, *THIS JOURNAL*, **44**, 207 (1940).

(53) R. W. Shearman and A. W. C. Menzies, *J. Am. Chem. Soc.*, **59**, 185 (1937).

(54) American Instrument Co., Silver Springs, Maryland, Catalog 406, 1947 Edition, pp. 41-44.

(55) Stupakoff Ceramic and Manufacturing Co., Latrobe, Penn., Catalog No. 453 on Kovar-Glass Seals, p. 24.

(56) Supplied by Stuart Oxygen Co., 211 Bay Street, San Francisco, Calif.

(57) J. W. Mellor, "A Comprehensive Treatise of Inorganic and Theoretical Chemistry," Vol. 3, Longmans, Green, and Co., New York, N. Y., 1923, pp. 387, 456-457.

sure fell approximately 1.4 kg. cm.<sup>-2</sup> whenever the gas sample was taken. Then the temperature was changed, and a new equilibrium was established. For most runs only eight samples were taken thus giving four points on the alpha versus temperature curve, though for some of the early runs over eight points were obtained for each curve. Samples were generally taken at about 120, 180, 240 and 340°. Usually the samples were taken in the order given, although several samples taken out of this order gave consistent values when compared to those resulting from ordered sampling.

After the samples were obtained from the pressure vessel, the traps were capped and placed in the purification train as soon as possible. The sample was distilled under vacuum into the first trap where it was treated with anhydrous potassium carbonate if any acidic material was suspected to have been distilled. If the salt used was difficult to dehydrate, the liquid-sample trap was placed in a bath of *n*-butyl phthalate heated above 100°. To test for completeness of dehydration the Dry Ice-acetone bath surrounding the first trap of the purification train was moved to cover a new section of glass, and if no moisture condensed on the newly covered section in over a minute, the dehydration was considered complete. After the sample had been treated in the first trap it was distilled into the sample holder. The sample was then removed from the purification train using a standard technique<sup>6</sup> and was analyzed for deuterium oxide after its pH had been checked.

Consideration of the vessel volume and the density of the gas and liquid phases shows that the liquid expands enough to keep the vessel more than half full of liquid phase up to the critical temperature. This allows both phases to be sampled without any special consideration as to the volume ratio if the samples are a small percentage of the total phase. The gas sample was bled very slowly as the gas phase had the largest percentage taken as a sample. The concentration of the liquid phase changes as more and more of the charge is in the gas phase. However, it is estimated that only 0.6% of a 50-ml. charge of pure water at 200° would be in the gas phase. Thus one would expect little change in the salt concentration due to part of the water being in the gas phase. Furthermore most of the solutions used were saturated, or very nearly saturated at 0.1 mole fraction of the salt used for most runs. The high heat capacity of the vessel prevented a drop in temperature if the gas sample were taken slowly.

The procedure which was used in a Rayleigh distillation was to charge the vessel with the mixed waters or with a saturated salt solution. The saturated salt solution was desirable so that the equilibrium alpha would not change due to a change in salt concentration. Then the vessel, while being shaken, was brought to the desired temperature. After the shaking was stopped, the gas valve was slightly opened to allow the first sample to escape into a Rayleigh trap immersed in a Dry Ice-acetone bath. Generally, one to two hours was required to collect over 50% of the charge. The sample was collected slowly so that the temperature and solution equilibrium would be maintained. After the first sample had been collected, the remainder of the water was collected much more rapidly in the second Rayleigh trap from the gas-sampling valve. The amount collected in each trap was determined by the use of a high-capacity balance sensitive to 10 mg. Part of each sample (approximately 1 g.) was transferred to the purification train and was processed in the ordinary manner so that the mole per cent. D<sub>2</sub>O could be determined.

### Calculations

The separation factor obtained at equilibrium could be checked by two general methods. In one method, a multiple plate fractionation column for extractive distillation with salts could be built. Here, the over-all separation factor (*A*) would be related to the single stage separation factor ( $\alpha$ ) by

$$A = \alpha^n \quad (2)$$

where *n* is the number of theoretical plates.<sup>58,59</sup> The other possible method uses Rayleigh distilla-

tion<sup>60,61</sup> in which a large part of the sample is evaporated, and thus the amount of separation is increased. Here, Rayleigh distillation was used to check the ordinary equilibrium distillation values. As the fraction evaporated ( $\theta$ ) approaches one, the differences between the concentration of heavy water in the gas and in the liquid phase become larger and, thus, the apparent separation factor ( $\alpha'$ ) for the evaporation of over 50% of the sample differs from one more than the equilibrium separation factor ( $\alpha$ ). If *n* and *N* represent the equilibrium values of mole per cent. of deuterium oxide in the gas and in the liquid phase, respectively, for the start of the distillation, and *n'* and *N'* are the mole % of deuterium oxide in the total distillate and the liquid residue, respectively, at the end of the evaporation, it follows that

$$\alpha = \frac{(1-n)N}{n(1-N)} \quad (3)$$

and

$$\alpha' = \frac{(1-n')N'}{n'(1-N')} \quad (4)$$

Use of a conservation relation plus equation 3, with  $\theta$  as the mole fraction distilled, allows one to write<sup>62,63</sup>

$$(1-\theta)^{1-\alpha} = \left(\frac{N'}{N}\right)^\alpha \left(\frac{1-N}{1-N'}\right) \quad (5)$$

Equation 5 would be quite satisfactory for use except that the experiment has been designed to measure the separation factors ( $\alpha$ 's) more accurately than the mole per cents. (*N*'s). Thus an equation in  $\alpha$ ,  $\alpha'$  and  $\theta$  is desired but appears to be unobtainable. Using a material balance and equation 4, equation 5 can be written

$$\left\{ \frac{(1-\theta)[\alpha'(1-N') + N']}{\theta + (1-\theta)[\alpha'(1-N') + N']} \right\}^{1-\alpha} = \left\{ \frac{\alpha' + N'(1-\theta)(1-\alpha')}{\theta + (1-\theta)[\alpha'(1-N') + N']} \right\} \quad (6)$$

Thus using equations 6 and 1 and the two experimental techniques previously described, the separation factor for a single stage can be determined by two independent methods.

The concentration normally used for these experiments was a salt mole fraction of 0.100. This high concentration was employed because, from the extractive-distillation viewpoint, high "solvent" (the salt considered as the solvent, here) concentration is necessary for a maximum effect on the relative volatility.<sup>8,64</sup> Googin and Smith<sup>6</sup> have found a linear relationship between the change in the separation factor and the concentration of a potassium iodide solution. Lithium iodide was chosen here to study the effect of concentration because it gave one of the lowest separation factors and was very soluble. From Fig. 1 it is observed

(60) K. Cohen, "The Theory of Isotope Separation as Applied to the Large-Scale Production of U<sup>235</sup>," McGraw-Hill Book Co., Inc., New York, N. Y., 1951, pp. 150-153.

(61) Lord Rayleigh, *Phil. Mag.*, [5] **42**, 493 (1896); [6] **4**, 521 (1902).

(62) H. C. Urey, F. G. Brickwedde and G. M. Murphy, *Phys. Rev.*, [2] **40**, 1 (1932).

(63) H. C. Urey and G. K. Teal, *Rev. Mod. Phys.*, **7**, 34 (1935).

(64) A. P. Colburn and E. M. Schoenborn, *Trans. Am. Inst. Chem. Engrs.*, **41**, 421 (1945).

(58) H. C. Urey and L. J. Greiff, *J. Am. Chem. Soc.*, **57**, 321 (1935).

(59) M. Randall and W. A. Webb, *Ind. Eng. Chem.*, **31**, 227 (1939).

that increasing the concentration does lower the curve a corresponding amount. If one plots the difference between the lowest alpha for the salt solution and for the mixed waters *versus* the difference between the crossover temperature for water and the corresponding salt solution, one obtains a straight line. However, if one plots either of these differences *versus* the mole fraction of lithium iodide in the solution some deviation from linearity is noted. Lithium iodide had many experimental difficulties, such as caking in traps, giving incomplete dehydration, and undergoing hydrolysis with the water. Errors from sources such as these could easily have caused the deviations observed. Anhydrous sodium fluoride was added to each liquid sample trap before the sample was distilled with the hope that the reaction



would occur and make dehydration easier. Using the free energy values of Latimer,<sup>65</sup> the free energy of such a reaction is found to be +1.33 kcal. This indicates that the reaction does not go to the extent desired, but as the results using sodium fluoride were more consistent and the time for acquiring dehydration (hours instead of days) was shorter, the addition of sodium fluoride was continued for the lithium iodide runs. If the prepared lithium iodide were considered to be dry, the mole fraction of its solution would be 0.143. It is likely that the curve does lie between the 0.150 and the 0.100 mole fraction curves using Mallinckrodt lithium iodide.

### Results and Discussion

The curve for the separation factor *versus* temperature for a mixture of heavy and light water is given in Fig. 2. The points below 100° are taken from Table IV in paper II of this series.<sup>3</sup> The points taken from Oliver, Grisard and Milton<sup>66</sup> were calculated from their vapor pressure data by the approximate equation

$$\alpha = \sqrt{\frac{p^0_{\text{H}_2\text{O}}}{p^0_{\text{D}_2\text{O}}}} \quad (8)$$

where  $p^0$  is the vapor pressure of the pure substance indicated by the subscript.<sup>9</sup> This graph indicates that the assumptions used in deriving equation 8 do not hold at the extremes of temperature. The agreement between  $\alpha$  and  $\sqrt{p^0_{\text{H}_2\text{O}}/p^0_{\text{D}_2\text{O}}}$  is fairly good, however.

The results obtained with salt solutions of the mixed waters are given in Table I.  $N_x$  is the mole fraction of salt  $x$  in the solution of the mixed waters. The curve, similar in shape to those curves in Figs. 1 and 2, of the alpha *versus* temperature was determined for the concentration of the salt given, and the crossover temperature and the lowest separation factor were read from this curve. The values in the delta crossover temperature and delta

(65) W. M. Latimer, "The Oxidation States of the Elements and Their Potentials in Aqueous Solution," 2nd ed., Prentice-Hall, Inc., New York, N. Y., 1952.

(66) G. D. Oliver, J. W. Grisard and H. T. Milton, Report K-874, Special, K-25 Plant, Carbide and Carbon Chemicals Co., Oak Ridge, Tennessee, Date of Issue: March 12, 1952, Unclassified: March 9, 1955; G. D. Oliver and J. W. Grisard, *J. Am. Chem. Soc.*, **78**, 561 (1956).

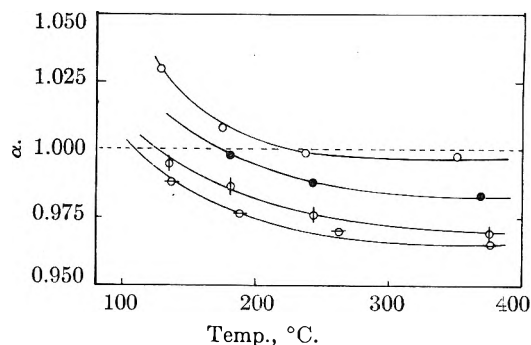


Fig. 1.—Separation factor *versus* temperature for lithium iodide solutions:  $\circ$ ,  $N_{\text{LiI}} = 0.0005$ ;  $\bullet$ ,  $N_{\text{LiI}} = 0.100$ ;  $\odot$ ,  $N_{\text{LiI}} = 0.150$ ;  $\ominus$ ,  $N_{\text{LiI}} = \text{approx. } 0.143$ , made with specially prepared LiI.

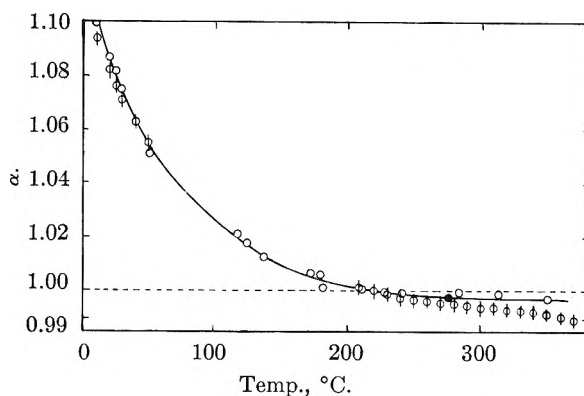


Fig. 2.—Separation factor *versus* temperature for a mixture of light and heavy water:  $\circ$ , points from direct determination of composition of liquid and vapor;  $\bullet$ , point from Rayleigh distillation;  $\ominus$ , points calculated from the approximation  $\alpha = \sqrt{p^0_{\text{H}_2\text{O}}/p^0_{\text{D}_2\text{O}}}$ .

alpha columns were determined by subtracting the values obtained for the salt solution from the value obtained for the pure waters. When the delta alpha values are plotted *versus* the delta crossover temperature values a few of the salts do not lie on the straight line obtained. Those salts giving anomalous values are sodium sulfate and potassium iodide. This could be due to changes in solubility as the temperature increases. The delta crossover temperature has a greater range than does

TABLE I  
RESULTS OBTAINED WITH THE SALT SOLUTIONS

Salt (x)	$N_x$	Cross-over temp.	Lowest $\alpha$	$\Delta$ Cross-over temp.	$\Delta\alpha$
None		220	0.997		
AgF	0.100	208	.998	12	0.009
KF	.100	190	.990	30	.007
KCl	.101	146	.989	74	.008
KBr	.101	152	.987	68	.010
KI	.103	139	.992	81	.005
NaI	.092	153	.990	67	.007
LiI	.150	106	.965	114	.032
LiI	.143(?)	124	.969	96	.028
LiI	.100	170	.983	50	.014
LiI	.0005	220	.997	0	000
ZnI <sub>2</sub>	.100	174	.986	46	011
Na <sub>2</sub> SO <sub>4</sub>	.100	220	.985	0	012
K <sub>2</sub> PO <sub>4</sub>	.100	83	.966	137	.031

delta alpha. Thus the change in the crossover temperature should show a change in the solution structure more readily than the change in alpha and will be used for comparisons with the other properties of solutions.

Some attempts were made to use potassium ferrocyanide, sodium tripolyphosphate, sodium lauryl sulfonate and zinc sulfate as the solute, but no satisfactory results were obtained with these salts. The difficulties involved were decompositions of the salt and reaction with the liner of the vessel. Many of the salts used (lithium iodide, zinc iodide and silver fluoride) gave acidic solutions for the samples. These samples were neutralized with anhydrous potassium carbonate, but if the hydrolysis reaction went to a large extent, this reaction could influence alpha more than does the distillation. The silver fluoride left a deposit of silver in the vessel even when the run was kept as short as possible (less than a day and a half).

The results of two Rayleigh distillations are presented in Table II for a mixture of the pure waters and for a salt solution. These measurements indicate the agreement of results obtained by ordinary distillation (equation 1) and by Rayleigh distillation (equation 8) is within 4 parts in 1000. The solubility of potassium orthophosphate is not given at high temperature by Seidell,<sup>67</sup> but the solubility at lower temperatures indicates that the solution used here ( $N_{K_2PO_4} = 0.100$ ) is almost saturated. For calculating the mole fraction evaporated,  $\theta$ , the molecular weight of heavy water<sup>28</sup> was chosen as 20.0284.

The results obtained are encouraging for the production of heavy water by extractive distillation since a salt solution does have a lower separation factor above the crossover temperature than does a mixture of the pure waters. Increasing the salt concentration does increase further the separation of light and heavy water at high temperatures. Of the salts investigated, lithium iodide and potassium orthophosphate gave the lowest separation factors. The curve of alpha versus temperature for most of the salt solutions falls rapidly during the first 60 to 100° after the crossover temperature, but then becomes an almost horizontal line out to the critical temperature. This horizontal portion of the curve, generally 100 to 200° in length, gives a wide range in which the fractionation processes can be carried out with almost the same separation factor.

TABLE II  
RESULTS OF RAYLEIGH DISTILLATIONS

Temp. range, °C.	Mixture of the pure waters	Potassium orthophosphate solution
	280-270	273-259
$\theta$	0.9696	0.6703
$\alpha'$	0.990 <sub>1</sub>	0.954 <sub>7</sub>
(Equation 8)	0.998 <sub>2</sub>	0.972 <sub>4</sub>
(Equation 1)	0.997 <sub>1</sub>	0.968 <sub>9</sub>

The lowering of the crossover temperature is used in discussing the structure of water solutions since,

(67) A. Seidell, "Solubilities of Inorganic and Metal Organic Compounds," Vol. 1, 3rd ed., D. Van Nostrand Co., Inc., New York, N. Y., 1940.

as indicated previously, it is a more sensitive function than the change in  $\alpha$ . Also, only the data for a salt mole fraction of 0.1 are considered here. Such a concentration will give one molecule of salt (at least two ions) per nine molecules of water. The lowering of the crossover temperature signifies that anything which is added to water breaks the hydrogen bonds involving the heavy water molecule in preference to the hydrogen bond involving the light water molecule. The shape of the alpha versus temperature curve reveals that there is a limiting structural difference which is reached somewhat above the crossover temperature. If no structure or association is assumed at these high temperatures, the data would denote that the escaping tendency of heavy water molecules as such is greater than that of light water molecules. However, the higher molecular weight of a heavy water molecule argues for a structure left in the liquid phase to account for the lower vapor pressure of light water above the crossover temperature and its higher critical temperature. As the presence of dissolved non-volatile salts has no influence on the vapor structure, it is the structure of the liquid phase which influences the crossover temperature and the separation factor in the temperature range under discussion. There is essentially no correspondence between the delta crossover temperature and the apparent volume of the ions in solution,<sup>14</sup> or with the ratio of the solubility of the salt at 50° to that at 0°.<sup>67</sup> There are trends revealed when the delta crossover temperature is compared with the solubility of the salt in water,<sup>67</sup> the ratio of the solubility in heavy water to that in light water,<sup>52,53</sup> the free energy of hydration,<sup>43,68</sup> the heat of hydration,<sup>43,68</sup> the heat of solution,<sup>14</sup> and the difference of the integral heat of solution for the salt in heavy water and in light water.<sup>69</sup> There are reasonable straight line relationships obtained when the lowering of the crossover temperature is compared to the entropy of hydration,<sup>43,68</sup> the molar fluidity elevation,<sup>70</sup> the  $B$ -coefficient of the Jones and Dole equation<sup>71</sup> for the viscosity of dilute solutions,<sup>44,72</sup> and with Googin and Smith's  $k$  values in some low temperature work on alpha.<sup>6</sup> Most of the above properties were measured at room temperature while the data given here were obtained at temperatures greater than 100°. This discloses order at high temperatures which can be compared to functions of order in solutions at room temperature. Gurney<sup>44</sup> has related the  $B$ -coefficient of the Jones and Dole equation for viscosity to the order or disorder produced in the water structure by the salt. A positive value of  $B$  (+0.147 for the lithium ion) indicates that the ion is order-producing while a negative value of  $B$  (-0.080 for the iodide ion) indicates a disorder-producing ion. The agreement between the  $B$ -coefficient and the delta crossover temperature is presented in Fig. 3. The multivalent ions are not on the line given by the univalent ions and could be on another line, but not enough

(68) W. M. Latimer, K. S. Pitzer and C. M. Slansky, *J. Chem. Phys.*, **7**, 108 (1939).

(69) E. Lange and W. Martin, *Z. physik. Chem.*, **A180**, 233 (1937).

(70) E. C. Bingham, *THIS JOURNAL*, **45**, 885 (1941).

(71) G. Jones and M. Dole, *J. Am. Chem. Soc.*, **51**, 2950 (1929).

(72) E. Asmus, *Z. Naturforsch.*, **4A**, 589 (1949).

data are available to prove this. When plots are made of the  $B$ -coefficient of the anion or the cation *versus* delta crossover temperature, the agreement is best using the anion values although it is not as good as when the  $B$ -coefficient for the salt is used. As the  $B$ -coefficient has been related to the temperature coefficient of electrical mobility, the lyotropic number, the ionic entropy and the activity coefficient of the ions,<sup>44</sup> the delta crossover temperature is likewise related to these properties. The  $B$ -coefficient is determined in very dilute solutions whereas the delta crossover temperature is determined in almost saturated solutions. For the other properties previously mentioned such as critical temperature and the dielectric constant, not more than two or three values could be found for comparison.

The above correlations demonstrate that the lowering of the crossover temperature and the separation factor are functions of the order-disorder in the solution and that the ions do cause changes in the structure of the water as well as form structures about themselves. Some additional factor must be taken into consideration for the multivalent ions as they did not follow the same relationships as the univalent ions.

Small ions, such as the lithium ion and the fluoride ion, do not tear up the water structure as much as do the large ions, such as the iodide ion and the phosphate ion. Further, anions do affect the sep-

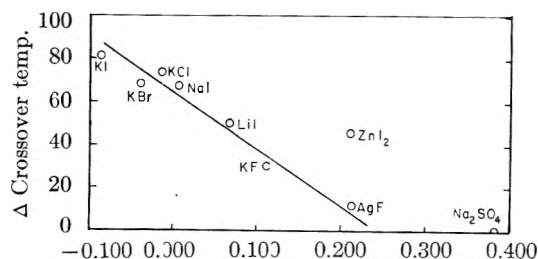


Fig. 3.—The lowering of the crossover temperature *versus* the viscosity  $B$ -coefficient for various salts.

aration, and thus the hydrogen bond, more than the cations. It is evident that potassium orthophosphate changes the structure of water to the greatest extent while sodium sulfate changes the structure the least. It is probable that the phosphate ion hydrates the light water preferentially and thus forms a structure about itself in addition to tearing up the water structure. The solubility of sodium sulfate was very slight (as indicated by plugging of the liquid sampling tube), and this could explain the results obtained.

This research demonstrates clearly that it is the structure of the liquid phase which causes the crossover temperature as well as a separation factor above and below the crossover temperature.

**Acknowledgment.**—The authors are indebted to the United States Atomic Energy Commission for support of this work.

## KINETICS OF THE CHLORATE-SULFITE REACTION

By E. H. GLEASON,\* G. MINO AND W. M. THOMAS

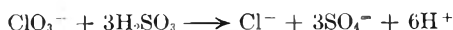
*Contribution from Stamford Laboratories, Research Division, American Cyanamid Company, Stamford, Conn.*

*Received October 11, 1956*

Kinetics of the chlorate-sulfite reaction in water were investigated at 0 and 20° at pH between 1 and 3.5. The rate of disappearance of sulfite was followed by iodometric titration and the rate of formation of chloride ions was determined amperometrically with silver nitrate. The data show that the reaction is second order and that the rate is pH dependent. A mechanism is proposed involving the reaction between  $H_2SO_3$  molecules and chlorate ions as the rate-determining step. In units of liters, moles and seconds, the reaction rates were formulated as  $-d[ClO_3^-]/dt = 3.3 \times 10^7 e^{-11000/RT}[ClO_3^-][H_2SO_3]$ . The reaction is not much influenced by traces of metals, even though these metals strongly accelerate polymerizations initiated by this system. The exact nature of the free-radical intermediates is thus still in doubt, but it seems likely that sulfoxy radical-ions and hydroxyl radicals are involved. Hydrogen ion concentration determines the  $H_2SO_3$  level and thus the reaction rate.

### I. Introduction

Although the iodate-sulfite reaction has been studied extensively, the only previous kinetic investigation of the chlorate-sulfite reaction appears to be that of Nixon and Krauskopf<sup>1</sup> in 1932. The reaction was assumed to be



or



Iodometric titration measured the loss of total sulfite and, from these data, a second-order rate constant  $K$  of 2.4 liters mole<sup>-1</sup> min.<sup>-1</sup> at 0° was calculated for the equation

\* New York State College of Forestry, Syracuse, New York.

(1) A. C. Nixon and K. B. Krauskopf, *J. Am. Chem. Soc.*, **54**, 4606 (1932).

$$-d[ClO_3^-]/dt = K[H_2SO_3][ClO_3^-] = \frac{2K}{K_0} [H^+][HSO_3^-][ClO_3^-]$$

From the fact that the chlorate-sulfite system can be used to initiate polymerization,<sup>2</sup> it might have been inferred that one or more intermediates are free radicals. Isotope exchange experiments<sup>3</sup> have shown that in the sequence  $ClO_3^- \rightarrow ClO^- \rightarrow Cl^-$  most of the oxygen is transferred directly from chlorine to sulfur.

### II. Experimental

Solutions of reagent grade  $Na_2SO_3$ ,  $NaClO_3$  and  $H_2SO_4$  in deaerated water were placed in a thermostated flask, acid being added last. The flask was arranged so that 25-ml.

(2) A. Cresswell, U. S. Patent 2,751,374 (1956), to American Cyanamid Co.; A. Hill, U. S. Patent 2,673,192 (1954), to Diamond Alkali Co.

(3) J. Halperin and H. Taube, *J. Am. Chem. Soc.*, **72**, 3319 (1950).

aliquots could be forced into a pipet by CO<sub>2</sub> pressure.

For sulfite determination, the aliquot was released into excess 0.1 *N* iodine solution and back-titrated with 0.025 *N* thiosulfate. For chloride determination, another aliquot was released into sufficient 2 *N* NaOH to neutralize the solution and stop the reaction. A solution of 10% Ba(NO<sub>3</sub>)<sub>2</sub> was added to precipitate SO<sub>3</sub><sup>2-</sup> and SO<sub>4</sub><sup>2-</sup>. After 20 minutes, the precipitate was filtered and washed free of Cl<sup>-</sup>. The filtrate was acidified with HNO<sub>3</sub> to pH 1 and titrated amperometrically with 0.05 *N* AgNO<sub>3</sub>, using a rotating platinum electrode and a calomel electrode.

For measurement of pH, Leeds and Northrup glass electrode 1199-44 was used at 0° and glass electrode 1199-30 at higher temperatures.

### III. Results

Rate of formation of the chloride ion was determined at 1° at a constant pH of 1.20. The rate of disappearance of sulfite was determined concomitantly on a duplicate solution. Results reported in Table I show that the rate of formation of chloride is one-third the rate of disappearance of sulfite. Since analysis for total sulfite is more con-

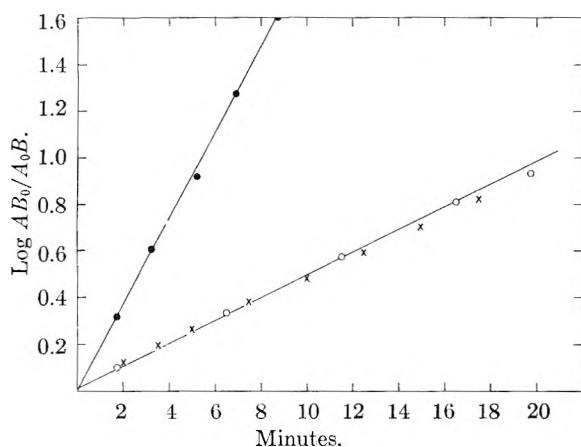


Fig. 1.—Second-order plots of the chlorate-sulfite reaction at pH 1: (●) run 17 at 20°; (○) run 1 at 0°; (×) data of reference 1.

venient than chloride determination, the kinetic runs discussed below relied entirely on total sulfite analysis at controlled pH.

TABLE I

STOICHIOMETRY OF THE CHLORATE-SULFITE REACTION				
Min-utes	ΣSO <sub>2</sub>	0.0524 -ΣSO <sub>2</sub>	Cl <sup>-</sup>	$\frac{\Delta\Sigma\text{SO}_2}{\Delta\text{Cl}^-}$
5	0.0288	0.0236	0.00790	2.99
10	.0208	.0310	.0103	3.02
15	.0163	.0361	.0116	3.11
20	.0135	.0389	.0123	3.16

Reaction rate could be followed roughly by change in pH, but the method lacked sensitivity, especially at low pH.

In the Discussion, equation 8, we derive the relationship

$$\frac{1}{3\rho A_0 - B_0} \ln \frac{AB_0}{A_0B} = Kt$$

where  $A = [\text{ClO}_3^-]$ ,  $B = [\text{H}_2\text{SO}_3]$ ,  $\rho = [\text{H}_2\text{SO}_3]/\Sigma\text{SO}_2$  and subscripts zero refer to time zero. Figure 1 shows typical plots of  $\log AB_0/A_0B$  vs.  $t$  (see Table II for conditions). Data of Nixon and Krauskopf<sup>1</sup> have been replotted according to our scheme. The first ionization constant of H<sub>2</sub>SO<sub>3</sub>,

used to compute  $\rho$ , was taken as  $3.10 \times 10^{-2}$  at 0° and  $1.91 \times 10^{-2}$  at 20°.<sup>4</sup>

At pH levels above 2, release of H<sup>+</sup> during the reaction is sufficient to shift the value of  $\rho$ . The rate equation was then taken as

$$\frac{\Delta\Sigma\text{SO}_2}{\Delta t} = 3K[\text{ClO}_3^-][\text{H}_2\text{SO}_3]$$

and  $K$  was calculated from tangents on plots of  $\Sigma\text{SO}_2$  (total sulfite) vs.  $t$ .

Results of these measurements are summarized in Table II. For the two temperatures  $K$  is given by

$$K = 2.0 \times 10^9 e^{-11000/RT} \text{ l. mole}^{-1} \text{ min.}^{-1}$$

$$K = 3.3 \times 10^7 e^{-11000/RT} \text{ l. mole}^{-1} \text{ sec.}^{-1}$$

Table II also summarizes the effect on rate of several additives. Agents expected to influence radical reactions had little effect, but NaCl and, particularly, Na<sub>2</sub>SO<sub>4</sub> retarded the reaction.

### IV. Discussion

From the dissociation constants of the sulfoxy acids, one can calculate readily that [SO<sub>3</sub><sup>2-</sup>] is negligible below pH 5. Below pH 4, both [HSO<sub>3</sub><sup>-</sup>] and [H<sub>2</sub>SO<sub>3</sub>] are important, with H<sub>2</sub>SO<sub>3</sub> comprising about 35% of the total sulfite (ΣSO<sub>2</sub>) at pH 2 and about 85% at pH 1. A small change near pH 2 drastically alters the ratio of [H<sub>2</sub>SO<sub>3</sub>] to [HSO<sub>3</sub><sup>-</sup>]. Since the reaction is faster as [H<sup>+</sup>] increases, one is led to identify H<sub>2</sub>SO<sub>3</sub> and ClO<sub>3</sub><sup>-</sup> as the active species.

It was shown that the rate of formation of chloride ions is one-third the rate of disappearance of the total sulfite

$$-\frac{d[\text{ClO}_3^-]}{dt} = \frac{d[\text{Cl}^-]}{dt} = -\frac{1}{3} \frac{d[\Sigma\text{SO}_2]}{dt}$$

If the bimolecular reaction takes place between a chlorate ion and a molecule of H<sub>2</sub>SO<sub>3</sub>, the reaction product, whatever it may be, must react very rapidly with two other molecules of H<sub>2</sub>SO<sub>3</sub> to give chloride ions. Only a mechanism of this type is consistent with the above rate expressions. The stepwise oxidation-reduction probably involves the reduction of the chlorate ion to chlorite ion (ClO<sub>2</sub><sup>-</sup>), followed by subsequent rapid reduction to hypochlorite ion (ClO<sup>-</sup>) and chloride ion (Cl<sup>-</sup>). The ratio of the total sulfite to H<sub>2</sub>SO<sub>3</sub> can be calculated, at low pH, as

$$[\text{H}_2\text{SO}_3] + [\text{HSO}_3^-] = \Sigma\text{SO}_2$$

$$[\text{HSO}_3^-] = \frac{K'}{[\text{H}^+]} [\text{H}_2\text{SO}_3]$$

$$\frac{[\text{H}_2\text{SO}_3]}{\Sigma\text{SO}_2} = \frac{1}{1 + K'/[\text{H}^+]} = \rho$$

where  $K'$  is the first dissociation constant of sulfurous acid.

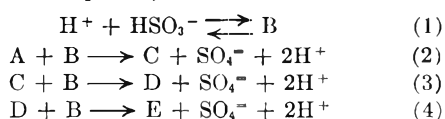
Since H<sub>2</sub>SO<sub>3</sub> and HSO<sub>3</sub><sup>-</sup> are in equilibrium,  $\rho$  remains constant throughout the reaction, at constant pH, and H<sub>2</sub>SO<sub>3</sub> is produced continuously by the ionic equilibrium  $\text{H}^+ + \text{HSO}_3^- \rightleftharpoons \text{H}_2\text{SO}_3$ . If  $A = [\text{ClO}_3^-]$ ,  $B = [\text{H}_2\text{SO}_3]$ ,  $C = [\text{ClO}_2^-]$ ,  $D = [\text{ClO}^-]$ ,  $E = [\text{Cl}^-]$  and  $X = \Sigma\text{SO}_2$ , the reaction

(4) Landolt-Börnstein, "Physikalisch-Chemische Tabellen," Vol. III, Julius Springer, Berlin, 1936, p. 2105; H. V. Tartar and H. H. Garretson, *J. Am. Chem. Soc.*, **63**, 808 (1941).

TABLE II  
SUMMARY OF RATE MEASUREMENTS

Run	Initial pH	[H <sub>2</sub> SO <sub>3</sub> ] <sub>0</sub>	[Na <sub>2</sub> SO <sub>3</sub> ] <sub>0</sub>	[NaClO <sub>3</sub> ] <sub>0</sub>	(l. mole <sup>-1</sup> min. <sup>-1</sup> ) K	Notes
Experiments at 0°						
..	..	0.1	0.01310	0.0160	3.97	Recalcd. from ref. 1
1	1.05	.1	.01200	.0160	4.20	
2	1.05	.1	.01310	.0160	3.77	
3	1.05	.1	.0262	.0080	3.58	
4	1.05	.1	.01922	.0200	3.71	
5	0.85	....	.01200	.0160	3.46	0.1 M HCl replacing H <sub>2</sub> SO <sub>3</sub>
6	1.05	.1	.01314	.0160	3.94	Soln. 1 M in acrylonitrile
7	1.05	.1	.01314	.0160	3.74	10 <sup>-3</sup> M Cu <sup>++</sup>
8	1.05	.1	.01314	.0160	3.80	10 <sup>-2</sup> M Fe <sup>++</sup>
9	2.4	.01	.01326	.0160	4.3	
10	2.4	.01	.01244	.0160	4.0, 4.5	Soln. 0.543 M in acrylonitrile
11	2.4	.01	.01388	.0160	4.5	0.0175% benzoquinone
12	ca. 2.3	.01	.01318	.0160	1.7	0.1 M Na <sub>2</sub> SO <sub>4</sub>
13	2.46	.01	.01335	.0160	3.2	0.3 M NaCl
14	3.37	.0068	.01250	.0160	3.4	
15	1.05	.1	.01970	.0150	3.98	
Experiments at 20°						
16	1.05	0.1	0.01314	0.01604	15.2	
17	1.05	.1	.01330	.01604	15.2	
18	1.05	.1	.0262	.00800	15.6	
19	2.4	.01	.01325	.01604	16.2	
20	2.4	.01	.01244	.01064	16.6	Soln. 0.543 M in acrylonitrile
21	3.0	.0011	.00135	.000567	19.5	

mechanism can be written as follows (omitting transient radical species)



At constant pH,  $B = \rho X$  and  $dB/dt = \rho(dX/dt)$  where  $dB/dt$  is the total rate of change of B. On the other hand, the rate of consumption of A is

$$-\frac{dA}{dt} = K_1AB = K_1\rho AX \quad (5)$$

and the total rates of change of D and B are

$$\frac{dC}{dt} = K_1AB - K_2BC \quad (6)$$

$$\frac{dD}{dt} = K_2BC - K_3DB \quad (7)$$

if reactions 3 and 4 are much faster than 6, C and D will be used up as formed. Under these conditions, the concentration of C and D will remain very small and a stationary state will be reached where

$$\frac{dC}{dt} = 0, \frac{dD}{dt} = 0$$

and  $K_1AB = K_2CB = K_3DB$ . The rate of disappearance of X is

$$-\frac{dX}{dt} = K_1AB + K_2BC + K_3DB = 3K_1AB$$

hence

$$\frac{dX}{dt} = 3 \frac{dA}{dt}$$

and, upon integration, one obtains

$$\begin{aligned}
 X &= X_0 + 3A - 3A_0 \\
 B &= B_0 + 3\rho A - 3\rho A_0
 \end{aligned}$$

Substituting this value of B into 5 gives a differen-

tial equation which can be readily integrated

$$-\frac{dA}{dt} = K_1AB = K_1A[B_0 + 3\rho A - 3\rho A_0]$$

$$\frac{1}{3\rho A_0 - B_0} \ln \frac{AB_0}{A_0B} = K_1t \quad (8)$$

Plots of  $2.3 \log AB_0/A_0B$  versus time are shown in Fig. 1. The slopes of these lines give the value  $K_1(3\rho A_0 - B_0)$ , from which the second-order rate constant  $K_1$  can be calculated.

Solving equation 8 for A gives

$$A = \frac{L}{\frac{B_0}{A_0} e^{K_1 L t} - 3\rho} \quad (9)$$

where  $L = B_0 - 3\rho A_0$ .

At constant pH, L is constant and is a measure of the excess of one reactant over the other. (Note that  $L/\rho = B_0 - 3A_0$ ;  $L/\rho = \Sigma \text{SO}_2 - 3[\text{ClC}_3^-]_0$ .)

Three situations should be considered.

1.  $L > 0$ ,  $B_0 > 3\rho A_0$ ; an excess of H<sub>2</sub>SO<sub>3</sub> is present. In this case  $e^{K_1 L t}$  will increase exponentially with time, while the function  $A(t)$  will tend to zero very rapidly if L is large. This means that, given several recipes, containing sulfite and chlorate in various ratios  $B_0/A_0$ , the concentration of the chlorate will decrease more rapidly the larger the excess of H<sub>2</sub>SO<sub>3</sub> present.

2.  $L < 0$ ; the chlorate is present in excess. In this case  $e^{K_1 L t}$  will decrease exponentially; consequently the concentration of the chlorate will tend to the limit  $-L/3\rho$  more rapidly as L increases.

3.  $L = 0$ ,  $B_0 = 3\rho A_0$ ; the chlorate and the sulfite are present in the quantities required by the stoichiometric equation. In this case equation 5 becomes indeterminate. Since  $B = 3\rho A$

$$\frac{dA}{dt} = -K_1AB = -K_13\rho A^2$$

and solving for  $A$

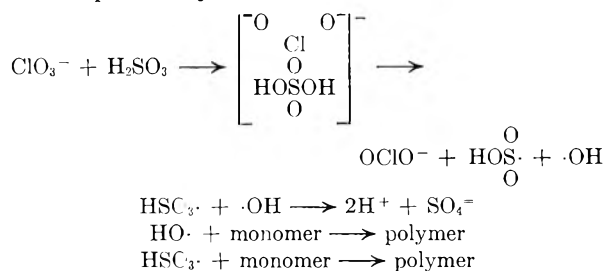
$$\frac{1}{A} = \frac{1}{A_0} + 3\rho K_1 t$$

Figure 2 shows how the product  $[\text{ClO}_3^-][\text{H}_2\text{SO}_3]$  decreases with time, in four different recipes containing the same initial product  $[\text{ClO}_3^-]_0[\text{H}_2\text{SO}_3]_0$  of  $5.73 \times 10^{-5}$ , but different  $L$ . The concentration of  $[\text{ClO}_3^-]$  at various instants was calculated from equation 9, taking  $K_1 = 4$  l. moles $^{-1}$  min. $^{-1}$  and  $\rho = 0.763$ .

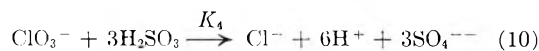
It is interesting to note that the product decreases with time more rapidly in systems containing either an excess of chlorate or sulfite than in systems containing stoichiometric quantities of the two reactants. The larger the absolute value of  $L$ , the faster the product tends to zero. This fact becomes very important when the rate of polymerization is studied as a function of the initiator concentration,<sup>5</sup> because systems having the same product  $[\text{ClO}_3^-][\text{H}_2\text{SO}_3]$ , but different concentration of  $[\text{ClO}_3^-]$  and  $[\text{H}_2\text{SO}_3]$ , will contain the same number of free radicals only initially.

This investigation has not established with certainty the nature of free radical intermediates.

One possibility in line with the data at hand is



The influence of metals like  $\text{Fe}^{++}$  and  $\text{Cu}^{++}$  is of interest. Our data indicate that small concentrations ( $10^{-3}$  mole $^{-1}$ ) of ferrous ions do not increase the over-all rate of the chlorite-sulfite reaction, but increase appreciably the rate of polymerization of acrylonitrile.<sup>5</sup> The following reactions can take place when  $\text{ClO}_3^-$ ,  $\text{H}_2\text{SO}_3$  and  $\text{Fe}^{++}$  react in acid medium



(5) W. M. Thomas, E. H. Gleason and G. Mino, *Polymer Sci.*, in press.

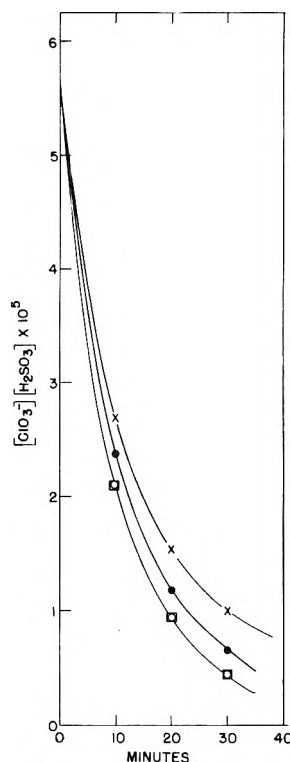
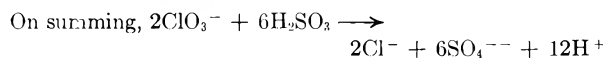
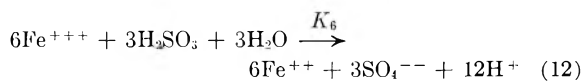
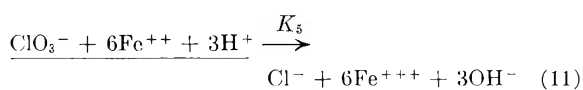


Fig. 2.—Variation in reaction rate with initial chlorate/sulfite ratio: (O)  $L = 17.2 \times 10^{-3}$ ; (X)  $L = 0$ ; (●)  $L = 12.2 \times 10^{-3}$ ; (□)  $L = -17.2 \times 10^{-3}$ .



Each of these reactions proceeds through a free radical mechanism and is capable of initiating polymerization. It is interesting to note that the iron present is continuously oxidized and reduced by reactions 11 and 12. If  $K_6$  is much larger than  $K_5$ , a steady state will be reached in which the concentration of the ferrous ion will remain constant.

## SOLID STATE ANOMALIES IN INFRARED SPECTROSCOPY

By ALVIN W. BAKER

Research Department, Western Division, The Dow Chemical Company, Pittsburg, California

Received October 15, 1956

Variations between mull and pellet spectra of organic compounds are due either to an induced physical isomerization or to the samples' having been rendered amorphous in the alkali halide pellet. Factors which influence these changes are: (1) crystal energy of the organic phase; (2) energy of grinding sample and matrix; (3) lattice energy of matrix; (4) particle size of matrix; (5) ability of sample to recrystallize in the pellet (related to crystal energy); and (6) relative stability of polymorphic forms. Relative merits of mull and pellet techniques are presented and it is shown how these can supplement each other. From the frequency of occurrence of polymorphism, it is concluded that this is a general rather than a rare problem facing the organic chemist.

When the potassium bromide pressed pellet technique<sup>1-3</sup> was introduced in 1952 to the field of infrared spectroscopy, it was received with considerable enthusiasm. It solved a number of difficult sampling problems, notably those encountered in obtaining spectra of certain polymers and of micro-

serious enough that some groups either never adopted it or else discarded it after a short trial. Spectra could not be reproduced to the desired degree for either quantitative or qualitative analyses, and gross differences were observed when mull and pellet spectra were compared. These difficulties

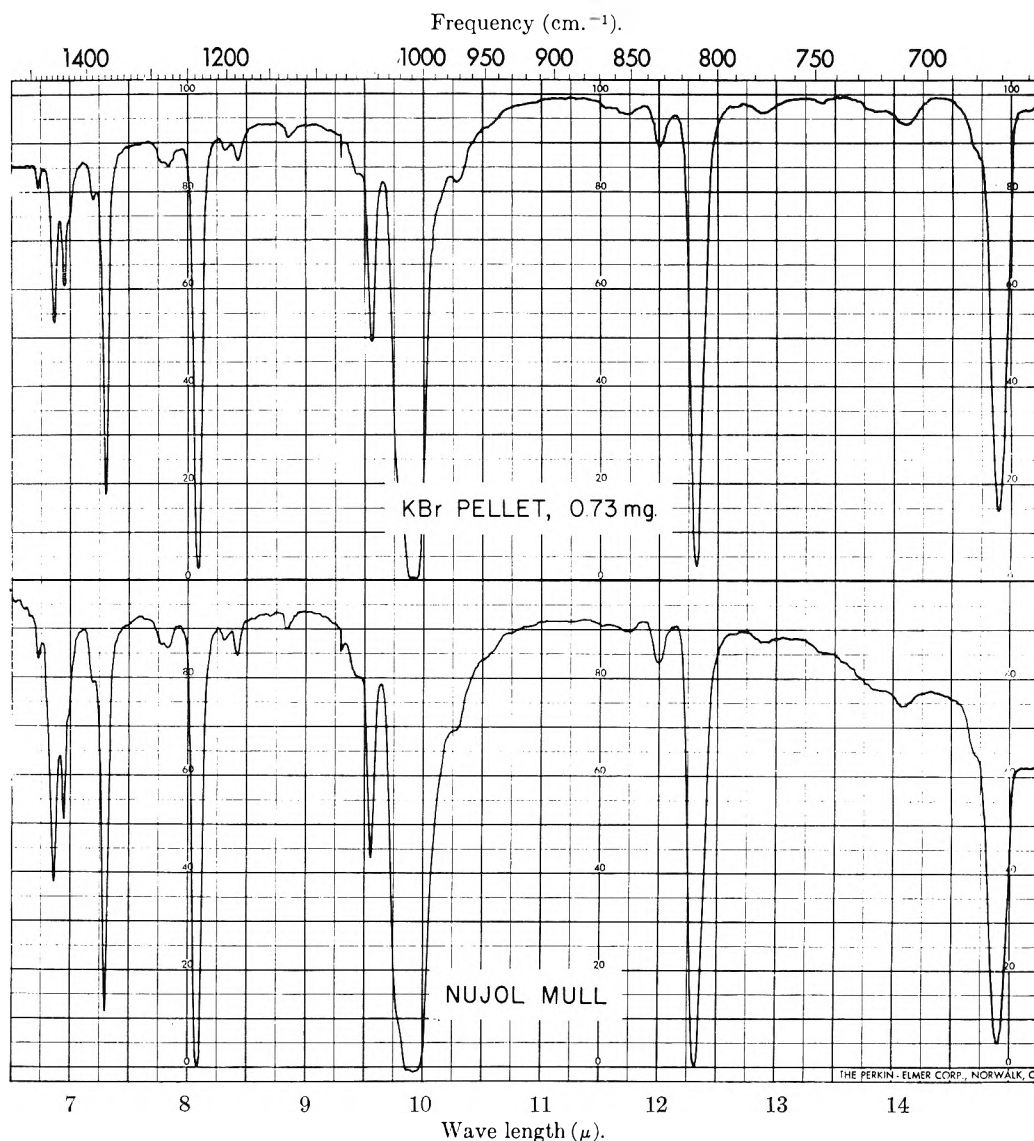


Fig. 1.—The spectrum of hexamethylenetetramine in KBr pellet and mineral oil mull. The pellet spectrum is equal in quality to that from the mull and shows no crystal changes upon pelleting.

samples. It also gave promise of being suitable for quantitative analyses.<sup>4,5</sup> Therefore, in some laboratories, particularly those investigating biological systems, it soon displaced the use of mineral oil (Nujol) mulls for obtaining spectra of insoluble materials.<sup>6</sup>

However, despite its ready acceptance, the pellet technique soon encountered difficulties<sup>7</sup> which were

will be discussed in this paper and an explanation for their occurrence will be presented.

Pellet spectra, when compared to good mull spectra, frequently display a broadening, a shifting or an elimination of some bands together with major changes in the relative absorption maxima of others.<sup>8</sup> Changes such as these (hereafter called changes of the first kind) are very similar to the changes encountered when comparing spectra of solid and liquid states and suggest that the sample has been rendered amorphous. In addition, some compounds exhibit a completely new group of

(1) M. M. Stimson and M. J. O'Donnell, *J. Am. Chem. Soc.*, **74**, 1805 (1952).

(2) U. Schiedt and H. Z. Rheinwein, *Naturforsch.*, **8b**, 66 (1953).

(3) U. Schiedt, *ibid.*, **7b**, 270 (1952).

(4) J. J. Kirkland, *Anal. Chem.*, **27**, 1537 (1955).

(5) R. S. Browning, S. E. Wiberley and F. C. Nachod, *ibid.*, **27**, 7 (1955).

(6) U. Schiedt, *Appl. Spectr.*, **7**, 75 (1953).

(7) R. D. Elsey and R. N. Haszeldine, *Chemistry and Industry*, 1177 (1954).

(8) S. A. Barker, *et al.*, *ibid.*, 1418 (1954).

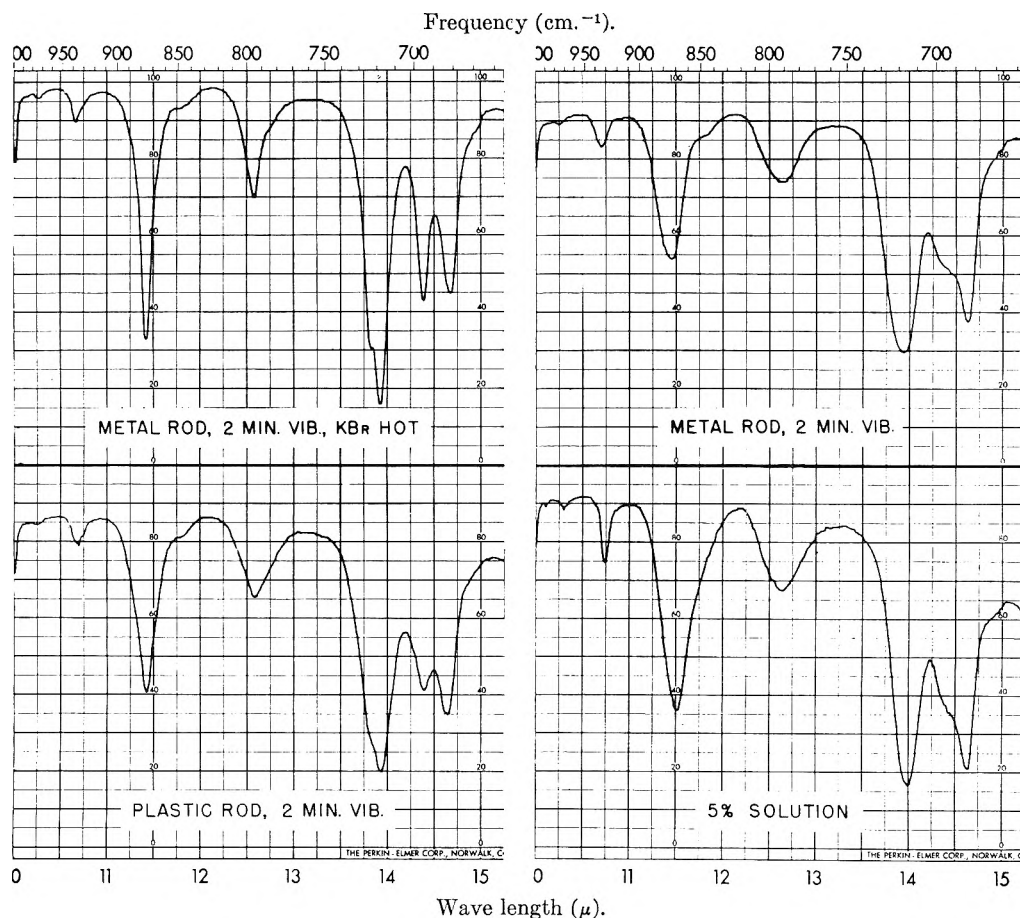


Fig. 2.—Spectrum of benzil, m.p.  $95^{\circ}$ , showing effect of temperature and variations in grinding energy. After grinding for two minutes with a metal hammer rod, the spectrum is very similar to that from a 5%  $\text{CS}_2$  solution.

sharp, well resolved bands, particularly when the sample is precipitated from a solvent<sup>9</sup> onto the KBr powder. These changes (of the second kind) are typical of polymorphic effects, and can in fact, be shown to be due to changes in crystalline structure. Either of these types of changes can be produced to any degree in susceptible samples by the use of proper techniques. Because of the many controlling factors, precise reproduction of any given degree of change is very difficult to obtain.

**Effects of Moisture.**—Pellet spectra also suffer from the presence of water bands of variable intensity at 2.9 and 6.1  $\mu$  which in many cases are more serious than the presence of C-H bands due to mineral oil. Since it is generally very difficult to eliminate moisture or prevent its adsorption in preparing the KBr discs, even with dry box techniques, one must tolerate band intensities at 2.9  $\mu$  of 4–30% or more. Moisture adsorption can be minimized if the pellets are prepared by depositing the sample from a solvent rather than by grinding.

In addition to its objectionable spectral absorbance, water can cause changes due to formation of hydrates (which can develop within the pellet) and to hydrolysis of compounds which will react with water.

**Factors Influencing Spectra.**—Some of the factors which influence the changes in pellet spectra

(9) D. N. Ingebrigtsen and A. L. Smith, *Anal. Chem.*, **26**, 1765 (1954).

are: (1) crystal energy of the organic phase; (2) total amount of energy used in grinding sample and matrix; (3) lattice energy of matrix; (4) particle size of matrix; (5) stress relaxation, (a) temperature of pellet or powder mixture, (b) time lapse between grinding the sample mixture and obtaining the spectrum; (6) occurrence of polymorphic transitions.

Two more factors are relatively unimportant in changing spectra, and have at most only second-order effects: (7) surface adsorption of sample upon matrix powder (molecular dispersion); (8) dielectric forces of the alkali halide.

Factors 7 and 8 can be discounted because, in even the most finely ground mixture, or in cases where samples are precipitated from a solvent upon the matrix powder, the included sample has particle sizes which contain large aggregates of molecules. Effects of surface forces<sup>10</sup> should therefore be limited to a small percentage of the total sample. For ionic compounds, the dielectric forces may be somewhat more effective in changing spectra, but the possibility of ion exchange with the alkali halide is even more important.

## Discussion

**I. Crystal Energy of the Organic Phase.** (a).—Compounds having high lattice energies generally have similar or nearly identical mull and pellet

(10) V. C. Farmer, *Chemistry and Industry*, 586 (1955).

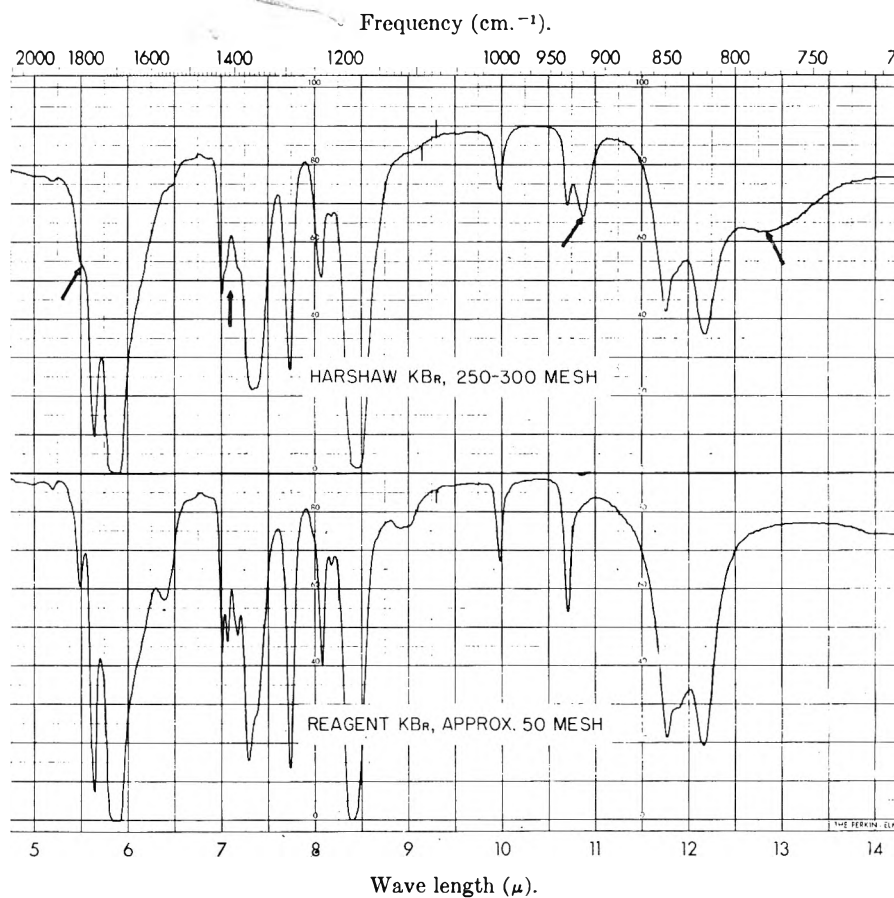


Fig. 3.—Spectrum of succinimide; both pellets were prepared in identical fashion except for the indicated difference in KBr particle size.

spectra. Exceptions will occur if polymorphic transitions can be induced in the pellet, but changes of the first kind either will not occur or will be minor. Lattice energies can be measured very approximately by melting points and, although the correlation is not very precise, it is probably within a factor of two. Experience has shown that the majority of compounds melting above approximately  $180\text{--}200^\circ$  have lattice energies which are high enough to prevent changes of the first kind if the grinding techniques are not excessively vigorous.

(b).—Low melting compounds, from room temperature to  $80\text{--}90^\circ$ , generally show changes in pellets of the band-broadening type (first kind). The pellets will probably give altered spectra even if the powder mixture is lightly hand ground or if the sample is precipitated from a solvent onto the matrix. For such samples, the actual operation of fusing the pellet under pressure, involving  $80,000\text{--}120,000\text{ lb./in.}^2$  is causing at least part of the crystal deformation. Changes of the second kind (polymorphism) may occur for some pelleting procedures but lattice energies are so low that crystallinity is easily destroyed, leading primarily to changes of the first kind.

(c).—Compounds melting at intermediate temperatures frequently will display changes of both kinds in the same pellet. The relative proportion of each can be altered by changes in matrix particle size, temperature, time of grinding, etc.; changes

of the first kind will be minimized if the sample is deposited from a solvent onto finely ground KBr powder but the possibility for changes of the second kind will be maximized. In the following arguments, consideration is centered primarily on changes produced by mechanical working of the powder mixture.

**II. Energy of Grinding.**—When pellets are prepared by grinding, the extent of spectral change, whether of the first or second kind, is a function of grinding time and vigor of grinding. For compounds showing changes of the first kind, continued grinding eventually will remove all indications of the original crystal structure and produce spectra nearly identical to liquid spectra. This is substantial indication that grinding is merely randomizing molecular orientation.

Hand grinding the powder mixture generally produces inferior spectra from both qualitative and quantitative standpoints. This difficulty can be solved by the use of mechanical vibrators; they are efficient mixers and are almost a necessity for this technique but, nevertheless, they must be used with caution because of their high energy output. To minimize spectral distortion, the energy of a vibrator can be moderated by the use of light plastic hammer rods and short vibration times. This may result in poor quantitative band intensities, but it is not always possible to achieve both qualitatively and quantitatively accurate spectra from pellets.

**III. Matrix Lattice Energy.**—The lattice en-

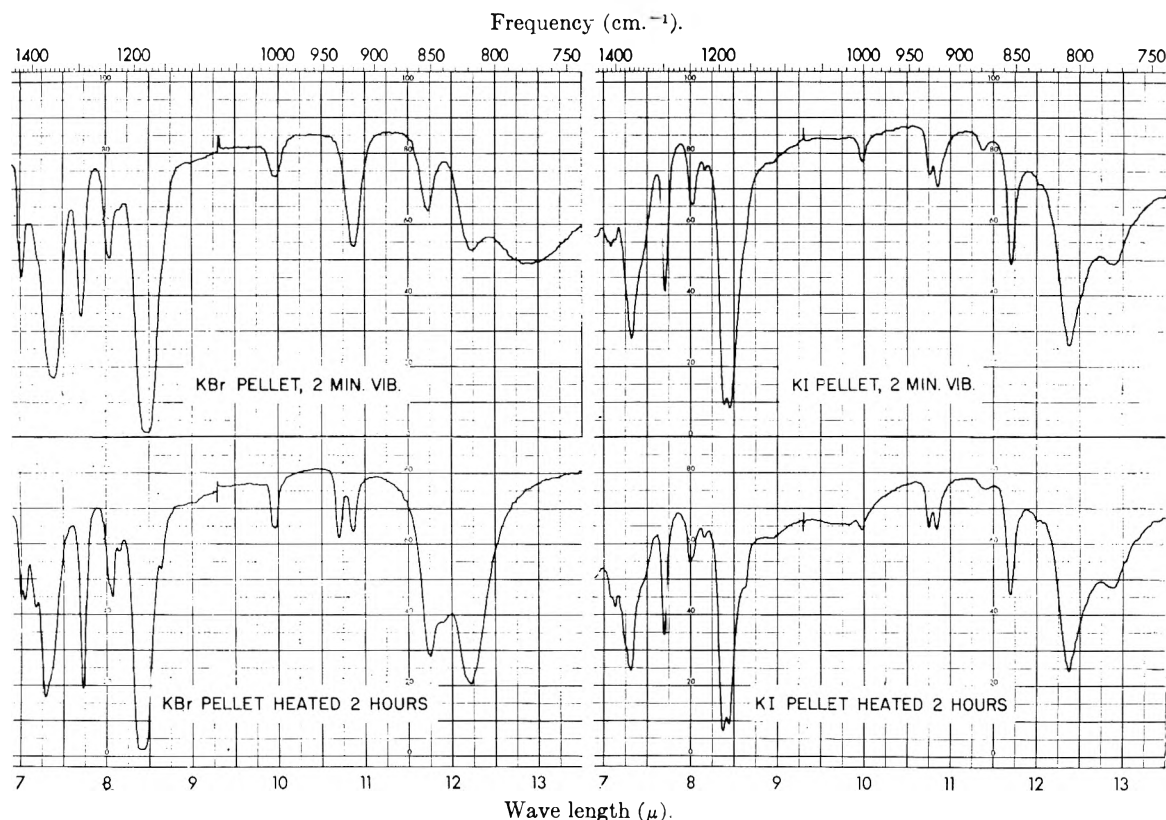


Fig. 4.—Succinimide: top left spectrum shows nearly complete destruction of original crystal structure. Upon heating this pellet, the crystal structure is regenerated (bottom left). The KI pellet (top right) gives evidence for polymorphic transition which is not changed by heating (bottom right).

ergy of the matrix controls to some extent the changes in pellet spectra because, under identical grinding conditions, the matrix having the lowest lattice energy will break down to the greatest extent. This permits an increased proportion of the grinding energy to go to the sample. Published lattice energies of the alkali halides are given in Table I.<sup>11</sup>

TABLE I

Compound	Lattice energy, kcal./mole	Compound	Lattice energy, kcal./mole
NaCl	184	KI	153
NaBr	177	CsCl	156
NaI	166	CsBr	150
KBr	162		
KCl	168	CsI	142

Both the ease of pelleting and the tendency for sample deformation increases with decreasing energy. Of the potassium halides, one would therefore choose KI for the clearest pellets but KCl for the best qualitative spectra. Since CsI, for example, is soft and plastic, pellets prepared from this matrix give extremely poor spectra because of the extensive crystal destruction. Its use is not recommended.

Although the sintering pressure of KCl (at room temperature) is about 80,000 lb./in.<sup>2</sup>, pressures exceeding 100,000 lb./in.<sup>2</sup> and careful techniques must be used to prepare consistently clear discs. Moisture pickup is approximately equal to that of KBr despite the lower water solubility of KCl.

(11) M. A. Ford and G. R. Wilkinson, *J. Sci. Inst.*, **31**, 338 (1954).

In contrast to KCl, KI will produce clear windows at pressures considerably less than 100,000 lb./in.<sup>2</sup>. Less care has to be taken to ensure even distribution of the powder in the die and the pressing times can be much shorter. If the powder mixtures are ground for a very short time, crystal deformation can be minimized and spectra can be obtained which, in most cases, are nearly as good as mulls. A second advantage of KI, at least in the form used in our laboratory, is the small moisture pickup in the pellet. This is less than in either KCl or KBr discs prepared by grinding, and gives an average absorption of from 3–10% at 2.9  $\mu$ . Using identical techniques, Harshaw KBr (250–300 mesh) has an absorption of 30–40% or greater, while the absorption of reagent KBr (20–50 mesh) is 10–20%.

**IV. Matrix Particle Size.**—As the initial size of the matrix particles is decreased, spectral distortion increases. For example, samples ground with 250–300 mesh KBr will usually show much greater spectral changes than if ground with 20–30 mesh KBr. In grinding a matrix-sample mixture, the particle size of each is reduced and each will absorb a certain amount of grinding energy. However, as the initial particle size of matrix is increased, a greater portion of the grinding energy must be expended in pulverizing the matrix, and the sample particles will be protected from too violent a grinding action.

The aim of the grinding procedure is to reduce the particle size of the sample into the 1–3  $\mu$  range. Since the lattice energy of organic compounds is less

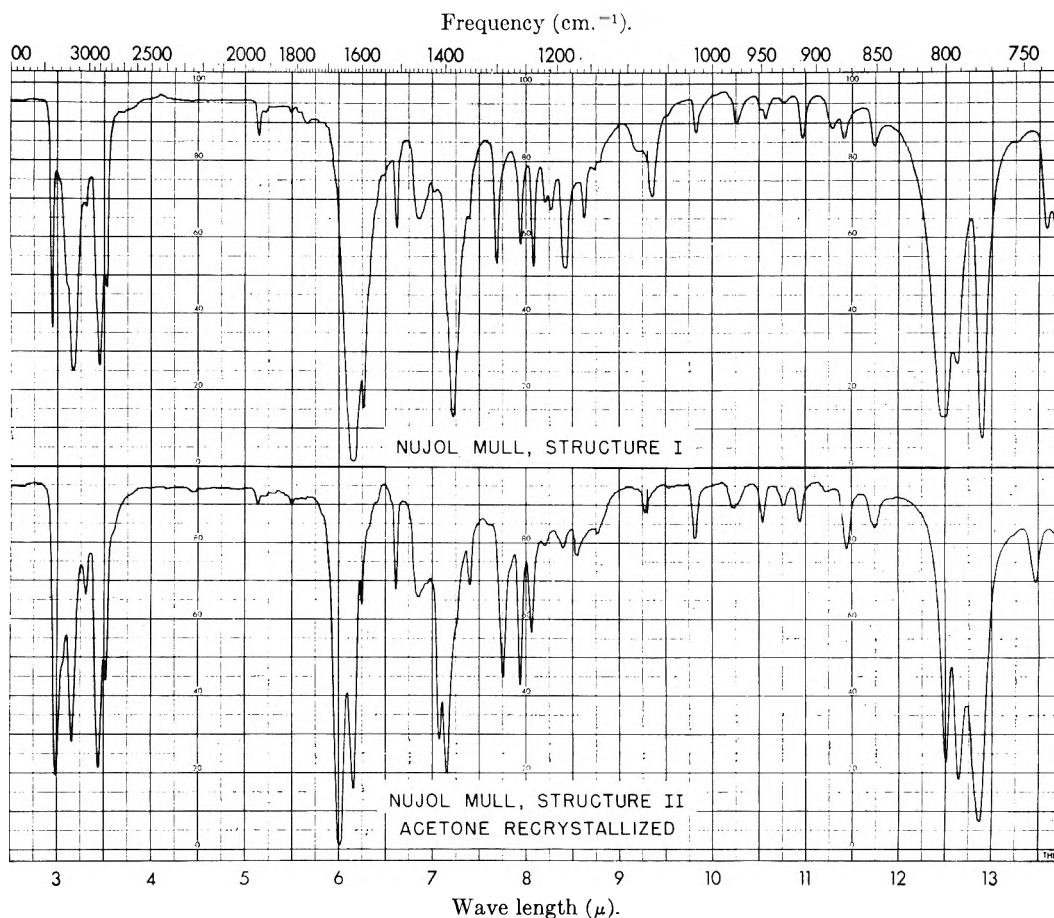


Fig. 5.— $\alpha$ -Naphthalene acetamide: mull spectra of two distinct crystalline structures.

than that of the alkali halides, this is easily accomplished before similar reduction occurs in the halide. However, when the matrix particles are of a size small enough that the sample is uniformly distributed across the pellet, further reduction in their size is unnecessary. At this point the matrix particles may still be much larger than the sample particles.

Satisfactory initial particle size for the matrix is probably about 20–30 mesh although Harshaw's 250–300 mesh is ideal for solvent deposition techniques.

An interesting variation of spectral alteration as a function of matrix particle size has been encountered with  $\alpha$ -glycerol allyl ether. This is a viscous, high boiling liquid very difficult to crystallize. Pellets from 20–50 mesh KI, KCl or KBr gave spectra very similar to that of the pure liquid. However, pellets from 250–300 mesh KBr gave sharp, well resolved spectra quite different from the liquid and undoubtedly due to the crystalline compound. The smaller mesh of the Harshaw KBr apparently has permitted sufficient pressure to be exerted on the sample during pelleting that the sample was forced into a crystalline or ordered state.

**V. Stress Relaxation.**—Spectra obtained from a single pellet frequently undergo changes as the pellet ages. Changes occurring when the pellet or powder is heated and those observed which increase with time after pelleting are manifestations of the same effects and will be discussed together. Contrary to some original expectations, pellets

may not necessarily give an unchanging record of the included sample, particularly if changes of the first kind have occurred. Ten pellets which originally showed changes of the first kind have been examined at 24-hour intervals for 7–10 days, and in each case the spectrum showed a reversal of the changes caused by pelleting (excluding effects such as chemical reactions or hydrate formation). Since the original crystal structure is being regenerated, as evidenced by the spectrum, there is little doubt that the sample is recrystallizing from a disordered or rearranged state.

When the crystal energy of the sample is high, recrystallization will proceed rapidly, being so fast in some compounds as to be difficult to observe. However, if the crystal energy is low, the pellet may remain unchanged for considerable periods of time. Interestingly enough, two compounds undergoing this change gave intermediate spectra which were different from those at either the beginning or end of the process.

Similar changes can be brought about in a shorter time by heating the pellet in a vacuum oven at a temperature below the melting point of the sample. Also, changes can sometimes be prevented if, after grinding, the powder is heated for a short time at the proper temperature. This may happen accidentally if KBr powder which has been stored in an oven is added hot to the sample and ground immediately.

If the temperature of the pellet while being heated exceeds the melting point of the included sam-

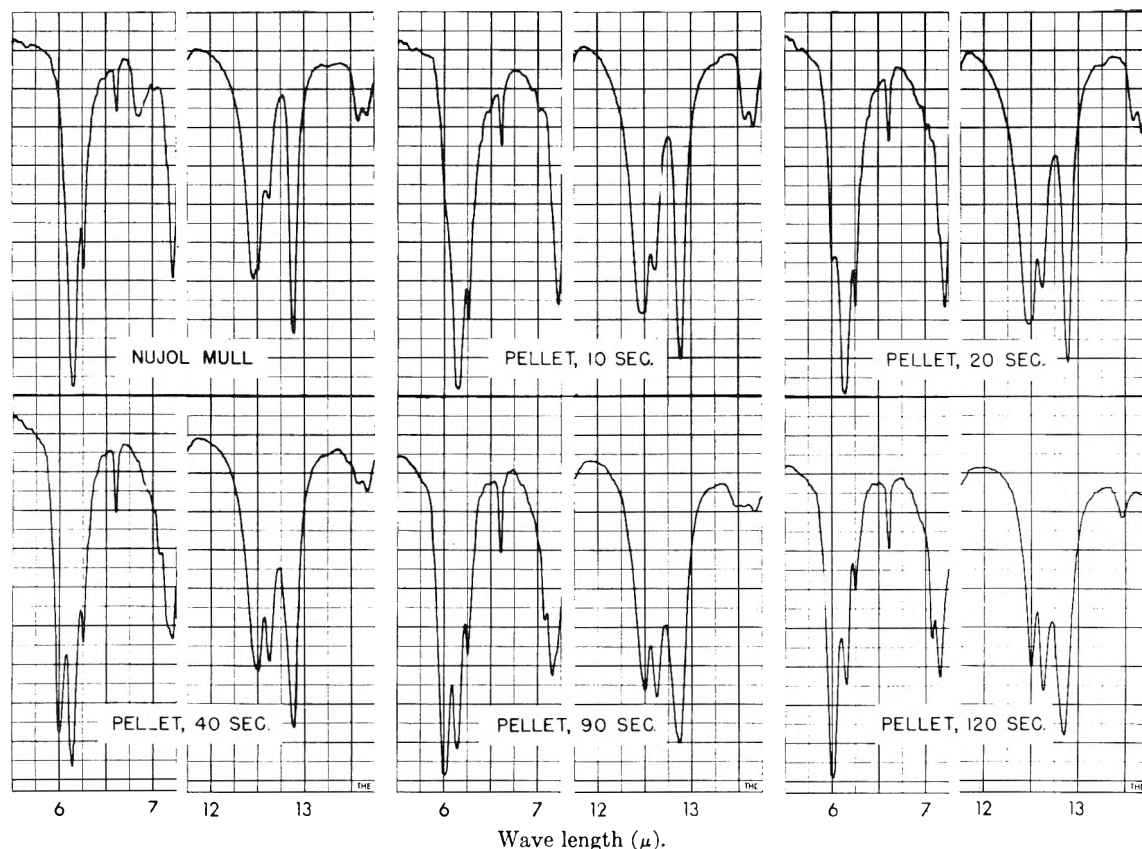


Fig. 6.— $\alpha$ -Naphthalene acetamide: top left, mineral oil mull; top middle, KI pellet ground for 10 sec. in Wig-L-Bug vibrator. Some slight changes are apparent even with very light grinding. The succeeding spectra show how the sample converts from structure I to structure II upon increasing the time of grinding.

ple, changes identical to those of the first kind can be obtained. These frequently can be reversed by reheating the pellet to a temperature below its melting point; in fact, conversions mull-like  $\rightleftharpoons$  liquid-like have been carried through as many as four cycles. Such reversal can only be due to interconversion between amorphous and crystalline states and confirms the statements made above about grinding.

Adsorbed moisture can be removed almost completely from some pellets by heating in a vacuum oven for several hours at  $100^\circ$ . The pellet will remain clear unless the sample is at the same time recrystallizing with an increase in volume. This requires some stress relaxation in the fused matrix, and if the increase in volume is sufficiently great, the pellet will become cloudy from minute fracturing.

**VI. Polymorphism.**—Many compounds can be physically isomerized by vigorous pelleting conditions. For this to occur, the compounds must have states which are relatively more stable under the conditions existing during the grinding and fusing operations. Crystalline structures which are thermodynamically unstable at normal temperature and pressure, are frequently obtained from organic preparations; these structures probably will undergo polymorphic transitions to more stable states if subjected to any sort of physical manipulation including mulling and pelleting. If the stability of the existing structure is low enough, spontaneous

transition to a more stable structure will occur on standing.

### Experimental Examples

The following examples present various aspects of solid state changes and were selected not for their uniqueness, but for clarity of presentation. They are typical of the samples which are encountered daily in our laboratory.

Hexamethylenetetramine sublimes at  $263^\circ$  and is representative of high melting compounds. Its spectrum obtained from both mull and pellet is given in Fig. 1. The top spectrum is from a KBr pellet which was ground with 0.73 mg. of sample for 30 sec. in a Wig-L-Bug vibrator and fused at  $110,000$  lb./in.<sup>2</sup>. The bottom spectrum is from a mineral oil mull prepared in the same vibrator. Both the wave lengths and band widths are essentially identical for each technique. Because the crystalline structure is neither altered nor destroyed in pelleting, accurate quantitative analyses can be obtained from samples containing this compound. Moreover, because pellets require less personal effort to prepare than mulls, many operators will generally produce better pellet spectra than mull spectra from such compounds.

Benzil has a low melting point ( $95^\circ$ ) and consequently has a comparatively small lattice energy. Figure 2 gives four different presentations of a portion of its spectrum which resemble a mull, a solution in  $CS_2$ , or a combination of these extremes. The first spectrum was obtained from 0.8 mg. of sample which was ground with hot ( $110^\circ$ ) 250–300 mesh KBr for two minutes. If any crystal deformation was induced, it has been eliminated since the spectrum is nearly as good as a mull. The second spectrum, prepared from cold KBr in exactly the same way, has a completely changed band structure and is very similar to the spectrum from a 5%  $CS_2$  solution (fourth). Because of the similarity of spectra 2 and 4, there is little doubt that the particles of benzil in pellet 2 are amorphous. Furthermore, spectrum 2 can be duplicated by heating a pellet containing crystalline

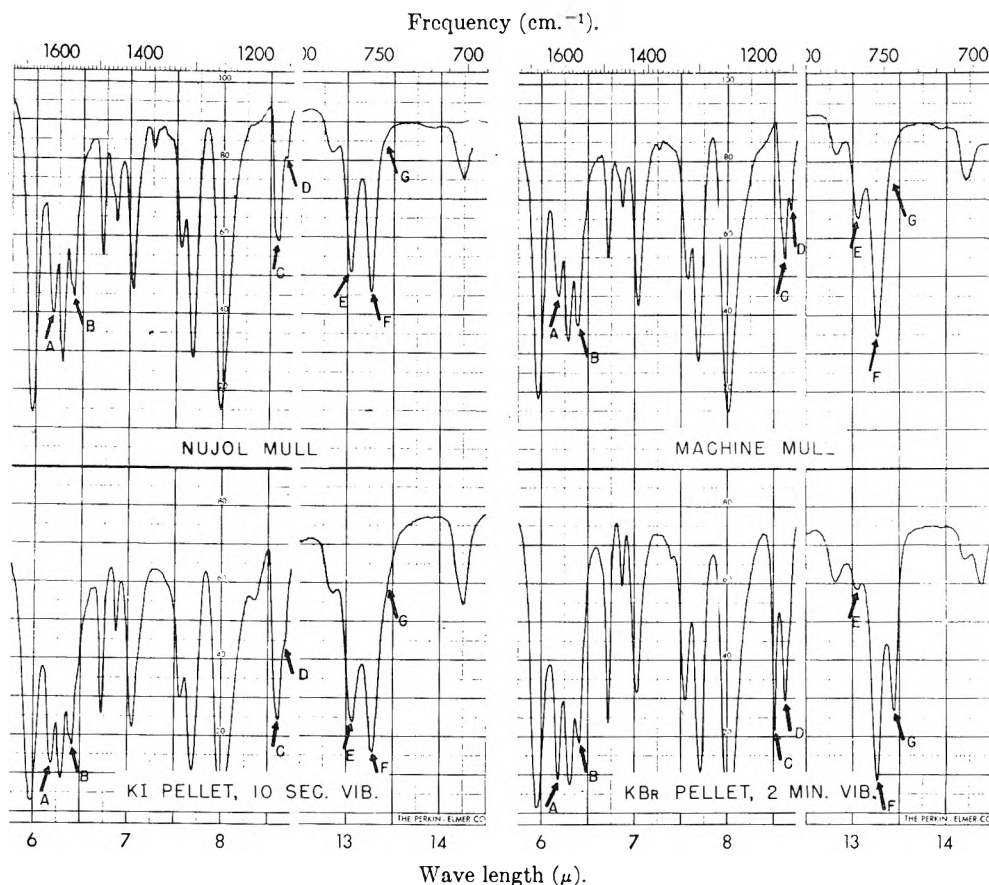


Fig. 7.—2-Aminobenzoic acid: top left, vigorous hand mull; top right, very vigorous machine mull using vibrator with metal hammer rod; bottom left, KI pellet, 10 sec. vib.; bottom right, KBr pellet, 2 min. vib.

benzil to a temperature above  $95^\circ$ , a result which cannot be due to molecular dispersion.

Pellet 3 was prepared from cold KBr using a plastic hammer rod, but identical grinding and pressing times as for pellets 1 and 2. The lighter hammer rod reduced the grinding energy so that only a part of the crystallinity was destroyed. Obviously band intensities change so greatly that quantitative analyses become very difficult.

**Succinimide.**—The effect of varying matrix particle size is shown in the spectrum of succinimide, Fig. 3. The pellet giving the top spectrum was made from Harshaw infrared grade KBr (250–300 mesh). The lower pellet was from reagent grade KBr which had an average mesh of 50, but which had some particles slightly larger than 20 mesh. Both pellets were ground and pressed in identical manner, but yet the spectrum from the 250–300 KBr pellet shows the occurrence of new bands, broadening of some, and almost a 50% reduction of the strong bands at  $12 \mu$ . In contrast, the bottom spectrum has sharp, well resolved bands and is nearly identical to a good mull.

The crystalline structure in the first pellet has been largely, though not completely, destroyed. This is concluded from a comparison with the first spectrum in Fig. 4 where the pelleting conditions were identical except for a longer grinding time. In the latter spectrum, the band at  $10.7 \mu$  has disappeared entirely, while the new bands and the remaining original bands have broadened considerably. By heating this pellet for two hours in a vacuum oven at  $100^\circ$ , the original structure has been almost entirely restored as can be seen in spectrum 3 of Fig. 4. However, the band at  $10.9 \mu$  indicates that the recrystallization was not complete.

Succinimide is interesting because in addition to these changes of the first kind, polymorphic changes can be produced by only a slight change in technique. Pellet 2 of Fig. 4 was prepared identically to pellet 1 except that the matrix was 10–20 mesh KI instead of 250–300 mesh KBr. The spectrum is markedly different from that of a mull or of a KBr pellet, particularly in respect to the position and sharpness of the new bands at  $11.68$  and  $12.3 \mu$ . Heating

this pellet did not restore the mull-like spectrum; rather, the existing bands (spectrum 4 of Fig. 4) sharpened to give cleaner resolution, particularly the bands at  $10.8$  and  $10.85 \mu$ . Evidently the difference in KBr and KI pellets is due to a polymorphic change which occurs in one and not the other. Particle size may be influencing the result but several other examples have been observed where crystal changes were not identical in KBr and KI of equal particle sizes.

**$\alpha$ -Naphthalene Acetamide.**—An example of polymorphism is given in Fig. 5 for two different crystalline structures of  $\alpha$ -naphthalene acetamide. The top spectrum is a mull of the sample as received from Eastman Kodak Company and the bottom is a mull of the sample recrystallized from acetone. That the change was due to polymorphism and not to chemical alteration was proven by recrystallization from ethanol and pyridine at room temperature. Both of these recrystallizations gave the same structure II as determined by infrared and X-ray diffraction. An identical transformation was obtained by vigorous pelleting techniques with KBr (no changes of the first kind were detected). In Fig. 6 the regions of maximum spectral changes are compared for five different grinding times, the amount of change being partially dependent upon the total applied energy. The first spectrum is a mull (structure I) and is included for reference with the second spectrum which was prepared from a KI pellet ground for 10 seconds. The spectrum from the pellet is nearly as good as that from the mull (as good as any from KBr pellets) although a small amount of structure II is present. With longer grinding times in KBr, an increased conversion from structure I to II is observed and at 120 seconds, the conversion is complete. Heating of the pellets in Fig. 6, rather than regenerating structure I, aided the change to the second structure. The rate of change was much slower, however, than in the case of compounds of similar melting points recrystallizing from amorphous states.

**Mulls.**—Changes in crystal structure have also been encountered in mulls, although these are less frequently observed than in pellets. In a sample of 3,4-dinitroaniline,

vigorous mulling caused a clear-cut polymorphic transition without any detectable changes of the first kind. Pelleting brought about the same conversion, but produced some amorphous regions at the same time. Heating the pellets quickly eliminated the amorphous phases and then slowly aided change to the second structure. Since the original crystal structure was subsequently found to be unstable at normal conditions, the effectiveness of mulling in aiding transition is easily understood.

Less readily explainable are the differences in the spectrum of stable 2-aminobenzoic acid given in Fig. 7. The first and second spectra are from a hand ground mull and a machine ground mull, respectively, and they show very marked differences in the bands indicated by arrows. Since the bands which show increased intensity after vigorous mulling have not broadened, the changes may be due to polymorphism. If so, then pelleting in KBr causes transition to still a different crystalline structure as shown in the fourth spectrum. The third spectrum is from a KI pellet ground for 10 sec. and is very similar to the first mull; the only changes are a slight broadening and decreased resolution of some bands, but the changes are much less than those produced by vigorous mulling.

Similar changes have been observed sufficiently often in a number of other compounds such as 2,4-dinitrophenylhydrazine, salicylic acid, etc., that any comparison of solid-state spectra, whether mulls or pellets, should allow for possible crystal changes.

### Conclusion

Although the pellet technique has some serious limitations, it is still eminently suited for obtaining

spectra of microsamples and of amorphous polymer or resin samples. With some precautions, crystal distortions usually can be minimized in all but the most sensitive samples, and the pellets, while occasionally giving spectra not quite as good as mulls, will yield spectra which are good enough qualitatively for most problems. In particular, cautious grinding followed by appropriate heat treatment will give many excellent spectra from pellets which would otherwise give very poor spectra.

On the other hand, rather than trying to avoid crystal changes, these have been induced purposely to solve problems encountered in polymorphism. This is usually easier and faster than recrystallization or cocrystallization. Rather than being relatively rare, polymorphism occurs very frequently in organic preparations, especially if stabilizing impurities are present or if different solvents are used in recrystallization.

For the reasons outlined above, the pellet technique should have a place beside the mineral oil mull in every laboratory. In combination, these two methods of obtaining spectra will yield more information about a sample than will either one alone.

## CORRELATIONS OF THE INFRARED SPECTRA OF SOME PYRIDINES

BY G. L. COOK<sup>1</sup> AND F. M. CHURCH

*Petroleum and Oil-Shale Experiment Station, Bureau of Mines, Laramie, Wyoming*

*Received October 15, 1956*

The spectra of pyridine and 33 substituted pyridines are compared to establish correlations of the absorption bands with the molecular structure of the compounds. Five groups of compounds are considered, namely, 2-, 3- and 4-monosubstituted, and di- and tri-substituted types. Absorption bands that are generally characteristic of an alkylpyridine system are found near 1600, 1570 and 1000  $\text{cm}^{-1}$ . For 3-alkylpyridines and 2,5-dialkylpyridines, the latter peak is removed to 1021–1034  $\text{cm}^{-1}$ . Peaks in the regions 1280–1330  $\text{cm}^{-1}$  and 1222–1255  $\text{cm}^{-1}$  are strong confirmatory evidence for the alkylpyridine system. The separation of the absorption bands near 1600 and 1570  $\text{cm}^{-1}$  is approximately 40  $\text{cm}^{-1}$  for 4-monoalkylpyridines and 20  $\text{cm}^{-1}$  for the other two types of monosubstituted pyridines. The 4-monosubstituted pyridines also have a band in the region 1067–1072  $\text{cm}^{-1}$ . The 2-monosubstituted pyridines have bands at 1050  $\text{cm}^{-1}$  and in the region 1146–1152  $\text{cm}^{-1}$ . The 3-monosubstituted pyridines have bands at 1117–1131  $\text{cm}^{-1}$  and 1180–1196  $\text{cm}^{-1}$ . Disubstituted pyridines all have a peak in the region 1099–1136  $\text{cm}^{-1}$ . No correlations were found in this region for trisubstituted pyridines. Out-of-plane deformation vibrations for 2-monoalkylpyridines were found in the region 743–750  $\text{cm}^{-1}$ ; for 3-monoalkylpyridines at 789–810  $\text{cm}^{-1}$  and 712–715  $\text{cm}^{-1}$ ; for 4-monoalkylpyridines at 785–822  $\text{cm}^{-1}$ ; for disubstituted pyridines at 816–833  $\text{cm}^{-1}$  and 725–743  $\text{cm}^{-1}$ ; and for trisubstituted pyridines at 724–732  $\text{cm}^{-1}$ . For monoalkylpyridines the relative intensity and location of absorption bands in the 1367–2030  $\text{cm}^{-1}$  region differ only if the position of substitution differs. Typical absorption patterns in the region are given for 2-, 3- and 4-monoalkylpyridines. Patterns are also suggested for 2,3-, 2,4-, 2,5- and 2,6-disubstituted pyridines. The patterns for the disubstituted compounds may need some modification as additional compounds become available.

Correlation of the infrared absorption bands of simple compounds with their structures can provide a means for determining the structure of more complex compounds. This paper presents correlations based on the infrared spectra of pyridine and 33 substituted pyridines. The infrared absorption spectra are discussed in relation to each of five classes. These are 2-, 3- and 4-monosubstituted, disubstituted and trisubstituted classes. A sufficient number of compounds of each monosubstituted type were examined to indicate the general applicability of the correlations. The disubstituted and trisubstituted compounds were principally methyl-substituted. Hence the ranges given for the correlations of the spectra of the latter

compounds may have to be broadened as additional compounds become available.

Most of the previous work has been based on the spectra of pyridine<sup>2-4</sup> and the methylpyridines.<sup>5</sup> Bellamy<sup>6</sup> has reviewed work through 1953 concerning the assignment of vibrations for pyridine, the monomethylpyridines, 2,6-dimethylpyridine and various alkaloids containing the pyridine

(2) C. H. Kline, Jr., and J. Turkevich, *J. Chem. Phys.*, **12**, 300 (1944).

(3) L. Corrsin, B. J. Fax and R. C. Lord, *ibid.*, **21**, 1170 (1953).

(4) H. M. Randall, R. G. Fowler, N. Fuson and J. R. Dangle, "Infrared Determination of Organic Structures," D. Van Nostrand Co., Inc., New York, N. Y., pp. 7, 17, 39, 42, 91, 225.

(5) L. J. Bellamy, "The Infrared Spectra of Complex Molecules," John Wiley and Sons, Inc., New York, N. Y., pp. 232–239 (22 references).

(1) Bureau of Mines, Region III, Laramie, Wyo.

TABLE I  
 1600-1400 CM.<sup>-1</sup> ABSORPTION BANDS IN THE SPECTRA OF PYRIDINES

Compound	Absorption bands, cm. <sup>-1</sup>							
Pyridine	1600	1582	1486	..	..	1460	..	..
2-Methylpyridine	1600	1577	..	..	..	1443	..	..
2-Ethylpyridine	1603	1577	..	..	..	1439	..	1403
2- <i>n</i> -Pentylpyridine	1600	1577	..	..	..	1468	..	1418
2-Hexylpyridine	1597	1577	..	1477	..	1437	..	..
2-(5-Nonyl)-pyridine	1597	1577	..	1474	..	1437	..	..
2-Benzylpyridine	1597	1575	1501	1477	1458	1437	..	..
3-Methylpyridine	1605	1587	1492	..	..	1453	..	1424
1-(3-Pyridyl)-4-methylaminobutane (dihydrometanicotine) <sup>a</sup>	1585	1572	..	1475	..	1443	..	1420
1-(3-Pyridyl)-4-methylamino-1-butene (metanicotine) <sup>a</sup>	1585	1570	..	1475	..	..	..	1416
3-(1-Methyl-2-pyrrolidyl)-pyridine (nicotine) <sup>a</sup>	1592	1577	..	1478	1458	1429	..	1418
3-(1-Methyl-2-pyrrolidyl)-pyridine (nicotyrine) <sup>a</sup>	1590	1568	1538	1486	..	..	..	1416
3-(2-Pyrrolidyl)-pyridine (normicotine) <sup>a</sup>	1590	1577	..	1479	1460	..	..	1427
4-Methylpyridine	1597	1555	1490	..	..	1437	..	1406
4-Ethylpyridine	1605	1570	1506	..	..	1466	..	1422
4- <i>n</i> -Propylpyridine	1613	1567	1508	..	..	1468	..	1420
4-Isopropylpyridine	1600	1555	1495	..	..	1464	..	1412
4-Pentylpyridine	1610	1570	1504	..	..	1468	..	1418
4-(5-Nonyl)-pyridine	1608	1565	1501	..	..	1471	..	1418
4-Benzylpyridine	1600	1563	1497	..	..	1456	1433	1416
2,3-Dimethylpyridine	..	1567	..	..	..	1451	1439	1420
2,4-Dimethylpyridine	1610	1567	1492	..	..	1451	..	1400
2,5-Dimethylpyridine	1608	1572	1492	..	..	1451	..	..
2,6-Dimethylpyridine	1597	1585	..	1473	..	1453	..	1414
3,4-Dimethylpyridine	1600	1564	..	..	..	1456	..	1412
2-Methyl-5-ethylpyridine	1603	1567	1490	..	..	1451	..	..
2-Methyl-4-ethylpyridine <sup>b</sup>	1605	1588	..	1479	..	1449	..	1412
3-Ethyl-4-methylpyridine	1600	1567	1497	..	..	1458	..	1410
2-Methyl-6-ethylpyridine <sup>b</sup>	..	1587	1499	1466	..	1439	..	..
2,3,6-Trimethylpyridine	1600	1582	..	1471	..	1443	..	..
2,4,6-Trimethylpyridine	1610	1572	1534	..	1468	1439	..	1410
2,4,5-Trimethylpyridine <sup>b</sup>	1610	1565	1555	1495	..	1451	..	1391
2,4-Dimethyl-6-ethylpyridine	1605	1570	..	..	1462	1441	..	1416
2,6-Dimethyl-4-ethylpyridine	1608	1570	1541	..	1450	1431	..	..

<sup>a</sup> C. R. Eddy and A. Eisner, *Anal. Chem.*, **26**, 1428 (1954).  
Edinburgh, Scotland.

<sup>b</sup> Spectra furnished by H. B. Nisbet, Heriot-Watt College,

nucleus. Besides indicating the generality of the correlations already established, this paper introduces several new correlations within the five classes of pyridines.

### Experimental

A Perkin-Elmer model 21 spectrophotometer equipped with sodium chloride optics was used to obtain the spectra. The spectra were run, using slit program 4 (slit opening 0.017 mm. at 2.0  $\mu$ ). Fixed cells 0.034 and 0.086 mm. thick were sufficient to bring out the features of the spectrum between 5 and 15  $\mu$ .

The 26 compounds used to obtain the spectra in this Laboratory were of commercial origin. The manufacturers placed the minimum purity of each at 95% or greater. As small impurity peaks could be expected to appear in the spectra, only relatively strong peaks for the most part were used for the correlations. The source of spectra, including literature references where appropriate, are given in Table I.

### Results and Discussion

The absorption bands from 650-2080 cm.<sup>-1</sup> are grouped into frequency ranges to facilitate the discussion of the spectra. Table I, in addition to indicating the compounds used, includes data for one of these frequency ranges—1600 to 1400 cm.<sup>-1</sup>. The sodium chloride optics have low disper-

sion in the 3000 cm.<sup>-1</sup> region. Hence, this region is omitted from the discussion.

**2080-1667 Cm.<sup>-1</sup> Region.**—Young, Duvall and Wright<sup>6</sup> presented average absorption patterns for benzenes in the 1600-2000 cm.<sup>-1</sup> region that were typical with respect to the position and number of substituent groups. It has been suggested<sup>3</sup> that many of the vibrations of pyridine are quite close to those of benzene. Therefore, similar correlations would be expected to exist for the pyridines.

Figure 1 presents typical absorption patterns for the 2-, 3- and 4-monosubstituted pyridine types. The pattern for pyridine is included in the figure for comparison. The patterns differ enough in position, number and relative intensity of the absorption peaks to be readily differentiated.

The variation from the typical patterns is indicated in Fig. 2, which shows the spectra of five 2-monosubstituted pyridines. The substituent alkyl groups varied from methyl to 5-nonyl. Apparently, the spectra of the five compounds can be nearly

(6) C. W. Young, R. B. Duvall and N. Wright, *Anal. Chem.*, **23**, 709 (1951).

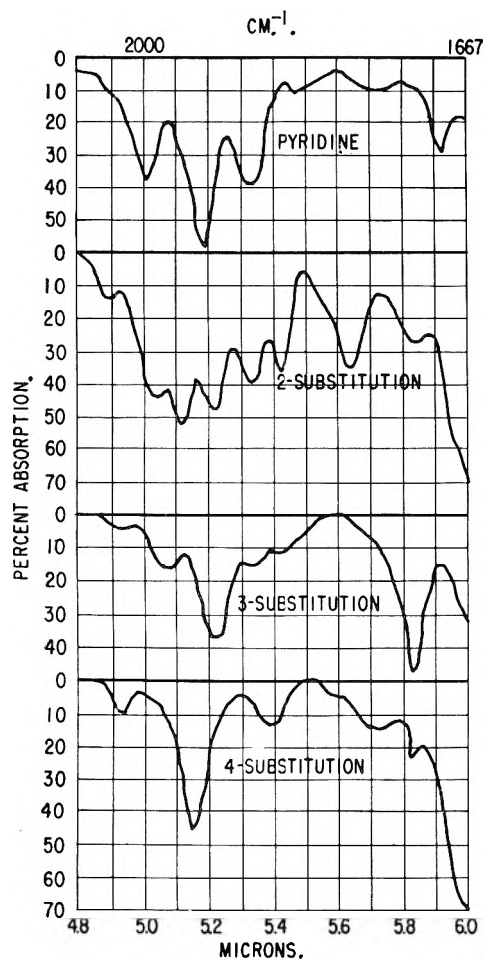


Fig. 1.—Typical absorption patterns for pyridine and three monosubstituted pyridines.

superimposed. Similar results were obtained for the 3- and 4-monosubstituted pyridines.

Figure 3 presents absorption patterns for 2,3-, 2,4-, 2,5- and 2,6-disubstituted pyridine types. The pattern for each type of substitution is quite distinctive. Only one or two compounds of each of the types illustrated were available. However, the remarkable similarity of the patterns (Fig. 2) for the 2-monosubstituted compounds as the chain length was increased suggests that the typical absorption patterns given for the disubstituted compounds will require little change as more compounds become available.

**1600-1400  $\text{cm}^{-1}$  Region.**—Two of the bands in the 1600-1400  $\text{cm}^{-1}$  region have been assigned to interactions between  $\text{C}=\text{C}$  and  $\text{C}=\text{N}$  vibrations of the pyridine rings.<sup>5</sup> The first of these bands occurs near 1600  $\text{cm}^{-1}$  and the second near 1500  $\text{cm}^{-1}$ . Bellamy<sup>5</sup> states that the 1600  $\text{cm}^{-1}$  band may show a double maximum, the second maximum occurring at a lower frequency than the 1600  $\text{cm}^{-1}$  band. With the exception of 2,3-dimethylpyridine and 2-methyl-6-ethylpyridine, all of the compounds given in Table I have absorption bands at 1588-1613  $\text{cm}^{-1}$  and at 1555-1588  $\text{cm}^{-1}$ . The bands in these two positions are assigned to the  $\text{C}=\text{C}$  and  $\text{C}=\text{N}$  groups, as suggested by Bellamy.

With the two exceptions noted, the disubstituted and trisubstituted pyridines had two absorption

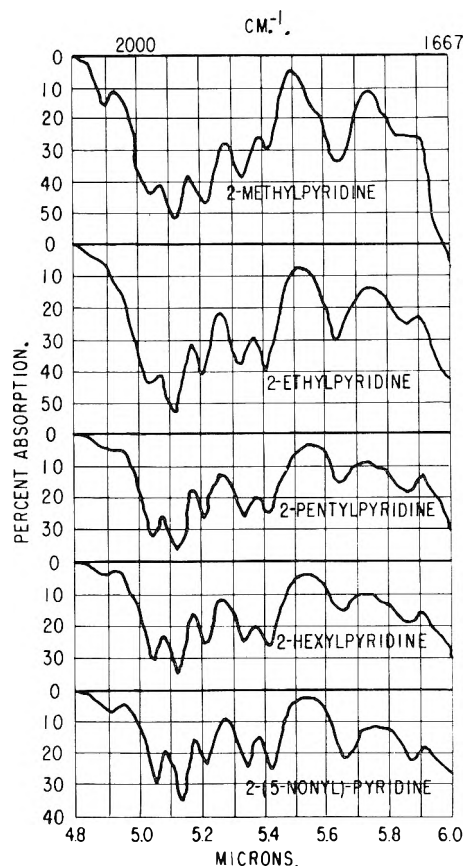


Fig. 2.—Spectra of five 2-monosubstituted pyridines in the 2000-1667  $\text{cm}^{-1}$  region.

maxima near 1600  $\text{cm}^{-1}$ . This double maximum appears to be a general characteristic of the pyridine nucleus and as such is similar to the phenyl compounds.<sup>5,6</sup> One of the exceptions noted, 2-methyl-6-ethylpyridine, exhibited an additional peak at 1529  $\text{cm}^{-1}$ , which was not included in Table I. This vibration is probably related to the double-bond system of pyridine, as are those in the 1600  $\text{cm}^{-1}$  region.

For monosubstituted pyridines the average separation of the two bands can be used to differentiate 2- or 3-monosubstituted pyridines from 4-monosubstituted pyridines. For 2- and 3-monosubstituted pyridines the average separation of the bands is 20  $\text{cm}^{-1}$ , but for 4-substituted pyridines the separation is 40  $\text{cm}^{-1}$ . The spectra of pyridines with a variety of monoalkyl substituents were examined, as shown in Table I, and the correlation was found to be valid for all.

In addition to the two bands in the 1550-1600  $\text{cm}^{-1}$  region, all the 4-monosubstituted pyridines showed an absorption band near 1500  $\text{cm}^{-1}$ . The 2-benzylpyridine and the 3-methylpyridine also exhibited peaks near 1500  $\text{cm}^{-1}$ , but the other 3-monosubstituted pyridines, the nicotines, did not have such a peak. The 1501  $\text{cm}^{-1}$  for 2-benzylpyridine probably results from a  $\text{C}=\text{C}$  vibration of the phenyl ring.<sup>5</sup> Hence, the presence of this peak in the 2-benzylpyridine spectrum does not invalidate the correlation of the peak with 4-substitution. The appearance of the peak in the spectrum of 3-methylpyridine suggests that the

correlation must be qualified to include possible interference from 3-alkylpyridines.

One or more additional absorption bands were found near 1475 and 1440 or 1460  $\text{cm}^{-1}$  in the spectra of the 2- and 3-monosubstituted compounds. In Table I these bands were grouped into columns, taking into consideration shape and intensity as well as position of the bands. On this basis, the 1468  $\text{cm}^{-1}$  peak for 2-*n*-pentylpyridine is placed in the sixth column of the table in preference to the fifth. Peaks in these three regions occur near the position assigned to vibrations of alkyl groups.<sup>5</sup> With the exception of 4-methylpyridine, the 4-monosubstituted compounds showed similar maxima near 1465  $\text{cm}^{-1}$ . All of the 3- and 4-monosubstituted compounds and 2-methyl- and 2-ethylpyridine had peaks in the 1403–1424  $\text{cm}^{-1}$  region. The origin of this vibration is not clear.

The disubstituted and trisubstituted compounds absorbed near 1450 or 1440  $\text{cm}^{-1}$  and near 1410  $\text{cm}^{-1}$ . The latter peak was found in the spectra of 22 of the 34 compounds shown in Table I. Hence, its presence in a spectrum can be used as additional evidence for the presence of the pyridine system, but the reverse is not necessarily true.

The peaks near 1500  $\text{cm}^{-1}$  in the spectra of the disubstituted compounds could interfere in differentiating 2- or 3-monosubstituted compounds from 4-monosubstituted compounds. However, the 1667–2080  $\text{cm}^{-1}$  region supplies a basis for the determination.

**1400–650  $\text{Cm}^{-1}$  Region.**—Table II presents the prominent peaks in the 1400–650  $\text{cm}^{-1}$  region shown by the spectra of the 34 pyridines. The compounds were grouped for the purpose of presentation in the table into 2-monosubstituted, 3-monosubstituted, 4-monosubstituted, disubstituted and trisubstituted types.

The methyl vibrations occur in the expected position, near 1380  $\text{cm}^{-1}$ .<sup>5</sup> For the 4-isopropylpyridine the split vibration of the methyl groups, although not shown specifically in the table, appeared at 1385 and 1364  $\text{cm}^{-1}$ . The two bands were of nearly equal intensity.

A peak at 1280–1330  $\text{cm}^{-1}$  appeared in the spectra of 32 of the 34 pyridines. The peak varied in intensity between compounds. It has been suggested<sup>3</sup> that this vibration in pyridine is due to an overtone of the fundamental that occurs near 650  $\text{cm}^{-1}$ . The variable intensity of the peak reduces its value for characterization studies.

A peak in the 1220–1250  $\text{cm}^{-1}$  region can probably be attributed to bending vibrations of the hydrogen atoms on the pyridine ring. An additional vibration at 1145–1152  $\text{cm}^{-1}$  for 2-monosubstituted pyridines probably arises from the same source. The latter vibration, which was especially constant in position, was found in the spectra of all the 2-monosubstituted pyridines. Both of these vibrations were medium to strong compared to the general level of absorption in the region. The spectra of the 3-monosubstituted pyridines showed an absorption band in the 1180–1196  $\text{cm}^{-1}$  region. This peak probably arises from hydrogen bending vibrations and is analogous

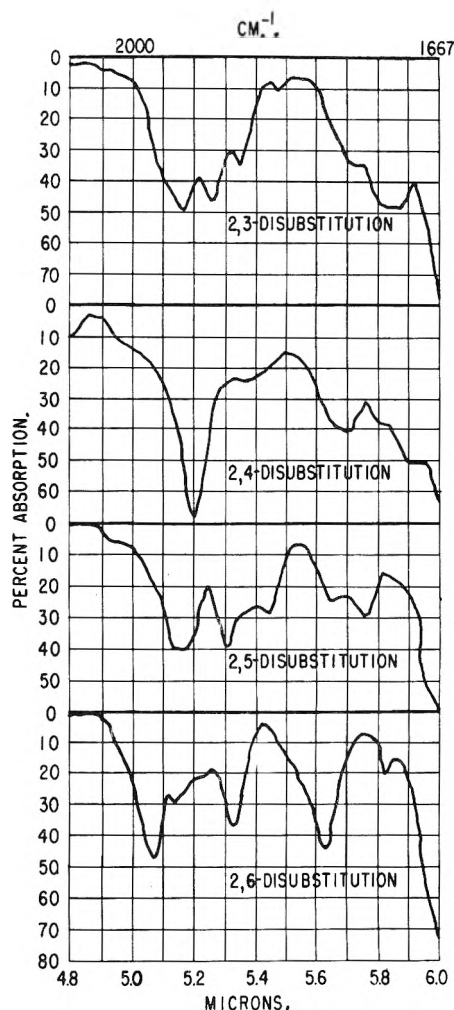


Fig. 3.—Typical absorption patterns for disubstituted pyridines.

to the 1146–1152  $\text{cm}^{-1}$  peak of the 2-monosubstituted pyridines.

Other bands in the hydrogen bending region, which were constant in position, were found at 1050–1052  $\text{cm}^{-1}$  for the 2-monosubstituted pyridines, at 1117–1131  $\text{cm}^{-1}$  for 3-monosubstituted pyridines, at 1067–1072  $\text{cm}^{-1}$  for 4-monosubstituted pyridines, and at 1099–1136  $\text{cm}^{-1}$  for the disubstituted pyridines. These were generally medium to strong bands in the spectra.

Bellamy<sup>5</sup> gives 1100–1000  $\text{cm}^{-1}$  as the range in which a ring vibration for pyridines<sup>3,3</sup> has been found. As shown in Table II, this band occurred in the very narrow range of 988–1001  $\text{cm}^{-1}$  for all of the pyridines except 3-monosubstituted and 2,5-disubstituted compounds. For the exceptions, a strong band appeared in the 1021–1034  $\text{cm}^{-1}$  region.

All of the 2-monosubstituted pyridines showed a strong band in the 745–750  $\text{cm}^{-1}$  region. This has been assigned to out-of-plane deformation vibrations of the ring hydrogens.<sup>5</sup> The vibrations are analogous to those of the phenyl hydrogens.<sup>5</sup> For the 3-monosubstituted compounds this band appeared in the 789–810  $\text{cm}^{-1}$  region, accompanied by a second band near 712  $\text{cm}^{-1}$ . For the

TABLE II  
1400-650 CM.<sup>-1</sup> INFRARED ABSORPTION PEAKS OF PYRIDINES

Compound	Frequencies of absorption regions in cm. <sup>-1</sup>							
	1377-	1299-	1225 <sup>a</sup>	1146-	1050-	995 <sup>a</sup>	743-	
2-Monosubstd.	1383	1311		1152			750	
3-Monosubstd.	1377-	1312-	1239-	1180-	1117-		789-	712-
	1383	1318	1253	1196	1131	1021-	810	715
						1034		
4-Monosubstd.	1377-	1299-	1222-		1067-	995-	785-	
	1383	1311	1253		1072	1000	822	
Disubstd.	1377-	1300-	1226-		1099-	1028 <sup>b</sup>	988- 816-	725-
	1383	1330	1250		1136		998 <sup>c</sup> 833	743
Trisubstd.	1377-	1280-	1222-			1032-	996-	724-
	1383	1330	1231			1040	1001	732

<sup>a</sup> The position of this band was constant; hence, no ranges are given. <sup>b</sup> Present only in spectra of 2,5-disubstituted pyridines. <sup>c</sup> Not present in spectra of 2,5-disubstituted pyridines

4-monosubstituted compounds the band appeared at 785-822 cm.<sup>-1</sup>. The disubstituted pyridines showed two such bands in the 650-1000 cm.<sup>-1</sup> region. These occurred at 816-833 cm.<sup>-1</sup> and 725-743 cm.<sup>-1</sup>. The trisubstituted compounds examined had only one strong peak (725-732 cm.<sup>-1</sup>) in the low-frequency region. In each instance the out-of-plane vibration bands were the strongest observed in the 650-1000 cm.<sup>-1</sup> region.

### Summary and Conclusions

Peaks near 1600, 1570 and 1000 cm.<sup>-1</sup> are characteristic of an alkyl-pyridine system. In 3-alkylpyridines and 2,5-dialkylpyridines the 1000 cm.<sup>-1</sup> peak is removed to 1021-1034 cm.<sup>-1</sup>. Peaks in the regions 1280-1330 cm.<sup>-1</sup> and 1222-1253 cm.<sup>-1</sup> are strong confirmatory evidence of the presence of an alkylpyridine.

The separation of the two peaks near 1600 and 1570 cm.<sup>-1</sup> is approximately 40 cm.<sup>-1</sup> for 4-monoalkylpyridines. This distinguishes the 4-monoalkylpyridines from the other monosubstituted pyridines; in these spectra the two peaks are separated by only 20 cm.<sup>-1</sup>.

In the region 1050-1200 cm.<sup>-1</sup> peaks at 1050 cm.<sup>-1</sup> and at 1146-1152 cm.<sup>-1</sup> characterize 2-monoalkylpyridines; peaks at 1117-1131 cm.<sup>-1</sup> and 1180-1196 cm.<sup>-1</sup> indicate 3-monoalkylpyridines; and a peak at 1067-1072 cm.<sup>-1</sup> indicates 4-mono-substitution. All the disubstituted pyridines examined have peaks in the 1099-1136 cm.<sup>-1</sup> region. This overlaps the vibration of 3-monoalkylpyridines. The distinction between these two types

would have to be made from other regions of the spectrum. As no correlations were made in this region for trisubstituted pyridines, the characterization of these must also be made from other spectral regions.

Out-of-plane deformation vibrations for 2-monoalkylpyridines were found in the region 743-750 cm.<sup>-1</sup>; for 3-monoalkylpyridines in the regions 789-810 cm.<sup>-1</sup> and 712-715 cm.<sup>-1</sup>; for 4-monoalkylpyridines in the region 785-822 cm.<sup>-1</sup>; for disubstituted pyridines in the regions 816-833 cm.<sup>-1</sup> and 725-743 cm.<sup>-1</sup>; and for trisubstituted pyridines in the region 724-732 cm.<sup>-1</sup>.

The location and relative intensity of the peaks in the 1667-2080 cm.<sup>-1</sup> region are characteristic of position of substitution for monoalkylpyridines. Changes in size and branching of the substituent group have little effect on the over-all appearance of the spectrum in this region. Assignments of typical substitution patterns for some disubstituted compounds are included. These may need modification as additional compounds of the types become available.

**Acknowledgment.**—This work was performed at the Bureau of Mines, Petroleum and Oil-Shale Experiment Station, Laramie, Wyo., under the general direction of H. P. Rue, H. M. Thorne and J. S. Ball. The authors wish to thank G. U. Dinnæen and H. H. Heady of this Laboratory for their review of the manuscript. The work was done under a coöperative agreement between the University of Wyoming and the Bureau of Mines, U. S. Department of the Interior.

## INTERFACIAL TENSION AND COMPLEX FORMATION

BY EDWARD A. HEINTZ AND DAVID N. HUME

Contribution from the Department of Chemistry and Laboratory for Nuclear Science of the Massachusetts Institute of Technology, Cambridge 39, Massachusetts

Received October 17, 1956

The interfacial tension method, proposed by Kazi and Desai for the study of complex formation in aqueous solution, has been examined critically and the effect of experimental variables on the results determined. The drop volume technique originally proposed was found to give results which were too erratic and unreliable to allow correlation with solution composition. Measurement of interfacial tension by the ring method, which was found to be much more accurate, showed no evidence of changes in interfacial tension due to complex formation alone.

During the last few years several workers have reported, in a long series of articles,<sup>1-4</sup> studies on

(1) H. J. Kazi and C. M. Desai, *J. Indian Chem. Soc.*, **30**, 287, 290, 291, 421, 423, 424, 426, 872, 873 (1953); **31**, 163, 165, 329, 331, 332, 415, 416, 418, 633, 636, 638, 640, 769 (1954); *Science and Culture*, **19**, 259 (1953).

complex formation in aqueous salt solutions carried out by measurement of the interfacial tension between the solutions and organic liquids "having

(2) H. J. Kazi, *J. Indian Chem. Soc.*, **31**, 763 (1954); **32**, 64 (1955).

(3) C. M. Desai, *ibid.*, **31**, 957 (1954).

(4) H. V. Barat and C. M. Desai, *ibid.*, **32**, 61 (1955).

an unstable H-bond ring structure." According to these workers, mixtures of salts corresponding to stoichiometric compound or complex formation showed strikingly higher interfacial tension against liquids such as *n*-butyl acetate than did similar mixtures which did not correspond to stoichiometric ratios. A typical set of their results is shown in the lower curve of Fig. 1. The observed effect persisted even in very dilute solutions and it was claimed in many instances that a larger number of complexes was formed in dilute (*e.g.*, 0.01 *M*) than in relatively more concentrated (0.5 *M*) solutions. The effects reported were large, sometimes as much as 3 dynes/cm. between peak and trough, and about the same for nearly all systems studied. Usually more complexes were reported for a given system than had been found by other workers using well-established potentiometric and spectrophotometric methods. From a study of the published results, it was evident that either the interfacial tension method must be a remarkable tool of hitherto unsuspected sensitivity, or it must be a trap for the unwary. In order to determine which, we have undertaken to repeat and extend some of the studies reported by previous workers, concentrating on systems the characteristics of which had also been well worked out by other investigators using established methods.

### Experimental

The first measurements of interfacial tension were made using the "drop volume" method as described by Kazi and Desai<sup>5</sup> and duplicating their technique as closely as possible. A Gilmont microburet was used to discharge and measure the drops of organic liquid. Tips of both glass and stainless steel were used to form the drops, with no significant differences being observed. Later experiments were performed by the ring method utilizing a du Noüy interfacial tensiometer as marketed by Central Scientific Company of Chicago, Illinois, under their catalog No. 70545. Measurements were performed in a constant temperature room at 23°, although it was observed that small temperature changes had very little effect.

Reagents and chemicals used were the best quality commercially available. Distilled, deionized water was used throughout. In order to avoid chance contamination by detergents or other surface-active agents, all glassware was cleaned with hot nitric-sulfuric acid and washed with distilled water.

### Results and Discussion

Several systems, of which the one involving mercuric and potassium chlorides is typical, were investigated following the procedure of Kazi and Desai. It was immediately observed that although satisfactory agreement could be obtained between successive observations of the volume of ten drops of *n*-butyl acetate delivered from the tip as long as the tip and solution remained undisturbed, emptying and refilling the apparatus often resulted in considerable changes in the apparent interfacial tension. Figure 2 shows the results of three independent runs made with the mercuric chloride-potassium chloride system, all supposedly identical.

In these runs the standard deviation of the measurements as estimated from the agreement between duplicate measurements made in immediate succession without any alteration or disturbance in experimental conditions, was 0.20 dyne/cm., based on 59 separate samples. On this basis, a

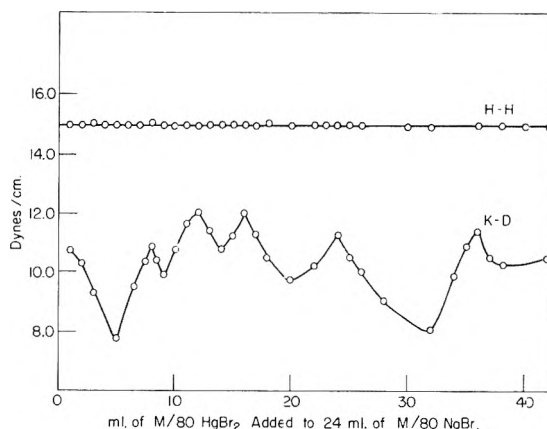


Fig. 1.—Interfacial tension between *n*-butyl acetate and mixtures of mercuric bromide and sodium bromide: upper curve, data of this investigation obtained by ring method, lower curve, data of Kazi and Desai.<sup>1</sup>

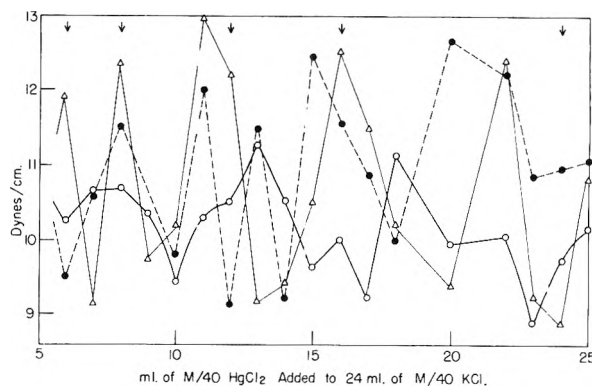


Fig. 2.—Interfacial tension between *n*-butyl acetate and mercuric chloride-potassium chloride mixtures, determined by the drop-volume method. Three separate runs are shown. The arrows correspond to the positions of peaks reported by previous workers.

difference of 0.56 dyne/cm. between two single observations would be statistically significant at the conventional 5% level. This, however, is not a valid way of estimating experimental error, inasmuch as it is always necessary in the actual experiments to compare results obtained on different solutions. Accordingly, the precision of the measurements was estimated by comparison of measurements on sets of identical replicate solutions. Here, the standard deviation was found to be 1.70 dynes/cm., based on 20 sets of triplicate samples. In order, then, to attribute statistical significance to a difference between two samples, the observed difference between them would have to be 4.8 dynes/cm. or more. Such differences were not observed in our work. The differences between solutions of different compositions were no greater than the differences between solutions of the same composition. Other systems investigated, including the lead nitrate-potassium nitrate and mercuric bromide-sodium bromide pairs, gave similar results. The range of values obtained in the present investigation was about the same as that previously reported.

It was noted that the drop volume, and therefore the apparent interfacial tension, was sensitive to small differences in the rate of delivery of the organic liquid through the capillary tip. When solu-

(5) H. J. Kazi and C. M. Desai, *J. Indian Chem. Soc.*, **30**, 209 (1953).

tions of known composition were being used, an unconscious tendency on the part of the operator to measure stoichiometric mixtures with greater care than solutions of less significance resulted in the occasional appearance of small peaks at stoichiometric compositions. When the samples were prepared by another person and run in random order under a blind code, these regularities disappeared and a random distribution of drop volumes with solution composition was obtained as in Fig. 2.

Although this result seemed clear-cut, we were far from satisfied, because as already indicated the precision of the drop-volume method was in our hands, rather low. The reproducibility was often not better than about  $\pm 0.5$  dyne/cm., and quite a number of the peaks shown in the literature are of that order of magnitude. Experimentation with various sizes, shapes and materials for the tips used and methods of manipulation led us to conclude that a significant increase in precision could only be achieved by a major effort in apparatus building, and this did not seem justified in view of the fact that the Indian workers had obtained their results apparently without difficulty using quite simple equipment. Room temperature changes were shown to be almost without effect. In an effort to get more reproducible data, we abandoned the drop-volume method and carried on the rest of the work with a du Noüy tensiometer. This instrument utilizes the well-known ring method of measuring surface tension and is adaptable both to ordinary surface tension and to interfacial tension measurements. In addition to being faster and more convenient than the drop-volume apparatus, it was found in our hands to be far more reproducible. For both surface tension and interfacial tension measurements, a precision of  $\pm 0.05$  dyne/cm. was obtained in regular use, in good agreement with the manufacturer's claims. The systems previously studied by the drop-volume method were then re-examined using the new apparatus. In the mercuric chloride-potassium chloride system, detailed examination of the region in the immediate vicinity of the alleged  $\text{HgCl}_4^-$  peak, using solutions of composition known to the investigator, showed at the most a difference of 0.2

dyne/cm. between the stoichiometric mixture and the lowest parts of the curve. Other experiments over a wide range of compositions and using solutions of composition unknown to the investigator showed no detectable differences between stoichiometric solutions and solutions of other compositions. A typical result is given in Fig. 1 in which the results of this investigation are compared with those of Kazi and Desai for the 80/M mercuric bromide-sodium bromide system. Our 36 observations showed no peaks whatever, and all the points lay within  $\pm 0.05$  dyne/cm. of the average value of 14.95 dynes/cm. Similar results were obtained with the mercuric chloride-potassium chloride system, although the scatter of points was a little greater. Control runs in which concentrations of potassium chloride alone and mercuric chloride alone were measured against *n*-butyl acetate showed only a slight trend of interfacial tension with concentration.

Potentiometric studies by a number of workers had indicated that although some complex formation between mercuric and potassium chlorides or bromides does take place, changes in physical properties of the solutions might not be great when dilute solutions were mixed. The ions  $\text{HgX}_3^-$  and  $\text{HgX}_4^{2-}$  are much less stable, relatively speaking, than the un-ionized  $\text{HgX}_2$ .<sup>6</sup> To give the interfacial tension method a greater chance of success, we used it to follow the addition of the first two chlorides to the mercuric ion by studying mixtures of mercuric nitrate and potassium chloride. This is a quantitative reaction which is used for analytical purposes and which gives a very striking end-point break in the potentiometric titration curve. Almost no effect was detected at the stoichiometric point, although a very slight rise just on the borderline of statistical significance could be seen.

It was reasoned that more definite results might be obtained using iodide ions, inasmuch as the capillary activity of iodide is greater than that of chloride or bromide. Addition of potassium iodide to water produced a small but definite drop in the interfacial tension. Mercuric nitrate was then titrated with potassium iodide and a very large drop (2 dynes/cm.) was indeed found at the stoichiometric point of  $\text{HgI}_2$  (Fig. 3). This, however, was not a clear-cut case of detection of complex formation; for, as is well known,  $\text{HgI}_4^{2-}$  forms immediately on addition of iodide and  $\text{HgHgI}_4$  is precipitated. After the stoichiometric point, the red precipitate begins to dissolve, forming yellow  $\text{HgI}_4^{2-}$  ions, and it was observed that the yellow color of the complex was being extracted into the organic phase. This fact is, in itself, sufficient to explain the change in interfacial tension. Not even the titration of calcium ions with sodium palmitate gave a clear-cut end-point by interfacial tension measurements. A rapid drop in interfacial tension was observed at the beginning of the titration, and very little further change took place in the vicinity of the end-point.

Parallel with a number of the interfacial studies, measurements were made on the surface tension of the solutions using the ring method. The results

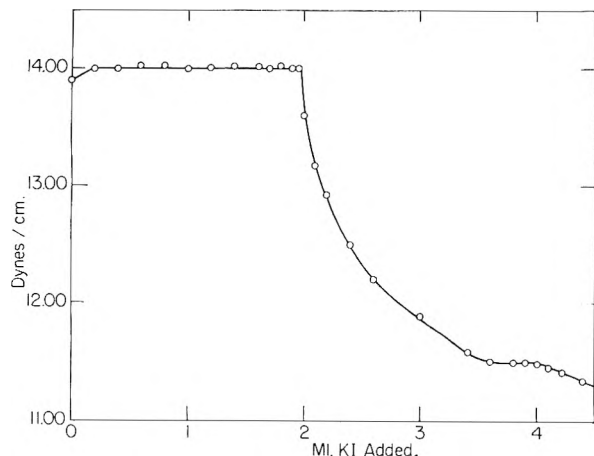


Fig. 3.—Interfacial tension between *n*-butyl acetate and 12.0 ml. of 0.025 *M* mercuric nitrate during titration with 0.30 *M* potassium iodide.

(6) L. G. Sillén, *Acta chem. Scand.*, **3**, 539 (1949).

were quite analogous and no evidence was found of the sharp drops at stoichiometric compositions which have been reported in surface tension *versus* composition curves by some previous workers.<sup>7-9</sup>

From all the evidence we have been able to gather, we can only conclude that within the pre-

(7) M. R. Nayar and C. S. Pande, *Proc. Indian Acad. Sci.*, **27A**, 343 (1948).

(8) M. R. Nayar and K. V. Nayar, *J. Indian Chem. Soc.*, **29**, 250 (1952).

(9) C. S. Pande and M. P. Bhatnagar, *ibid.*, **31**, 405, 537 (1954).

cision of our measurement, the interfacial tension of aqueous salt mixtures with liquids such as *n*-butyl acetate does not assume peak values at stoichiometric compositions corresponding to complex formation, and that previous workers have been misled by unrecognized procedural bias and a failure to evaluate observed differences in terms of a validly estimated experimental error.

**Acknowledgment.**—This work was supported in part by the United States Atomic Energy Commission.

## DILUTE SOLUTION MEASUREMENTS OF MOLAR KERR CONSTANTS OF SOME HALOBENZENES, MONOHALOBENZOTRIFLUORIDES AND BENZOTRIFLUORIDE<sup>1,2</sup>

By L. V. CHERRY, M. E. HOBBS AND H. A. STROBEL

*Contribution from the Department of Chemistry, Duke University, Durham, N. C.*

*Received October 20, 1956*

The Kerr constants of three halobenzenes, benzotrifluoride and nine monohalobenzotrifluorides were measured by a relative method in benzene at concentrations below 0.015 mole fraction of solute. In this range the Kerr constants were found to vary linearly with concentration. A method developed by Otterbein for calculating molar Kerr constants of disubstituted benzene derivatives has been modified by use of the Silberstein molecular model to include effects of possible interaction between substituents on the benzene ring. The molar Kerr constants calculated by this method are generally in better agreement with experimental values than those calculated by the Otterbein method without correction. The principal polarizabilities of all compounds studied were calculated from the Kerr constants and refractivity data on benzene and its monohalogen derivatives. The results for benzene and the monohalobenzenes agreed with the values reported by LeFèvre and LeFèvre, on the average, to within  $\pm 3\%$ .

Theoretical treatments of the Kerr effect relate the Kerr constant of a molecule to its polarizability and the components of the permanent dipole moment in the directions of the principal polarizabilities of the molecule. As shown mathematically by Langevin<sup>3</sup> and Born,<sup>4</sup> it is these quantities which determine the orientation of the molecule in an external electric field. The relation between the Kerr constant and the above mentioned molecular properties can be used, as Stuart<sup>5</sup> has pointed out in his excellent review article, to provide a considerable amount of information concerning molecular structure.

The objective of the present investigation was to learn how reliably the Kerr constant and polarizabilities of disubstituted benzene derivatives can be predicted by combination of appropriate properties of the corresponding monosubstituted benzenes. The compounds chosen for the study were benzotrifluoride,  $C_6H_5CF_3$ , the halobenzenes,  $C_6H_5X$ , and the monohalobenzotrifluorides,  $CF_3C_6H_4X$ , where  $X = F, Cl$  or  $Br$ .

Measurements were made in dilute solution since this offered a good compromise between the theoretically favorable gaseous state and the experimentally favorable pure liquid state. No sys-

tematic observations of the Kerr constant have been reported on a well-defined series of compounds in the dilute concentration range (mole fraction  $\leq 0.015$ ) although many solution measurements on benzene derivatives have been reported by Briegleb,<sup>6</sup> Otterbein,<sup>7</sup> and others.<sup>8-11</sup>

### Experimental

**Materials.**—Reagent-grade Jones and Laughlin benzene was refluxed overnight over sodium, then distilled twice over sodium through a 6-ft. Dufton column. The middle fraction boiling over a range of less than  $0.02^\circ$  was used. The benzene was recovered by essentially the same treatment.

Eastman Kodak Co. white label fluorobenzene, chlorobenzene and bromobenzene were shaken first with portions of cold concentrated sulfuric acid, then with dilute sodium bicarbonate solution, and finally with water. After storage for two days over anhydrous magnesium sulfate, the liquids were distilled, as were all the other substances studied through a 60-cm. jacketed column packed with glass helices. There were sufficient quantities of most materials to permit redistillation of the middle cuts obtained from the first fractionation.

Samples of benzotrifluoride and the three chlorobenzotrifluorides, obtained from the Hooker Electrochemical Company, were distilled without treatment.

The *o*-bromobenzotrifluoride and *o*-fluorobenzotrifluoride were prepared using the method of Jones.<sup>12</sup>

The *m*- and *p*-fluorobenzotrifluoride were synthesized by the method of Booth, Elsey and Burchfield.<sup>13</sup>

(1) Presented before the Division of Physical and Inorganic Chemistry of the American Chemical Society at the 130th National Meeting, Atlantic City, September, 1956.

(2) Taken in part from a dissertation submitted by L. V. Cherry to the Graduate School of Duke University in partial fulfillment of the requirements for the degree of Doctor of Philosophy, June, 1953.

(3) P. Langevin, *Compt. rend.*, **151**, 475 (1910).

(4) M. Born, *Ann. Physik*, [4] **55**, 177 (1918).

(5) H. A. Stuart, *Hand und Jahrbuch chem. Physik*, **10**, 27 (1939).

(6) G. Briegleb, *Z. physik. Chem.*, **14B**, 97 (1931); **16B**, 249 (1932).

(7) G. Otterbein, *Physik. Z.*, **35**, 249 (1934).

(8) A. Lippmann, *Z. Elektrochem.*, **17**, 15 (1911).

(9) R. Lieser, *Physik. Z.*, **12**, 955 (1911).

(10) A. Pickara, *Acta Phys. Polon.*, **10**, 37, 107 (1950).

(11) C. G. LeFèvre and R. J. W. LeFèvre, *J. Chem. Soc.*, 4041 (1953); 1577 (1954).

(12) R. G. Jones, *J. Am. Chem. Soc.*, **69**, 2346 (1947).

(13) H. S. Booth, H. M. Elsey and P. E. Burchfield, *ibid.*, **57**, 2066 (1935).

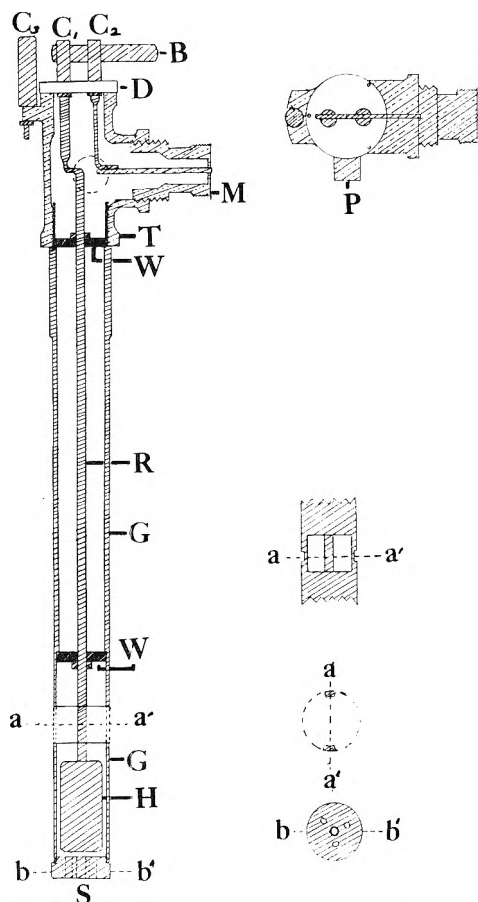


Fig. 1.—Dielectric constant cell.

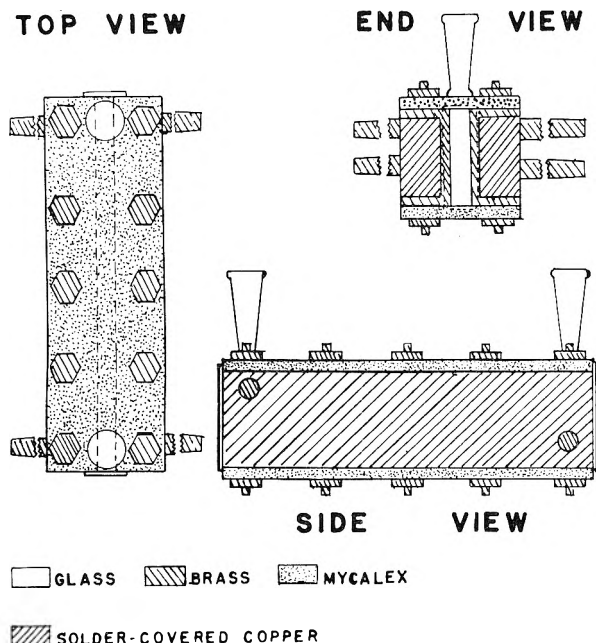


Fig. 2.—Kerr cell.

Both the method of Simons and Ramler<sup>14</sup> and a modification of the preparative procedure described by Adams and Johnson<sup>15</sup> for *o*-chlorotoluene were used in making *m*-bromobenzotrifluoride.

(14) J. H. Simons and E. O. Ramler, *J. Am. Chem. Soc.*, **65**, 389 (1943).

(15) R. Adams and J. R. Johnson, "Elementary Laboratory Ex-

periment in Organic Chemistry," The Macmillan Co., New York, N. Y., 1943, p. 263.

Finally, *p*-bromobenzotrifluoride was produced by direct bromination of Hooker *m*-aminobenzotrifluoride and demethylation of the resulting 3-amino-4-bromobenzotrifluoride.

**Apparatus.**—Refractive indices were measured at the wave length of the sodium D line with a calibrated Spencer-Abbe refractometer. Calibrated glass pycnometers similar in design to those described by Vosburgh, Connell and Butler<sup>16</sup> were used to obtain densities.

Dielectric constants were determined by the heterodyne beat method. The equipment consisted of a modified Clough-Brcngle (C. B.) Beat Frequency Oscillator connected in parallel with a calibrated General Radio Precision Condenser, Type 722-D, and a special measuring cell, shown in Fig. 1. The cell consists of a grounded cylindrical conductor G made from 1/2-inch monel metal pipe, and inner solid monel cylinder forming the high-potential section H. The upper end of H is attached to a threaded length of 1/8 inch monel rod R which is held rigidly in place by Teflon washers W. The upper end of the rod is connected to the central terminal C<sub>1</sub> of an s.p.d.t. knife switch B. A second terminal C<sub>2</sub> leads to the insulated contact of a microphone connector M, and the third terminal C<sub>3</sub> is grounded. The components C<sub>1</sub> and C<sub>2</sub> are mounted on a polystyrene disk D which is rigidly fixed to a 1/8-inch brass pipe tee T fastened over the upper end of G. Access to connections within the tee is permitted by a plug P. The lower end of G is closed with a small screw cap S which contains four holes so as to permit filling and drainage of the high-potential section of the cell. At about 5 mm. above the junction of H and R, a major section of the 1/2-inch pipe is cut away to reduce the effect of slight variation in liquid level on the value of the capacitance.

In use, the cell was placed in a 30-ml. glass vial into which 5 ml. of liquid had been introduced by means of a calibrated pipet. The blade of the switch was set at either C<sub>2</sub> or C<sub>3</sub>, and the precision condenser adjusted to give a zero beat condition in the oscillator. Capacitance readings were then made in the usual manner. The cell was calibrated with benzene, using a value of the dielectric constant,  $\epsilon^{20} = 2.263$ , given by Hartshorn and Oliver.<sup>17</sup> The values of the dielectric constant obtained in this way are considered accurate to about half a per cent.

**Kerr Constants.**—A relative method involving two Kerr cells suggested by Des Coudres<sup>18</sup> and subsequently employed by others<sup>19-22</sup> was used in determining Kerr constants.

The type of Kerr cell used in this work is shown diagrammatically in Fig. 2. The electrodes, which served as cell walls, were sections of hollow rectangular brass stock 97 × 12 × 21 mm., which had been milled out and then closed by soldering on a copper plate. Oil from a thermostat was circulated through each of the hollow electrodes. The electrode separation was 5 mm., being maintained by strips of 1/8-inch Mycalex which formed the top and bottom of each cell. To seal the Mycalex to the brass sides Goodyear Pliobond-30 was applied and carefully cured. The top of each cell was provided with two 5/20 ground glass standard taper joints for filling purposes. These inlets were sealed to the Mycalex with heat-cured Bakelite Varnish No. 1600. A short length of wire soldered to each electrode provided an electrical connection. About 11 ml. of liquid sample was required to fill an assembled cell.

The end windows of each cell were cover glasses of 0.5 mm. thickness certified as to planarity of surface by the National Bureau of Standards. They were sealed directly to the electrodes by means of cured Bakelite varnish. Occasionally one was replaced without any apparent effect on the geometrical constant *k* of eq. 3 below.

Each cell rested in a Bakelite cradle and was so oriented that the direction of the electric field in the cell was at an

periments in Organic Chemistry," The Macmillan Co., New York, N. Y., 1943, p. 263.

(16) W. C. Vosburgh, L. Connell and J. Butler, *J. Chem. Soc.*, 933 (1933).

(17) L. Hartshorn and D. A. Oliver, *Proc. Roy. Soc. (London)*, **A123**, 634 (1929).

(18) T. Des Coudres, *Verhand. deut. Ges. Deutsch. Natur. Ärzte*, **65**, No. 2, 67 (1893).

(19) W. Schmidt, *Ann. Physik*, **7**, 142 (1902).

(20) R. Leiser, *Physik. Z.*, **12**, 955 (1911).

(21) W. Ilberg, *ibid.*, **29**, 670 (1928).

(22) H. A. Scheraga, M. E. Hobbs and P. M. Gross, *J. Opt. Soc. Amer.*, **39**, 410 (1949).

angle of 45° from the horizontal. The first cell mount had three translational and two rotational degrees of freedom, the second, an additional rotational degree of freedom. Set screws in appropriate places served to lock the cradles in any desired position; the cells could be removed and subsequently replaced without observable changes in the optical alignment.

In Fig. 3 the optical system is shown. The light source I was a Western Union Type M100 concentrated-arc lamp operating from a d.c. supply. Its spectral range was limited by a Farrand interference filter F having a peak transmission wave length of 555 m $\mu$  and a half-band width of 15 m $\mu$ . The lens L, the lamp housing slot and slits S<sub>1</sub> and S<sub>2</sub> served to collimate and limit the light beam. The light was polarized by a Nicol prism N<sub>1</sub> after which it passed through a third slit S<sub>3</sub> and entered the Kerr cell, K<sub>1</sub>. Since the beam diverged somewhat in passing through liquid, it was again limited by slit S<sub>4</sub> prior to entering the second cell K<sub>2</sub>. The latter was oriented so that its electric field was perpendicular to the field in K<sub>1</sub>. An analyzing Nicol N<sub>2</sub> crossed with respect to N<sub>1</sub>, resolved the light emerging from K<sub>2</sub>. Finally, the light from N<sub>2</sub> struck the 1P21 photomultiplier tube P of a Farrand Photometer. All of these elements were mounted on an optical bench, and all but the light source were enclosed in a light-tight box which was blackened inside.

In practice a little light was incident on the photomultiplier tube at all times even when the Nicols were crossed and no electrical fields applied. Actually, this was partly by design, since the sensitivity of detection of small changes in intensity in a polarimetric system is small at the condition of complete extinction.<sup>23</sup> By reaching balance between Kerr cells when some residual light entered the detector, a much greater sensitivity was achieved.

The electrical system, which was similar to that described by Scheraga,<sup>22</sup> produced high potential a.c. by means of two Thordarson type T-51916 115 to 10000 volt transformers, each of which was calibrated for different loads. A Sola constant voltage transformer in the primary circuit minimized the effects of fluctuations in the line voltage.

**Procedure for Measurements.**—One of the cells was filled with a standard substance and the other with the solution under investigation by means of a hypodermic syringe. When the two liquid samples were judged to be at thermal equilibrium, a predetermined a.c. voltage was applied to the primary circuit of the transformer of the standard cell. The deflection thus produced on the detector galvanometer was cancelled as quickly as practicable by applying in-phase a.c. to the primary circuit of the solution cell. From the observed values of the primary potentials the actual secondary voltages across the cells could be determined easily by reference to the transformer calibration curves. Though the step-up ratios were load-dependent, the measurements on the dilute benzene solutions were not affected since their resistance was high.

The estimated standard deviation of the reported relative Kerr constant is 3–4%.

## Results

In Table I are listed the pertinent physical properties of the compounds investigated. Except where otherwise indicated, the constants are for the samples prepared for this investigation. When available, comparison values obtained in other laboratories are given. The distillation range listed first for each substance has been corrected to 760 mm. pressure and was obtained using a calibrated thermometer. The disparity between values of the benzotrifluoride constants may indicate that the present sample contained impurities. Other measurements in this Laboratory, however, support the current results and they were used in all calculations.

It was shown by Kerr<sup>5</sup> that the phase difference  $D$  in radians produced in electrical double refraction is given by

(23) W. Heller in A. Weissberger, Ed., "Technique of Organic Chemistry," Part II, Vol. I, Interscience Publishers, Inc., New York, N. Y., 1949, p. 1523.

$$D = 2\pi BLE^2 \quad (1)$$

where  $B$ , the Kerr constant, is defined as

$$B = \frac{n_p - n_s}{n\lambda} \times \frac{1}{E^2} \quad (2)$$

In the equations  $l$  is the path length in the medium,  $E$  is the electrical field strength,  $n_p$  and  $n_s$  are the refractive indices of the medium parallel and per-

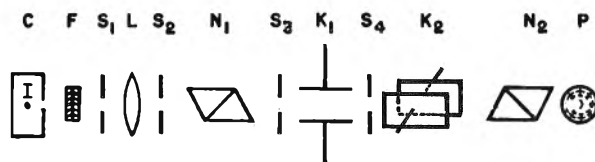


Fig. 3.—Optical system employed in determining Kerr constants by the relative method.

pendicular to the field,  $\lambda$  is the wave length of light in the medium and  $n$  the refractive index in the absence of a field. In the relative method of measurement the phase differences introduced by the Kerr cells at balance are equal. Equations 1 and 2 may be combined to yield

$$\frac{B'}{B} = k \left( \frac{V}{V'} \right)^2 \quad (3)$$

where the primed quantities refer to cell-2 and the unprimed ones to cell-1,  $V$  is the voltage across a cell,  $k$  is a geometrical constant reflecting the asymmetry of the system. Observations at several voltage ratios with benzene in both cells showed  $k$  to be 1.003 with a standard deviation of 0.0004.

Kerr effect measurements were made at  $30.4 \pm 0.5^\circ$ . In general, the mole fraction  $f_2$  of solute in the solutions measured was 0.015 or less, though some observations were made on solutions of chloro- and bromobenzene as high as  $f_2 = 0.05$  and 0.04, respectively. Observations on each solution were made at several different voltage ratios and averaged. The r.m.s. field strengths used ranged from 4000–20,000 volts/cm. The relative Kerr constants of the solutions calculated using eq. 3 are plotted as a function of the mole fraction of solute in Figs. 4 through 8.

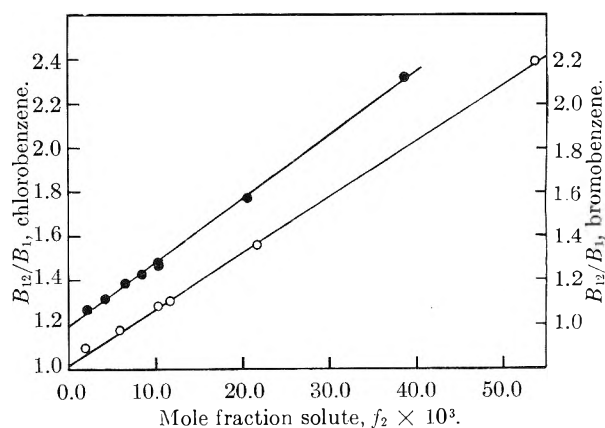


Fig. 4.—Relative Kerr constants of benzene solutions vs. the mole fraction of solute: O, C<sub>6</sub>H<sub>5</sub>Cl; ●, C<sub>6</sub>H<sub>5</sub>Br.

The values of  $B_{12}/B_{\phi H}$  were found to increase linearly with concentration in the dilute range investigated and to have an intercept equal to  $k$  within experimental error. For that reason the

TABLE I  
 PHYSICAL PROPERTIES OF THE COMPOUNDS STUDIED

Compound	Distilling range, °C. (cor. to 760 mm.)	$n_D^{20}$	$d_4^{20}$ , g./ml.	$\epsilon_{30}$
$C_6H_6$	80.12–80.14	1.4947		
	80.05–80.15 <sup>a</sup>	1.4949 <sup>a</sup>	0.8684 <sup>a</sup>	2.263 <sup>b</sup>
$C_6H_5F$	84.79–84.82	1.4604		5.24
	84.75–84.9 <sup>a</sup>	1.4610 <sup>a</sup>	1.0131 <sup>a</sup>	5.42 (25°) <sup>f</sup>
$C_6H_5Cl$	131.95–131.99	1.5190		5.53
	131.7–132.0 <sup>a</sup>	1.5192 <sup>a</sup>	1.0954 <sup>a</sup>	5.62 (25°) <sup>f</sup>
$C_6H_5Br$	156.25–156.30	1.5544		5.31
	156.16 <sup>a</sup>	1.5553 <sup>a</sup>	1.4815 <sup>a</sup>	5.32 <sup>a</sup>
$C_6H_5CF_3$	102.50–102.54	1.4097	1.174 <sup>c</sup>	9.14
	102.06 <sup>f</sup>	1.3999 <sup>f</sup>	1.1742 <sup>f</sup>	9.04 (25°) <sup>f</sup>
<i>o</i> -CF <sub>3</sub> C <sub>6</sub> H <sub>4</sub> F	115.70–115.76	1.4016	1.294	19.4
	114.5 (750 mm.) <sup>b</sup>	1.4040 (25°) <sup>b</sup>	1.293 (26°) <sup>b</sup>	
<i>o</i> -CF <sub>3</sub> C <sub>6</sub> H <sub>4</sub> Cl	152.70–152.74	1.4516	1.356	16.0
<i>o</i> -CF <sub>3</sub> C <sub>6</sub> H <sub>4</sub> Br	171.55–171.56	1.4785	1.651	14.2
	167.5–168 (745 mm.) <sup>b</sup>	1.4805 (25°) <sup>b</sup>	1.656 (25°) <sup>b</sup>	
<i>m</i> -CF <sub>3</sub> C <sub>6</sub> H <sub>4</sub> F	101.08–101.12	1.3965	1.274	7.22
	100.9 <sup>c</sup>	1.3980 (25°) <sup>c</sup>	1.289 (25°) <sup>c</sup>	
<i>m</i> -CF <sub>3</sub> C <sub>6</sub> H <sub>4</sub> Cl	137.92–137.96	1.4412	1.330	6.51
<i>m</i> -CF <sub>3</sub> C <sub>6</sub> H <sub>4</sub> Br	156.83–156.89	1.4683	1.616	6.78
	151–152 <sup>d</sup>	1.4749 (20°) <sup>d</sup>	1.606 <sup>d</sup>	
	154–156 <sup>e</sup>	1.4713 (25°) <sup>e</sup>	1.637 (25°) <sup>e</sup>	
<i>p</i> -CF <sub>3</sub> C <sub>6</sub> H <sub>4</sub> F	103.05–103.09	1.3965	1.285	3.23
	102.8 <sup>e</sup>	1.3996 (22°) <sup>e</sup>	1.293 (25°) <sup>e</sup>	
<i>p</i> -CF <sub>3</sub> C <sub>6</sub> H <sub>4</sub> Cl	138.91–138.97	1.4419	1.328	3.23
<i>p</i> -CF <sub>3</sub> C <sub>6</sub> H <sub>4</sub> Br	158.05–158.10	1.4681	1.614	3.50
	160.0–160.5 <sup>b</sup>	1.4710 (25°) <sup>b</sup>	1.614 (20°) <sup>b</sup>	

<sup>a</sup> J. Timmermans, "Physico-Chemical Constants of Pure Organic Compounds," Elsevier Pub. Co., Inc., New York, N. Y., 1950, pp. 281–295; value corrected to 30° where necessary. <sup>b</sup> Reference 12. <sup>c</sup> Reference 13. <sup>d</sup> Reference 14. <sup>e</sup> G. B. Bachman and L. L. Lewis, *J. Am. Chem. Soc.*, 69, 2022 (1947). <sup>f</sup> R. R. Driesbach, "Physical Properties of Chemical Substances," Dow Chem. Co., 1952. <sup>g</sup> Estimated from data of W. M. Heston, E. J. Hennelly and C. P. Smyth, *J. Am. Chem. Soc.*, 72, 2071 (1950).

 TABLE II  
 OBSERVED AND CALCULATED KERR CONSTANTS

Compound	Rel. Kerr const. $B/B_{C_6H_6}$ <sup>a</sup>	Abs. Kerr const. $B \times 10^7$	Molar Kerr constant, $mK \times 10^{12}$		
			Obsd.	Calcd <sup>b</sup>	Calcd. <sup>c</sup>
$C_6H_5F$	11.2	4.36	61.8	..	..
			56.8 <sub>20</sub> <sup>d</sup>		
$C_6H_5Cl$	26.6	10.3	142	..	..
			145 <sub>20</sub> <sup>d</sup>		
$C_6H_5Br$	29.8	11.6	160	..	..
			171 <sub>25</sub> <sup>d</sup>		
$C_6H_5CF_3$	40.5	15.8	206	..	..
<i>o</i> -CF <sub>3</sub> C <sub>6</sub> H <sub>4</sub> F	74.3	28.9	403	390	390
<i>o</i> -CF <sub>3</sub> C <sub>6</sub> H <sub>4</sub> Cl	83.6	32.5	448	570	505
<i>o</i> -CF <sub>3</sub> C <sub>6</sub> H <sub>4</sub> Br	84.9	33.0	460	605	500
<i>m</i> -CF <sub>3</sub> C <sub>6</sub> H <sub>4</sub> F	27.3	10.6	149	113	100
<i>m</i> -CF <sub>3</sub> C <sub>6</sub> H <sub>4</sub> Cl	16.0	6.22	91.5	58	96
<i>m</i> -CF <sub>3</sub> C <sub>6</sub> H <sub>4</sub> Br	15.1	5.87	94.3	47	93
<i>p</i> -CF <sub>3</sub> C <sub>6</sub> H <sub>4</sub> F	10.7	4.16	63.1	50	50
<i>p</i> -CF <sub>3</sub> C <sub>6</sub> H <sub>4</sub> Cl	16.7	6.50	93.0	80	83
<i>p</i> -CF <sub>3</sub> C <sub>6</sub> H <sub>4</sub> Br	19.4	7.54	106	89	93

<sup>a</sup> Each result is the mean of nine observations. <sup>b</sup> Calculated by Otterbein method, no corrections applied. <sup>c</sup> Calculated by the modified Otterbein method. <sup>d</sup> C. G. LeFevre and R. J. W. LeFevre, *J. Chem. Soc.*, 1577 (1954); their values were obtained in CCl<sub>4</sub> solution.

slopes were taken as identical with the limiting slopes and used to calculate the relative Kerr constant of the solute,  $B_2/B_{\phi H}$ . The actual mechanics

of doing so involved formulating a least-squares equation for each substance and solving it at  $f_2 = 1$ . Values of  $B_2$  were calculated using the absolute

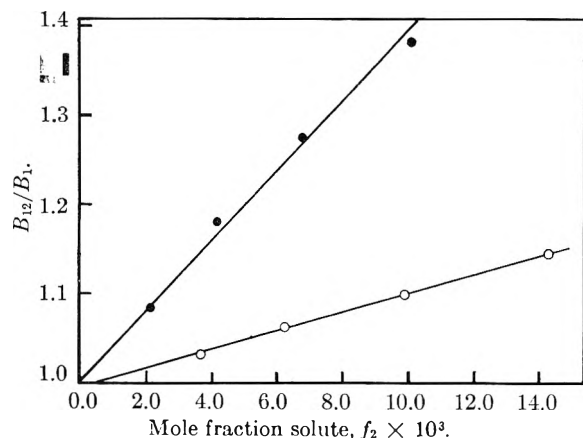


Fig. 5.—Relative Kerr constants of benzene solutions vs. the mole fraction of solute:  $\circ$ ,  $C_6H_5F$ ;  $\bullet$ ,  $C_6H_5CF_3$ .

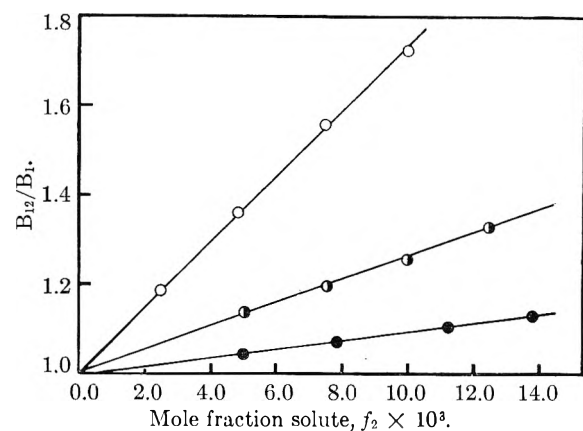


Fig. 6.—Relative Kerr constants of benzene solutions vs. the mole fraction of solute:  $\circ$ ,  $o-CF_3C_6H_4F$ ;  $\ominus$ ,  $m-CF_3C_6H_4F$ ;  $\bullet$ ,  $p-CF_3C_6H_4F$ .

value for benzene at  $20^\circ$  and  $546\text{ m}\mu$  of  $0.407 \times 10^{-7}$  given by Stuart.<sup>5</sup> Corrected to  $30^\circ$  and  $555\text{ m}\mu$ ,  $B_{\phi H}$  is  $0.389 \times 10^{-7}$ .

The results of these calculations are presented in Table II, together with values of the molar Kerr constant discussed below. Values of the molar Kerr constants of three halobenzenes obtained by LeFèvre and LeFèvre<sup>11</sup> from measurements in dilute solutions in  $CCl_4$  have been included for comparison. The agreement is quite satisfactory considering the difference in solvent. The authors know of no previous work on the Kerr constants of solutions of benzotrifluoride or its derivatives except for that of Kohn,<sup>24</sup> who investigated these compounds at higher concentrations using chlorobenzene as a standard.

#### Discussion

Otterbein<sup>7</sup> has defined the "molar Kerr constant,"  $mK_{12}$ , of a dilute solution as

$$mK_{12} = \frac{6n_{12}^2}{(n_{12} + 2)^2} \times \frac{1}{(\epsilon_1 + 2)^2} \times \frac{M_{12}^*}{d_{12}} \times K_{12} \quad (4)$$

where  $K_{12}$  is the Kerr constant of the solution,  $n_{12}$  its refractive index,  $d_{12}$  its density,  $M_{12}^*$  its "molecular weight," and  $\epsilon_1$  is the dielectric constant of the pure solvent. The refractive indices and densities for the solutions were obtained by the linear interpolation between the lowest values measured by

(24) E. M. Kohn, H. A. Strobel and P. M. Gross, to be published.

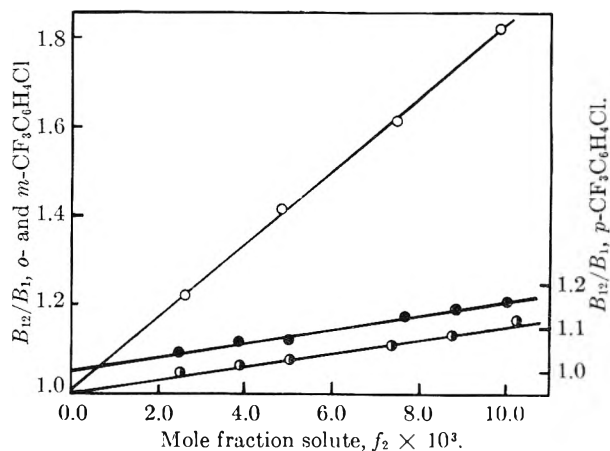


Fig. 7.—Relative Kerr constants of benzene solutions vs. the mole fraction of solute:  $\circ$ ,  $o-CF_3C_6H_4Cl$ ;  $\ominus$ ,  $m-CF_3C_6H_4Cl$ ;  $\bullet$ ,  $p-CF_3C_6H_4Cl$ .

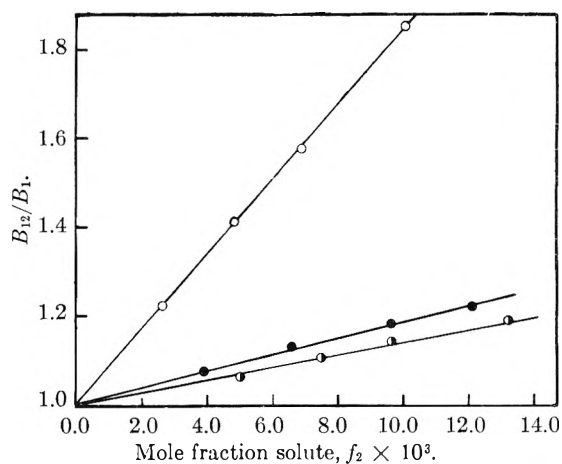


Fig. 8.—Relative Kerr constants of benzene solutions vs. the mole fraction of solute:  $\circ$ ,  $o-CF_3C_6H_4Br$ ;  $\ominus$ ,  $m-CF_3C_6H_4Br$ ;  $\bullet$ ,  $p-CF_3C_6H_4Br$ .

Kohn<sup>24</sup> and those for pure benzene. To find  $M_{12}$  the additive relation  $M_{12} = M_1f_1 + M_2f_2$  is used, and  $K_{12}$  is determined from the experimental  $B_2$  defined by eq. 2 using the relation<sup>3</sup>

$$K = B\lambda \quad (5)$$

where  $\lambda$  is again in the wave length of light in the medium.

More importantly, the molar Kerr constant is also expressible in terms of principal molecular polarizabilities  $b_1$ ,  $b_2$  and  $b_3$ , and dipole moments  $\mu_1$ ,  $\mu_2$  and  $\mu_3$  for the substance. Using Otterbein's definition the relation is

$$mK = J \{ (b_1 - b_2)^2 + (b_2 - b_3)^2 + (b_3 - b_1)^2 + \frac{1}{KT} [ (\mu_1^2 - \mu_2^2)(b_1 - b_2) + (\mu_2^2 - \mu_3^2)(b_2 - b_3) + (\mu_3^2 - \mu_1^2)(b_3 - b_1) ] \} \quad (6)$$

where  $J = (2\pi N_0/9) (1/45kT)$ ,  $k$  is the Boltzmann constant,  $T$  the absolute temperature,  $N_0$  Avogadro's number.

**Otterbein Calculation.**—Meyer and Otterbein<sup>25</sup> proposed a method for determining the molar constant of disubstituted benzene derivatives from measurements on the appropriate monosubstituted

(25) E. H. L. Meyer and G. Otterbein, *Physik. Z.*, **32**, 290 (1931).

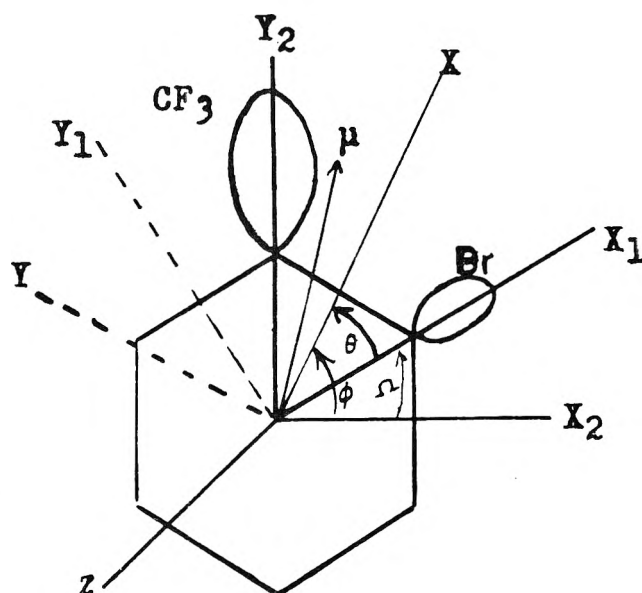


Fig. 9.—Sketch showing rotation of axes necessary to calculate polarizabilities and molar Kerr constants of disubstituted benzene by the Otterbein method.

compounds using the Silberstein<sup>26</sup> model of the atomic dipole as a basis. Later Otterbein<sup>5,27</sup> applied the technique to dichlorobenzenes.

The procedure involves estimating the changes in the principal polarizabilities of the benzene ring caused by the introduction of a substituent. The experimental quantities involved are refractions, molar Kerr constants and dipole moments. Once polarizability contributions of the substituents are known, they provide the basis for calculating, by a combination method, the molecular polarizabilities and the molar Kerr constants of disubstituted compounds.

A brief illustration of the Otterbein method as applied to *o*-bromobenzotrifluoride will suffice. In Fig. 9 there is a sketch of the *o*-bromo-BTF molecule showing some of the quantities of interest. The polarizability of each substituent is assumed to be an ellipsoid of rotation whose *Z*-axis is perpendicular to the plane of the benzene ring. As indicated in Fig. 9 axis-*X*<sub>1</sub> is along the benzene-bromine bond (in bromobenzene) and *X*<sub>2</sub> along the benzene-CF<sub>3</sub> bond (benzotrifluoride). To obtain the polarizabilities of the disubstituted compound along the as-yet-unknown principal axes *X*, *Y* and *Z* of its polarization ellipsoid, the contributions of the various groups as estimated from the results with the mono-substituted benzenes must be added. This can be accomplished by finding the components of these contributions along the new axes *X*, *Y*, *Z*. Mathematically, this amounts to a rotation of the two other sets of orthogonal axes about the common *Z*-axis. The appropriate angles  $\theta$  and  $\varphi$  may be calculated by formulating the potential energies of the various groups resulting from the interaction of the induced moments and the components of the applied field along *X*, *Y*, *Z*, and applying the condition that the cross terms in *XY* be

zero. The final potential energy expression has the form

$$-2U = AX^2 + BY^2 + CZ^2 \quad (7)$$

where *A*, *B* and *C* are the principal polarizabilities of the disubstituted molecule and *U* is the potential energy. The coefficients *A*, *B*, *C* are, of course, additive functions of the substituent and ring matrix polarizabilities.

The polarizabilities of a bonded substituent are calculated in each case as follows. For example, in bromobenzene the polarizabilities are taken to be  $b_1 = \alpha_1 + \beta_2$ ,  $b_2 = \alpha_1 + \alpha_2$ ,  $b_3 = \gamma_1 + \alpha_2$  where  $\alpha_1$  is the polarizability of benzene in the plane of the ring,  $\alpha_2$  is the transverse polarizability of bromine,  $\beta_2$  the polarizability along its bond with carbon and  $\gamma_1$  the polarizability of benzene perpendicular to its ring. All of these can be estimated approximately from the molar refraction and Kerr data for benzene and bromobenzene.

The necessary molar refraction data for the monosubstituted benzenes were calculated from the refractive indices at infinite wave length. These in turn were obtained by extrapolating as a function of the square of the frequency. The dispersion curve of benzotrifluoride was unknown, however, and was assumed similar to that of fluorobenzene.<sup>28</sup> Dipole moment data for the disubstituted compounds were either not available in the literature, or the reported values were in disagreement. For that reason the moments were approximated by vector addition. The moments for the monosubstituted analogs were used and central angles of 60 and 120° were assumed for *ortho* and *meta* compounds, respectively. It should be noted that even though the molar Kerr constant is quite sensitive to the magnitude of the dipole moment, the ratio of the values calculated by the Otterbein and the aggregate method discussed below is about the same even if a moment is altered by 0.1 debye.

It must also be noted that the Otterbein additivity method includes no direct provision for interaction between substituents on a benzene ring. Consequently, it is not surprising in the case of the *o*-halobenzotrifluorides that the values of *mK* calculated by this method do not agree well with the observed values. For the *meta* compounds the deviation between observed and calculated results also seems larger than would be expected unless there is interaction between the substituent groups.

In general the fluorobenzotrifluorides show the smallest deviations between theory and experiment, probably because the small size and polarizability of the fluorine atom limits its interaction with the CF<sub>3</sub> cluster. The bromo derivatives with their large and highly polarizable bromine atoms show the largest deviations.

**Interaction between Substituents.**—If the deviations between the measured molar Kerr constants and the values calculated by Otterbein's method are due to interactions, either directly or indirectly, the calculations may be modified to take these interactions partially into account.

(26) L. Silberstein, *Phil. Mag.*, [6] **33**, 92, 215, 521 (1917).

(27) G. Otterbein, *Physik. Z.*, **34**, 645 (1933).

(28) "International Critical Tables," McGraw-Hill Book Co., New York, N. Y., 1930.

Otterbein effectively made an allowance for interaction in *o*-dichlorobenzene by assuming a central angle of  $83.4^\circ$  between the two substituents rather than  $60^\circ$ . To support the assumption he cited the fact that the actual dipole moment of the substance is smaller than that expected from vector addition of the two group moments.

Another approach is afforded by applying the Silberstein treatment to the substituent groups.<sup>26</sup> Silberstein's theory was originally developed for a simple model of a rigid molecule. Silberstein assumed that the dipole induced in an atom by an external electric field induces secondary dipoles in neighboring atoms. The result is a strengthening or a weakening of such original moment depending on the direction of polarization. Though the approach usually has been restricted to bonded atoms, it should be applicable, at least as a correction factor, to non-bonded neighbors whose relative positions are more or less fixed.

**Aggregate Method.**—Accordingly, the Silberstein model has been used to allow for the mutual effects of substituents in the disubstituted benzene compounds. The procedure differs from that of Otterbein in the intermediate step; here principal polarizabilities are obtained for the two substituents as a unit or aggregate rather than separately. These are then added in straightforward fashion to the polarizabilities of the benzene ring. The term "aggregate" will be used to identify this method.

Several assumptions have been made in applying the Silberstein treatment. First, polarizability values have been assigned to the substituent groups on the ring as in the Otterbein method, by calculating the differences in corresponding directions between the polarizabilities of the monosubstituted benzenes and the polarizabilities of benzene. This procedure is related to the method used by Denbigh<sup>29</sup> to obtain bond polarizabilities and assumes additivity. Therefore, since interactions with the benzene ring have, to a first approximation, been considered in the foregoing procedure, the presence of the ring has been ignored from this point on in calculating the polarizabilities of the "aggregate" formed by the substituents in the di-derivatives. Second, these groups have been treated as though their radii were much smaller than the intergroup distance, although this is not the case for the *o*-substituents. Third, the  $\text{CF}_3$  group has been treated as a single atom, with the carbon atom as its center. Finally, for simplicity the principal polarizabilities of the molecule have been assumed to lie along and perpendicular to the direction of the line joining the centers of the substituents. This is believed to be a fairly close approximation to the polarizability ellipsoid of the molecule.

To illustrate the modified method of calculation of molar Kerr constants, the procedure will be considered in some detail for *o*-bromobenzotrifluoride. A drawing showing the pertinent molecular parameters is given in Fig. 10. From the law of cosines, the center-to-center distance  $r$  between the  $\text{CF}_3$  and Br groups is found to be  $3.13 \text{ \AA}$ . Since these substituents are not spherically symmetrical, the polarizabilities of each group, parallel and per-

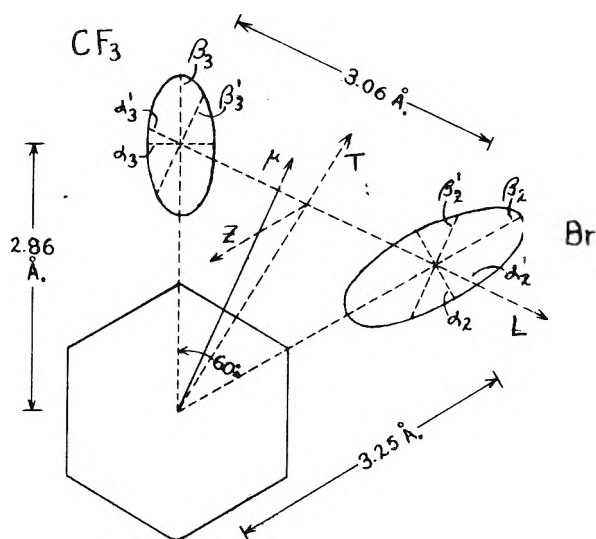


Fig. 10.—Sketch showing quantities involved in calculation of polarizabilities and molar Kerr constants of disubstituted benzenes by the modified Otterbein or aggregate method.

pendicular to the line joining their centers, must be estimated. This may be done for each substituent once the polarizabilities of the substituents parallel and perpendicular to the ring-substituent bond have been determined. The previously-mentioned polarizabilities,  $\alpha_2$ ,  $\beta_2$ , etc., become  $\alpha_2^1$ ,  $\beta_2^1$ , etc. For the  $\text{CF}_3$  group  $\alpha_3$  is the polarizability along the C- $\text{CF}_3$  bond,  $\beta_3$  that transverse to the bond in any direction. The polarizabilities of the substituents as an aggregate are<sup>27</sup>

$$a_L = [\alpha_2^1 + \alpha_3^1 + 4\alpha_2^1\alpha_3^1r^{-3}]/[1 - 4\alpha_2^1\alpha_3^1r^{-6}]$$

along the line joining the group centers

$$a_T = [\beta_2^1 + \beta_3^1 - 2\beta_2^1\beta_3^1r^{-3}]/[1 - \beta_2^1\beta_3^1r^{-6}] \quad (8)$$

perpendicular to  $a_L$  but in the plane of the benzene ring, and

$$a_Z = [\alpha_2^1 + \alpha_3^1 - 2\alpha_2^1\alpha_3^1r^{-3}]/[1 - \alpha_2^1\alpha_3^1r^{-6}]$$

perpendicular to both  $a_L$  and  $a_T$ . For *o*-bromobenzotrifluoride,  $a_L = 53.0 \times 10^{-25}$ ,  $a_T = 58.8 \times 10^{-25}$ , and  $a_Z = 29.8 \times 10^{-25}$ .

The principal polarizabilities of the benzene ring,  $\alpha_1$ ,  $\alpha_1$ ,  $\gamma_1$ , may be considered as being in the same directions as  $a_L$ ,  $a_T$  and  $a_Z$  without loss of generality. As determined by the method outlined above,  $\alpha_1 = 111.4 \times 10^{-25}$  and  $\gamma_1 = 76.9 \times 10^{-25}$ . The polarizabilities of the disubstituted molecule are given by  $b_1 = \alpha_1 + a_T$ ,  $b_2 = \alpha_1 + a_L$ , and  $b_3 = \gamma_1 + a_Z$ , or  $b_1 = 170.2 \times 10^{-25}$ ,  $b_2 = 164.4 \times 10^{-25}$ ,  $b_3 = 106.6 \times 10^{-25}$ . These quantities, together with the value of the dipole moment obtained by vector addition of the group moments,  $3.62D$  are substituted in eq. 6 to give the value of  $mK$ ,  $502 \times 10^{-12}$  e.s.u. The molar Kerr constants calculated in this way are shown in Table II.

When calculated by Otterbein's method the molar Kerr constants of the chloro- and bromobenzotrifluorides deviate an average of 30% from the experimental values. The values calculated by the aggregate method for these six compounds deviate on the average less than 10% from the measured ones, which appears to be a significant improvement.

(29) K. G. Denbigh, *Trans. Faraday Soc.*, **36**, 936 (1940).

Corrected  $mK$ 's are reported for the fluorobenzotrifluorides for the sake of completeness, though they are believed less reliable. As with the other substituents, the polarizability of a fluorine on a benzene ring was obtained by difference, which led to a negative value for the transverse polarizabilities  $b_2$  and  $b_3$  of  $-3.05 \times 10^{-25}$  since  $R_{\phi H} > R_{\phi F}$ . In some cases the use of these values leads to the contradictory result that the aggregate polarizability along the line joining the centers of the substituents is depressed while the transverse polarizability is enhanced. From Table II it is apparent that the modified calculation leads to substantially the same results as does the Otterbein treatment.

It is of interest to apply the aggregate method to Otterbein's own data<sup>7</sup> for *o*- and *m*-dichlorobenzene in carbon tetrachloride. Using his values for chlorobenzene and benzene this procedure gives molar Kerr constant values of  $284 \times 10^{-12}$  and  $51 \times 10^{-12}$  for the *ortho* and *meta* compounds, respectively. These figures are to be compared with

his calculated results<sup>30</sup> of  $240 \times 10^{-12}$  and  $50 \times 10^{-12}$  and the experimental data of  $234 \times 10^{-12}$  and  $64 \times 10^{-12}$ . The agreement of the aggregate method values with experiment might have been better if  $R_{\infty}$  were used instead of Otterbein's listed  $R_{546} m\mu$ . Though it would be of interest to do so, the present data for  $C_6H_5Cl$  were not used in these calculations since Otterbein has shown that the magnitude of  $mK$  is very much influenced by the choice of solvent. Also, the requisite experimental data for comparison are not available for very dilute benzene solutions of dihalogenated benzenes.

**Polarizabilities.**—The calculated principal molecular polarizabilities of the compounds used in this work are listed in Table III. The values obtained by LeFèvre and LeFèvre<sup>11</sup> for certain of the substances are given for comparison. Their results differ about 3% from the presently reported values which, considering the precision of both sets of measurement, is reasonable agreement. For the disubstituted chloro- and bromobenzotrifluorides values are given for both the Otterbein calculation and the aggregate method calculation. Estimates of the polarizabilities of *p*-dichlorobenzene and *p*-dibromobenzene based on this investigation are also included and compared with those of LeFèvre and LeFèvre.

A direct check on the internal consistency of these polarizabilities and indirectly on the Otterbein and aggregate method calculations can be made: the average polarizability,  $\alpha$ , of each of the disubstituted compounds may be compared with that obtained from the molar refraction  $R_{\infty}$ . To find the average polarizability, the  $R_{\infty}$  values listed in Table III must be multiplied by  $0.03964 \times 10^{-23}$ . For the *m*- and *p*-compounds, the average polarizabilities calculated by the aggregate method were found to be in slightly better agreement with the  $\alpha$ 's determined from  $R_{\infty}$  than those found by the Otterbein procedure. The two methods of calculation yielded almost identical polarizabilities for the *o*-compounds. In all cases the disagreement is at most two units in the third significant figure. Of itself, this agreement does not establish the validity of the aggregate method. Two reasons should be noted. First, the average polarizability is not an especially sensitive indicator of changes in the individual principal polarizabilities. Second, the reliability of the  $R_{\infty}$  data, which were estimated from extrapolated values of  $n_D$ , remains to be confirmed by experiment. If there had been a serious disagreement between values of  $\alpha$  from  $R_{\infty}$  and those from the Otterbein or aggregate calculations, however, these methods of calculating  $mK$  would have appeared quite questionable.

**Acknowledgment.**—The authors are grateful to Dr. E. M. Kohn, formerly of this Laboratory, for preparing four of the compounds used in this research and for making many of the measurements of the physical constants of the solutions.

Compound	$b_1 \times 10^{23}$	$b_2 \times 10^{23}$	$b_3 \times 10^{23}$	$R_{\infty}$ (est), cc.
$C_6H_6$	1.11 <sub>4</sub>	1.11 <sub>4</sub>	0.76 <sub>8</sub>	25.1 <sub>0</sub>
	1.11 <sub>4</sub> <sup>b</sup>	1.11 <sub>4</sub> <sup>b</sup>	.73 <sub>8</sub> <sup>b</sup>	25.0 <sub>5</sub> <sup>b</sup>
$C_6H_5F$	1.14 <sub>2</sub>	1.08 <sub>4</sub>	.73 <sub>8</sub>	24.9 <sub>3</sub>
	1.12 <sub>5</sub> <sup>b</sup>	1.10 <sub>5</sub> <sup>b</sup>	.71 <sub>1</sub> <sup>b</sup>	24.9 <sup>b</sup>
$C_6H_5Cl$	1.50 <sub>6</sub>	1.20 <sub>0</sub>	.85 <sub>4</sub>	29.9 <sub>5</sub>
	1.47 <sub>2</sub> <sup>b</sup>	1.24 <sub>4</sub> <sup>b</sup>	.81 <sub>8</sub> <sup>b</sup>	29.9 <sup>b</sup>
$C_6H_5Br$	1.65 <sub>1</sub>	1.28 <sub>7</sub>	.94 <sub>1</sub>	32.6 <sub>1</sub>
	1.68 <sub>4</sub> <sup>b</sup>	1.21 <sub>3</sub> <sup>b</sup>	.95 <sub>6</sub> <sup>c</sup>	32.6 <sup>b</sup>
$C_6H_5CF_3$	1.36 <sub>5</sub>	1.25 <sub>5</sub>	.90 <sub>9</sub>	29.6 <sub>8</sub>
<i>o</i> - $CF_3C_6H_4F$	1.35 <sub>7</sub>	1.26 <sub>1</sub>	.87 <sub>8</sub>	29.7 <sub>2</sub>
<i>o</i> - $CF_3C_6H_4Cl$	1.68 <sub>3</sub>	1.41 <sub>5</sub>	.99 <sub>5</sub>	34.6 <sub>3</sub>
	1.59 <sub>8</sub> <sup>c</sup>	1.50 <sub>8</sub> <sup>c</sup>	.98 <sup>c</sup>	
<i>o</i> - $CF_3C_6H_4Br$	1.82 <sub>7</sub>	1.50 <sub>4</sub>	1.08 <sub>2</sub>	37.2 <sub>3</sub>
	1.70 <sub>5</sub> <sup>c</sup>	1.64 <sub>4</sub> <sup>c</sup>	1.06 <sub>8</sub> <sup>c</sup>	
<i>m</i> - $CF_3C_6H_4F$	1.35 <sub>7</sub>	1.26 <sub>1</sub>	0.87 <sub>8</sub>	29.8 <sub>6</sub>
<i>m</i> - $CF_3C_6H_4Cl$	1.68 <sub>2</sub>	1.41 <sub>5</sub>	.99 <sub>5</sub>	34.6 <sub>3</sub>
	1.67 <sub>8</sub> <sup>c</sup>	1.43 <sub>6</sub> <sup>c</sup>	.99 <sub>5</sub> <sup>c</sup>	
<i>m</i> - $CF_3C_6H_4Br$	1.82 <sub>4</sub>	1.50 <sub>3</sub>	1.08 <sub>2</sub>	37.3 <sub>6</sub>
	1.81 <sub>7</sub> <sup>c</sup>	1.53 <sub>4</sub> <sup>c</sup>	1.07 <sub>8</sub> <sup>c</sup>	
<i>p</i> - $CF_3C_6H_4F$	1.39 <sub>3</sub>	1.22 <sub>4</sub>	0.87 <sub>8</sub>	29.6 <sub>1</sub>
<i>p</i> - $CF_3C_6H_4Cl$	1.75 <sub>7</sub>	1.34 <sub>1</sub>	.99 <sub>5</sub>	34.7 <sub>3</sub>
	1.77 <sub>8</sub> <sup>c</sup>	1.33 <sub>9</sub> <sup>c</sup>	.99 <sub>5</sub> <sup>c</sup>	
<i>p</i> - $CF_3C_6H_4Br$	1.90 <sub>2</sub>	1.42 <sub>8</sub>	1.08 <sub>2</sub>	37.3 <sub>8</sub>
	1.92 <sub>5</sub> <sup>c</sup>	1.42 <sub>8</sub> <sup>c</sup>	1.08 <sub>0</sub> <sup>c</sup>	
<i>p</i> - $C_6H_4Cl_2$	1.92 <sub>5</sub> <sup>b</sup>	1.27 <sub>0</sub> <sup>b</sup>	0.90 <sub>3</sub> <sup>b</sup>	34.7 <sup>b</sup>
	1.89 <sub>9</sub>	1.28 <sub>7</sub>	.94 <sub>1</sub>	
	1.92 <sub>5</sub> <sup>c</sup>	1.27 <sub>3</sub> <sup>c</sup>	.92 <sub>7</sub> <sup>c</sup>	
<i>p</i> - $C_6H_4Br_2$	2.18 <sub>8</sub> <sup>b</sup>	1.37 <sub>5</sub> <sup>b</sup>	1.17 <sub>9</sub> <sup>b</sup>	40.1 <sup>b</sup>
	2.18 <sub>8</sub>	1.46 <sub>0</sub>	1.11 <sub>4</sub>	
	2.22 <sub>0</sub> <sup>c</sup>	1.43 <sub>9</sub> <sup>c</sup>	1.09 <sub>3</sub> <sup>c</sup>	

<sup>a</sup> Calculated by Otterbein method, unless otherwise noted. <sup>b</sup> Values given by C. G. LeFèvre and R. J. W. LeFèvre, *J. Chem. Soc.*, 1577 (1954). <sup>c</sup> Calculated by aggregate method.

(30) Otterbein's values were calculated for central angles between substituents of 83.4 and 123°, respectively. If one uses 60 and 120° for the *o*- and *m*-compounds, he obtains  $325 \times 10^{-12}$  and  $59 \times 10^{-12}$ .

# HYDROTHERMAL REACTIONS BETWEEN CALCIUM HYDROXIDE AND AMORPHOUS SILICA; THE REACTIONS BETWEEN 180 AND 220°

BY GUNNAR O. ASSARSSON

*Chemical Laboratory of the Geological Survey, Stockholm 50, Sweden*

*Received October 23, 1956*

The reaction between calcium hydroxide and amorphous silica was studied within the temperature range 180–220°. Three stages of the reaction are distinguished. The first one is the rapid combination of the calcium hydroxide with the reactive silica, forming the poorly crystallized low temperature phase B, which has no definitive proportion lime:silica, as has been described earlier. The second reaction stage is a recrystallization of the phase B forming distinct compounds; lower content of lime, 0–1 mole CaO per mole silica, yields a compound, hitherto unknown as a mineral and designated Z in this paper; the content of 0.67–2.0 mole CaO per mole silica yields the tobermorite-like compound; with a lime content of 1–2 mole CaO per mole silica, uncombined lime represents an unstable phase. The third reaction stage leads to the final formation of phases in equilibrium; they are the compounds resembling gyrolite, xonotlite and hillebrandite. The existence ranges of the unstable as well as the stable compounds overlap each other according to the phase rule. With a lime content >2 mole per mole silica, uncombined lime is the compound existing besides the hillebrandite compound; no phase richer in lime than the dicalcium silicate was detected within the temperature range examined.

In some earlier papers<sup>1</sup> the present author has given the results of the hydrothermal reactions between amorphous silica and calcium hydroxide within the range of 120–220° and 0–24 hr. Two types of products were to be distinguished. A low temperature phase which is poorly crystallized and which obviously consists of more than one compound is formed below 180° and during short periods of time; its X-ray pattern, however, is very indistinct; it has been considered to correspond to the mineral tobermorite.<sup>2</sup> The high temperature phases are well crystallized and rather easy to distinguish. The subsequent work with the problems showed that special reactions take place under certain conditions. It was also found that the reactions between calcium hydroxide and quartz or some silicates could be elucidated by the reactions calcium hydroxide–amorphous silica, these reactions being of importance in the solution of mineralogical and theoretical as well as of practical problems. It seems therefore to be necessary to study the reactions at special temperatures more in detail. For this purpose the temperature range immediately above the transition boundary low temperature–high temperature phase at 180°, 24 hr. is considered to be the best basis for a further investigation, as the results of the earlier particularized investigations can be employed. The present investigation therefore involves the formation of the phases in saturated steam at the temperature 220°, and the molar ratio calcium oxide:amorphous silica in the reaction mixtures was changed gradually.

## Experimental

The autoclave and the materials used for the mixtures calcium oxide–amorphous silica were the same as those earlier described; the amorphous silica was the pure silica gel slightly desiccated on the steam-bath (80°).

By the use of some new X-ray cameras of good resolving power it was possible to distinguish the diffraction lines more accurately than in the earlier investigation. The smallest Bragg angle which could be measured with reasonable accuracy using the improved instruments corresponds to a  $d$ -value of about 35 Å.

(1) G. O. Assarsson, *et al.*, *THIS JOURNAL*, **60**, 397 (1956); **60**, 1559 (1956).

(2) G. F. Claringbull and M. H. Hey, *Min. Mag.*, **29**, 960 (1952); J. D. C. McConnell, *ibid.*, **30**, 293 (1954); H. Megaw, *Nature*, **177**, 390 (1956).

## Results and Discussion

**The Identification of the Phases.**—As some new results concerning the X-ray diffraction of the compounds have been available in the literature it may be expedient to give a short summary of the possibility of identifying the phases in mixtures which are formed during the hydrothermal reactions. For the present there are six calcium silicate hydrates which occur in the autoclave products at 220°: namely, the low temperature phase B, the compounds resembling gyrolite, tobermorite, xonotlite, hillebrandite and finally a new phase which will be designated phase Z in this paper, in the absence of a better name. In connection with the X-ray identification of the phases it must be remarked that objections could be raised against some older measurements. The imperfection of the X-ray cameras was mentioned above, but also the purity of some mineral specimens, used as comparison material, may be questioned. Some of these minerals seem to have been very difficult to obtain in a pure state.

Minute crystallites with low degree of repeating patterns could generally be a consequence of the rather short periods of reaction time which have been one of the principal conditions in the present investigation. In most cases, however, the measurements of the X-ray photographs are easily performed upon the substances produced after a reaction period of 24 hr. at 220°, showing a sufficient growth of the crystallites, even if it is impossible to investigate the products microscopically.

The X-ray powder data most suitable for the identification of the phases are listed in Table I. New measurements of the spacings have given rise to a short discussion of some of the phases below.

**Phase Z.**—A re-examination of the reaction products poor in lime showed that there must occur an unknown new-formed phase. The examination reported below shows an existence range which is very limited with regard to both the molar ratio lime:silica and the reaction temperature and time. The phase Z can only exist during a relatively short period of time and as a consequence of this there is not sufficient time to ensure its being well crystallized. The only characteristic spacing which has been discerned hitherto in the X-ray photographs is a line 15.3 Å. which has a very strong intensity



Skye mineral is not within the scope of this investigation.

**Xonotlite.**—In the present investigation the X-ray photograph of a specimen of xonotlite from Xonotla, Mexico, has been used at the comparison of the synthetic compounds.

As far as known to the author X-ray powder data of an analytically and microscopically controlled specimen of the mineral have not been published<sup>5</sup>; some notes will therefore be made in connection with this investigation. The mineral is a white, tough, fibrous material. The analysis (Table III) shows a monocalcium silicate which contains a small amount of Mn, Fe and Mg replacing Ca in the pattern; the content of water is somewhat lower than the ideal formula 3:3:1 shows. The X-ray powder data of a preparation synthesized by autoclaving a mixture lime-silica = 1:1 at 220° for 144 hr. are given in Table IV together with the powder data of the mineral. The cell dimensions of the mineral are calculated to be  $a = 16.90$ ,  $b = 7.32$ ,  $c = 7.03$  Å. The analysis of the synthetic preparation showed the composition  $\text{CaO}:\text{SiO}_2:\text{H}_2\text{O} = 1:1:0.34$ . The synthetic compound has one line (11.1 Å., w) showing the presence of a small residual amount of the tobermorite compound which had not been transformed into the xonotlite compound in spite of the extended time of autoclaving; in other respects the agreement between the two series of measurements is excellent (see also Fig. 2).

TABLE III

CHEMICAL ANALYSIS OF XONOTLITE, TETELE DI XONOTLA, MEXICO

(Mus. of Nat. Hist. of Sweden, Min. Dep. No. g. 20272)  
Anal. A. Aaremae

	Molar ratio		
$\text{SiO}_2$	48.55	0.809	
$\text{Al}_2\text{O}_3$	0.30	...	
$\text{FeO}$	0.51	.007	
$\text{MnO}$	1.00	.014	Calcd. for (Ca, Mg, Fe,
$\text{CaO}$	45.17	.806	Mn)O: $\text{SiO}_2:\text{H}_2\text{O} =$
$\text{MgO}$	0.28	.007	1.02:1:0.24
$\text{K}_2\text{O}, \text{Na}_2\text{O}$	0.10	...	( $\text{CaCO}_3 = 0.73\%$ )
$\text{H}_2\text{O}$	3.57	.198	
$\text{CO}_2$	0.32	.007	
	99.80		

**The Existence Range of the Phase Z.**—To the phase Z must be ascribed a certain importance from the mineralogical point of view and the conditions of its formation have therefore been studied more thoroughly in the present investigation. A survey of its existence range is given in Table V. It is clear from the experiments cited in the table that the phase Z is formed only in mixture low in lime ( $\text{CaO}:\text{SiO}_2 = <1:1$ ). At lower temperature (160°) it is not formed within a reasonable period of time (24 hr.). When synthesized at 180° its formation can first be discerned after about 24 hr. by the diffraction line 15.3 Å., and extended autoclave treatment of the mixture (48 hr.) results in

(5) W. Jander and B. Franke, *Z. anorg. Chem.*, **247**, 161 (1941); E. Thilo, H. Funk and E. M. Wichmann, *Abh. Akad. Wissensch. zu Berlin, Jahrg.*, 1950 nr 4 (1951); H. F. W. Taylor, *Min. Mag.*, **30**, 338 (1954); concerning the cell dimensions: Ch. S. Mamedov and N. W. Belov, *Doklady Akad. Nauk S.S.S.R.*, **104**, 615 (1955).

TABLE IV

X-RAY POWDER DATA FOR THE SYNTHETIC PREPARATION  
 $\text{CaO}:\text{SiO}_2 = 1:1$ , 220°, 144 hr. and Xonotlite (Table III)

Synth. prep. Int.	d	Xonotlite Int.	d	Synth. prep. Int.	d	Xonotlite Int.	d
(w)	(11.1)			ww	2.427	ww	2.415
ww	8.44	ww	8.50	w	2.340	w	2.330
s	7.03	s	6.98	w	2.246	m	2.246
ww	6.29	ww	6.27	w, d	2.189	ww, d	2.188
s	4.23	s	4.24			ww, d	2.122
		ww, d	3.98	s	2.037	s	2.032
		ww, d	3.86	s	1.949	s	1.943
s	3.638	s	3.634	m	1.833	m	1.832
		ww, d	3.484	w	1.770	w	1.765
		ww, d	3.395	ww	1.753		
s	3.230	s	3.230	m	1.708	m	1.707
ss	3.076	sss	3.076	ww	1.642	w	1.643
ww	3.018	ww, d	2.986	ww	1.588	ww	1.593
		ww, d	2.915	ww	1.571	ww	1.575
s	2.817	s	2.820			ww	1.543
s	2.696	s-m	2.696	w	1.518	m	1.517
ww	2.626	w	2.623			w	1.433
		ww	2.583			w	1.395
m	2.497	m	2.500				

the formation of crystals of better growth. The autoclave products at 200° show its characteristic line with strong intensity after 12 and after 24 hr., but at higher temperatures (220 and 240°) autoclave treatment produces the phase during short

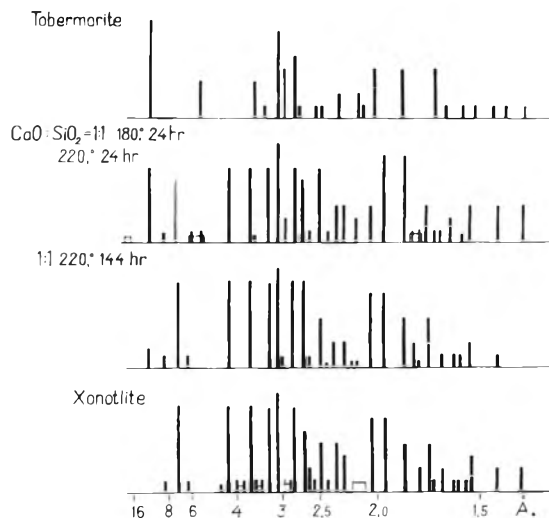


Fig. 2.—X-Ray powder data of some autoclaved preparations of the molar proportion lime:silica = 1:1 compared with the powder data of tobermorite (Claringbull and Hey<sup>2</sup>) and of xonotlite from Tetele di Xonotla (Table IV).

periods of time only, while autoclaving for longer periods causes a recrystallization of the crystals previously formed. The compounds which co-exist with the phase Z are the low temperature (180°) phase B during the first period of its formation, while later the compound resembling gyrolite appears, obviously to the same degree that the phase Z disappears, slowly at 180° but rapidly at 220–240°. The only distinct spacing of the phase Z, 15.3 Å., seems to represent a basal reflection. Other reflections which could be identified are missing; the plausible conclusion might be drawn, that the phase Z is present as very thin plates, the growth of

TABLE V

## OCCURRENCE OF THE PHASE Z IN AUTOCLAVED PRODUCTS CALCIUM HYDROXIDE-AMORPHOUS SILICA

The diffraction lines 22, 11.1 (the gyrolite-like compound) and 15.3 Å. (phase Z) in X-ray photographs; the line 11.1 Å. occurring alone indicates the tobermorite-like phase.<sup>a</sup> Symbols of the phases: B = low temperature phase; Z = phase of unknown composition; G, T, X = compounds resembling the minerals gyrolite (G), tobermorite (T), xonotlite (X).

Temp., °C.	Autoclave		Molar ratio of the mixtures CaO:SiO <sub>2</sub>						Phase
	Time, hr.	22 Å.	15.3 Å.	0.67:1 11.1 Å.	22 Å.	15.3 Å.	1:1 11.1 Å.		
160	2-24	0	0	0	B	0	0	0	B
180	2-16	0	0	0	B	0	0	0	B
	24	0	w	0	B,Z	0	0	0	B
	48	0	m	0	B,Z	ww	0	s	T,X(BG)
200	2	0	0	0	B	0	0	ww	B(T)
	12	ww	s	ww	Z,B(G)	0	0	m	X,T(B)
	24	ss	s	s	Z,G,B	ww, d	0	s	X,T(G)
220	3	0	m	0	Z,B	0	0	m	X,T,B
	12	ss	ww	s	G,B(Z)	0	0	m	X,T(BG)
	24	ss	0	s	G(B)	0	0	m	X,T
240	2	0	m	0	Z,B	...	..	..	
	24	ss	0	s	G	...	..	..	

<sup>a</sup> Intensities: ss = very strong; s = strong; m = medium strong; w = weak; ww = very weak; 0 = not discernible.

which proceeds during continued autoclaving chiefly in the direction perpendicular to the *c*-axis. Characteristic for the two phases gyrolite and Z is therefore that they are both of a lamellar habit.

Other minerals described recently by Gard and Taylor,<sup>6</sup> okenite and nekoite, could possibly occur in the autoclaved mixtures poor in lime, but their characteristic reflections have not been discerned in the photographs.

The new compound Z belongs to the high temperature phases and a lowering of the vapor pressure influences its crystallization in the same way as was described earlier concerning the other high temperature phases.<sup>1</sup>

The crystallization of the phases poor in lime shows that the low temperature phase B contains compounds which are not in equilibrium when the temperature is raised to about 180° or higher. The formation of the phase Z may therefore be regarded as a transformation of a certain part of the phase B or of a certain saturation stage of the amorphous silica resulting in crystals with gradually growing patterns which are sufficiently repeated to be observed by means of the diffraction 15.3 Å. of strong intensity. As the phase Z is a transition phase and not in equilibrium it recrystallizes rather rapidly into the gyrolite-like compound on an extended autoclave treatment.

The phase Z has not yet been prepared in anything like pure state; its real composition has not been established by analysis and is therefore unknown. As it seems to be formed from mixtures poor in lime and is obviously transformed into the gyrolite-compound, it is most probable that it contains lime and silica in the same proportion as does this compound. The phase B disappears to the same degree that the gyrolite-like compound crystallizes and it is probable that this transformation always occurs through the intermediate Z-phase, the transformation of which could therefore establish the composition.

**The Phases Formed at 220°, 24 hr.**—The systematic variation of the lime ratio was brought about in order to find the connection between this

variation, the phases formed successively, and the approximate minimum content of the phases which could be discerned in the X-ray photographs. In the more detailed discussion which follows, the series will be divided into several ranges, according to their characteristic compounds.

**The Gyrolite Range.**—The compound resembling gyrolite can be discerned easily with the aid of the spacing 22 Å. in the mixture with a lime:silica ratio down to about 0.35:1, probably also to a much lower lime content (Fig. 3). In mixtures richer in lime up to about 0.80:1 the characteristic line is very distinct but at the ratio 0.90:1 it has become a band of a very weak intensity. The photograph of the preparation of the lime ratio 1:1 shows a very, very weak rather broad band at the position 22 Å., but in a special preparation of this mixture at 220° for 144 hr. every trace of the band at 22 Å. has disappeared (Fig. 2). Photographs of mixtures somewhat richer in lime than 1:1 seem to contain only very weak shadows of the line in question. The two reflections 3.16 and 3.10 Å. change their intensities in the same way and could also be suitable for an identification, but one of them, 3.10 Å., belongs also to the compounds richer in lime and the occurrence of the line 3.16 Å. is therefore not decisive without a camera of very good dispersion.

The gyrolite range covers the molar ratio calcium oxide:silica = 0:1 up to 1:1 according to the X-ray photographs. The mineral gyrolite contains lime-silica-water in the proportion 2:3:2. The mixtures poorer in lime than 2:3 must therefore contain an excess of silica which is not combined with lime. In order to examine whether the gyrolite-like compound could be a stable phase or possibly be transformed into other substances, some samples (molar ratio lime:silica = 0.35:1 and 0.67:1) were autoclaved at 220° for 144 hr. An analysis of the product from the latter showed the composition CaO:SiO<sub>2</sub>:H<sub>2</sub>O = 0.67:1:0.67 which exactly corresponds to that of gyrolite. The X-ray photographs of the two preparations showed only a pattern identical with those obtained by autoclaving at the same temperature for 24 hr. (Fig. 1). The low temperature phase B, once formed, seems therefore to re-

(6) J. A. Gard and H. F. W. Taylor, *Min. Mag.*, **31**, 5 (1956).

crystallize rather easily forming the stable compound resembling gyrolite, with the phase Z as a transition compound, as mentioned above. On the other hand, when the mixtures are richer in lime, up to a molar ratio of 1:1, the gyrolite compound is mixed with the other compounds rich in lime, which also belong to this range. It is therefore rather easy to prepare pure samples of the compound resembling gyrolite, if the correct proportion lime:silica, a suitable period of time and a temperature of 200–220° are chosen for the synthesis. The preparations are synthetic and their patterns are therefore not necessarily in detailed agreement with that of a specimen of the mineral, the pattern of which varies in some details according to the specimen.

**The Xonotlite Range.**—After the gyrolite compound, the next substance in order of ascending lime content is xonotlite, having the composition  $\text{CaO}:\text{SiO}_2:\text{H}_2\text{O} = 3:3:1$ . The water content has sometimes been assumed to be somewhat lower. Its characteristic spacings can be discerned in the X-ray photographs of samples of the molar ratio 0.80:1 up to 1.90:1 autoclaved at 220°, 24 hr. (Fig. 3). As the xonotlite compound is a monocalcium silicate hydrate, preparations poorer in lime contain the next compound in order of descending lime content, the gyrolite compound, which is formed from the transition compound Z. A more thorough examination of the X-ray photographs shows also the presence of the tobermorite compound in the autoclave products of the mixtures of about 1:1. The characteristic spacing of this compound (11.1 Å.) occurs in the photographs of the mixtures 0.90:1 and of 1:1. In the mixture 1.20:1 the spacing 11.1 Å. is not discernible. As the two compounds resembling xonotlite and tobermorite are monosilicates and occur in the same preparations, one of them must be stable at the temperature in question. In order to test the stability of the phases, samples of the molar ratio 1:1 were autoclaved at 220° for 144 hr.; the measurements were mentioned above. The characteristic spacings of the tobermorite compound have not disappeared completely after the more intensive autoclave treatment; the intensity of its spacing 11.1 Å., however, is reduced considerably (Fig. 2, Table IV). The xonotlite compound has no diffraction of this value which can also be concluded from the fact that in the preparation lime:silica = 1.20:1, 220°, 24 hr. every trace of this line is lacking (Fig. 3). The tobermorite substance may therefore be interpreted as a transition compound of the same kind as was described concerning the relation the Z-phase—the gyrolite compound; the rate of the transformation is obviously slower for the tobermorite compound than for the Z-phase. As a consequence of this it follows that the tobermorite compound will be rather difficult to prepare in pure state by autoclaving mixtures of calcium hydroxide and amorphous silica within the temperature range 180–220°. The initial substance for the tobermorite-compound must also be the phase B containing a certain minimum quantity of lime. For the composition of tobermorite varying formulas have been proposed.<sup>2,7</sup> Due to the transformation tobermorite-xonotlite

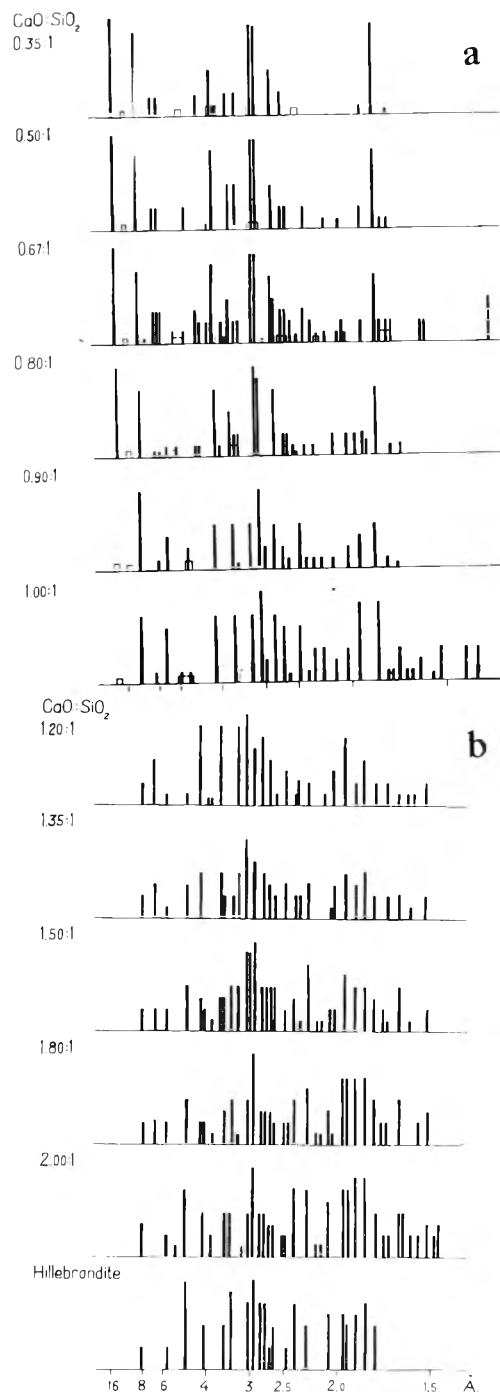


Fig. 3.—X-Ray powder data of preparations of varying content of lime, autoclaved at 220°, 24 hr.

mentioned above, it seems, however, as if a monocalcium silicate composition would best correspond to the synthetic compound and that non-Berzelian formulas might possibly be connected with some mineral specimens. Another argument for the monosilicate formula is that homogenous synthetic substances, crystallizing as the compound in question, very seldom deviate in composition from the rule of whole numbers and synthetic substances not corresponding to such formulas have in most cases been shown to be mixtures, or compounds decomposed to some extent or solid solutions. If the tobermorite compound would be poorer in lime than a

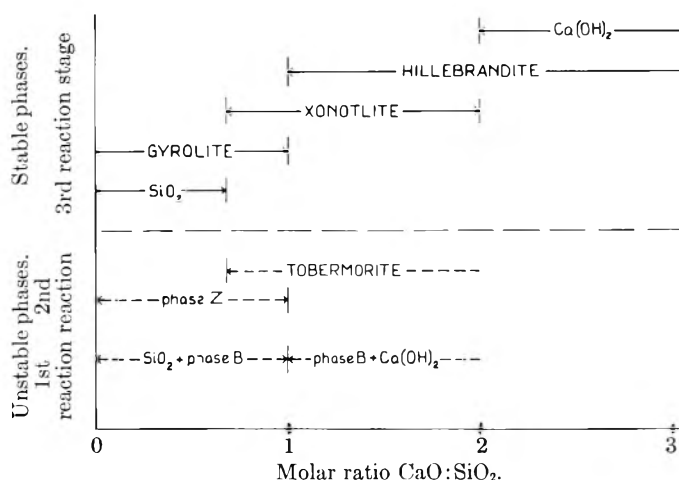


Fig. 4.—The existence range of the unstable and stable phases between 180 and 220°.

monosilicate the autoclaved mixtures of the proportion lime:silica = 1:1 should contain a certain amount of uncombined lime or hillebrandite which might easily be shown by X-rays or by analysis; a content of these compounds, however, has never been established in the experiments.

**The Hillebrandite Range.**—The compound resembling hillebrandite was observed in X-ray photographs of a preparation of the molar ratio 1.20:1. This mixture, as well as those richer in lime, contains this compound together with the compound resembling xonotlite. The content of the latter substance in the preparations decreases at the same time as the content of the hillebrandite-like compound increases. No other compound was observed in the preparations with lime contents up to the molar ratio 2:1. Mixtures still richer in lime up to the molar ratio 3:1 (2.30:1; 2.60:1; 3.00:1) were found to contain only the hillebrandite-phase together with uncombined calcium hydroxide, even when the period of time for the autoclaving was extended to 7 days. A consequence of this is that no compound richer in lime than the dicalcium silicate can be formed from calcium hydroxide and amorphous silica between 180 and 220°. No trace of the spacings of a trisilicate or of other disilicates mentioned in the literature have been observed in the X-ray photographs of the preparations. The silicates formed within the range of lime:silica = 1:1 and 2:1 and stable at 220° are therefore the compounds resembling xonotlite and hillebrandite. By analogy with the formation of the phases in mixtures poorer in lime than the disilicate proportion, it is to be expected that transition compounds might also occur in the mixtures rich in lime, when the xonotlite and hillebrandite compounds are formed. The substance first formed is the phase B rich in lime, which recrystallizes forming the tobermorite compound and after this reaction the phases resembling xonotlite and hillebrandite are produced by combination of the available amount of free lime. In mixtures with the lime ratio 1.5:1 and autoclaved at 200° for 16 hr. the spacing 11.1 Å. of the tobermorite compound was observed as a band of very weak intensity. These transition stages cannot be distinguished in mixtures very rich in lime because of an increased

reaction rate but the above conclusion must be plausible.

**Discussion of the Results.**—The reactions between calcium hydroxide and amorphous silica described in the earlier papers<sup>1</sup> were not necessarily allowed to react to a definite equilibrium, but were designed to throw light on the first stages of the hydrothermal reaction. The results above render possible the conclusion that the formation of the phases within the temperature range 180–220° passes through three stages: the formation of the phase B; of the transition phases Z and the tobermorite compound; and of the compounds finally stable.

The formation of phase B is rapid and the product is poorly crystallized because of the short reaction time; only small differences in the patterns can be observed between the products poor or rich in lime. This phase B deriving from a mixture of a certain composition has the same properties whether it is prepared at a low temperature (160°) or at higher temperatures (180–220°); the phases formed at its recrystallization should therefore depend on the initial lime content.

The second stage of the formation of the solids involves the crystallization of the metastable transition compounds, the phases Z, tobermorite and, in mixtures rich in lime, also calcium hydroxide. As they are unstable in the reaction mixture they are transformed more or less rapidly (phase Z, tobermorite) or combined with the silicates (calcium hydroxide). The transformation was shown within the ranges where the transformation reaction requires a relatively long period of time; the conclusion, however, may be drawn that two reaction stages of unstable phases can occur within ranges where two principal transition reactions would take place. Such a range exists between the molar ratio 0.67:1 and 1:1. Within this range there is a formation of two stable substances, the gyrolite and the xonotlite compounds. Both of them seem to originate from unstable compounds, the Z-phase and the tobermorite phase. Thus two unstable transition phases may be formed more or less rapidly during the recrystallization of the phase B, a reaction resulting in final formation of the stable phases. In this way also the ranges of the unstable phases overlap one another. When the lime content is higher than the molar ratio 1:1, the tobermorite compound originating from the phase B or the xonotlite phase obviously reacts with the other unstable phase within this range, the calcium hydroxide; a reaction which seems to be very rapid and very difficult to distinguish beside the formation of the stable phases, the xonotlite and the hillebrandite compounds.

The third stage of the formation of the solids leads to a final crystallization of the phases in equilibrium. The three compounds resembling gyrolite, xonotlite and hillebrandite represent therefore different degrees of saturation of the silica by the lime and their mutual proportions can be calculated when the amounts of lime and reactive silica are known, provided that an equilibrium exists. An excess of calcium hydroxide together

with the dicalcium silicate hillebrandite shows, on the other hand, a complete saturation of the reactive silica.

The results of earlier investigations<sup>1</sup> have established a recrystallization of the phase B starting just below 180° within about 24–48 hr. and leading to the formation of the phases mentioned above. The reactions and the equilibria described in the present paper must therefore also be of a similar kind within the whole temperature range 180–220°.

The results described above are illustrated by Fig. 4. The stages of the formation of the phases and of their existence range are elucidated when the compounds are or are not in equilibrium, within the temperature range 180–220°.

**Acknowledgment.**—The author wishes to express his gratitude to the International Ytong Co. of Stockholm for a grant which made possible this investigation.

## STANDARD PARTIAL MOLAL COMPRESSIBILITIES BY ULTRASONICS.

### I. SODIUM CHLORIDE AND POTASSIUM CHLORIDE AT 25°<sup>1,2</sup>

BY BENTON B. OWEN AND HAROLD L. SIMONS

Contribution No. 1403 from the Sterling Chemistry Laboratory, Yale University, New Haven, Conn.

Received October 24, 1956

The velocity of sound in dilute aqueous solutions of sodium chloride and potassium chloride is reported at 25°, and at frequencies of 2.5, 5 and 10 megacy./sec. The velocity in pure water (saturated with air) is reported as 1496.7 m./sec. The complete calculation of *isothermal* partial molal compressibilities at infinite dilution,  $\bar{K}_2^0$ , from these data is illustrated. By suitable equations and numerical examples it is shown that the neglect of the correction of adiabatic to isothermal compressibilities causes an error of 7.5% in  $\bar{K}_2^0$  for sodium chloride and potassium chloride at 25°.

#### Introduction

The partial molal compressibilities required for the calculation<sup>3</sup> of the effects of pressure upon ionic equilibria have been derived from two kinds of data, bulk compressions and sound velocities. Compression measurements are well suited for determining compressibilities as a function of pressure above two or three hundred atmospheres, but compressibilities at one atmosphere, which are of great practical importance, require a long extrapolation in their evaluation. This extrapolation, usually based upon some modification of the Tait equation,<sup>4,5</sup> is not completely satisfactory. Compressibilities calculated from sound velocities at one atmosphere avoid extrapolation by the Tait equation, but are, of course, adiabatic compressibilities,  $\beta_s$ , which differ from the desired isothermal compressibilities,  $\beta$ , by the quantity

$$\delta = \beta - \beta_s = 0.02391\alpha^2T'/\sigma \quad (1)$$

where  $\alpha$  is the expansibility of the solution, and  $\sigma$  is its volume specific heat in cal./deg. cm.<sup>3</sup> For convenience  $\sigma$  has been introduced for the product  $c_p d$ . It is a serious mistake to assume that  $\delta$  can be disregarded in the estimation of apparent molal compressibilities. Although  $\delta_c$ , the difference at zero concentration is small at room temperatures, and becomes zero at 4° where  $\alpha$  is zero, the derivative  $d\alpha/dc$  plays an important role in the calculation of apparent molal compressibilities, even at infinite dilution, and this derivative does not

necessarily vanish at 4°. It is the purpose of this communication to report precise data on the velocity of sound in dilute aqueous solutions of sodium chloride and of potassium chloride at 25°, and to illustrate the complete calculation of isothermal partial molal compressibilities at infinite dilution from these data.

#### Experimental

**Materials.**—The salts were J. T. Baker "Analytical Reagent" grade, used without further purification. Concentrations were determined by withdrawing portions of the solutions from the acoustic interferometer after each sound velocity measurement, and titrating them against standard silver nitrate with dichlorofluorescein as indicator.

**Apparatus and Technique.**—Sound velocities were measured in an acoustic interferometer of the movable reflector type illustrated in Fig. 1. More detailed drawings by the authors may be found elsewhere.<sup>6</sup> Except for the bronze nut (5), and several moving parts specifically described, the apparatus is constructed of #303 stainless steel. The quartz crystal transducers are mounted in a cylindrical assembly (1) attached to the heavy base-plate (2) of the interferometer by means of three bolts which permit adjustment to exact parallelism with the 1" plane reflector (3). The X-cut, silver-sputtered crystal of the transducer has an exposed radiating surface 1 in. in diameter, and is in direct contact with the solution through a hole 1 1/8 in. in diameter in the base-plate (2). The lower face of the crystal is air-loaded. The crystal circuit is carefully peaked, and is operated close to fundamental resonance frequency. Interchangeable crystal holders permit operation at various frequencies between 0.5 and 10 megacycles per second.

The 1/2 in. micrometer screw (6) has 24 threads per inch ground over a total length of seven inches. Its pitch was measured at 17 points by Pratt and Whitney. The screw operates through a 1.5 in. tobin bronze nut (5) at the top of the hollow cylinder to which the reflector is attached. Exact axial alignment of the cylinder and reflector is assured by two polished guide rods (4) and four lapped monel sleeves. A third rod, similar and parallel to the guides but not shown in the diagram, was added to improve the rigidity of the assembly when the outer shell (shown as broken lines in Fig. 1) is removed for cleaning. The inside diameter of the shell is 3 in.

(1) This communication contains material from a thesis presented by Harold L. Simons to the Graduate School of Yale University in partial fulfillment of the requirements for the degree of Doctor of Philosophy, June, 1953.

(2) This research was carried out under Contract SAR/DA-19-059-ORD-1287 between the Office of Ordnance Research and Yale University.

(3) B. B. Owen and S. R. Brinkley, Jr., *Chem. Revs.*, **29**, 461 (1941).

(4) R. E. Gibson, *J. Am. Chem. Soc.* **56**, 4 (1934); **57**, 284 (1935).

(5) H. S. Harned and B. B. Owen, "The Physical Chemistry of Electrolytic Solutions," Reinhold Publ. Corp., New York, N. Y., 1950.

(6) B. B. Owen, H. L. Simons and C. E. Milner, Final Report Contract SAR/DA-19-059-ORD-1287, Yale University, Dec. 15, 1953.

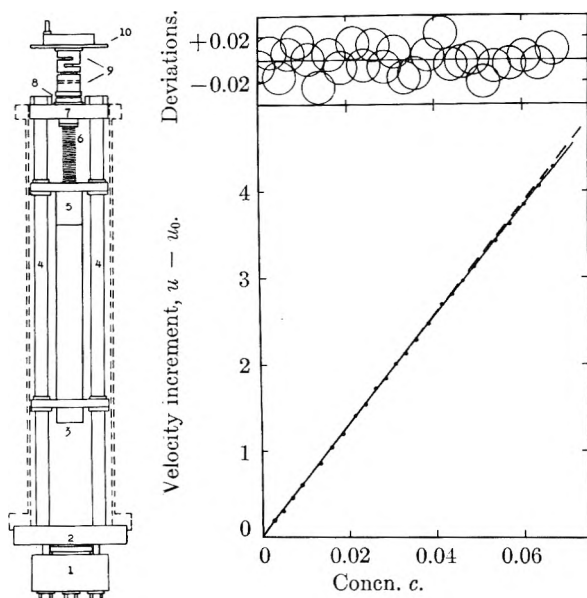


Fig. 1.—The ultrasonic interferometer.

Fig. 2.—Variation of the velocity of sound with concentration of sodium chloride in water at 25°. The broken straight line is drawn with slope  $A_u$ . The deviations of the experimental points from equation 2 are plotted in the upper section of the figure.

A hardened collar on the screw bears against a tobin bronze bearing in the head-plate (7). An even force against this bearing is maintained by the brass spring (9) pressing against a thrust ball bearing (8). This spring, designed to be free from back-lash, is simply a thick brass cylinder sawn radially at four equally spaced positions 90° apart, and serves its purpose admirably.

Full turns of the screw are indicated by a counter (not shown) and fractional turns are read on a 100-division dial (10) equipped with a vernier permitting readings to  $1/1000$  turn, or about 1  $\mu$ . After the crystal circuit has been sharply tuned and the crystal and reflector have been adjusted to exact parallelism, as evidenced by verticality, symmetry and maximum depth of the voltage dips produced across the crystal transducer circuit at nodal settings, the dial, the screw and its bearings are simultaneously calibrated by assuming that the velocity of sound along the axis of the interferometer is rigorously constant throughout the working range, 2 to 6 in. above the transducer. This calibration leads to a sinusoidal correction curve with maximum corrections of two vernier divisions. Back-lash is also of this order, so each set of readings was always made in the same direction of motion of the reflector, and multiple readings were averaged. These precautions resulted in a reproducibility of about one vernier division, as can be seen by inspection of the deviations plotted at the top of Fig. 2. The nodal positions were determined from voltage minima read on a sensitive vacuum tube voltmeter across the transducer. Since these positions were reproducible to about  $1/1000$  turn, and the reflector travel was 100 turns, the velocity of sound was measured with a reproducibility of about 0.001%, or about 0.02 meter per second.

The oscillator driving the transducers is controlled by AT-cut quartz crystals whose frequencies (multiples of 0.5 mcgy./sec.) were periodically compared with the frequencies broadcast by the National Bureau of Standards over Station WWV. Since the oscillator frequency was always known to better than 0.001%, no appreciable error was contributed from this source. The temperature of the interferometer water-bath was controlled by an off-balance bridge type thyatron thermoregulator designed by Sturtevant.<sup>7</sup> Regulation within a range of 0.003° was considered satisfactory during a series of measurements, because a drift of 0.005° was required to cause an error of 0.001% in the velocity of sound at 25°. Temperatures were measured with a Mueller bridge and a platinum resistance thermometer calibrated by the National Bureau of Standards.

(7) J. M. Sturtevant, *Rev. Sci. Instr.*, **9**, 276 (1938).

## Results of Velocity Measurements

Our experimental results are readily summarized in terms of the equation

$$u = u_0 + A_u c + B_u c^{3/2} \quad (2)$$

in which the velocity of sound,  $u$ , through the solutions is expressed as a function of its concentration,  $c$ . The parameters of this equation, evaluated from the data by the method of least squares, are given in Table I. The accuracy with which the data conform to this equation is represented by the probable error,  $P_u$ , recorded in the last column. The experimental results, and hence the equation, are limited to concentrations less than 0.07 mole per liter.

The results of a typical run, expressed graphically in Fig. 2, show at a glance that the deviations of the data from the equation are seldom more than 0.02 meter per second. On the other hand, values of  $u_0$  reported in Table I may differ by as much as 0.17 m./sec., if we compare the maximum and minimum values which resulted from measurements at 2.5 and 10 megacycles per second. Although our measurements were designed to yield thermodynamic information which, as we will see later, depends upon  $A_u$  rather than on  $u_0$ , it will be useful to consider briefly the accuracy with which  $u_0$  is determined with our apparatus. The change in  $u_0$  from one run to another results in part, at least, from removing the outer shell between runs for cleaning and repairs. Referring to Fig. 1, it can be seen that since the guide rods (4) and the end-plates (2 and 7) form a long narrow framework, the apparatus derives much of its rigidity from the outer shell. In reassembling after cleaning it is difficult to re-align the guide rods perfectly, and if these rods depart by 1° from the perpendicular to the base-plate this could cause the nut (5) to rotate as much as 0.011 revolution during the usual 11 cm. travel of the reflector, and thus account for a change of 0.15 m./sec. in  $u_0$ .

TABLE I  
SUMMARY OF RESULTS<sup>a</sup> IN TERMS OF EQUATION 2

Run	Salt freq.	$u_0$	$A_u$	$B_u$	$10^4 \phi^b \kappa$	$P_u$	
1	KCl	1496.824	57.02	-3.73	-40.48	0.0114	
2	KCl	1496.696	58.50	-9.06	-41.50	.0141	
3	KCl	1496.784	57.57	-8.52	-40.93	.0120	
4	KCl	1496.743	55.46	-0.85	-39.66	.0083	
"com"	KCl	..	1496.762	57.20	-6.0	-40.72	.0153
5	NaCl	1496.697	63.31	3.95	-45.92	0.0099	
6	NaCl	1496.698	65.17	-4.60	-47.03	.0088	
7	NaCl	1496.748	64.60	-4.58	-46.69	.0081	
8	NaCl	1496.653	63.52	-1.57	-46.05	.0087	
"com"	NaCl	..	1496.695	64.53	-3.0	-46.65	.0154

<sup>a</sup> Temperature, 25°; frequencies, mcgy./sec.; velocity  $u_0$ , m./sec.;  $\phi^b \kappa$ , cc./mole;  $P_u = 0.675 [\sum \Delta^2 / (n - 3)]^{1/2}$ , where  $\Delta = u(\text{obsd.}) - u(\text{calcd.})$ , and  $n$  is the number of experimental values  $u(\text{obsd.})$ . The composite series, designated as "com," were derived from the combined data for four runs with the same salt. The differences  $u - u_0$  were calculated for each run, and then this composite set of data was fitted to eq. 2 in the form  $u - u_0 = A_u c + B_u c^{3/2}$  by the method of least squares.

The value 1,496.73 m./sec. is the average of the eight independently determined values of  $u_0$  in Table I, and represents all of our data within 0.1 m./sec. for the velocity of sound in air-saturated distilled water at 25° and 1 atmosphere. Making

allowance for the difference in temperatures, our figure 1,496.73 at 25° agrees satisfactorily with the value 1,509.85 at 30° recommended by Del Grosso, Smura and Fougere<sup>8</sup> as the result of a very elaborate experimental and theoretical investigation of the moving reflector type interferometer. Their paper also contains an extensive bibliography.

#### Evaluation of $\phi^0_K$ , or $\bar{K}^0_2$

The velocity of sound (m./sec.) through a liquid is related to the density (g./cm.<sup>3</sup>) and the adiabatic compressibility (bar<sup>-1</sup>) of the fluid by

$$\beta_s = 100/u^2d \quad (3)$$

Through eq. 1 it is possible to calculate  $\beta$  from  $\beta_s + \delta$ , and hence the apparent molal compressibility from the equation<sup>9</sup>

$$\phi_K = \frac{1000}{c} (\beta - \beta_0) + \beta_0\phi_v \quad (4)$$

providing, of course, that data are available for evaluating  $\delta$  and  $\phi_v$ . Subsequent extrapolation of a series of values of  $\phi_K$  against  $c^{1/2}$  would lead to the limiting value  $\phi^0_K$ , which is numerically equal to the desired standard thermodynamic quantity  $\bar{K}^0_2$ . So long as the procedure relies upon extrapolation of apparent molal quantities against  $c^{1/2}$ , rather than a function involving the  $\alpha$ -parameter,<sup>10</sup> the dependence of  $\phi^0_K$  upon the various factors entering into its calculation is simply formulated.

Thus, if the concentration dependence of the apparent molal quantities  $\phi_X$  ( $X = V, K, E, C_p$ ) in dilute solutions may be represented by equations of the form

$$\phi_X = \phi^0_X - S_X c^{1/2} \quad (5)$$

then the corresponding directly measurable quantities ( $y = d, \beta, \alpha, \sigma$ ) must follow equations of the form

$$y = y_0 + A_y c + B_y c^{3/2} \quad (6)$$

in dilute solutions. Combination of such equations for  $d, \beta, \alpha$  and  $\sigma$  with eq. 1 and 3 results in infinite series expressions which we write

$$u = u_0 + A_u c + B_u c^{3/2} + \dots \quad (7)$$

$$\delta = \delta_0 + A_\delta c + B_\delta c^{3/2} + \dots \quad (8)$$

The first three terms in eq. 7 are the same as those in eq. 2. Among the equations connecting the coefficients of corresponding equations of types 5 and 6, we will have need of the following

$$1000A_{d1} = M_2 - d_0\phi^0_v \quad (9)$$

$$1000A_\beta = \phi^0_K - \beta_0\phi^0_v \quad (10)$$

$$1000A_\alpha = \phi^0_E - \alpha_0\phi^0_v \quad (11)$$

$$1000A_\sigma = \phi^0_{C_p} - \sigma_0\phi^0_v \quad (12)$$

In addition we will need two new equations

$$A_\beta = A_\delta - \beta_{0s}(2A_u/u_0 + A_d/d_0) \quad (13)$$

$$A_\delta = \delta_0(2A_\alpha/\alpha_0 - A_\sigma/\sigma_0) \quad (14)$$

(8) V. A. Del Grosso, E. J. Smura and P. F. Fougere, "Accuracy of Ultrasonic Interferometer Velocity Determinations," Naval Research Laboratory Report 4439, 1954. In this paper a number of measurements of  $u_0$  by other investigators at various temperatures are compared at 30° by means of temperature coefficients based upon earlier work of Del Grosso [Naval Research Laboratory Report 4002, 1952].

(9) For other definitions and appropriate symbols consult Chapter 8 of ref. 5.

(10) B. B. Owen and S. R. Brinkley, Jr., *Ann. N. Y. Acad. Sci.*, **51**, 753 (1949).

which bring the first coefficients of eq. 6 and 8 into the scheme. It follows by combination of these equations that  $\phi^0_K$  can be directly expressed in terms of the parameters obtained from sound velocity data. Thus

$$\phi^0_K = 1000A_\delta + \delta_0\phi^0_v + (2\phi^0_v - M_2/d_0 - 2000A_u/u_0)\beta_{0s} \quad (15)$$

An equation of this type was derived by Barnartt,<sup>11</sup> but because he neglected to consider the variation of the ratio  $C_p/C_v$  with concentration, his expression lacks the important terms  $1000A_\delta$  and  $\delta_0\phi^0_v$ . In order to show the magnitude of these terms relative to the others in eq. 15, the thermodynamic quantities and coefficients which enter into the application of this equation are collected in Table II. Also included are the composite values ("com") of  $u_0$  and of  $A_u$  from Table I, and the final calculated values of  $\beta_0, A_\beta$  and  $\phi^0_K$ . The magnitude of the individual terms that contribute to  $\phi^0_K$  for sodium chloride have been calculated from the data in Table II, and are written below in the order in which they occur in eq. 15. Thus

$$10^4 \phi^0_K = 3.441 + 0.076 + (14.685 - 26.248 - 38.606) \quad (15a)$$

Comparison of eq. 15 and 15a brings out several important results at once. In the first place, the sum  $(1000A_\delta + \delta_0\phi^0_v)10^4$  is  $3.441 + 0.076 = 3.517$ , or 7.5% of  $(-46.65)$  the numerical value of  $10^4\phi^0_K$ . Thus at 25°, neglect of  $\delta$  and  $\delta_0$  would cause an error in  $\phi^0_K$  of more than twice the sum of the experimental and curve-fitting errors combined. Due to the presence of  $\delta_0$  as a factor<sup>12</sup> in eq. 14,  $A_\delta$  is zero at the temperature of maximum density where  $\alpha_0$  vanishes.

TABLE II

QUANTITIES <sup>a</sup> USED IN THE EVALUATION OF $\phi^0_K$	NaCl	KCl
Quantity		
$M_2$	58.454	74.553
$\phi^0_v$	16.40	26.52
$d_0$	0.99707	0.99707
$A_d$	0.04210	0.04811
$\phi^0_E$	0.0930	0.0850
$\alpha_0 10^4$	2.55	2.55
$A_\alpha 10^4$	0.89	0.78
$\phi^0_{C_p}$	-23.8	-29.0
$\sigma_0$	0.99473	0.99473
$A_\sigma$	-0.04011	-0.05538
$\delta_0 10^7$	4.660	4.660
$A_\delta 10^7$	3.441	3.110
$u_0$	1496.70	1496.76
$A_u$	64.53	57.20
$\beta_{0s} 10^4$	0.44772	0.44769
$\beta_0 10^4$	0.45238	0.45235
$A_\beta 10^4$	-0.05407	-0.05271
$\phi^0_K 10^4$	-46.65	-40.72

<sup>a</sup> For the sources of the thermodynamic quantities not derived in this paper, consult reference 5.

Reference to Table I shows that extreme values of  $u_0$  differ by about 0.01%, so the uncertainty in the value of  $\beta_{0s}$  could contribute an error of only

(11) S. Barnartt, *J. Chem. Phys.*, **20**, 278 (1952).

(12) This factor was overlooked in a statement in reference 6 where it was concluded that further experimental work would be necessary to show that  $A_\delta$  is zero at the temperature of maximum density.

0.02% of the sum of the terms in parenthesis in eq. 15a, or 0.01 to  $\phi^0_K$ . The values of  $A_u$  show considerable variation between runs, and in view of the sensitivity of this parameter to the vagaries of curve-fitting, we estimate that  $A_u$  may be in doubt by 1.5 units. This could contribute an error of 0.9 to  $10^4\phi^0_K$  for sodium chloride, and it seems reasonable to set 1.0 as the total probable error in  $10^4\phi^0_K$  directly associated with the ultrasonic measurements and the analytical evaluation of  $A_u$ . The value of  $\phi^0_V$  used for sodium chloride is scarcely in doubt by more than 0.3 cc./mole, which corresponds to an error of 0.27 in  $10^4\phi^0_K$ . Thus in the evaluation of  $10^4\phi^0_K$  for sodium chloride the sum of the estimated experimental errors is 1.28 compared to 3.44 contributed by the term  $1000A_s$ .

The situation is very much the same for potassium chloride, for the term  $1000A_s$  contributes 7.6% to  $10^4\phi^0_K$ . The values of  $10^4\phi^0_K$  derived<sup>13</sup> from compression measurements are about 10% more negative than those in Table II, being  $-51.6$  for sodium chloride and  $-45.2$  for potassium chloride.

**Acknowledgments.**—The authors wish to express their gratitude to Mr. Charles M. Pond of Niles, Bement and Pond Division of Pratt Whitney, West Hartford, for calibration of the micrometer screw, to Mr. Walther Andersen of Andersen Laboratories, West Hartford, for design of electronic equipment, and to the Office of Ordnance Research for financial assistance.

(13) Reference 5, p. 270.

## DIELECTRIC CONSTANT MEASUREMENTS ON GASES AT MICROWAVE FREQUENCIES<sup>1</sup>

BY JAMES E. BOGGS, CULLEN M. CRAIN AND JAMES E. WHITEFORD

*Electrical Engineering Research Laboratory and Departments of Chemistry and Electrical Engineering,  
The University of Texas, Austin, Texas*

*Received November 10, 1956*

Dielectric constant measurements have been made on 15 gases at 30, 60 and 90°, using a frequency of 9400 megacycles. For HCl, SO<sub>2</sub>, H<sub>2</sub>S, CO, CH<sub>3</sub>COCH<sub>3</sub> and CClF<sub>2</sub>CClF<sub>2</sub>, values for the molar polarization and for the dipole moment comparable to those reported at lower frequency were obtained. For CH<sub>2</sub>ClF, CF<sub>2</sub>=CClF and *cis*-C<sub>2</sub>H<sub>4</sub>=C<sub>2</sub>H<sub>4</sub>, no values at lower frequency are available in the literature for comparison. For CH<sub>3</sub>Cl, CHClF<sub>2</sub>, CHCl<sub>2</sub>F, CH<sub>3</sub>Br, and possibly CClF<sub>3</sub> and CCl<sub>3</sub>F, the dielectric constant at 9400 megacycles is distinctly lower than that at lower frequency. Possible explanations for the lowering are discussed.

Most of the measurements of dielectric constants of gases reported in the literature have been made at relatively low frequency; generally less than 1 megacycle. The measurements are difficult and great pains must be taken to ensure high precision. In recent years, equipment for making similar measurements in the microwave region has become available and is capable of greater precision with much greater ease of operation.

A relatively small number of gases has been investigated at microwave frequencies. Consequently it was considered of interest to make a survey to determine whether dielectric constant values measured at these frequencies were identical with those measured at low frequencies (the so-called static values).

From theoretical considerations, one would expect that the static dielectric constant value would be obtained at all frequencies below the lowest resonance frequency of the dipole being measured. In the region of such a frequency, resonance dispersion would be observed and, at still higher frequencies, the dielectric constant would have a value lower than the static value. Normally, one would predict that the lowest such resonance frequency would be the one corresponding to the transition from the zero to the first rotational energy level. Only for rather heavy molecules would this resonance frequency be lower than the frequencies usu-

ally used for microwave measurements. Nevertheless, the possibility that some unknown type of transition might occur at lower frequency and alter the value of the dielectric constant cannot be ruled out without actual measurement.

In the current study, dielectric constants have been measured for 15 gases and the results compared, when possible, with lower frequency measurements reported in the literature.

### Experimental

Measurements on all of the gases were made using a Crain refractometer.<sup>2</sup> The gas sample was contained in a cavity resonator which controlled the frequency of a Pound-type stabilized oscillator. The cavity was immersed in a constant-temperature bath and was connected to a vacuum system through which the sample could be admitted. The temperature of the constant-temperature bath was maintained within  $\pm 0.05^\circ$ . The gas pressure was read on an ordinary mercury manometer. A second cavity, evacuated and sealed, was immersed in the same bath and used to stabilize a second oscillator. The frequency difference between the two stabilized oscillators was read with the sample cavity evacuated, and the change noted when the sample was introduced. Then,  $\Delta f/f = \sqrt{\epsilon} - 1$ , where  $\Delta f$  is the change in beat frequency,  $f$  is the resonant frequency of the evacuated measuring cavity, and  $\epsilon$  is the dielectric constant of the gas.

All of the free gases used were purchased from The Matheson Company and were purified by fractional distillation on a vacuum line. The acetone was of reagent grade and was further purified by fractional distillation. The authors wish to express their appreciation to Mrs. Helene P. Mosher for her assistance in purifying the samples.

In a typical measurement, the sample cavity was evacuated and the frequency of the beat note between the two os-

(1) This work has been supported by Air Force Contract AF 33(616)-2842. It was presented in part at the 129th National Meeting of the American Chemical Society, Dallas, Texas, April 9-13, 1956.

(2) C. M. Crain, *Rev. Sci. Instr.*, **21**, 456 (1950).

TABLE I

Gas	Micro-wave $P$ (cc.)	"Static" $P$ (cc.)	Micro-wave $P_D$ (cc.)	"Static" $P_D$ (cc.)	Micro-wave $\mu$ (Debyes)	"Static" $\mu$ (Debyes)
HCl	31.5	30.5 <sup>a</sup>	7.2	7.0 <sup>a</sup>	1.10	1.08 <sup>a</sup>
SO <sub>2</sub>	63.7	64.2 <sup>b</sup>	10.2	10.8 <sup>b</sup>	1.63	1.63 <sup>b</sup>
H <sub>2</sub> S	28.1	27.0 <sup>c</sup>	8.8	10.0 <sup>c</sup>	0.98	0.92 <sup>c</sup>
CO	5.04	4.9 <sup>d</sup>	4.65	4.65 <sup>d</sup>	0.14	0.12 <sup>d</sup>
CH <sub>3</sub> COCH <sub>3</sub>	184.4	183. <sup>e</sup>	17.7	<sup>f</sup>	2.88	2.88 <sup>e</sup>
CClF <sub>2</sub> CClF <sub>2</sub>	33.8	34.4 <sup>g</sup>	29.5	<sup>h</sup>	0.46	<sup>i</sup>

<sup>a</sup> R. P. Bell and I. E. Coop, *Trans. Faraday Soc.*, **34**, 1909 (1938). <sup>b</sup> R. J. W. LeFevre, J. W. Mulley and B. M. Smythe, *J. Chem. Soc.*, 276 (1950). <sup>c</sup> C. T. Zahn and J. B. Miles, *Phys. Rev.*, **32**, 497 (1928). <sup>d</sup> A. van Itterbeek and K. de Clippeleir, *Physica*, **14**, 349 (1948). <sup>e</sup> C. T. Zahn, *Physik. Z.*, **33**, 686 (1932). <sup>f</sup> The distortion polarization of acetone has not been reported. The molar refraction is 16.2 cc. <sup>g</sup> R. M. Fuoss, *J. Am. Chem. Soc.*, **60**, 1633 (1938). <sup>h</sup> The distortion polarization of this compound has not been reported. The molar refraction is 21.5 cc. <sup>i</sup> Fuoss measured this compound at only one temperature, so the dipole moment could not be determined accurately.

cillators was measured. Gas was then admitted to the sample cavity at a measured pressure and allowed to come to temperature equilibrium. The beat frequency between the two oscillators was determined again. The shift in beat frequency varied from 0.5 to 15 megacycles, depending on the gas and its pressure. Such measurements were made at a series of pressures and extrapolated graphically to 760 mm. pressure. The molar polarization was then calculated by the relation

$$P = \frac{\epsilon - 1}{\epsilon + 2} V$$

where  $V$ , the molar volume, was calculated by the ideal gas law. The molar polarization can, of course, be thought of as the sum of the distortion polarization (electronic plus atomic) and the orientation polarization. Plotting the molar polarization against the reciprocal of the absolute temperature gave a straight line from which the dipole moment and distortion polarization of the gas could be determined.

### Results

The results obtained with acetone vapor are presented as typical. Figure 1 shows the measured dielectric constant plotted against gas pressure at 30, 60 and 90°. In Fig. 2 the resulting values for the molar polarization are plotted against reciprocal temperature. The results from a similar treatment of each of the gases are shown in the tables.

Table I shows the results for 6 of the compounds measured. The total molar polarization at 30° ( $P$ ), the distortion polarization ( $P_D$ ) and the dipole moment ( $\mu$ ), as measured by us at 9400 megacycles, are given for each compound together with similar values calculated from literature data at low frequency. The value for the total polarization should be accurate to better than 1% and the dipole moment to  $\pm 0.01$  Debye. The distortion polarization is less accurate, since it involves a rather considerable extrapolation. It can be seen that the values at the two frequencies agree within experimental error in every case except for the dipole moment of H<sub>2</sub>S. We believe that the value of 0.92 reported by Zahn and Miles in 1928 for the dipole moment of H<sub>2</sub>S is too low, since Hillger and Strandberg,<sup>3</sup> in 1950, reported a dipole moment of 1.02 for H<sub>2</sub>S as measured from the Stark effect on the microwave absorption spectrum, and one would not anticipate this large an isotope effect.

In addition to the compounds listed in Table I, Crain<sup>4</sup> and Birnbaum and Chatterjee<sup>5</sup> have meas-

(3) R. E. Hillger and M. W. P. Strandberg, Technical Report 180, Laboratory of Electronics, Massachusetts Institute of Technology, 1950.

(4) C. M. Crain, *Phys. Rev.*, **14**, 691 (1948).

(5) G. Birnbaum and S. K. Chatterjee, *J. Appl. Phys.*, **23**, 220 (1952).

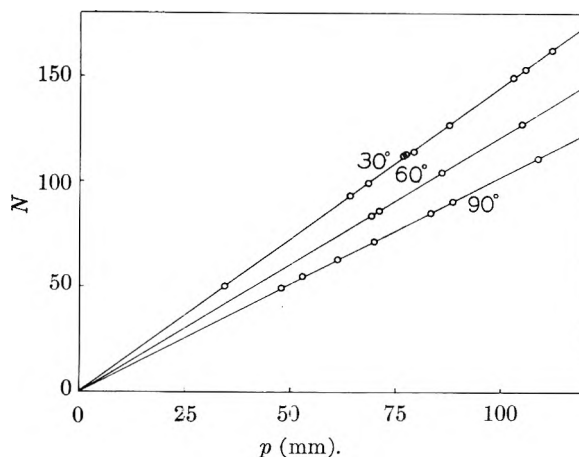


Fig. 1.—Dielectric constant of acetone as a function of pressure at 30, 60 and 90°:  $N = (\sqrt{\epsilon} - 1) \times 10^6$ .

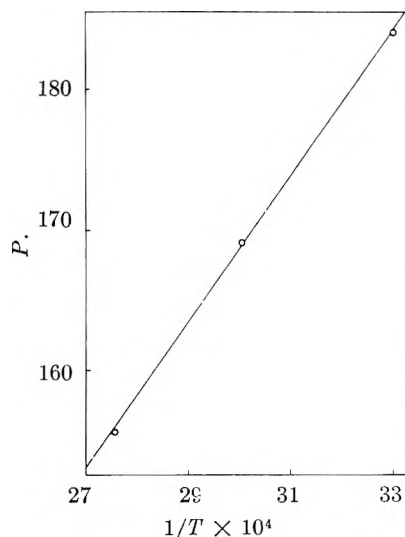


Fig. 2.—Molar polarization of acetone as a function of the reciprocal of the absolute temperature;  $\mu = 2.88$ ;  $P_D = 17.7$ .

ured the dielectric constant of water vapor at 9400 megacycles and obtained the same value as at lower frequencies.

Similar data are shown in Table II for six halo-methanes. For the first four of these compounds there is a real discrepancy between the total polarization values measured at microwave frequencies and those reported at lower frequencies. The un-

TABLE II

Gas	Micro-wave P (cc.)	"Static" P (cc.)	Micro-wave P <sub>D</sub> (cc.)	"Static" P <sub>D</sub> (cc.)	Lowest rotational frequency (Mc.)
CH <sub>3</sub> Cl	78.0	84.4 <sup>a</sup>	14.2	14.1 <sup>a</sup>	26,176-26,586 <sup>b</sup>
CHClF <sub>2</sub>	46.7	54.9 <sup>c</sup>	11.1	14.9 <sup>c</sup>	...
CHCl <sub>2</sub> F	43.6	50.8 <sup>c</sup>	15.6	17.2 <sup>c</sup>	...
CH <sub>3</sub> Br	76.2	80.3 <sup>d</sup>	14.6	15.2 <sup>d</sup>	19,064-19,136 <sup>b</sup>
CClF <sub>3</sub>	18.4	18.8 <sup>e</sup> -19.9 <sup>f</sup>	14.3	15.7 <sup>e</sup>	6,503-6,671 <sup>g</sup>
CCl <sub>3</sub> F	27.3	28.0 <sup>e</sup> -30.6 <sup>f</sup>	22.5	23.9 <sup>e</sup>	...

<sup>a</sup> R. Sanger, O. Steiger and K. Gächter, *Helv. Phys. Acta*, **5**, 200 (1932). <sup>b</sup> W. Gordy, J. W. Simmons and A. G. Smith, *Phys. Rev.*, **74**, 243 (1948); J. W. Simmons and W. E. Anderson, *ibid.*, **80**, 338 (1950). <sup>c</sup> C. P. Smyth and K. B. McAlpine, *J. Chem. Phys.*, **1**, 190 (1933). <sup>d</sup> C. P. Smyth and K. B. McAlpine, *ibid.*, **2**, 499 (1934). <sup>e</sup> G. W. Epprecht, *Z. angew. Math. Phys.*, **1**, 138 (1950). <sup>f</sup> R. M. Fuoss, *J. Am. Chem. Soc.*, **60**, 1633 (1938). <sup>g</sup> D. K. Coles and R. H. Hughes, *Phys. Rev.*, **76**, 858 (1949).

certainties of measurement for CClF<sub>3</sub> and CCl<sub>3</sub>F are such that no statement can be made about the effect of frequency. For the others, the molar polarization measured at microwave frequency is distinctly lower. It can be seen that the distortion polarization values agree within experimental error at the two frequencies. Thus, the discrepancy appears in the orientation polarization term. The dipole moments of these compounds cannot be calculated from our data, since such a calculation requires a knowledge of the static dielectric constant. For reference, the frequency of the lowest rotational absorption transition as determined from microwave spectroscopy is given where known. The range of frequency values covers the region in which different isotopic species absorb.

Three other gases were measured by the same method, but low frequency values for comparison are not available. The microwave results obtained are shown in Table III. The dipole moments have been calculated on the assumption that the microwave dielectric constants are really identical with the static values. As some check on the validity of the measurements, the molar refractions of the compounds are also given.

TABLE III

Gas	Micro-wave P (cc.)	Micro-wave P <sub>D</sub> (cc.)	Molar refraction R (cc.)	Micro-wave μ (Debyes)
CH <sub>2</sub> ClF	78.9	12.3	11.8	1.82
CF <sub>2</sub> =CClF	22.6	15.1	16.2	0.61
<i>cis</i> -C <sub>2</sub> H <sub>4</sub> =				
C <sub>2</sub> H <sub>4</sub>	22.4	20.2	20.2	0.33

Magnuson<sup>6</sup> has also measured the dielectric constant and computed the dipole moment of a number of compounds at a frequency of 9400 megacycles. He obtains a dipole moment of 0.554 for ClF<sub>3</sub>, 0.533 for C<sub>2</sub>Cl<sub>2</sub>F<sub>4</sub>, and 0.85 for C<sub>4</sub>Cl<sub>3</sub>F<sub>7</sub>. Measurement of these compounds at lower frequency would be very interesting to see if there is any frequency effect on the dielectric constant.

(6) D. W. Magnuson, *J. Chem. Phys.*, **20**, 229 (1952); **24**, 334 (1956).

## Discussion

For certain of the compounds measured, the total polarization at 9400 megacycles has come out as much as 15% lower than literature values at low frequencies. Since the accuracy of our measurements should be better than 1% and various values reported in the literature show nearly this good agreement among themselves, it is evident that the discrepancy is real. Of the compounds measured so far, the discrepancy has appeared only in a group of halomethanes.

The lower dielectric constant at high frequency cannot be attributed to resonance dispersion involving a pure rotational transition, since, for CH<sub>3</sub>Cl and CH<sub>3</sub>Br at least, the measurement frequency is below the frequency of the first rotational spectral line. In the case of CClF<sub>3</sub>, such an effect might be expected, but here the orientation polarization is so small that a decrease in it would be difficult to observe with certainty.

The lowering of the dielectric constant could be explained if there were some resonant frequency connected with the molecules which occurred at a frequency intermediate between 9400 megacycles and the frequency used in the "static" measurements. One possible explanation is suggested by the work of Bleaney and Loubser,<sup>7</sup> who detected absorption in the high pressure microwave spectrum of CH<sub>3</sub>Cl and CH<sub>3</sub>Br which they attributed to the pressure broadening of a low frequency inversion transition. While it is more difficult to picture an inversion of a molecule like CH<sub>3</sub>Cl than in the well-known example of NH<sub>3</sub>, it is certainly true that there are two mirror image configurations and that the potential barrier between them is not infinite. Such a double potential well would lead to splitting of the energy levels and the possibility of a transition between the split levels. The extent of splitting, and hence the frequency of the absorption line, would depend on the height of the barrier. Unfortunately no way of calculating this appears to be immediately evident.

(7) B. Bleaney and J. H. N. Loubser, *Proc. Phys. Soc. (London)*, **A63**, 483 (1950).

## TRANSFERENCE IN BINARY MOLTEN SALT SOLUTIONS

BY BENSON ROSS SUNDHEIM

*Department of Chemistry, Washington Square College, New York University, New York, N. Y.**Received November 12, 1956*

The coupling between diffusion and electrical conduction is treated for a solution of two molten salts having an ion in common. The quantities of transport are related to transference numbers, diffusion potential and the steady state in electrolysis.

It has been observed<sup>1</sup> that the quantity ordinarily termed transference number in a pure molten salt has a value which is determined by the conditions of measurement and by the reference point chosen for the velocities. An investigation is made here of the significance of transference numbers and junction potentials in electrochemical cells of certain molten salt solutions. The diffusion process has been studied repeatedly from the point of view of the thermodynamics of irreversible processes.<sup>2</sup> Ordinarily the motion of the individual ionic components is studied, leading to the use of single ion chemical or electrochemical potentials. In the derivation presented below the introduction of such unmeasurable quantities is avoided. In addition, the usual treatment of the diffusion potential uses the expression  $\text{grad}(\mu_i + z_i\phi)$  for the force on a single ion. This immediately implies that the Nernst-Einstein equation applies, relating the diffusion coefficient and mobility of the ion. No such special assumption is imbedded in the present treatment.

**The Phenomenological Equations.**—Consider a cell containing a mixture of two molten salts, the local concentrations being designated as  $c_1$ ,  $c_2$  moles/cc. We restrict ourselves to the particularly simple case where the salts have an ion in common since the important results are seen most clearly here. The general multi-component case will be treated elsewhere. The first component is  $A_nB_m$  and the second  $C_pB_q$  and the cell also contains a pair of electrodes reversible to one of the ionic species. The frictional drag of cell walls and electrodes is assumed to be negligible. A porous plug may be inserted in the cell to establish a reference point for measurements. (This arrangement corresponds to that of various experimental cells used to measure transference numbers or junction potentials in molten salts.) Designate by

$\vec{J}_1$  ( $\vec{J}_2$ ) the flux (moles/cm.<sup>2</sup> sec.) of (neutral) salt 1 (2) and by  $\vec{I}$  the electrical current density (Faradays/cm.<sup>2</sup> sec.), all measured with respect to the mass average velocity of the solution. Let  $\bar{v}_1$ ,  $\bar{v}_2$  be the respective partial molar volumes,  $M_1$ ,  $M_2$  the appropriate formula weights and  $z_A$ ,  $z_B$ ,  $z_C$  the ionic valences. In view of the essential incompressibility of liquids, of the requirements of electroneutrality and of the fact that momentum is conserved in such systems<sup>1</sup> the set of interrelations occurs

$$\begin{aligned} M_1\vec{J}_1 + M_2\vec{J}_2 &= 0 & (a) \\ \vec{J}_2 &= -(M_1/M_2)\vec{J}_1 \end{aligned}$$

$$\vec{J}_A = n\vec{J}_1 \quad (b)$$

$$\vec{J}_C = p\vec{J}_2 = -p(M_1/M_2)\vec{J}_1 \quad (c) \quad (1)$$

$$\vec{J}_B = (\vec{I} - z_A\vec{J}_A - z_C\vec{J}_C)/z_B \quad (d)$$

$$= [\vec{I} - nz_C\vec{J}_1 + pz_C(M_1/M_2)\vec{J}_1]/z_B$$

$$c_2 = (1 - c_1\bar{v}_1)/\bar{v}_2 \quad (e)$$

$$z_A z_A + c_B z_B + c_C z_C = 0 \quad (f)$$

It is seen readily that all the measurable fluxes are expressed in terms of  $\vec{J}_1$  and  $\vec{I}$  and that only the concentration  $c_1$  is needed to specify the composition of the solution at any point.

The forces corresponding to the fluxes  $\vec{J}_i$  and  $\vec{I}$  are,<sup>2</sup> respectively,  $-\text{grad} \mu_i$  and  $-\text{grad} \phi$  where  $\mu_i$  is the chemical potential and  $\phi$  is the electrostatic potential. In these terms the phenomenological equations express a linear relation between the forces and fluxes

$$\vec{J}_1 = -L_{11} \text{grad} \mu_1 - L_{12} \text{grad} \mu_2 - L_{13} \text{grad} \phi \quad (2)$$

$$\vec{J}_2 = -L_{21} \text{grad} \mu_1 - L_{22} \text{grad} \mu_2 - L_{23} \text{grad} \phi$$

$$\vec{I} = -L_{31} \text{grad} \mu_1 - L_{32} \text{grad} \mu_2 - L_{33} \text{grad} \phi$$

Certain of the coefficients are readily identified<sup>3</sup>

$$L_{ik} = D_{ik}c_i / \left[ 1 + \frac{\delta \ln \gamma_i}{\delta c_i} \right] \quad i, k = 1, 2 \quad (3)$$

$$L_{33} = \kappa$$

Here  $\kappa$  is the isothermal specific electrical conductance measured in faradays,  $\gamma_i$  the activity coefficient of the  $i$ th component and  $D_{ik}$  the interdiffusion coefficient of the  $i$ th and  $k$ th components. The Onsager relations then state that  $L_{ik} = L_{ki}$ . Designate the quantity  $L_{13} = L_{31}$  by  $\kappa t_1$ ,  $L_{32}$  by  $\kappa t_2$ . The quantity  $\text{grad} \mu_2$  can be eliminated from (2) by use of the Gibbs-Duhem equation,  $(\sum c_i \text{grad} \mu_i)_{T,P} = 0$

$$\vec{J}_1 = (-L_{11} - L_{12}c_1/c_2) \text{grad} \mu_1 - \kappa t \text{grad} \phi \quad (4)$$

$$\vec{J}_2 = -(L_{21} - L_{22}c_1/c_2) \text{grad} \mu_1 - \kappa t_2 \text{grad} \phi$$

$$\vec{I} = -(t_1 - t_2c_1/c_2)\kappa \text{grad} \mu_1 - \kappa \text{grad} \phi$$

Using (1a) and designating  $[L_{11} - L_{12}c_1/c_2]$  by  $\mathcal{L}$ , (4) becomes

$$\vec{J}_1 = -\mathcal{L} \text{grad} \mu_1 - \kappa t_1 \text{grad} \phi$$

$$\vec{J}_2 = +(M_1/M_2)\mathcal{L} \text{grad} \mu_1 + (M_1/M_2)\kappa t_1 \text{grad} \phi$$

$$\vec{I} = -[1 + (M_1c_1)/M_2c_2]\kappa t_1 \text{grad} \mu_1 - \kappa \text{grad} \phi \quad (5)$$

Only one diffusion coefficient,  $\mathcal{L}$ , occurs in accord-

(1) B. R. Sundheim, *THIS JOURNAL*, **60**, 1381 (1956).

(2) S. R. de Groot, "Thermodynamics of Irreversible Processes," Interscience Publishers, Inc., New York, N. Y., 1952.

(3) (a) J. G. Kirkwood in "Ion Transport Across Membranes," edited by H. T. Clarke, Academic Press, Inc., New York, N. Y., 1954, p. 119 ff; (b) H. Fujita and L. J. Gosting, *J. Am. Chem. Soc.*, **78**, 1099 (1956).

ance with the fact that only one composition variable is required and the fact that the fluxes are coupled through (1a).

The following quantities are of particular interest.

A.  $(J_1/I)\mu_1 = t_1$ .—Thus  $t_1$  is seen to be the amount of component one convected along with a unit current in a uniform fluid. We shall call it the electrochemical transport coefficient of component one.

B.  $[\text{grad } \phi / \text{grad } \mu_1]_{I=0} = -t_1[1 + M_1c_1/(M_2c_2)]$ .—Here  $\text{grad } \phi$  is the diffusion potential,  $\overline{E}_d$ .

$$\overline{E}_d = -t_1[1 + M_1c_1/(M_2c_2)] \text{grad } \mu_1$$

$$\Delta \overline{E}_d = \phi(a) - \phi(0) = -\int_0^a t_1[1 + M_1c_1/(M_2c_2)] \text{grad } \mu_1 dx$$

With the use of this expression the equation for the current becomes

$$\overline{I} = -\kappa \overline{E}_d - \kappa \text{grad } \phi$$

$$\text{grad } \phi = \overline{E}_d - \overline{I}/\kappa$$

stating that the potential difference across  $dx$  is equal to the diffusion potential minus the  $IR$  drop.

C.  $[\text{grad } \mu_1 / \text{grad } \phi]_{J_1=\text{const.}} = \kappa t_1/\mathcal{L} - [J_1/(\mathcal{L} \text{grad } \phi)]$ .— $\text{Grad } \mu_1$  here is the gradient of the chemical potential, from which the gradient of the concentration can be obtained, during the steady state of electrolysis of the solution.<sup>4</sup> Since  $\mathcal{L}$ ,  $t_1$  and  $\kappa$  are functions of the concentration, integration of this expression involves solution of the diffusion equation and is ordinarily a formidable task.

**The Electrochemical Transport Coefficient.**—With the aid of expressions 1 the transference numbers of the individual ions may be expressed in terms of the electrochemical transport coefficient of one of the components.

(4) P. Drossback, *Z. Elektrochem.*, **58**, 66 (1954).

$$t_2 = t_1(-M_1/M_2) \quad (6)$$

$$t_A = nz_A t_1$$

$$t_B = [1 - nz_A t_1 + p(M_1/M_2)z_A t_1]$$

$$t_C = -p(M_1/M_2)z_C t_1$$

It is clear that there is only one significant transport quantity describing this system and it may be chosen to be any of the above as well as  $t_1$  itself. The numerical value of the transport quantities depends upon the point of reference used in defining the velocities. If a new reference point, moving with a velocity  $v_0$  with respect to the former one (the mass average velocity) is chosen, then the new fluxes, identified with primes become

$$\overline{J}_i' = (\overline{v}_i + \overline{v}_0)c_i = \overline{J}_i + \overline{v}_0 c_i \quad (7)$$

$$\overline{I}' = \Sigma(\overline{v}_i + \overline{v}_0)c_i z_i = \overline{I} + \overline{v}_0 \Sigma c_i z_i = \overline{I}$$

The transport coefficients are then changed to

$$t_1' = t_1 + \overline{v}_0 c_1 / \overline{I} \quad (8)$$

$$t_i' = \overline{J}_i' z_i / \overline{I}' = t_i + \overline{v}_0 c_i z_i / \overline{I}$$

In this way the transport coefficients may be referred to any desired reference point. One reference point seems to be particularly convenient. A porous plug inserted in the liquid will have the mass average velocity of the liquid provided that viscous drag along the walls is negligible and provided that the plug is free of electrophoretic effects. Diffusion potentials and transference numbers in molten salts are ordinarily measured with reference to such a porous plug. In any event it is important that the transference number occurring in the expression for the diffusion potential be expressed in terms of the same reference velocity as is used in expressing the gradients of concentration and potential.

It is a pleasure to acknowledge assistance to this work from the United States Atomic Energy Commission (Contract AT 30-1 1837).

## THE ADSORPTION OF CATIONS BY ANIONIC FOAMS<sup>1</sup>

BY CHEVES WALLING,<sup>2</sup> EDGAR E. RUFF AND JAMES L. THORNTON, JR.

Contribution from the Research and Development Division of Lever Brothers Co., Edgewater, N. J.

Received November 23, 1956

A study of the relative adsorption of calcium and sodium ion by N-palmitoyl methyl taurine foams indicates a strong preferential adsorption of calcium ion by the anionic surface layer. Quantitative interpretation of the phenomenon is however complicated by a competitive preferential adsorption of calcium ion by micelles in the solution being foamed. Similar preferential adsorption of a number of other cations by anionic foams has also been demonstrated, polyvalent ions being, in general, the most strongly held, and the relation of this absorption to foam properties is discussed.

The layer of an anionic surfactant adsorbed at an air-water interface must have associated with it an equivalent quantity of cations in order to neutralize its electric charge. In general such ions, bound by a colloid phase are termed "gegenions." The fact that insoluble surface films such as stearic acid, show very strong preferential adsorption of certain

ions was strikingly demonstrated many years ago by Langmuir and Shaefer,<sup>3</sup> and the subject has recently been investigated further by Havinga.<sup>4</sup> The possibility that a similar preferential adsorption might take place with soluble films occurred to us, and has now been investigated, using the apparatus for the study of foam compositions and foam drainage properties which we have recently de-

(1) Presented in part before the Colloid Division at the meeting of the American Chemical Society, Buffalo, New York, March, 1952.

(2) Department of Chemistry, Columbia University, New York 27, N. Y.

(3) I. Langmuir and V. J. Schaefer, *J. Am. Chem. Soc.*, **59**, 2400 (1937).

(4) E. Havinga, *Rec. trav. chim.*, **71**, 72 (1952).

scribed.<sup>5</sup> Results indicate that surface films do show a strong preferential adsorption of polyvalent ions such as calcium and magnesium, even in systems where the calcium and magnesium salts of the surfactant employed are entirely soluble.

### Experimental

The foam apparatus employed is essentially a device for producing and collecting foam from surfactant solutions under such conditions that the amount (and, in particular, the relative amount) of any component adsorbed in the foam surface may be calculated from an analysis of the foam. It has been described in detail in our previous paper.<sup>5</sup>

The surfactant employed in most of our measurements was a single preparation of the sodium salt of palmitoyl methyl taurine (NaPMT), *i.e.*,  $C_{15}H_{31}CON(CH_3)CH_2CH_2SO_3Na$ . It was prepared from a batch of technical material containing soap and inorganic salts, by slurring with hot 95% ethanol, adjusting to pH 4, filtering hot with the aid of Super-cel and allowing to crystallize. The crystalline product was washed with acetone and cold water, redissolved in hot alcohol, refiltered through Super-cel until clear, and again allowed to crystallize. The product was given a final wash with acetone and dried *in vacuo* at 60°. The final material was free from soap, but probably contained traces of stearyl methyl taurine, since the initial palmitic acid was a technical grade consisting of 90% palmitic, 4% oleic and 6% stearic acids. In experiments using additional surfactants, sodium "Oronite" (the sodium salt of technical dodecylbenzenesulfonic acid) was the same sample as used in the work described previously.<sup>5</sup> Initial experiments with NaPMT were carried out using ordinary laboratory distilled water. However, although this water had a conductivity corresponding to only 2 p.p.m. of sodium chloride, it was found to contain significant quantities of cations which were strongly adsorbed by PMT foams. In the collected foams these had the titration properties of calcium or magnesium by our analytical method (see below). Continued foaming of such a NaPMT solution until no more strongly adsorbed ions could be detected in the foam indicated an initial concentration of the ions of  $9.5 \times 10^{-6} M$ . That the NaPMT was not the source of the contaminating ions was shown by adding more to the "cleansed" solution at this point and collecting additional foam. This foam gave no titration for  $Ca^{++}$  or  $Mg^{++}$ . Investigation of water deionized through a mixed bed of cation- and anion-exchange resins showed that it was free of whatever strongly adsorbed ions were present in the distilled water although it had a similar conductivity. The preliminary results reported earlier<sup>1</sup> were determined before this difficulty was recognized, and have accordingly been revised somewhat here.

In the analyses of collected foams, PMT and "Oronite" ions were determined by cetylpyridinium bromide (CPB) titration.<sup>5</sup> Calcium, magnesium and zinc were determined by titration with ethylenediaminetetraacetic acid, using Eriochrome black as indicator, as described by Betz and Noll.<sup>7</sup> Other ions were determined by essentially standard quantitative procedures.

In analyzing our data, the difference in concentration of any component in a collected foam and in the solution from which the foam has been generated has been considered as material adsorbed at the surface or (in the case of a gegenion) held by the surface-adsorbed layer. The basis and validity of this assumption is discussed in detail in our previous paper.<sup>5</sup> Thus, if concentrations are expressed in moles/l., the resulting difference is a concentration of surface-adsorbed material in moles/l. of collapsed foam. In most of our work here, relative values of this quantity for different ions are all that are required. However, since the foam area/liter of collapsed foam may be determined from the foam density and average bubble size, the concentration per unit area of foam surface (usually expressed  $\text{\AA}^2/\text{molecule}$ ) also may be calculated. In our studies, the concentrations of surfactant and "added" ion were generally determined directly by analysis, and the amount of sodium ion held in

the surface determined as the amount required to neutralize the charge of the additional surfactant not associated with the other cation. Such a calculation would be in error if additional anion (*e.g.*, chloride ion) were somehow held by the foam surface. This possibility has been investigated for the NaPMT +  $CaCl_2$  system, and no concentration of chloride ion in the foam was found above that in the bulk solution. Since such an occurrence seems unlikely on other grounds, it has been assumed not to occur in the other systems. In experiments involving very strongly adsorbed ions, additional sodium ion (as sodium chloride) was generally added to the solution in order to provide a high sodium to other ion ratio and still have enough of the other ion present to prevent its rapid depletion during the foaming of the solution. By this device, changes in concentration of the strongly adsorbed ion have been kept down to under 25%. Whenever they have exceeded 10%, averaged values of the concentration in the foamed solution have been employed in calculation of distribution-ratios (see below).

All experiments were carried out at a rate of foam rise of 5.41 mm./sec. and, with the exception of the experiment with silver ion, at 28°. Results of all foaming experiments are listed in the tables.

Ion-exchange experiments were carried out by stirring solutions with IR-120 cation-exchange resin (a sulfonated cross-linked polystyrene manufactured by the Rohm & Haas Co.) in the sodium form for 1 hr., followed by titration of the supernatant solution for calcium ion. Since the solutions were very dilute ( $5 \times 10^{-4} M$ ) 500-ml. aliquots were taken and concentrated to 100–150 cc. before titration. The capacity of the resin was determined by conversion to the hydrogen form and titrating with 0.5 *N* NaOH to the phenolphthalein end-point.

### Discussion of Results

**Ca-Na-PMT System.**—Results of foaming experiments on  $Ca^{++}$ - $Na^+$ -PMT systems are listed in Table I, with the tendency of the foam surface to absorb one ion preferentially expressed in terms of an empirical distribution coefficient *R* such that

$$R = \frac{b_s/a_s}{b/a} \quad (1)$$

Here *a* and *b* are concentrations of  $Na^+$  and  $Ca^{++}$ , respectively, and subscript *s*'s refer to gegenions held by the surface layer. Since *R*'s are larger than unity they show that our foams selectively remove  $Ca^{++}$  in preference to  $Na^+$  by an appreciable factor and thus provide a convenient index of the amount of gegenion fractionation achieved by the system. On the other hand, *R*'s vary almost 4-fold between experiments, and, while we have not been able to devise a quantitative model for our system, we believe that a qualitative explanation of at least part of the variation can be given along the following lines.

One of the characteristic properties of surfactant solutions is that the surfactant molecules coalesce into clumps or micelles above some critical concentration for micelle formation (CMC). Further, the CMC is in general depressed by adding electrolytes, the effect depending primarily upon the ion of opposite charge to the surfactant<sup>8</sup> and increasing markedly with polyvalent ions.<sup>9,10</sup> Since these micelles strongly adsorb ions of opposite charge, and surround themselves with a cloud of gegenions, if present they may be expected to have a profound effect on the availability of such ions for adsorption

(5) C. Walling, E. E. Ruff and J. L. Thornton, Jr., *THIS JOURNAL*, **56**, 989 (1952).

(6) J. H. Jones, *J. Asen. Off. Agricultural Chemists*, **28**, 398 (1945).

(7) J. D. Betz and C. A. Noll, *J. Am. Water Wks. Assn.*, **42**, No. 1 (Jan. 1950).

(8) M. L. Corrin and W. D. Harkins, *J. Am. Chem. Soc.*, **69**, 683 (1947).

(9) A. W. Ralston, D. N. Eggenberger and F. K. Broome, *ibid.*, **71**, 2145 (1949).

(10) H. Langer, *Koll. Z.*, **121**, 66 (1951).

TABLE I  
 ADSORPTION OF CALCIUM ION BY PMT FOAMS

Run	70	82	83	84	85	95
Foam collected, g./hr.	100	104	105	98	86	84
Av. bubble dia. (cm.)	0.34	0.35	0.35	0.42	0.44	0.40
Soln., moles/l. $\times 10^3$						
PMT	1.25	1.25	1.25	1.25	1.25	.50
Ca <sup>++</sup>	0.055	0.125	.0263	.25	.50	.125
Na <sup>+</sup>	1.25	1.25	1.25	2.50	5.00	1.25
Foam, moles/l. $\times 10^3$						
PMT	8.55	8.46	7.79	8.91	9.38	9.26
Ca <sup>++</sup>	1.75	2.42	.99	3.24	3.99	3.71
Na <sup>+</sup>	5.16	3.87	5.86	4.18	6.15	2.84
Surface, moles/l. $\times 10^3$						
PMT	7.30	7.21	6.54	7.66	8.13	8.76
Ca <sup>++</sup>	1.70	2.30	.97	2.99	3.49	3.59
Na <sup>+</sup>	3.91	2.62	4.61	1.68	1.15	1.59
$\bar{A}^2$ /PMT mcl.	54	48	56	43	44	48
R	9.9	8.8	10.0	17.8	30.3	21.8

by the surface layer of surfactant in our foams.<sup>11</sup> Further, since the physical structure of a micelle is considered to consist of a clump of surfactant molecules with their hydrocarbon "tails" together and their ionic groups exposed to the surrounding solution, it might be expected to show selective properties in its choice of gegenions similar to that of a surfactant layer in the surface of a foam.<sup>13</sup> If so, the micelles should exert a sequestering action on calcium ion, and, the greater the ratio of PMT in micellar form to calcium ion, the less Ca<sup>++</sup> should be available for surface adsorption. Such a picture is qualitatively in agreement with the data—the largest values of *R* in Table I are found when either the amount of Ca<sup>++</sup> is high (expt. 84–85) or when the amount of PMT is reduced (expt. 95), while the smallest value goes with the least amount of Ca<sup>++</sup> (expt. 83).

The sequestering action of PMT micelles can also be demonstrated independently and directly by equilibration with a cation-exchange resin. In Table II below, the relative amounts of Ca<sup>++</sup> and Na<sup>+</sup> ions adsorbed by IR-120 cation-exchange resin (a sulfonated cross-linked polystyrene) equilibrated with a solution containing NaCl and CaCl<sub>2</sub> is compared with the amounts adsorbed when a portion of the NaCl was replaced with NaPMT. A quantity of resin containing  $1 \times 10^{-3}$  moles of  $-\text{SO}_3^-$  groups was used in a liter of solution having the same ionic concentrations as expt. 85 in Table I. It is evident from Table II that the presence of PMT preferentially reduces the availability of Ca<sup>++</sup> in the solution, to a marked extent, since the frac-

tion of  $-\text{SO}_3^-$  groups in the resin binding Ca<sup>++</sup> at equilibrium is reduced from 0.241 to 0.077.

 TABLE II  
 EQUILIBRATION OF Ca<sup>++</sup>-Na<sup>+</sup> SOLUTIONS (1 LITER) WITH IR-120 CATION-EXCHANGE RESIN

Expt.	92	93
Initial quantities (moles $\times 10^3$ )		
IR-120 (Na form)	1.0	1.0
CaCl <sub>2</sub>	0.50	0.50
NaCl	4.50	3.25
NaPMT	0	1.25
Equilibrated		
Ca <sup>++</sup> in resin	0.241	0.077
Na <sup>+</sup> in resin	0.518	0.846

**Adsorption of Other Cations.**—In addition to our study of the Na<sup>+</sup>-Ca<sup>++</sup>-PMT system, a number of experiments have been carried out with eight other cations. Table III lists results obtained with Mg<sup>++</sup> in both NaPMT and "Oronite" forms. Results are similar for the two surfactants and indicate that Mg<sup>++</sup> is preferentially adsorbed somewhat more strongly than Ca<sup>++</sup>, although the differences in concentration prevent accurate comparison. Data on the remaining systems are shown in more condensed form in Table IV.

The results for Ag<sup>+</sup>, Cu<sup>++</sup> and Fe<sup>+++</sup> are less precise than the single value given implies, since they represent single experiments carried out using distilled rather than deionized water. The relatively low apparent adsorption for these ions may be due to partial filling of the surface by other polyvalent cations from the distilled water (*cf.* Experimental Part). Further, it should be pointed out that, in view of our experience with Ca<sup>++</sup>, for any ion the difference of *R* from unity should increase with a larger ratio of total cations to surfactant in micellar form.

The results among the univalent ions suggest an order of increasing adsorption  $\text{H}^+ < \text{Na}^+ < \text{K}^+ < \text{NH}_4^+$ . This order resembles that found with cation-exchange resins except for the apparent rather strong adsorption of  $\text{NH}_4^+$ , and at this point it

(11) Determination of the CMC of PMT solutions by the dye technique of Corrin and Harkins, *ref. 12*.

(12) M. L. Corrin and W. D. Harkins, *J. Am. Chem. Soc.*, **69**, 679 (1947), gives approximate values of  $4.5 \times 10^{-4} M$  in the absence of Ca<sup>++</sup> ion. Thus, in our system much of the surfactant is in micellar form.

(13) A similar picture of preferential adsorption of calcium ion by alkyl sulfonate micelles was suggested several years ago by H. V. Tartar and R. D. Cadle, *THIS JOURNAL*, **43**, 1173 (1939), to explain the solubility properties of mixed sodium and calcium alkyl sulfonates. For a more recent case involving anion adsorption by cationic micelles, *cf.* I. M. Kolthoff and W. F. Johnson, *J. Am. Chem. Soc.*, **74**, 20 (1952).

TABLE III  
ADSORPTION OF MAGNESIUM ION BY PMT AND THE OROHITE FOAMS

Run	71	72	74	58	59	61
Surfactant	PMT	PMT	PMT	Na Or.	Mg Or.	Na Or.
Foam collected, g./hr.	90	106	102	99	103	91
Av. bubble diam. (cm.)	0.44	0.40	0.40	0.36	0.35	0.38
Soln., moles/l. $\times 10^3$						
Surfactant	1.25	1.25	1.25	1.42	1.42	1.42
Mg <sup>++</sup>	0.114	0.250	0.0586	0.71	0.71	0.0233
Na <sup>+</sup>	6.25	6.25	3.125	15.64	14.64	1.42
Å. <sup>2</sup> /surfactant mol.	32	38	71	46	42	47
R	49.0	28.2	41.7	45.5	39.9	43.7

TABLE IV

ADSORPTION OF ADDITIONAL IONS BY PMT FOAM  
All solutions initially  $1.25 \times 10^{-3}$  PMT plus added ions.

Ion	Amt., (moles/l. $\times 10^3$ )	Foam col- lected, g./hr.	Å. <sup>2</sup> /PMT in sur- face	R
NH <sub>4</sub>	0.44	115	49	6.25
NH <sub>4</sub>	0.44	116	61	9.78
NH <sub>4</sub>	1.25	89	49	1.27
NH <sub>4</sub>	1.76	85	42	1.60
H <sup>+</sup>	0.54	77	57	0.70
H <sup>+</sup>	1.25	70	88	.58
H <sup>+</sup>	2.16	75	54	.72
K <sup>+</sup>	0.164	90	861	2.0
K <sup>+</sup>	0.658	45	135	1.2
K <sup>+</sup>	1.25	55	108	1.9
Zn <sup>++</sup>	0.0124	103	66	12.7
Zn <sup>++</sup>	.025	102	65	17.2
Zn <sup>++</sup>	.053	106	57	7.2
Ag <sup>+</sup> (50°)	1.25	59	48	0.76
Ca <sup>++</sup>	0.025	80	66	1.0
Fe <sup>+++</sup>	0.0198	89	51	4.3

might be noted that ion distributions between solution and both micelles and foam surfaces have rather obvious analogies to those existing between solutions and ion-exchange resins. This in turn suggests a plausible basis for a quantitative treatment of the phenomena which we have described. We have, in fact, attempted such an analysis of the situation, but it soon became evident that our data are inadequate for suitable test, and an independent determination of the micelle-solution distribution would be needed.

As far as we know, the results reported here are almost the only studies available of selective adsorption of gegenions by surface films of soluble surfactants. Recently Salley and co-workers<sup>14</sup> have noted an apparent surface hydrolysis (*i.e.*, adsorption of hydrogen or hydroxyl ions, respectively) by sodium di-*n*-octylsulfosuccinate and stearamidopropyl-2-hydroxyethylammonium sulfate, a result quite different from the small affinity for hydrogen ion shown by the anionic surfactant in our system. Since the reported hydrolysis occurred only at high dilution, and was detected as a

deficiency of sodium or sulfate (measured radiochemically) in the surface, this disagreement and our difficulties with distilled water suggest that the effect was actually produced by displacement of Na<sup>+</sup> or SO<sub>4</sub><sup>=</sup> by minute traces of more strongly adsorbed ions, rather than an actual hydrolysis.

**Effect of Adsorbed Ions on Foam Properties.**—The data in Tables I, III and IV also permit some observations on the effect of different cations on the drainage properties of PMT foams, and on the closeness of packing of the adsorbed surfactant layer at the bubble surfaces. NaPMT alone, at various concentrations, gives foams with the properties shown in Table VI.

TABLE V

PROPERTIES OF NaPMT FOAM					
5.41 mm./sec. bubble rise in 137 cm. column					
NaPMT concn. $\times 10^3$	5	2.5	1.25	0.625	0.468
Foam density (g./hr.)	81	80	73	69	60
Bubble diam. (cm.)	0.35	0.36	0.38	0.42	0.44
Surface excess $\times 10^3$	6.18	6.77	7.05	6.75	6.65
Å. <sup>2</sup> /molecule	77	69	69	73	77

Addition of even small quantities of the strongly adsorbed divalent ions Ca<sup>++</sup>, Mg<sup>++</sup> and Zn<sup>++</sup> leads to considerably wetter foams (90–106 g./hr.) and closer packing of the PMT surface layer (32–66 Å.<sup>2</sup>/molecule).

In contrast, addition of univalent ions produces variable results. Ammonium ion gives a wet foam with a closely packed surface, potassium gives a relatively dry foam with a loosely packed surface, while hydrogen ion, which is only weakly adsorbed, has little effect on foam density and slightly increases packing.

The results with the divalent ions appear reasonable, since as each is bound to the surface-layer by the charges of two surfactant molecules, the resulting unit (perhaps in the form of an actual ion-triplet) might well be rather compact. They are also interesting in that they suggest a mechanism for the different foaming properties of synthetic detergents in hard and soft water, in spite of their complete solubility in the presence of divalent ions.

(14) C. M. Judson, A. A. Lerew, J. K. Dixon and D. J. Salley *J. Chem. Phys.*, **20**, 519 (1952).

# THE CRYSTAL STRUCTURE OF TETRAPHENYLARSONIUM TETRACHLOROFERRATE(III), $(C_6H_5)_4AsFeCl_4$

BY B. ZASLOW AND R. E. RUNDLE

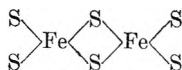
Contribution No. 499 from the Institute for Atomic Research and Department of Chemistry, Iowa State College, Ames, Iowa  
[Work was performed in the Ames Laboratory of the U. S. Atomic Energy Commission]

Received December 17, 1956

The crystal structure of  $(C_6H_5)_4AsFeCl_4$  is tetragonal,  $a = 13.16 \text{ \AA}$ . and  $c = 7.15 \text{ \AA}$ ., with space group  $I\bar{4}$ , and two formula units per unit cell. The  $FeCl_4^-$  ion is a tetrahedron, flattened along  $z$ , with an Fe-Cl bond distance of  $2.19 \pm 0.03 \text{ \AA}$ . and Cl-Fe-Cl bond angles of  $114.5$  and  $107.0^\circ$ . In contrast with the iodide salt, where the tetraphenylarsonium ion has at least very nearly  $D_{2d}$  symmetry with the phenyl planes normal to the mirror planes, the cation mirror planes are destroyed in the tetrachloroferrate(III) compound by a  $28^\circ$  rotation of the planes of the phenyl groups about the As-C bonds. Although the  $FeCl_4^-$  ion is tetrahedral with five unpaired electrons, both the short Fe-Cl distance and an MO treatment suggests that iron 3d-orbitals are involved in bonding to chlorine.

## Introduction

There is convincing chemical evidence for a  $FeCl_4^-$  ion with five unpaired electrons.<sup>1,2</sup> The usual directed-valence approach interprets this to mean that no  $d$ -orbitals are involved in the bonding, which then makes use only of the fourth shell  $sp^3$  metal orbitals to give a tetrahedral structure. Such a geometrical configuration is not unique to this complex. The electron diffraction data of Hassel and Viervoll<sup>3</sup> are compatible with a tetrahedral bridge structure for the gaseous dimer of  $FeCl_3$ , and tetrahedral



chains are found in  $KFeS_2$ .<sup>4</sup>

The  $(C_6H_5)_4As^+$  ion has already been studied by single crystal X-ray diffraction in the iodide salt.<sup>5</sup> Here the point symmetry of the ion is at least approximately  $D_{2d}$ , with phenyl rings normal to the mirror planes, although the crystallographic point symmetry at the arsenic atom is only 4.

This paper both confirms and extends the existing information on the  $FeCl_4^-$  and  $(C_6H_5)_4As^+$  species. It suggests, as well, that the hybrid-orbital, directed-valence interpretation of the electronic structure of the  $FeCl_4^-$  ion is inappropriate.

## Experimental Methods

The tetraphenylarsonium tetrachloroferrate(III) crystals, furnished by Professor Harold Friedman, were yellow, tetragonal needles, elongated along  $c$ , and stable to air; the crystal used for intensity measurements had faces of the forms  $\{100\}$  and  $\{110\}$  (only six of the eight were sufficiently well-developed to measure with an optical goniometer), and approximated a cylinder of  $0.04 \text{ mm}$ . radius.

The  $\{hkl\}$  data were taken on a Weissenberg camera, using Cu K radiation and a combined timed exposure and multiple film technique, while a precession camera using Mo K radiation with the timed exposure method supplied the  $\{h0l\}$  data. Intensity estimates were determined visually.

General reflections  $\{hkl\}$  were examined on higher levels of both Weissenberg and precession photographs so as to confirm the Laue class, but intensity measurements of these reflections were not made.

## Determination of the Structure

Lattice constants of  $(C_6H_5)_4AsFeCl_4$  are  $a = 13.160 \pm 0.005 \text{ \AA}$ . (from a back-reflection Weis-

senberg photograph) and  $c = 7.15 \pm 0.02 \text{ \AA}$ . The Laue class is  $C_{4h}$ . A calculated density of  $1.56 \text{ g./cc.}$  for two formula units in the unit cell agrees with an experimental density of  $1.55 \text{ g./cc.}$  obtained by the flotation method.

Systematic extinction of  $\{hkl\}$  reflections occurs for  $h + k + l = 2n + 1$ . Since, of the  $\{00l\}$  reflections, only (008) was observed, the following were admitted as possible space groups:  $I\bar{4}$ ,  $I4_1$ ,  $I4$  and  $I4/m$ . However, requiring a fourfold inversion axis for the central atom of either the  $(C_6H_5)_4As^+$  ion or the  $FeCl_4^-$  ion is sufficient to fix the space group as  $I\bar{4}$ .

The appropriate Lorentz and polarization factors were used to correct the intensity estimates to structure factors. No corrections were made for absorption; the James and Brindley atom form factors<sup>6</sup> were employed in structure factor computations. No calculations were made involving hydrogen atoms. The two sets of data,  $\{hk0\}$  and  $\{h0l\}$ , were treated independently.

TABLE I

ATOMIC PARAMETERS ASSOCIATED WITH THE  $b$ -AXIS AND  $c$ -AXIS PROJECTIONS<sup>a</sup>

	$z_b$	$x_c$	$y_b$	$y_c$	$z_b$
As	0.000		0.000		0.000
Fe	.000		.500		.250
Cl		0.038	.364	0.366	.084
C <sub>1</sub>	.047	.047	.112	.111	.841
C <sub>2</sub>	.978	.984	.157	.162	.722
C <sub>3</sub>	.010	.003	.238	.231	.608
C <sub>4</sub>	.112	.100	.271	.268	.616
C <sub>5</sub>	.180	.176	.224	.219	.736
C <sub>6</sub>	.147	.147	.143	.139	.850

<sup>a</sup>  $x_b$ ,  $y_b$  and  $z_b$  are parameters from the  $b$ -axis projection;  $x_c$  and  $y_c$  are from the  $c$ -axis projection. The  $y$  parameters for the chlorine and carbon atoms also appear in the  $b$ -projection as the  $x$  values of an alternate set of general positions.

Only the  $c$ -axis projection is centrosymmetric, and it, therefore, represented a favorable starting point in the structural analysis. Arsenic and iron atoms were placed at the special positions (a) and (c), *i.e.*,  $000$ ,  $1/2^1/2^1/2$ , and  $0^1/2^1/4$ ,  $1/2^03/4$ . These two sets of atoms scatter in phase for wave amplitudes in the  $\{hk0\}$  data set having an even  $h$  index. The  $x$  and  $y$  chlorine parameters were obtained

(6) "Internationale Tabellen zur Bestimmung von Kristallstrukturen," Borntraeger, Berlin, 1935, p. 571.

(1) H. L. Friedman, *J. Am. Chem. Soc.*, **74**, 5 (1952).  
 (2) D. E. Metzler and R. J. Myers, *ibid.*, **72**, 3776 (1950).  
 (3) O. Hassel and H. Viervoll, *Acta Chem. Scand.*, **1**, 149 (1947).  
 (4) J. W. Boon and C. H. MacGillavry, *Rec. trav. chim. Pays-Bas*, **61**, 910 (1942).  
 (5) R. C. L. Moorley, *J. Am. Chem. Soc.*, **62**, 2995 (1940).

from an electron density computation using only this partial set of amplitudes.

The phases resulting from structure factor calculations with As, Fe and Cl atoms did not, however, lead to resolution of the phenyl ring in the subsequent electron density map. A regular tetrahedral configuration was assumed for the  $\text{FeCl}_4^-$  ion, and a trial model was constructed for the  $(\text{C}_6\text{H}_5)_4\text{As}^+$  ion, the orientation of which was varied by rotation about the  $c$ -axis in order to obtain the most acceptable interionic contacts. Resulting carbon parameters provided phases good enough to resolve a projected phenyl ring.

The trial model represented the  $(\text{C}_6\text{H}_5)_4\text{As}^+$  ion structure as having the following features: regular tetrahedral symmetry of carbon atoms about the As atom, retention of the known geometry of the benzene ring, an  $\text{As}-\text{C}_1$  distance of 1.95 Å., colinearity for  $\text{As}-\text{C}_1-\text{C}_4$ , and the restriction that  $\text{C}_2$  and  $\text{C}_6$  have the same  $z$  parameter. In this description the carbon atom notation of Fig. 1 was used. Refinement necessitated a shift from the original  $(\text{C}_6\text{H}_5)_4\text{As}^+$  ion orientation, and the tipping of the benzene ring about the  $\text{As}-\text{C}_1-\text{C}_4$  axis to the extent of  $28^\circ$ , lowering the ion symmetry to  $\bar{4}$ .

For the  $\{hk0\}$  data, Fig. 2 represents a final electron density map. The atomic parameters, corrected for series termination error using a calculated Fourier, are listed in Table I, while the corresponding phases are given in Table II.<sup>7</sup> Peak maxima were located using Booth's method.<sup>8</sup>

The  $b$ -axis projection affords resolution of the chlorine  $z$  parameter, which is needed in order to obtain a good Fe-Cl bond distance. Carbon coordinates,  $x_b$ ,  $y_b$  and  $z_b$  used for this analysis are listed in Table I; these are assumed coordinates which correspond within 0.02 Å. to the refined trial model of the  $(\text{C}_6\text{H}_5)_4\text{As}^+$  ion described above. Starting with a regular tetrahedral  $\text{FeCl}_4^-$  ion, refinement cycles employing back-shift corrections were made until no further parameter shifts resulted for the Cl atom. The carbon positions were not moved during this analysis.

Final values for chlorine coordinates are listed in the  $y$  and  $z$  columns of Table I; the electron den-

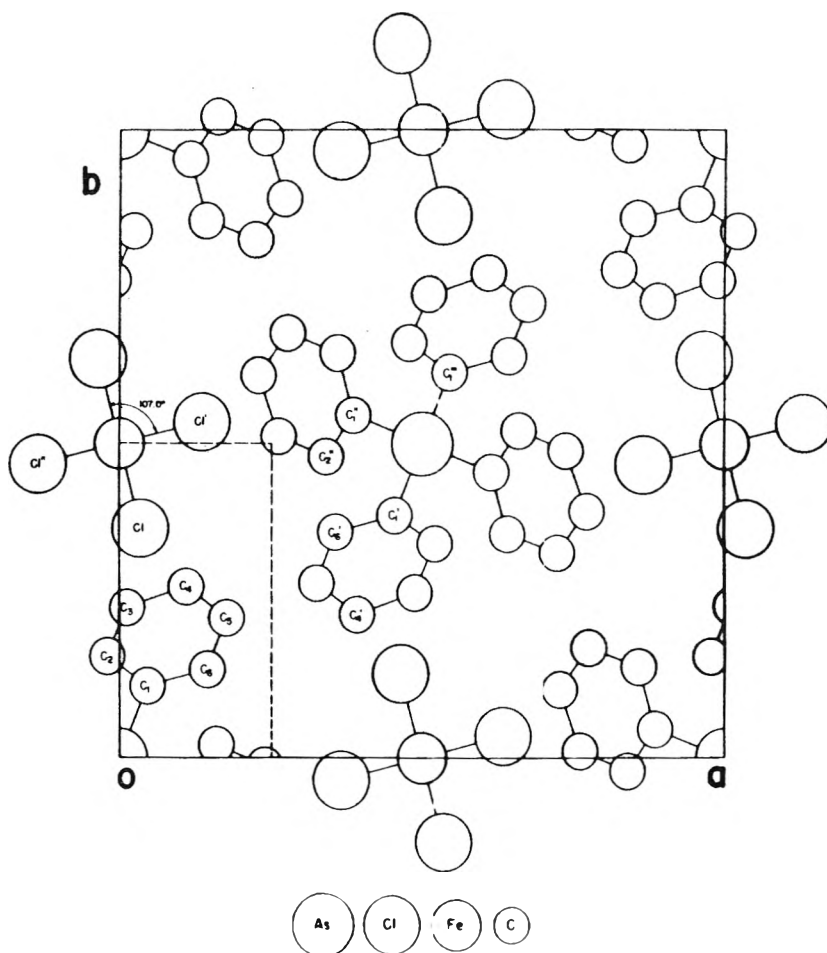


Fig. 1.—Atomic arrangement in the  $c$ -axis projection. The asymmetric unit is shown by broken lines.

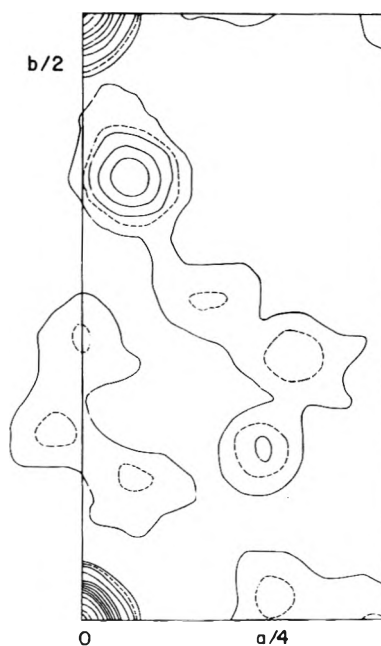


Fig. 2.—Projection of the asymmetric unit in the unit cell along the  $c$ -axis. Solid contours are equally spaced and of arbitrary increment; the dotted contour represents a  $1/2$  increment.

(7) For Table II order Document 5132 from the American Documentation Institute, Auxiliary Publication Project, Photoduplication Service, Library of Congress, Washington 6, D. C., remitting \$1.25 for microfilm or \$1.25 for photocopies by check or money order payable to Chief of Photoduplication Service, Library of Congress.

(8) A. D. Booth, "Fourier Techniques in X-ray Organic Structure Analysis," University Press, Cambridge, 1948, pp. 62-65.

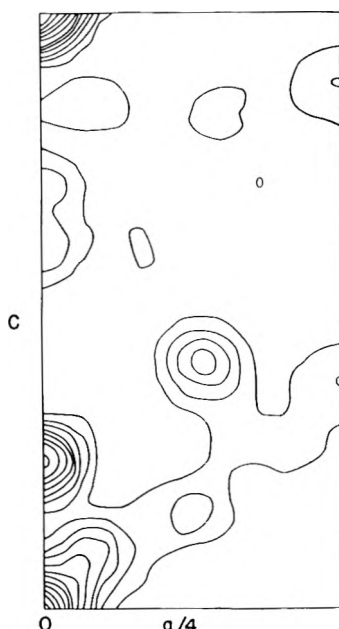


Fig. 3.—Projection of the asymmetric unit in the unit cell along the  $b$ -axis. Contours are equally spaced and of arbitrary increment.

sity map and the corresponding atomic arrangement are shown in Figs. 3 and 4. Overlap prevents a determination of the chlorine coordinate that would appear in the  $x_b$  column of Table I. The phases employed with the  $\{h0l\}$  data appear in Table II.

#### Error Treatment

Standard deviations of random errors were determined using Cruickshank's procedure,<sup>9</sup> which was modified appropriately for two dimensional electron density projections. For the  $c$ -axis projection  $\sigma(A_h) = 3.05 \text{ e./\AA}^3$ ; for the  $b$ -axis projection  $\sigma(A_h) = 2.51 \text{ e./\AA}^3$  and  $\sigma(A_l) = 2.43 \text{ e./\AA}^3$ . The  $(\partial^2\rho/\partial r^2)_{r=0}$  value and the resultant  $\sigma(x)$  and  $\sigma(z)$  values are listed in Table III;  $\sigma$ -values from the non-centro-symmetric data have been doubled.<sup>10</sup>

TABLE III

	c-Axis projection		b-Axis projection		
	$(\frac{\partial^2\rho}{\partial r^2})_{r=0}$ , e./\AA. <sup>3</sup>	$\sigma(x)$ , \AA.	$(\frac{\partial^2\rho}{\partial r^2})_{r=0}$ , e./\AA. <sup>3</sup>	$\sigma(x)$ , \AA.	$\sigma(z)$ , \AA.
Cl	-250	0.01	-240	0.02	0.02
C	-75	.04	...	...	...

The carbon atoms exert a strong influence on the calculated  $\{hk0\}$  structure factors, while at the same time they are difficult to locate accurately on an electron density map. Shifts in the phenyl ring location, which must move as a unit, can easily cause phase changes for small structure factors. To obtain an estimate of the magnitude of the displacement of a peak maximum due to a single incorrect phase angle, an electron density projection with the change in sign from positive to negative for the  $(2,12,0)$  term, a typical term with a

small structure factor, was calculated. Coördinate differentials were thus obtained. For the Cl maximum, the shift amounted to 0.01 \AA. for each coordinate; if each carbon shift is treated as a residual, the standard deviation of this error for carbon coordinate parameters is 0.03 \AA.

We feel that  $\pm 0.03 \text{ \AA.}$  represents a good estimate for  $\sigma(d)$ , the standard deviation of the Fe-Cl bond.

#### Discussion

**Description of the Crystal Structure.**—The parameters listed in Table I represent an approximate tetraphenylarsonium ion structure, although the carbon positions are sufficiently well located so as not to interfere with an Fe-Cl bond distance determination. The reliability index,  $R_{(hkl)} = \sum_{hkl} |F_0| - |F_c| \div \sum_{hkl} |F_0|$ , omitting unobserved reflections, is 0.18 for  $\{hk0\}$  data and 0.12 for  $\{h0l\}$  data; the constants used in the isotropic temperature factor corrections for these two data sets are 2.71 and 3.52, respectively.

The large standard deviations found for the carbon parameters tend to discourage any additional refinement procedure using only two-dimensional data. One such attempt retaining As-C<sub>1</sub>-C<sub>4</sub> colinearity, but with a 1.97 \AA. As-C<sub>1</sub> distance and a 105.5° C<sub>1</sub>'-As-C<sub>1</sub>''' angle, led to poorer reliability indices than those reported above.

Contact distances are listed in Table IV; these distances were calculated using  $b$ -projection parameters from Table I, and are not significant to better than 0.10 \AA. All carbon atoms of a phenyl ring are approximately equidistant from an associated Cl atom, although close contact with other Cl atoms exists for C<sub>3</sub>, C<sub>4</sub> and C<sub>6</sub>. Carbon-carbon contacts between atoms of neighboring phenyl groups on the same (C<sub>6</sub>H<sub>5</sub>)<sub>4</sub>As<sup>+</sup> ion are comparable to distances found by Mooney<sup>5</sup> for the iodide salt; however, the closest interionic C-C distance in the FeCl<sub>4</sub><sup>-</sup> compound is 0.35 \AA. larger than that found in the iodide structure.

Mooney<sup>5</sup> established that the tetraphenylarsonium ion configuration in the iodide salt was approximately D<sub>2d</sub>, with phenyl groups normal to the mirror planes. In the FeCl<sub>4</sub><sup>-</sup> compound, rotation of the phenyl groups about the As-C axis destroys the mirror planes. This versatility of form undoubtedly helps account for the effectiveness of the (C<sub>6</sub>H<sub>5</sub>)<sub>4</sub>As<sup>+</sup> ion as a precipitating agent.

The FeCl<sub>4</sub><sup>-</sup> ion in the tetraphenylarsonium compound is a flattened tetrahedron with a true 4 axis; the Cl-Fe-Cl angles are 114.5  $\pm$  1.5° and 107.0  $\pm$  1.5°, and the Fe-Cl bond distance is

TABLE IV

ION CONTACT DISTANCES			
Distance, \AA.		Distance, \AA.	
Atoms	Distance, \AA.	Atoms	Distance, \AA.
C <sub>1</sub> '-C <sub>1</sub> '''	3.20	C <sub>1</sub> -Cl	3.75
C <sub>6</sub> '-C <sub>1</sub> '''	3.40	C <sub>2</sub> -Cl	3.85
C <sub>6</sub> '-C <sub>2</sub> '''	3.45	C <sub>3</sub> -Cl	3.80
C <sub>5</sub> -C <sub>4</sub> '	3.85	C <sub>4</sub> -Cl	3.70
C <sub>4</sub> -Cl'	3.80	C <sub>5</sub> -Cl	3.65
C <sub>6</sub> '-Cl'	3.75	C <sub>6</sub> -Cl	3.65
C <sub>3</sub> -Cl''	3.80		

\* Intraionic. Others are interionic.

(9) D. W. J. Cruickshank, *Acta Cryst.*, **2**, 65 (1949).

(10) D. W. J. Cruickshank, *ibid.*, **3**, 72 (1950).

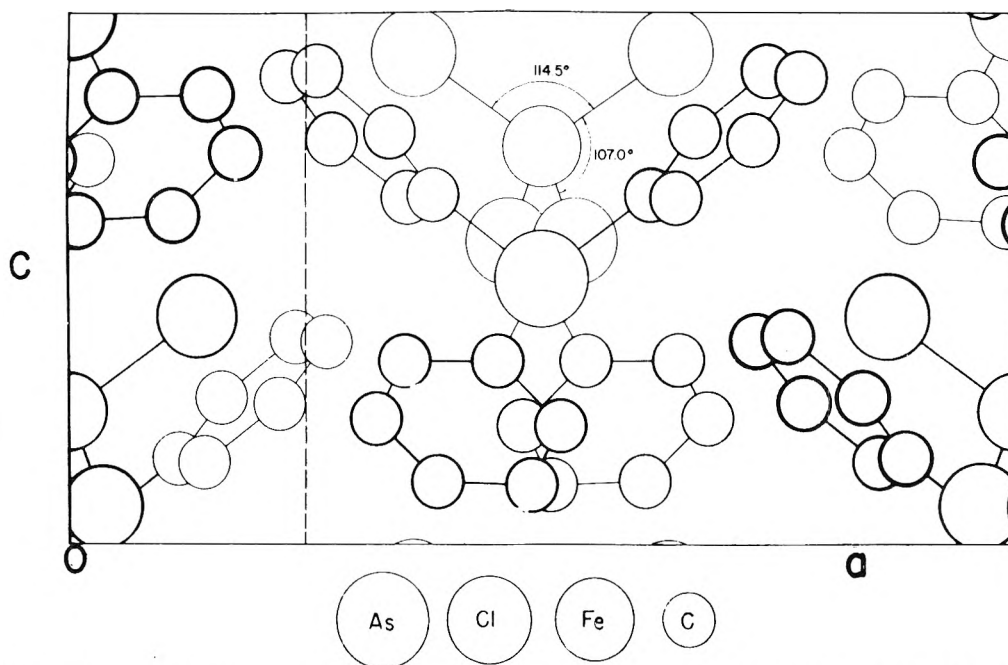


Fig. 4.—Atomic arrangement in the *b*-axis projection. The asymmetric unit is shown by broken lines.

$2.19 \pm 0.03$  Å. This distance is comparable to 2.17 Å., the shortest Fe-Cl distance found in the  $\text{FeCl}_2$  gaseous dimer as determined by electron diffraction.<sup>3</sup>

Although tetrahedral covalent and ionic radii are not directly available for computing Fe-Cl bond lengths, it is of interest to obtain estimates of these quantities. The single bond, tetrahedral, and predominantly covalent radius for Ga(III) can be used to set a lower limit for an Fe(III) radius in which only 4s and 4p orbitals of iron are used in bonding; this leads to a covalent distance of  $> 2.25$  Å.

Solid  $\text{FeCl}_3$ , with octahedral coordination of Cl about Fe, has a magnetic moment corresponding to five unpaired electrons and an Fe-Cl distance<sup>11</sup> of 2.48 Å. Using the magnetic data as an indication (by no means conclusive) of ionic bonding, a correction for the effect of change of coordination number from six to four results in a 2.41 Å. bond length for a predominantly ionic Fe-Cl bond.

**Electronic Structure of the  $\text{FeCl}_4^-$  ion.**—The Fe-Cl distance of 2.19 Å. is shorter than a bond length expected from valence bond considerations for a  $\text{FeCl}_4^-$  ion of either covalent  $4s4p^3$  or ionic character. This suggests that 3d orbitals participate in the bonding in the complex. It is noteworthy that the single-bond metallic radius of iron, where 3d-orbitals are used,<sup>12</sup> plus the chlorine radius lead to an Fe-Cl distance of 2.16 Å., in reasonable agreement with the observed distance. This is incompatible with the usual hybrid-orbital directed-valence theory.

It is becoming increasingly clear that the directed-valence theory, in its usual form, is unreliable when applied to transition metal complexes with odd-electrons, since evidence is accumulating that odd-electrons are usually contained in anti-

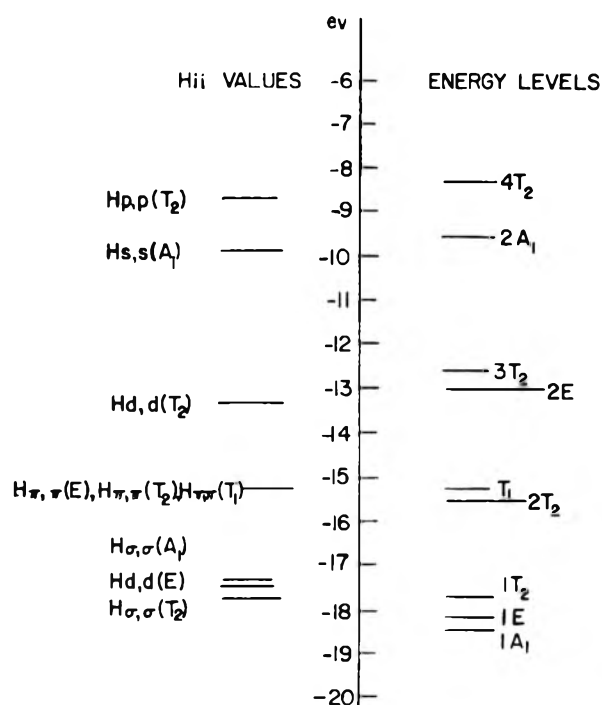


Fig. 5.—Energy levels for a  $\text{FeCl}_4^-$  complex having a +1.40 charge on the Fe atom. On the left are the energy levels determined by a crystal-field treatment for an ion with the final charge distribution.  $\sigma$  and  $\pi$  refer to chlorine (ligand) orbitals, while d, s, and p refer to the 3d-, 4s- and 4p-orbitals of iron. On the right are the resulting MO's for the  $\text{FeCl}_4^-$  ion. E, A and T are symbols for the various irreducible representations and are identical with those used by Wolfsberg and Helmholz.<sup>14</sup>

bonding orbitals,<sup>13</sup> and these orbitals are usually omitted from consideration in valence bond treatments. Moreover, transition metal-halide complexes often contain  $\pi$ -type interactions of a type

(11) N. W. Gregory, *J. Am. Chem. Soc.*, **73**, 472 (1951).

(12) L. Pauling, *ibid.* **69**, 542 (1947).

(13) J. H. E. Griffiths and J. Owens, *Proc. Roy. Soc. (London)*, **A226**, 6 (1954); B. P. McGarvey, *This Journal*, **60**, 71 (1956).

awkward to describe in valence bond terms, and not easy to fit into the bond-overlap criteria of Pauling. The directed-valence theory can be "made to fit" these complexes by three-electron bond schemes, etc., but under these circumstances it loses its simplicity and most of its usefulness.

We have undertaken some molecular orbital calculations to study the bonding in  $\text{FeCl}_4^-$  from an alternate viewpoint. The complex ion was assumed to be a regular tetrahedron, and the orbitals considered were the same as those of Wolfsberg and Helmholz.<sup>14</sup> The Wolfsberg-Helmholz approximation did not prove to be appropriate to this problem; instead, crystal-field effects which could not be ignored here, were accounted for in the evaluation of matrix elements, according to a method developed by Richardson.<sup>15</sup> Exchange, however, was completely neglected in these calculations. Computational details will be published elsewhere.

The final charge distribution resulting from the self-consistent cyclic process used was +1.40 for the Fe atom and -0.60 for each Cl atom. This is indicative of a complex of mixed ionic and covalent character. Energy levels are shown in Fig. 5. With 24 electrons filling the lower molecular orbitals, the remaining five available electrons can be placed unpaired in the 2E and 3T<sub>2</sub> levels which have nearly the same energy (Fig. 5). The resultant energy scheme is consistent with the magnetic properties of the complex, and also with the observed spectrum.<sup>2</sup> The pertinent wave functions are listed in Table V.

Final 1A<sub>1</sub> and 1T<sub>2</sub> functions, though energetically bonding, took on an antibonding appearance,

(14) M. Wolfsberg and L. Helmholz, *J. Chem. Phys.*, **20**, 837 (1942).

(15) J. W. Richardson, Ph.D. thesis, Iowa State College Library, Ames, Iowa, 1956.

probably as a consequence of the omission of exchange terms. The 1E molecular orbital (d- $\pi$  interaction) was strongly bonding and, as a consequence,

TABLE V

MOLECULAR WAVE FUNCTIONS FOR  $\text{Fe}^{+1.40}\text{Cl}^{-0.60}$ 

Representation	Wave function
1 A <sub>1</sub>	0.41 (4s) - 1.15 ( $\sigma$ )
1 E	.80 (3d) + 0.36 ( $\pi$ )
2 E	.74 (3d) - 1.02 ( $\pi$ )
1 T <sub>2</sub>	1.02 ( $\sigma$ ) - .10 ( $\pi$ ) - 0.01 (3d) - 0.14 (4p)
2 T <sub>2</sub>	0.01 ( $\sigma$ ) + .98 ( $\pi$ ) + .18 (3d) + .15 (4p)
3 T <sub>2</sub>	.17 ( $\sigma$ ) + .42 ( $\pi$ ) - 1.03 (3d) + .07 (4p)

the 2E level, containing two of the unpaired electrons, is antibonding with considerable chlorine contribution. Even 3T<sub>2</sub> contains ligand (chlorine)  $\sigma$ - and  $\pi$ - character. The 3d-orbitals of the iron atom are relatively unimportant in forming  $\sigma$ -bonds, but they are important in  $\pi$ -bonding, thereby helping to explain the short Fe-Cl distance. It appears that neither the hybrid-orbital directed-valence theory nor the crystal-field theory is sufficiently accurate to account for the electronic structure of the  $\text{FeCl}_4^-$  ion, since the MO's for the odd electrons are not localized on iron, but are antibonding, and since the energy levels are quite dependent upon overlap. Though it is desirable to repeat this calculation including exchange, the above conclusions seem qualitatively reliable.

**Acknowledgments.**—The authors are indebted to Prof. Harold Friedman not only for supplying crystals of the compound, but also for calling our attention to this problem. The aid of Dr. James W. Richardson in the MO treatment is also gratefully acknowledged.

## NOTES

### THE POLYTUNGSTATES AND THE COLLOIDAL NATURE AND THE AMPHOTERIC CHARACTER OF TUNGSTIC ACID

BY S. E. S. EL WAKKAD AND H. A. RIZK

Department of Chemistry, Faculty of Science, University of Cairo, Cairo, Egypt

Received July 20, 1956

Earlier study of tungstic acid by the titration of an alkali tungstate with hydrochloric acid was due to Hundeshagen,<sup>1</sup> Herting,<sup>2</sup> and Lind and Trueblood.<sup>3</sup> Afterwards, Britton<sup>4</sup> by back-titrating an alkaline solution of sodium tungstate with hydro-

chloric acid in the presence of the hydrogen electrode was able to carry out measurement until pH 4. Later, Britton and German<sup>5</sup> using the quinhydrone electrode followed the complete titration. The results obtained in that investigation threw light on the paratungstate and the metatungstate. This is here further clarified by studying the variations in both the hydrogen and the chloride ion activities during the successive additions of hydrochloric acid. The amphoteric character of tungstic acid was investigated by determining the solubility of tungsten trioxide in hydrochloric acid solutions of different concentrations.

#### Experimental

(A).—The sodium tungstate solutions were prepared by dissolving the Analar sample of sodium tungstate (99.97%) in three times redistilled water. Protection of the solutions

(1) F. Hundeshagen, *Chem.-Z.*, **18**, 547 (1894).

(2) O. Herting, *Z. angew. Chem.*, **14**, 165 (1901).

(3) S. C. Lind and B. C. Trueblood, *J. Am. Chem. Soc.*, **29**, 477 (1907).

(4) H. T. S. Britton, *J. Chem. Soc.*, **131**, 148 (1927).

(5) H. T. S. Britton and W. German, *ibid.*, **137**, 1249 (1930).

from carbon dioxide was effected by covering the containing vessels with carefully made ground joint stoppers and keeping them in a compartment guarded with sodalime tube and fitted with bubblers containing chromous chloride through which pure nitrogen was passed. The hydrochloric acid solutions were prepared by diluting the constant boiling acid with water or concentrating it with HCl gas. Tungstic acid was prepared by a method similar to that given by Archibald<sup>6</sup> using the sodium tungstate. The tungsten trioxide produced was bright canary-yellow powder of particles of average diameter equal to 0.096 mm. as determined by the polarizing microscope.

(B).—For the determination of the isoelectric point of tungstic acid solubility measurements of the trioxide in hydrochloric acid solutions of varying concentrations from 0.015 to 7.20 *M* were carried out by the chronometric method which was previously developed.<sup>7</sup> The tungsten trioxide solutions were made by shaking the trioxide with the hydrochloric acid solutions in Jena flasks coated internally with paraffin wax at 35° for 60 hours, a period which was found sufficient for saturation. The flasks were then left in an air-thermostat at 35 ± 0.02° for three months. The mixture in each flask was filtered with the aid of a high pressure ultra-filtration apparatus. The solutions obtained were free from colloidal particles of tungstic acid as indicated by the Tyndall effect non-formation.

(C).—The electrical measurements were carried out in an air-thermostat fixed at 35 ± 0.02°. The *pH* and *pCl* values of the solutions were followed by the quinhydrone and silver-silver chloride electrodes, respectively. The results were reproducible to within ±0.01 *pH* or *pCl* unit. The standard potential of the latter electrode which was prepared according to Carmody,<sup>8</sup> was evaluated at 35 ± 0.02° by using hydrochloric acid solutions of known activities in a cell without liquid junction of the type Ag:AgCl||HCl:H<sub>2</sub> and the value obtained was 0.2156 v. The reference half cell in the e.m.f. measurements was the saturated calomel electrode of *E*<sub>0</sub> equal to 0.2379 v. at 35 ± 0.02° as determined by the method of Harned and Owen.<sup>9</sup>

### Results and Discussion

Figure 1 represents the variation in the *pH* value of 10 cc. of 0.200 *N* sodium tungstate solution with the successive additions of 0.200 *N* HCl. Figure 2 represents the same measurements on 100 cc. of 0.010 *N* sodium tungstate solution with the successive additions of 0.100 *N* HCl. In this case the effect of time was considered. Curves 1, 2 and 3 in Fig. 2 represent the measurements after 10 minutes, 3 hours and 24 hours, respectively. The corresponding differential curves are shown in Figs. 3 and 4 for the concentrated and the diluted solutions, respectively. Figure 3 indicates two inflections: the first starts after the addition of 4.50 cc. of the acid and ends after the addition of 7.25 cc. thus corresponding to a *pH* range from 6.50 to 4.40, and the second inflection is between 7.25 cc. and 8.75 cc. of HCl within a *pH* range from 4.40 to 2.25. In the diluted solutions there are three inflections for the measurements taken after 10 minutes. The first begins after the addition of 4.50 cc. of HCl and ends at 6.50 cc., the second is from 6.50 to 9.25 cc. of HCl and the third is from 9.25 to 10.50 cc. of HCl. The corresponding *pH* ranges are 5.85–5.45, 5.45–4.15 and 4.15–3.10, respectively. For measurements taken after 3 or 24 hours, there is only one inflection between 8.50 cc. and 10.50 cc. of HCl with *pH* range from 5.12 to 2.90.

(6) E. H. Archibald, "The Preparation of Pure Inorganic Substances," John Wiley & Sons, Inc., New York, N. Y., 1932, p. 285.

(7) S. E. S. El Wakkad and H. A. Rizk, *Analyst*, **77**, 161 (1952).

(8) W. Carmody, *J. Am. Chem. Soc.*, **54**, 189 (1932).

(9) H. Harned and B. Owen, "The Physical Chemistry of Electrolytic Solutions," Reinhold Publishing Corp., New York, N. Y., 1943, p. 321.

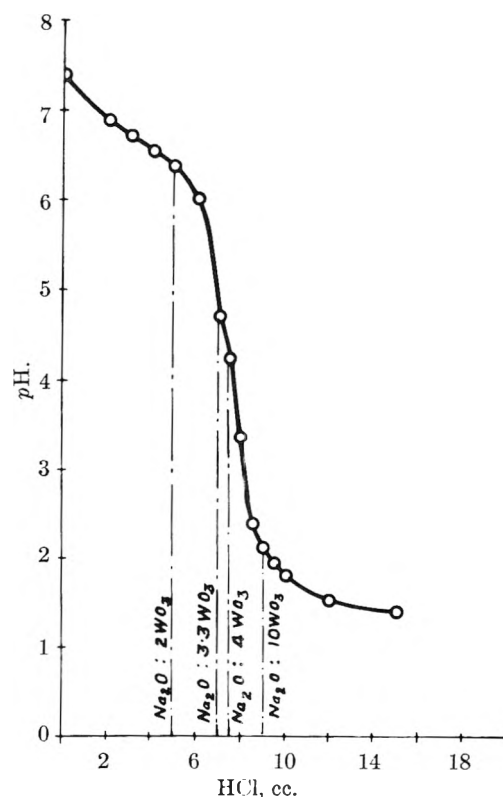


Fig. 1.—Titration of 10 cc. of 0.200 *N*  $\text{Na}_2\text{WO}_4 \cdot 2\text{H}_2\text{O}$  against 0.200 *N* HCl.

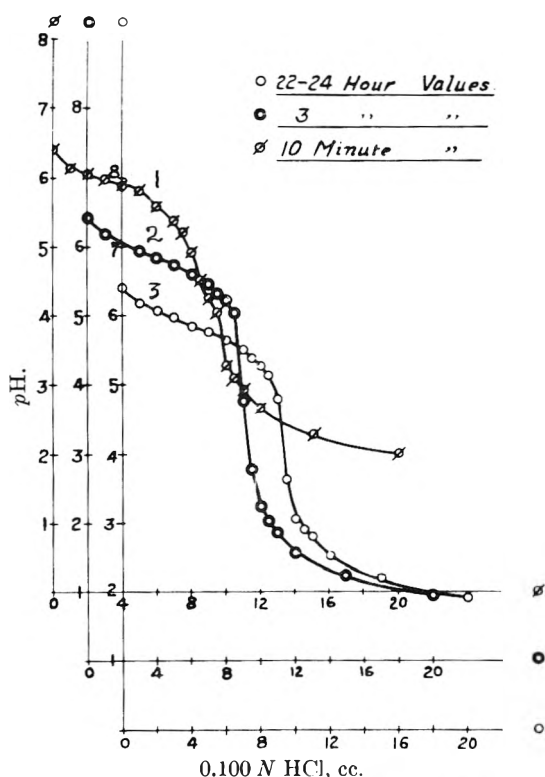


Fig. 2.—Titration of 10 cc. 0.010 *N*  $\text{Na}_2\text{WO}_4 \cdot 2\text{H}_2\text{O}$  + 90 cc. conductivity water against 0.100 *N* HCl.

It can be deduced from above that in the case of 0.200 *N* solutions the paratungstate,  $\text{Na}_2\text{O} \cdot 2.4\text{WO}_3$ , is formed at *pH* 6.1 and the metatungstate  $\text{Na}_2\text{O} \cdot 4\text{WO}_3$  is formed at *pH* 4.2. In the case of 0.010 *N*

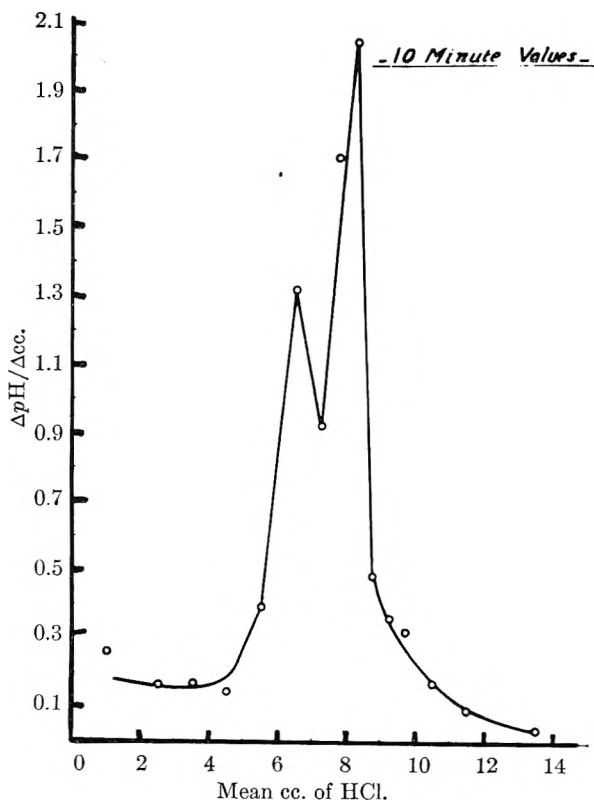


Fig. 3.—Titration of 10 cc. of 0.200  $N$   $\text{Na}_2\text{WO}_4 \cdot 2\text{H}_2\text{O}$  against 0.200  $N$   $\text{HCl}$ .

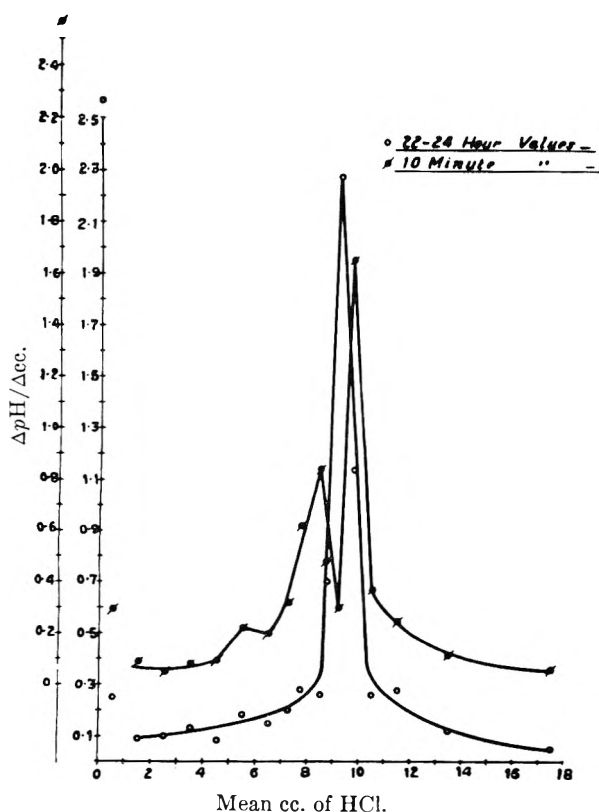


Fig. 4.—Titration of 10 cc. of 0.100  $N$   $\text{Na}_2\text{WO}_4 \cdot 2\text{H}_2\text{O}$  + 90 cc. conductivity water against 0.100  $N$   $\text{HCl}$ .

solutions, the paratungstate and the metatungstate are formed at  $p\text{H}$  5.6 and 5.2, respectively. Britton and German<sup>5</sup> considered the metatungstate formed

after the addition of 1.5 moles of  $\text{HCl}$  per mole  $\text{Na}_2\text{WO}_4 \cdot 2\text{H}_2\text{O}$  to be a salt of a stronger acid than  $\text{HCl}$  acid, and therefore it could not be attacked by further addition of  $\text{HCl}$ . The increased acidity recognized after the addition of 1.5 moles of  $\text{HCl}$  per mole of sodium tungstate was thus attributed to the free  $\text{HCl}$  and the acid property of the metatungstate. We tried in this investigation to test this assumption by calculating the  $p\text{H}$  values after the addition of 1.5 moles of  $\text{HCl}$  to one mole of sodium tungstate for each next introduction of  $\text{HCl}$ . In these calculations we considered at every point the measured  $p\text{H}$  value at the point just previous to it, and the excess amount of the acid introduced was assumed as free unreacting acid. In this way, we found that the measured  $p\text{H}$  values became lower than the calculated values not after the addition of 1.5 moles of  $\text{HCl}$  but after the addition of 1.8 moles in the case of 0.200  $N$  solutions and after 1.9 moles in the case of 0.010  $N$  solutions. The corresponding polytungstates are thus  $\text{Na}_2\text{O} \cdot 10\text{WO}_3$  and  $\text{Na}_2 \cdot 20\text{WO}_3$  which are responsible for the noticed acidity. Therefore, it can be concluded that the  $\text{HCl}$  action on the polytungstates is not limited by the metatungstate  $\text{Na}_2\text{O} \cdot 4\text{WO}_3$  formation but it depends on the concentration of the solutions involved.

When the  $p\text{H}$  and the  $p\text{Cl}$  values were measured as a function of time, namely, 10 minutes, 1, 2, 3 and 24 hours for the 0.010  $N$  solutions, the following was observed.

(1) Up to the addition of one mole  $\text{HCl}$ , the  $p\text{H}$  values measured after 10 minutes remained fairly constant within the next 24 hours. On the other hand, when adding more than one mole of the acid the  $p\text{H}$  values were found to increase with time. This could be considered to be due to a further reaction between the hydrogen ions and the complex polytungstates which needed time due to the colloidal nature of the latter. The complex formation as an intermediate stage in the colloidal formation was suggested by Dumanski, *et al.*<sup>10</sup>

(2) The  $p\text{Cl}$  values measured after 10 minutes were found to decrease with time till the addition of 1.9 moles of  $\text{HCl}$ . This may be due to the colloidal nature of the polytungstates which on standing would undergo coagulation or dissolution. After the addition of 1.9 moles of  $\text{HCl}$ , a slight increase in the  $p\text{Cl}$  values was noticed with time. At this stage, one might expect that tungstic acid was liberated and being of colloidal nature the chloride ions might be taken as the charging ions. The  $p\text{Cl}$  values were calculated at every point after the addition of 1.9 moles of  $\text{HCl}$  considering, as mentioned above, the  $p\text{Cl}$  value at the point just previous to that point and the excess amount of the acid to be free. It was found that the measured  $p\text{Cl}$  values were higher than the calculated values thus probably indicating the adsorption of the chloride ions by the micelles of the colloidal polytungstates.

For further support of this colloidal nature, tungsten trioxide sol was prepared in hydrochloric acid solutions of varying concentrations ranging from 0.0001 to 5.50  $M$ . It was found, by carrying out

(10) A. Dumanski, A. P. Euntin and A. G. Kniga, *Kolloid Z.*, **38**, 208 (1926).

electrophoretic experiments, that the colloidal particles were negatively charged when the molarity of the hydrochloric acid used was in the range 0.0001 to 0.110, and that they were positively charged at molarities higher than 0.500. On the measurement of the  $pCl$  of the hydrochloric acid solutions in which the sol particles were formed, the following was remarked.

(1) In the range 0.0001 to 0.110  $M$   $HCl$  the  $pCl$  values measured after the colloid formation were greater than the original values.

(2) At 0.500  $M$   $HCl$  the  $pCl$  values before and after the colloid formation were identical.

(3) At concentrations higher than 0.500  $M$   $HCl$  the  $pCl$  values measured before were higher than those measured after the colloid formation.

It is thus clear that the colloidal micelles of tungstic acid in hydrochloric acid solutions of molarity less than 0.500 are negatively charged by the chloride ions. The  $pH$  values of the colloidal solutions at concentrations greater than 0.500  $M$  of  $HCl$  were found to be higher than the corresponding original values. This indicates that the charging ions for the colloidal micelles of tungstic acid at such concentrations are the hydrogen ions. Therefore, the isoelectric point of tungstic acid would be expected to be at a molarity of hydrochloric acid equal to 0.500 which is of a  $pH$  value 0.43. To support this view, the amphoteric character of tungstic acid was studied by determining the solubility in hydrochloric acid solutions of varying concentrations. The results obtained are shown in Table I.

TABLE I

$HCl, M$	$WO_3 \times 10^4,$ mole/l.	$HCl, M$	$WO_3 \times 10^4,$ mole/l.
7.20	38.4	1.00	7.11
6.85	27.4	0.500	5.37
5.50	18.4	.110	8.59
4.17	15.3	.075	9.20
2.78	10.8	.015	11.0
1.41	9.0		

It is evident from this table that the solubility of the tungsten trioxide decreases with the increase of concentration of hydrochloric acid till a certain stage after which it increases. By extrapolating the main slopes of the solubility- $HCl$  concentration curve on each side of the minimum, the interception was found at a molarity of  $HCl$  of about 0.50, *i.e.*, at a  $pH$  of about 0.43.

## THE HEAT OF COMBUSTION OF YTTRIUM<sup>1</sup>

By ELMER J. HUBER, JR., EARL L. HEAD AND CHARLES E. HOLLEY, JR.

Contribution from the University of California, Los Alamos Scientific Laboratory, Los Alamos, New Mexico

Received October 8, 1956

Because of its occurrence with the rare earths and because of its similar chemical properties, yttrium is being included in a series of measurements of the heats of formation of the rare earth oxides.<sup>2-8</sup>

(1) This work was performed under the auspices of the A. E. C.  
(2) E. J. Huber, Jr., and C. E. Holley, Jr., *J. Am. Chem. Soc.*, **74**, 5530 (1952).

(3) E. J. Huber, Jr., and C. E. Holley, Jr., *ibid.*, **75**, 3594 (1953).

(4) E. J. Huber, Jr., and C. E. Holley, Jr., *ibid.*, **76**, 5645 (1953).

The method, involving the determination of the heat evolved from the combustion of a weighed sample of the metal in a bomb calorimeter at a known initial pressure of oxygen, has been described elsewhere.<sup>6</sup> The same units and conventions are used here.

**Yttrium Metal.**—The yttrium metal was analyzed and found to have the following per cent. impurities: C, 0.042; H, 0.031; O, 0.693; N, 0.0088; Ca, 0.05; Mg, 0.005. No other metallic impurities were detected. The metal thus contained about 0.8% impurities.

An X-ray pattern of the yttrium showed a two atom hexagonal close-packed unit cell and a calculated density of 4.46 g./cc. Both  $YO$  and  $Y_2O_3$  were observed as impurities. If it is assumed that the C, H and N are combined with yttrium as the carbide, hydride and nitride and that the oxygen is combined as  $YO$  and  $Y_2O_3$  in equi-molar quantities, the yttrium is 96.30 mole % metal (atomic weight  $Y = 88.92$ ).

**Combustion of Yttrium.**—The yttrium was burned on sintered discs of yttrium oxide in oxygen at 25 atmospheres pressure. The oxide, obtained from Jarrell-Ash Co., Newtonville, Mass., was approximately 99.9% pure. The metal showed no increase in weight when exposed to  $O_2$  at 25 atm. pressure for one hour. Combustion varied from 99.82 to 100.00% of completion. The average initial temperature for the runs was 25.3°. The results are listed in Table I.

This average value of 10,351.4  $\pm$  3.8 joules/g. must be corrected for the impurities present.

**Correction for Impurities.**—The calculated percentage composition of the yttrium by weight is Y metal 94.86;  $YH_2$ , 1.40;  $Y_2O_3$ , 2.44;  $YO$ , 1.14;  $YN$ , 0.066; C, 0.042; Ca, 0.05; Mg, 0.005. The carbon is probably present as  $YC_2$  but its heat of formation is not known and is probably small. The heat of combustion of Y metal corrected<sup>6</sup> for impurities is 10,691.7 j./g. The correction due to impurities amounts to 3.29% of the uncorrected value.<sup>10</sup> This value would be decreased by 0.17% to 10,673.6 if the  $CO_2$ ,  $H_2O$  and  $NO_2$  were assumed to react with the  $Y_2O_3$  to form  $Y_2(CO_3)_3$ ,  $Y(OH)_3$  and  $Y(NO_3)_3$ .

**Calculation of the Uncertainty.**—The uncertainty to be attached to the corrected value includes the uncertainty in the energy equivalent which is 0.04%, the uncertainty in the calorimetric measurements which is 3.8 j./g. or 0.04% and the

(5) E. J. Huber, Jr., and C. E. Holley, Jr., *ibid.*, **77**, 1444 (1955).

(6) E. J. Huber, C. O. Matthews and C. E. Holley, Jr., *ibid.*, **77**, 6493 (1955).

(7) E. J. Huber, Jr., E. L. Head and C. E. Holley, Jr., *This Journal*, **60**, 1457 (1956).

(8) E. J. Huber, Jr., E. L. Head and C. E. Holley, Jr., *ibid.*, **60**, 1582 (1956).

(9) The specific heat of  $Y_2O_3$  is estimated to be 0.43 joule/g./°.

(10) The heat of formation of  $YH_2$  is taken as -52 kcal./mole from the unpublished work of R. N. R. Mulford of this Laboratory. The heat of formation of  $YN$  is estimated at -75 kcal./mole from the published values of  $LaN$  and  $CeN$ . See Selected Values of Chemical Thermodynamic Properties, N.B.S. Circular 500, 1952, pp. 350, 354. The heat of formation of  $YO$  is estimated at -155 kcal./mole. The heats of combustion of graphite (to  $CO_2$ ), calcium (to  $CaO$ ) and magnesium (to  $MgO$ ), are taken as 33,000, 15,800 and 24,670 j./g., respectively. The heats of formation of  $H_2O(g)$  and  $NO_2$  are taken as -58 and +8 kcal./mole.

TABLE I  
THE HEAT OF COMBUSTION OF YTTRIUM

Mass Y burned, g.	Wt. Mg, mg.	Wt. Y <sub>2</sub> O <sub>3</sub> , g.	Joules/deg., total <sup>9</sup>	$\Delta T$ , °K.	Firing, j.	Energy from Y, j./g.	Dev. from mean
1.2237	7.11	40.1	10037.1	1.2812	11.2	10356.2	4.8
1.1507	7.03	31.4	10033.4	1.2054	11.2	10350.0	1.4
1.1454	7.06	31.9	10033.6	1.1999	13.0	10347.7	3.7
1.0926	6.43	52.9	10042.6	1.1425	10.5	10346.5	4.9
1.1571	7.20	39.8	10037.0	1.2131	10.4	10360.3	8.9
1.1400	7.51	39.8	10037.0	1.1953	12.5	10350.4	1.0
1.1945	7.94	42.2	10038.0	1.2523	13.1	10348.8	2.6
						Av. 10351.4	3.9
						Stand dev. 1.9	

uncertainty introduced in the correction for the impurities<sup>6</sup> which is estimated to be 0.11%. The determination of the uncertainty in the correction for impurities also includes the possibility that the ratio of YO to Y<sub>2</sub>O<sub>3</sub> may be as high as 3 and as low as 1/3.

The combined uncertainty is 12.8 joules/g. which does not include the possibility that the CO<sub>2</sub>, H<sub>2</sub>O and NO<sub>2</sub> react with the Y<sub>2</sub>O<sub>3</sub>. The value for the heat of combustion gives for the reaction in the bomb a value of  $\Delta E_{25.0^\circ} = -1901.4 \pm 2.3$  kj./mole.

**Composition of the Yttrium Oxide.**—The oxide formed was light tan in color. An X-ray pattern showed it to be the cubic form with a calculated density of 5.03 g./cc. Analysis by the method of Barthauer and Pierce<sup>11</sup> showed no oxygen above that necessary for the sesquioxide.

**Heat of Formation of Y<sub>2</sub>O<sub>3</sub>.**—Using methods of calculation reported elsewhere<sup>6</sup> the heat of formation of Y<sub>2</sub>O<sub>3</sub>,  $\Delta H_{25^\circ} = -1905.6 \pm 2.3$  kj./mole. In defined calories this is  $-455.45 \pm 0.54$  kcal./mole. Two estimated values in the literature are those of Brewer,<sup>12</sup>  $-420 \pm 9$ , and Roth and Becker,<sup>13</sup>  $-440$  kcal./mole. This high value,  $-151.82 \pm 0.18$  kcal./g. atom O, appears to deserve some comment.

The only other oxides known to have heats of formation greater in magnitude than  $-150$  kcal./g. atom O are CaO ( $-151.79 \pm 0.21$  kcal./mole)<sup>14</sup> and Er<sub>2</sub>O<sub>3</sub> ( $-151.20 \pm 0.15$  kcal./g. atom O).<sup>8</sup> Dysprosium oxide, Dy<sub>2</sub>O<sub>3</sub>, is close, having a heat of formation of  $-148.61 \pm 0.31$  kcal./g. atom O.<sup>7</sup> The other rare earth sesquioxides which have been measured have values for the heat of formation around  $-144$  kcal./g. atom O.<sup>2-7</sup> Since yttrium has an ionic radius and chemical properties similar to those of dysprosium and erbium the heat of formation of its oxide would probably be expected to be of the same order of magnitude. Also, since the heat of formation of the alkali and alkaline earth oxides increase in each series as the atomic weight decreases, it might be expected that yttrium oxide would have a higher heat of formation than lanthanum oxide. In this connection, the heat of formation of scandium oxide, Sc<sub>2</sub>O<sub>3</sub>, should be very interesting, and the authors hope to measure it as soon

as they are able to acquire some pure scandium metal.

**Acknowledgments.**—The authors wish to acknowledge the valuable assistance of D. Pavone, F. H. Ellinger, O. R. Simi and E. Van Kooten in the analytical work.

They also appreciate the courtesy of Dr. F. H. Spedding of the Ames Laboratory, A.E.C., through whom the metal was obtained.

## THE LIQUID DENSITY, VAPOR PRESSURE AND CRITICAL TEMPERATURE AND PRESSURE OF PERCHLORYL FLUORIDE<sup>1,2</sup>

BY ROGER L. JARRY

Pennsylvania Salt Manufacturing Company, Research and Development Department, Whitmarsh Research Laboratories, Wyndmoor, Pa.

Received October 1, 1956

Perchloryl fluoride (ClO<sub>3</sub>F) was first prepared by Engelbrecht and Atzwanger,<sup>3</sup> and in the cited article and in a later one by the same authors<sup>4</sup> information on the physical and chemical properties is given. The infrared spectrum has been examined by Lide and Mann.<sup>5</sup> Barth-Wehrenalp<sup>6</sup> reviewed the methods of preparation of perchloryl fluoride. The current study has extended the range of measurements reported by Engelbrecht and Atzwanger<sup>3,4</sup> and presents data of a higher precision.

**Apparatus and Procedure.**—The density was measured in a glass dilatometer consisting of a 4 cm.<sup>3</sup> bulb and 10 cm. of 2 mm. i.d. capillary tubing. This apparatus and its operation were described in a previous publication.<sup>7</sup> The only change in procedure was in filling the dilatometer; in this case the perchloryl fluoride was charged from a storage cylinder and the amount obtained by weight difference.

Vapor pressures to two atmospheres were measured in an all-metal system which was described in previous publications.<sup>7,8</sup> Pressures were read on a mercury manometer by means of a cathetometer to a precision of  $\pm 0.05$  mm. The vapor pressure to the critical region was measured in a metal

(1) Presented before the Fluorine Symposium, Division of Industrial and Engineering Chemistry, 130th National Meeting of the American Chemical Society, September 20, 1956.

(2) This paper represents the results of one phase of research carried out under Contract No. 18(600)-761, supported by the United States Air Force through the Air Force Office of Scientific Research of the Air Research and Development Command.

(3) A. Engelbrecht and H. Atzwanger, *Monatsh. Chem.*, **83**, 1087 (1952).

(4) A. Engelbrecht and H. Atzwanger, *J. Inorg. Nuclear Chem.*, **2**, 348 (1956).

(5) D. R. Lide, Jr., and D. E. Mann, National Bureau of Standards Report #4399, Nov. 1, 1955.

(6) G. Barth-Wehrenalp, *J. Inorg. Nuclear Chem.*, **2**, 266 (1956).

(7) R. L. Jarry and H. C. Miller, *THIS JOURNAL*, **60**, 1412 (1956).

(8) R. L. Jarry and H. C. Miller, *J. Am. Chem. Soc.*, **78**, 1552 (1956).

(11) G. L. Barthauer and D. W. Pierce, *Ind. Eng. Chem.*, **18**, 479 (1946).

(12) L. Brewer, *Chem. Revs.*, **52**, 1 (1953).

(13) W. A. Roth and G. Becker, *Z. physik. Chem.*, **A159**, 1 (1932).

(14) E. J. Huber, Jr., and C. E. Holley, Jr., *THIS JOURNAL*, **60**, 498 (1956).

system immersed in a constant temperature bath. The lines to the bourdon gage as well as the gage itself were kept at a temperature above that in the bath. The 1000 p.s.i.g. bourdon gage used in these measurements had a stated accuracy of  $\pm 1/4$  of 1%.

Critical temperature was measured on samples sealed in 2 mm. i.d. capillary tubing. The tube was placed directly into a constant temperature bath and observations made on the disappearance and reappearance of the meniscus.

Temperature was measured during the density and precise vapor pressure determinations either by means of a platinum resistance thermometer or by means of thermocouples which have been compared with the thermometer. The thermometer had been compared with the National Bureau of Standards temperature scale. During the equilibrium periods of 15-20 min. during which measurements were taken, the temperature drift in the metal system or the dilatometer was no more than  $0.002^\circ/\text{min.}$  and  $0.004^\circ/\text{min.}$ , respectively. For the critical temperature and high vapor pressure determinations a mercury in glass thermometer calibrated by the National Bureau of Standards was used.

**Material.**—The perchloryl fluoride for these measurements was prepared and purified by A. Engelbrecht at this Laboratory. Purification was accomplished by fractional distillations. Purity was assayed by infrared analysis and by mass spectrometer analysis kindly furnished by the staff of the National Bureau of Standards. The mass spectrometer analysis showed a purity of 99.9+ mole %.

**Results and Discussion.**—The data obtained for the liquid density are given in Table I, and are represented by the equation

$$d = 2.266 - 1.603 \times 10^{-3}T - 4.080 \times 10^{-6}T^2 \quad (1)$$

where  $d$  is the density in  $\text{g./cm.}^3$  at the absolute temperature  $T$ . Deviations between the experimental and values calculated using equation 1 are given in column 3 of Table I.

TABLE I

THE DENSITY OF LIQUID PERCHLORYL FLUORIDE BETWEEN 131 AND  $234^\circ\text{K.}$  ( $0^\circ\text{C.} = 273.16^\circ\text{K.}$ )

$T, ^\circ\text{K.}$	Density, $\text{g./cm.}^3$	Deviation obsd. - calcd.	$T, ^\circ\text{K.}$	Density, $\text{g./cm.}^3$	Deviation obsd. - calcd.
131.31	1.989	0.004	189.50	1.816	0.001
144.46	1.950	.001	194.44	1.801	.001
149.58	1.935	.000	199.38	1.786	.002
154.79	1.920	.000	204.34	1.770	.002
159.84	1.905	.000	209.21	1.751	-.001
164.66	1.891	.000	214.21	1.734	-.001
169.62	1.877	.001	219.15	1.718	.000
174.50	1.862	.000	224.11	1.701	-.001
179.52	1.846	.000	229.23	1.684	.000
184.54	1.831	.000	234.22	1.667	.003

The uncertainty of the measurements is estimated to be  $\pm 0.1\%$ . Temperature was known to  $\pm 0.05^\circ$ .

The volume values for the dilatometer were corrected using the expansion coefficient data of Buffington and Latimer.<sup>9</sup> Corrections were applied for the quantity of material in the dead space above the liquid.

The vapor pressure data are given in Table II. The data to two atmospheres have been fitted by the equation

$$\log_{10}P(\text{mm.}) = 18.90112 - \frac{1443.467}{T} - 4.09566 \log_{10}T \quad (2)$$

The normal boiling point calculated using equation

(9) R. M. Buffington and W. M. Latimer, *J. Am. Chem. Soc.*, **48**, 2305 (1926).

TABLE II

THE VAPOR PRESSURE OF PERCHLORYL FLUORIDE ( $0^\circ\text{C.} = 273.16^\circ\text{K.}$ )

Temp., $^\circ\text{K.}$	Pressure, mm.	Deviation, mm. obsd. - calcd.	Temp., $^\circ\text{K.}$	Pressure, atm.	Deviation, atm. obsd. - calcd.
152.81	3.08	-0.15	227.09	1.033	-0.008
157.67	5.53	-.03	232.04	1.290	-.006
162.58	9.31	-.05	237.14	1.606	-.001
167.50	14.97	.02	242.09	1.969	.004
172.33	23.19	-.10	251.99	2.891	.025
177.40	35.73	-.03	262.07	4.048	-.041
182.33	53.05	-.01	272.04	5.748	.086
187.31	77.13	.02	282.10	7.789	.108
192.25	109.48	.12	292.13	10.170	-.027
197.19	151.77	.23	292.24	10.177	-.050
202.11	207.50	.38	302.17	13.361	.074
207.19	279.66	-.35	312.21	17.034	.012
212.20	370.73	-.08	322.33	21.388	-.122
217.13	481.49	-.20	332.41	26.490	-.285
222.13	619.33	-.10	342.50	32.782	-.127
227.09	785.44	1.00	352.66	39.959	-.066
232.04	980.28	-0.97	362.92	48.259	.024
237.14	1220.89	-0.80			
242.09	1496.31	1.20			

2 is  $226.40^\circ\text{K.}$  The data to the critical region are represented by the equation

$$\log_{10}P(\text{atm.}) = 4.46862 - \frac{1010.81}{T} \quad (3)$$

Deviations between the experimental and calculated values for these two equations are given in column three of Table II. Temperature was known in these measurements to  $\pm 0.05^\circ$  for the data to 2 atmospheres and to  $\pm 0.10^\circ$  for the data to the critical region. The heat of vaporization at the normal boiling point calculated using equation 2 and a gas imperfection correction of  $-3.21\%$ , derived from the Betheot equation, is 4609 cal./mole.

The critical temperature was determined to be  $368.33 \pm 0.10^\circ\text{K.}$  From this value the critical pressure was calculated using equation 3 to be 53.0 atm. absolute.

**Acknowledgments.**—The author wishes to express his appreciation to Dr. J. J. Fritz of the Pennsylvania State University and Mr. H. C. Miller of the Pennsylvania Salt Manufacturing Company for their advice during the course of this work. He also wishes to thank Dr. A. Engelbrecht, now at the University of Innsbruck, for purifying the sample of perchloryl fluoride, and Mr. Gordon E. Webb of the Pennsylvania Salt Manufacturing Co. for his excellent assistance.

## POLYMORPHISM IN MONOCHLOROACETIC ACID

BY R. E. KAGARISE

Naval Research Laboratory, Washington 25, D. C.

Received October 25, 1956

It is well known that monochloroacetic acid exists in at least three distinct crystalline varieties.<sup>1</sup> Re-

(1) "Beilsteins Handbuch der Organischen Chemie," Julius Springer, Berlin, Fourth Edition, H2, 194, 1920; E.12, 87 (1929); E112, 187 (1942).

cent thermodynamic studies<sup>2,3</sup> have shown that these three varieties form a monotropic system consisting of a stable  $\alpha$ -form and metastable  $\beta$ - and  $\gamma$ -forms. The melting points of the three forms are 62.0, 56.5 and 50.5°, respectively. Moreover, these investigations have shown that the varieties are capable of isolation provided the proper cooling techniques are employed.

The problem of determining the crystal structure of these three species does not appear to have been studied previously, except for several investigations of the pure quadrupole spectra. Allen<sup>4</sup> observed two Cl<sup>35</sup> resonance frequencies in the spectrum of the ordinary acid ( $\alpha$ -form) which he attributed to the acid dimer. More recently, Negita<sup>5</sup> has observed the pure quadrupole spectrum of all three crystalline species and found only single resonance frequencies in the metastable  $\beta$ - and  $\gamma$ -forms. Moreover, the frequency in the  $\beta$ -form is near the higher frequency of the  $\alpha$ -modification, while that of the  $\gamma$ -form is very close to the lower one of the  $\alpha$ -form. These results have been interpreted in terms of two forms of the dimer resulting from the hindered rotation of the  $-\text{CH}_2\text{Cl}$  groups about the C-C bond. Thus the  $\gamma$ -modification is regarded as the *gauche*-form, the  $\beta$ -modification as the *trans*-form, and the  $\alpha$ -modification as an equilibrium mixture of the two.

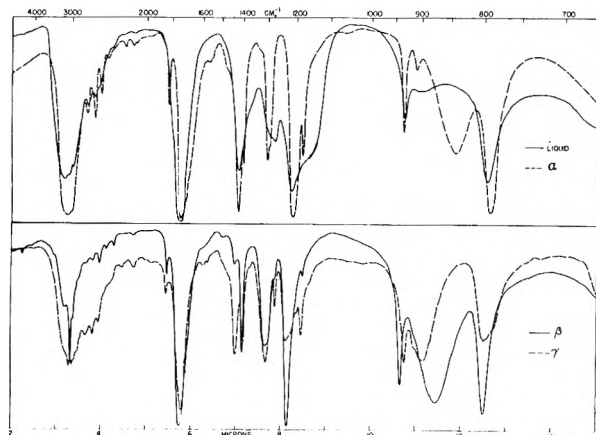


Fig. 1.—Infrared spectra of liquid and the  $\alpha$ -,  $\beta$ - and  $\gamma$ -crystalline forms of monochloroacetic acid. Thickness of samples is approximately 0.01 mm.

In view of the successful application of infrared absorption spectroscopy to similar studies on *sym*-tetrabromoethane<sup>6</sup> it was considered worthwhile to examine the infrared spectra of the various crystalline species of monochloroacetic acid.

#### Experimental

The sample of chloroacetic acid used in this investigation was an Eastman Kodak White label product, which was recrystallized five times from benzene. The product was stored over  $\text{P}_2\text{O}_5$  in a vacuum desiccator to remove final traces of water and benzene.

(2) M. Aumeras and R. Minangay, *Bull. soc. chim. France*, 1100 (1948).

(3) L. M. Katayeva and Z. S. Smutkina, *Zhur. fg. Khim.*, **29**, 428 (1955).

(4) H. C. Allen, *Fhys. Rev.*, **87**, 227 (1952); *J. Am. Chem. Soc.*, **74**, 6074 (1952); *THIS JOURNAL*, **57**, 501 (1953).

(5) H. Negita, *J. Chem. Phys.*, **23**, 214 (1955).

(6) R. E. Kagaris, *ibid.*, **24**, 300 (1956).

All absorption spectra were obtained with a Perkin-Elmer Model 21 spectrophotometer equipped with NaCl optics. The absorption cell consisted of a conventional liquid cell which was heated by means of an electrical heater wound around the periphery of the cell. Since  $\text{CH}_2\text{ClCOOH}$  is a solid at room temperature, it was necessary to fill the absorption cell in the following manner. Two sodium chloride windows were heated to a temperature slightly above the melting point of the acid. An appropriate amount of sample was placed on one window and allowed to melt. The second window and a Teflon spacer were placed on top of the first and the cell assembled in the usual manner. The temperature of the sample was measured with an iron-constantan thermocouple.

To prepare specimens of the various crystalline forms the following cooling procedures were employed. The  $\alpha$ -form was obtained readily by slowly cooling the liquid while the  $\gamma$ -form usually resulted when the liquid was rapidly cooled. The  $\beta$ -form was very difficult to prepare *in situ* since most of the procedures advocated by earlier workers<sup>2,3,6</sup> are not applicable to closed systems. It was observed, however, that under certain conditions (which were not definable) the  $\gamma$ -form was converted to the  $\beta$ -form with aging. The various forms were identified by observing their melting points.

#### Discussion of Results

The observed infrared absorption spectra of liquid and the  $\alpha$ -,  $\beta$ - and  $\gamma$ -modifications of crystalline monochloroacetic acid are shown in Fig. 1, while the wave lengths and wave numbers of the absorption maxima are listed in Table I. An examination of Fig. 1 shows that the four spectra are quite different and the individual spectra cannot be represented by a combination of the others. For example, in the region between 10.75 and 12.25  $\mu$  none of the three crystalline forms have bands in common. The spectra are also appreciably different in the neighborhood of 7  $\mu$ . These observations are in contrast to those previously reported for *sym*-tetrabromoethane.<sup>6</sup> In this case the observed spectrum of the liquid was very similar to the synthetic spectrum obtained by a superposition of the spectra of the two crystalline forms. According to the interpretation of Negita,<sup>5</sup> one would have predicted that the spectrum of the  $\alpha$ -form would be similar to the sum of those of the  $\beta$ - and  $\gamma$ -forms.

An examination of the region beyond 12  $\mu$  in Fig. 1, shows that apparently only a single band is present which can be attributed to a C-Cl stretching mode. One must conclude, therefore, that if several isomeric species are present, the stretching frequency of the carbon-chlorine bond is the same in each. This is also in opposition to observations on other halogenated compounds which are known to possess rotational isomers.<sup>7</sup> Moreover, the observed conversion of the  $\gamma$ -form to the  $\beta$ -form appears to contradict the interpretation of Negita. If the stable  $\alpha$ -form is an equilibrium mixture of  $\beta$  and  $\gamma$  such a conversion would be highly improbable. It seems certain, therefore, that the various crystalline species of monochloroacetic acid cannot be attributed simply to different species of rotational isomers.

Before discussing the differences between the spectra of the various crystalline species it is appropriate to consider briefly the possible modes of vibration of the dimeric molecule. This question has been treated quite extensively by Hadzi and

(7) S. Mizushima, "Structure of Molecules and Internal Rotation," Academic Press Inc., New York, N. Y., 1954.

TABLE I  
INFRARED ABSORPTION SPECTRA OF LIQUID AND  $\alpha$ -,  $\beta$ - AND  $\gamma$ -FORMS OF  $\text{CH}_2\text{ClCOOH}$

Liquid		$\alpha$ -Crystal		$\beta$ -Crystal		$\gamma$ -Crystal		Interpretation
$\lambda$ ( $\mu$ )	$\nu$ ( $\text{cm.}^{-1}$ )	$\lambda$ ( $\mu$ )	$\nu$ ( $\text{cm.}^{-1}$ )	$\lambda$ ( $\mu$ )	$\nu$ ( $\text{cm.}^{-1}$ )	$\lambda$ ( $\mu$ )	$\nu$ ( $\text{cm.}^{-1}$ )	
3.18s	3144	3.25vs	3076	3.18m	3144	3.20sh	3125	$\nu$ (O-H)
...	...	...	...	3.31s	3021	3.28s	3048	$\nu$ (O-H)
3.36w	2976	...	...	3.36sh	2976	3.35s	2985	$\nu$ (C-H)
3.69w	2710	3.68w	2717	3.65vw	2739	3.65w	2739	
3.85w	2597	3.85w	2597	3.82vw	2617	3.80w	2631	
...	...	3.99w	2506	3.96w	2525	3.94w	2538	
4.22	2360	4.14vw	2415	4.11vw	2433	4.25sh	2350	
...	...	4.52vw	2212	4.28vw	2336	4.47vw	2237	
...	...	4.70vw	2127	4.71vw	2123	4.72w	2118	
...	...	5.49w	1821	5.46w	1831	5.44w	1838	
5.74vs	1742	5.75vs	1739	5.75vs	1739	5.78vs	1730	$\nu$ (C=O)
7.05s	1418	7.04s	1420	6.96w	1436	6.98m	1432	COOH-I
...	...	7.16m	1396	7.13m	1402	7.15m	1398	$\delta$ (C-H)
7.75sh	1290	7.68m	1302	7.65m	1307	7.67m	1303	COOH-II
7.86m	1272	7.75m	1290	7.70sh	1298	7.86m	1272	
8.23s	1215	8.26vs	1210	8.14vs	1228	8.10m	1234	COOH-III
...	...	8.48m	1179	8.48vw	1179	8.45m	1183	
10.74m	931	10.73m	932	10.66s	938	10.75m	930	$\nu$ (C-C)
...	...	11.01vw	908	...	...	11.15m	897	$\delta$ (OH)
...	...	...	...	11.45s	873	...	...	$\delta$ (OH)
...	...	11.88s	842	...	...	...	...	$\delta$ (OH)
12.58s	795	12.65s	790	12.51s	799	12.52m	799	$\nu$ (C-Cl)

Sheppard.<sup>8</sup> They conclude that in the region of the spectrum between 1500 and 700  $\text{cm.}^{-1}$ , one might expect to observe absorptions due to the C-O stretching, C-O-H angle bending, and the motion corresponding principally to the motion of the hydrogen atom of the OH group perpendicular to the plane of the dimer. These conclusions are based on the assumption that the dimers have either  $C_{2H}$  or  $C_i$  symmetry. In either case, the rule of mutual exclusion applies, so that there is a corresponding set of frequencies which are active only in the Raman effect. In addition to the above mentioned modes, one would also expect to observe the O-H and C=O stretching frequencies in the NaCl region of the spectrum. The assignment of the latter two modes is firmly established, and Hadzi and Sheppard have given strong evidence that the out-of-plane bending mode absorbs in the region from about 870 to 940  $\text{cm.}^{-1}$ . The two remaining modes, namely, the C-O stretching and C-O-H angle bending are attributed to the absorption frequencies around 1400 and 1300  $\text{cm.}^{-1}$ . However, the degree of interaction between these two vibrations is so great, that one cannot make an unequivocal assignment. Therefore, the absorption bands in the 1200-1400  $\text{cm.}^{-1}$  are referred to as COOH-I, II and III.

An examination of the data shows that those absorption bands due to the  $-\text{CH}_2\text{Cl}$  end groups, *e.g.*,  $\nu$ (C-H),  $\delta$ (C-H),  $\nu$ (C-C) and  $\nu$ (C-Cl), remain relatively constant in both intensity and frequency in all of the spectra. Those bands attributable to the  $-\text{COOH}$  portion of the molecule, on the other hand, vary considerably both in intensity and frequency. Consider, for example, the band at  $\sim 3150$   $\text{cm.}^{-1}$  due to the O-H stretching mode. In the  $\alpha$ -form, the absorption is quite strong and completely over-

laps the nearby C-H stretching band at  $\sim 3025$   $\text{cm.}^{-1}$ , while in the  $\beta$ -modification the OH band is relatively weak. The same situation prevails in the case of the COOH-I band near 1420  $\text{cm.}^{-1}$ . It is also apparent that considerable frequency shifts take place since the out-of-plane OH deformation band falls at 842, 873 and 897  $\text{cm.}^{-1}$  in the  $\alpha$ -,  $\beta$ - and  $\gamma$ -species, respectively.

As previously mentioned, one would predict two frequencies in the 1200-1400  $\text{cm.}^{-1}$  region for dimers having  $C_{2H}$  or  $C_i$  symmetry. Since three frequencies due to COOH group vibrations are observed in this region one must conclude that either the dimers are of lower symmetry, or other molecular species (*e.g.*, trimers or higher polymers) are present. Indeed, recent studies (see Chapman<sup>9</sup>) have shown that the molecules of solid formic acid are linked by hydrogen bonds at both ends, forming extended chains and not dimeric units. However, since little is known about the crystal structure of these compounds, one cannot differentiate between these two possibilities.

### Conclusions

The infrared absorption spectra of liquid and the  $\alpha$ -,  $\beta$ - and  $\gamma$ -crystalline forms of monochloroacetic acid are significantly different. These differences cannot be explained logically in terms of rotational isomers, since the more pronounced changes occur in absorption bands characteristic of the bonded-COOH groups. This being the case, it seems logical to conclude that the kind and degree of hydrogen bonding is appreciably different in the various crystalline forms.

A more detailed study of this problem can perhaps be carried out when crystallographic data become available. These data together with infrared polarization studies of oriented crystals are

(8) D. Hadzi and N. Sheppard, *Proc. Roy. Soc. (London)*, **216**, 247 (1953).

(9) D. Chapman, *J. Chem. Soc.*, 225 (1956).

needed before one can make any conclusions with regard to the structure or symmetry of the crystalline species of monochloroacetic acid.

## COMPARISON OF THE INFRARED AND RAMAN SPECTRA OF SOME CRYSTALLINE HYDROXIDES<sup>1</sup>

BY BETTY A. PHILLIPS AND WILLIAM R. BUSING<sup>2</sup>

Contribution No. 1404 from the Sterling Chemistry Laboratory, Yale University, New Haven, Connecticut

Received October 5, 1956

The crystal structures of  $\text{LiOH}$ ,<sup>3</sup>  $\text{LiOH}\cdot\text{H}_2\text{O}$ ,<sup>4</sup>  $\text{NaOH}$ <sup>5</sup> and  $\text{Ca}(\text{OH})_2$ <sup>6-9</sup> are known from X-ray or neutron diffraction studies, and, while the atomic arrangements of these substances are all different, their structures have one feature in common: in each primitive unit cell there are two hydroxide ions and these are related to each other by a center of symmetry. This means that in the vibrational spectrum of each material there will be two fundamental OH stretching modes, one of which will be symmetric with respect to the symmetry center and Raman active, while the other will be antisymmetric with respect to this center and infrared active. The frequency difference between these vibrational modes is a measure of the coupling between the vibrations of the two hydroxide ions.<sup>10</sup>

The infrared spectra of these compounds have been observed,<sup>11-13</sup> and the hydroxide stretching frequencies are listed in Table I. The probable errors of these frequencies are all about  $1\text{ cm.}^{-1}$ . The purpose of this note is to report some careful measurements of the corresponding Raman frequencies, since the published values of these frequencies<sup>14,15</sup> are given to the nearest  $10\text{ cm.}^{-1}$  only.

The samples used were white crystalline powders of  $\text{LiOH}$  and  $\text{LiOH}\cdot\text{H}_2\text{O}$ , reagent grade pellets of  $\text{NaOH}$  (assay 97.0% minimum), and coarsely crystalline  $\text{Ca}(\text{OH})_2$  obtained by slow precipitation from interdiffusing solutions.<sup>16</sup>

(1) This research was supported in part by the U. S. Air Force under contract monitored by the Office of Scientific Research, Air Research and Development Command. The material is taken from a thesis to be submitted to Yale University by Betty A. Phillips in partial fulfillment of the requirements for the degree of doctor of philosophy.

(2) Chemistry Division, Oak Ridge National Laboratory, Oak Ridge, Tennessee.

(3) T. Ernst, *Z. physik. Chem.*, **20B**, 65 (1933).

(4) R. Pepinsky, *Z. Krist.*, **A102**, 119 (1939).

(5) T. Ernst, *Nachr. Akad. Wiss. Göttingen, Math.-physik. Kl., Math.-physik. chem. Abt.*, 76 (1946).

(6) J. D. Bernal and H. D. Megaw, *Proc. Roy. Soc. (London)*, **A151**, 384 (1935).

(7) H. E. Petch and H. D. Megaw, *J. Opt. Soc. Am.*, **44**, 744 (1954).

(8) H. E. Petch, *Phys. Rev.*, **99**, 1635 (1955).

(9) W. R. Busing and H. A. Levy, *J. Chem. Phys.*, in press.

(10) D. F. Hornig, *Disc. Faraday Soc.*, **9**, 115 (1950).

(11) L. H. Jones, *J. Chem. Phys.*, **22**, 217 (1954);  $\text{LiOH}$  and  $\text{LiOH}\cdot\text{H}_2\text{O}$ .

(12) W. R. Busing, *ibid.*, **23**, 933 (1955). This is a detailed discussion of the spectrum of  $\text{NaOH}$  which refers to the Raman work presented here.

(13) H. W. Morgan and W. R. Busing, to be published. The infrared spectrum of  $\text{Ca}(\text{OH})_2$  is complicated by the appearance of a number of bands believed to be due to the combination of vibrational modes with the stretching fundamental, but the latter is easily recognized by its strong polarization in the c-direction.

(14) P. Krishnamurti, *Ind. J. Phys.*, **5**, 651 (1930).

(15) G. S. Landsberg and F. S. Baryshanskaya, *Izvest. Akad. Nauk SSSR, Ser. Fiz.*, **10**, 509 (1946).

(16) F. W. Ashton and R. Wilson, *Am. J. Sci.*, **13**, 209 (1927).

Suitable spectra of these inhomogeneous samples were obtained by using a Wood's tube in which the exit window was replaced by a Pyrex cone extending about 4 cm. into the sample.

Six AH-2 mercury lamps supplied the exciting light which passed through a filter jacket surrounding the sample. A filter solution of gentian violet and *p*-nitrotoluene in isopropyl alcohol was used to isolate the 4358 Å. Hg line, and a few measurements were made with the 4047 Å. Hg line isolated by a filter of iodine in  $\text{CCl}_4$ . The spectra were photographed with an *f*/12 Schmidt and Haensch spectrograph using two glass prisms. Exposure times ranged from 20 to 48 hours.

Only one Raman line was observed for each sample and in each case it was a fairly sharp line in the OH stretching region. The fine structure found in the infrared spectrum of  $\text{Ca}(\text{OH})_2$ <sup>7,13</sup> was not observed in these Raman spectra. Any low frequency bands which may have been present were obscured by the halation from the exciting line, and even the water bands of the  $\text{LiOH}\cdot\text{H}_2\text{O}$  were too weak to be seen against the background.

TABLE I

A COMPARISON OF THE INFRARED AND RAMAN OH STRETCHING FREQUENCIES IN SOME CRYSTALLINE HYDROXIDES

Compound	Frequency ( $\text{cm.}^{-1}$ )		Difference
	Infrared <sup>11-13</sup>	Raman	
$\text{LiOH}$	3678	3664	14
$\text{LiOH}\cdot\text{H}_2\text{O}$	3574	3563	11
$\text{NaOH}$	3637	3633	4
$\text{Ca}(\text{OH})_2$	3644	3618	26

The spectrum of a neon discharge was superimposed on each Raman spectrum for calibration. The Raman frequencies were determined in the usual way, correcting to vacuum, and the final values which are the averages of from three to eight measurements are listed in Table I. The probable errors as determined from the deviations of the observations are about  $1\text{ cm.}^{-1}$ , and test measurements of the 4916 Å. Hg line and of the Raman spectrum of benzene indicate that this estimate of the errors is realistic. With the exception of the  $\text{LiOH}$  frequency, these results are all within  $8\text{ cm.}^{-1}$  of the previously reported Raman values.<sup>14,15</sup> The literature value of  $3630\text{ cm.}^{-1}$  for  $\text{LiOH}$  appears to be in error.

The observed spectra are consistent with the symmetries of these crystals in that one infrared active fundamental and one Raman active one have been observed in each case. Comparing the frequency differences, it is seen that the coupling of the hydroxide ion vibrations is greatest in  $\text{Ca}(\text{OH})_2$  and least in  $\text{NaOH}$ , and that the sign of the interaction force constant is the same for all of these compounds.

## THE SYSTEM 2,4,6-TRINITROTOLUENE-2,4,6-TRINITRO-*m*-XYLENE

BY LOHR A. BURKARDT

Chemistry Division, U. S. Naval Ordnance Test Station, China Lake, California

Received October 29, 1956

In the course of investigations of the viscosities of liquid mixtures of 2,4,6-trinitrotoluene and 2,4,6-trinitro-*m*-xylene it became evident that the freezing point data reported by Efremov and Tikhomi-

rova,<sup>1</sup> Bell and Sawyer,<sup>2</sup> and Efremov, Khaishbashev and Frolova,<sup>3</sup> data which had been essentially reproduced by the present author, did not represent equilibrium conditions.

A study of this system was made by using an apparatus described elsewhere<sup>4</sup> which permitted a stepwise melting approach to the liquidus point with the provision for determining by means of the light transmission of the sample that solid-liquid equilibrium had been reached before proceeding to the next thermal step.

#### Experimental

The 2,4,6-trinitrotoluene used was recrystallized from benzene and ethyl alcohol. Following recrystallization it was fused and allowed to freeze under a vacuum twice. The melting point then was 80.9°. The 2,4,6-trinitro-*m*-xylene was recrystallized twice from methyl ethyl ketone. It then had a melting point of 182.2°.

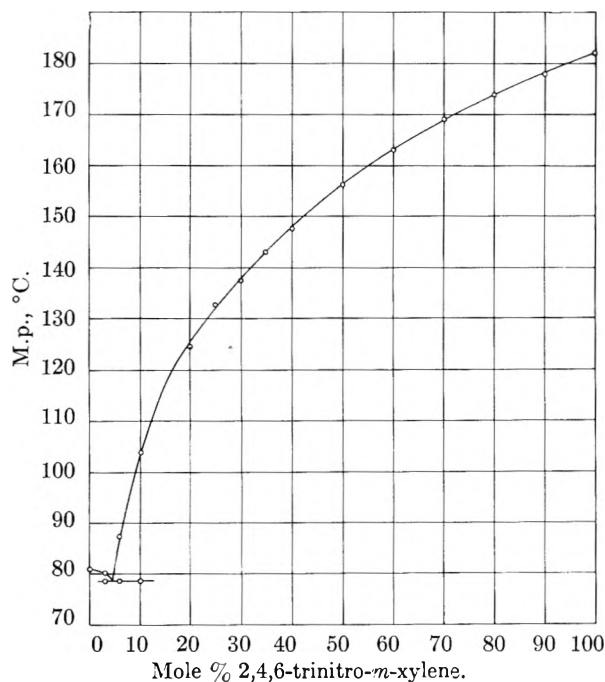


Fig. 1.

Six-gram samples of the required compositions were melted and stirred thoroughly. The temperature of the sample was then allowed to fall until a small amount of solid was formed. The temperature of the sample was then raised stepwise holding the sample at each temperature until the light transmission of the sample became constant. In this manner the temperature was raised to the point at which a few crystals were in equilibrium with the liquid. The temperature was then raised in small increments until these crystals disappeared, the last temperature being taken as the liquidus temperature.

Eutectic melting points were obtained by heating the completely solid sample through the eutectic melting point with a 0.1° temperature gradient between the bath and sample. With a small enough temperature gradient a flat is obtained at the eutectic melting point.

#### Results

This system forms a simple eutectic containing 4.6 mole % of 2,4,6-trinitro-*m*-xylene. The eutectic

(1) N. N. Efremov and A. M. Tikhomirova, *Ann. Inst. Phys. Chim. (Leningrad)*, **4**, 65 (1928).

(2) J. M. Bell and J. P. Sawyer, *Ind. Eng. Chem.*, **11**, 1025 (1919).

(3) N. N. Efremov, O. K. Khaishbashev and A. A. Frolova, *Izvest. Sektora Fiz.-Khim. Anal. Inst. Obshchei i Neorg. Khim., Akad. Nauk. USSR*, **17**, 160 (1949).

(4) L. A. Burkardt, W. S. McEwan and H. W. Pitman, *Rev. Sci. Inst.*, **27**, 693 (1956).

TABLE I

MELTING POINT DATA FOR THE SYSTEM 2,4,6-TRINITRO-TOLUENE-2,4,6-TRINITRO-*m*-XYLENE

Trinitro- <i>m</i> -xylene, mole %	M. p., °C.	Eutectic m. p., °C.	Trinitro- <i>m</i> -xylene, mole %	M. p., °C.
0	80.9		40	147.8
3	80.2	78.7	50	156.3
6	87.5	78.7	60	163.2
10	103.9	78.7	70	169.3
20	124.7		80	174.0
25	131.8		90	178.2
30	137.7		100	182.2
35	143.2			

melts at 78.7°. The concentration of 2,4,6-trinitro-*m*-xylene in the eutectic was found to be lower and the melting point higher than that obtained by previous investigators using the freezing point approach. The liquidus points were found to be markedly higher than those given by previous investigators.

Melting point data for this system is presented in Table I and given in graphical form in Fig. 1.

**Acknowledgments.**—The 2,4,6-trinitro-*m*-xylene used in this study was prepared and recrystallized by Donald W. Moore.

## THE VISCOSITY AND SURFACE TENSION OF PERCHLORYL FLUORIDE<sup>1</sup>

BY JOSEPH SIMKIN AND ROGER L. JARRY

*Pennsylvania Salt Manufacturing Company, Research and Development Department, Whitmarsh Research Laboratories, Wyndmoor, Pa.*

Received November 23, 1956

During the course of a program of physical measurements on perchloryl fluoride, determinations of viscosity and surface tension were made at selected points between -77 and 54°. A viscometer of the Scarpa design, as described by Elverum and Doescher,<sup>2</sup> was used for the measurements below 0°. The same operating procedure as described in their article was used in this work. For measurements at higher temperatures and pressures a modified Kuenen and Visser viscometer as described by Barr<sup>3</sup> was used. This glass viscometer with metal valves was constructed to withstand 300 p.s.i.g.

The viscosity measurements were relative and the reference material was acetone. Density and viscosity data for acetone were obtained from the International Critical Tables. Density data for perchloryl fluoride below 0° were from work done in this Laboratory to be published in this journal in the near future. For the points at 29.9 and 53.8° determinations were specifically made giving values of 1.390 and 1.276 g./cc., respectively.

Surface tension measurements were based on the

(1) This paper is the result of one phase of research carried out under Contract No. 19(600)761, supported by the United States Air Force through the Air Force Office of Scientific Research of the Air Research and Development Command.

(2) G. W. Elverum Jr., and R. N. Doescher, *J. Chem. Phys.*, **20**, 1834 (1952).

(3) G. Barr, "A Monograph of Viscometry," Oxford University Press, London, 1931, p. 123.

capillary rise in the Scarpa viscometer. The equation

$$\gamma = 1/2rhg(d_l - d_v) \quad (1)$$

where  $\gamma$  is the surface tension,  $r$  the radius,  $h$  the capillary rise,  $g$  the acceleration due to gravity and  $d_l$  and  $d_v$  are the densities of the liquid and vapor, respectively, was used for the calculation.

The viscosity data obtained are listed in Table I.

TABLE I  
VISCOSITY OF PERCHLORYL FLUORIDE

$t, ^\circ\text{C.}$	$\eta$ , centipoise	Dev. obsd. - calcd.
-76.5	0.572	-0.010
-75.0	.563	-.004
-65.9	.500	+.013
29.9	.173	+.003
53.8	.142	-.002

These data are fitted by the linear formula

$$\log \eta \text{ (centipoise)} = \frac{299}{T} - 1.755 \quad (2)$$

Deviations between the observed values and those calculated using equation 2 are shown in column three of Table I.

The surface tension data are listed in Table II.

TABLE II  
SURFACE TENSION OF PERCHLORYL FLUORIDE

$t, ^\circ\text{C.}$	Surface tension (dynes/cm.)
-75.2	24.1
-65.8	22.3
-55.6	21.3

The estimated uncertainty in the viscosity and surface tension data is  $\pm 2\%$ . Temperature measurements were made with calibrated thermocouples and were known to  $\pm 0.1^\circ$ .

**Acknowledgment.**—The writers wish to express their appreciation to Mr. W. J. Barry, of The Pennsylvania Salt Manufacturing Company, for performing the high temperature measurements.

## DISSOCIATION CONSTANTS OF POLYETHYLENEAMINES. II. THE DISSOCIATION CONSTANTS OF TETRAETHYLENEPENTAMINE<sup>1</sup>

BY HANS B. JONASSEN, FRED W. FREY AND ANNEKE SCHAAFSMA

Contribution from the Richardson Chemistry Laboratory, Tulane University, New Orleans, Louisiana

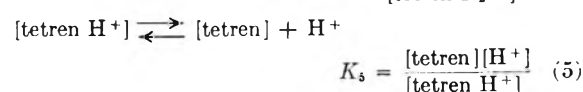
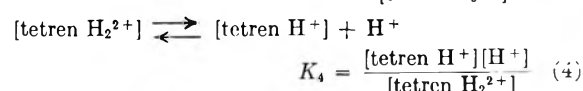
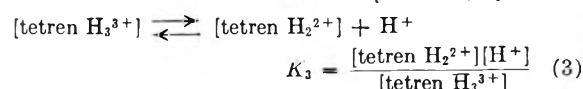
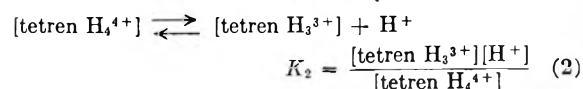
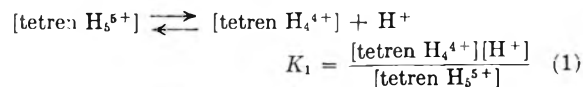
Received October 10, 1956

The dissociation constants of the three lower members of this polyethyleneamine series, as well as their complexity constants with various metal ions, have been determined previously by several investigators.

This paper reports methods of purification of tetren and the determination of its acid base constants.

(1) Abstracted from the Doctoral Dissertations of F. Frey, June, 1954, A. Schaafsma, June, 1953, Tulane University, New Orleans, Louisiana.

**Calculation of Constants.**—According to Bjerrum,<sup>2</sup> the dissociation or "hydrolysis" constants of a polyethyleneamine, in this case tetren, can be determined from the equilibria which are present in an aqueous solution



These five constants can be calculated from  $pH$  measurements of solutions containing known concentrations of the amine and an inorganic acid. Using Bjerrum's method the following equations can be derived where  $\bar{n}$  = the mean number of hydrogen ions attached to the amine molecule.

$$pK_1 = pH + \log \left[ \frac{\bar{n} - 4}{5 - \bar{n}} \right] \quad (6)$$

$$pK_2 = pH + \log \left[ \frac{\bar{n} - 3}{4 - \bar{n}} \right] + \log \left( 1 + \frac{K_3(\bar{n} - 2)}{[\text{H}^+](\bar{n} - 3)} \right) \quad (7)$$

$$pK_3 = pH + \log \left[ \frac{\bar{n} - 2}{3 - \bar{n}} \right] + \log \left( 1 + \frac{K_4(\bar{n} - 1)}{[\text{H}^+](\bar{n} - 2)} \right) \quad (8)$$

$$pK_4 = pH + \log \left[ \frac{\bar{n} - 1}{2 - \bar{n}} \right] + \log \left( 1 + \frac{K_5(\bar{n})}{[\text{H}^+](\bar{n} - 1)} \right) \quad (9)$$

$$pK_5 = pH + \log \left[ \frac{\bar{n}}{1 - \bar{n}} \right] - \log \left( 1 + \frac{(2 - \bar{n})\text{H}^+}{(1 - \bar{n})K_3} \right) \quad (10)$$

### Experimental

The technical grade amine purchased from Carbide and Carbon Chemicals was redistilled *in vacuo*. The tetren distilled at 169–171° under pressure of 0.05 mm. However, as indicated by potentiometric titration with a standard acid solution, distillation alone did not purify the amine sufficiently, and several other methods were used to prepare pure amine salts.

**I. Purification of Tetren by Precipitation of the Penta Acid Salts. a. Tetren Pentahydrochloride.**—About 150 g. of the distilled amine was dissolved in 300 ml. of 95% ethanol and the solution cooled to 10° in an ice-bath. One hundred eighty ml. of concentrated HCl was added dropwise so that the temperature of the solution did not exceed 20°. A white precipitate appeared during addition of the last 30 ml. The precipitate was filtered, recrystallized three times from ethanol and water, and washed with ether after the last recrystallization. The precipitate was dried by suction.

A weighed sample of the precipitate was titrated potentiometrically with standard sodium hydroxide solution; 0.1114 g. of the precipitate required 6.00 ml. of 0.2318 *M* NaOH for neutralization, indicating that the salt formed is the pentahydrochloride.

(2) J. Bjerrum, "Metal Amine Formation in Aqueous Solution, Theory of the Reversible Step Reaction," P. Haase and Son, Copenhagen, 1941.

The precipitate was also analyzed for chloride by titration with  $\text{AgNO}_3$  using thiocyanate as the indicator.

*Anal.* Calcd. for Tetren  $\cdot 5\text{HCl}$ : Cl, 47.7. Found: Cl, 47.2, 47.1.

The low chloride analysis is due to incomplete drying of the sample. Attempts to obtain a completely dried sample always resulted in partial decomposition of the salt.

b. **Tetren Pentahydrate.**—About 150 g. of the distilled amine was dissolved in 200 ml. of 95% ethanol and the solution cooled to 10°. One hundred ml. of concentrated  $\text{HNO}_3$  was added dropwise so that the temperature did not exceed 20°. The white precipitate was filtered by suction, recrystallized five times from ethanol and water, and washed with alcohol and ether after the last recrystallization. The precipitate was dried by suction.

A weighed sample of the salt was titrated potentiometrically with standard sodium hydroxide solution; 0.1289 g. of the salt required 5.20 ml. of 0.2318 *M* NaOH, indicating that the salt formed is the pentahydrate.

Paper chromatographic tests on all salt samples indicated the presence of only one component.

II. **Preparation of Solution.**—The standard aqueous amine solution was prepared by dissolving a weighed amount of the nitrate (chloride) salt. The solution was standardized by potentiometric titration with standard sodium hydroxide solution. This solution was then diluted to give a 0.001 *M* tetren hydronitrate solution.

A carbonate-free sodium hydroxide solution was prepared in the usual manner. After dilution it was standardized by titration with standard acid solution using modified methyl red as the indicator. A 0.05000 *M* sodium hydroxide solution was then prepared from this stock solution.

III. **Determination of Dissociation Constants.**—The dissociation constants of the tetren were determined by titrating 50 ml. of 0.001 *M* solution of the nitrate and chloride salts, with 0.05 *M* NaOH, using a Beckman model G pH meter and a Beckman all-purpose glass electrode. The titration was accomplished in a 4-neck flask, three necks symmetrically located around the center neck. The center neck was equipped with a stirring rod for mechanical stirring. The calomel and glass electrodes were placed in two of the other necks. The sodium hydroxide was introduced from a 10-ml. buret into the fourth neck. Nitrogen was bubbled through this neck during the titration.

The titrations were made at 25 ± 0.1°, 35 ± 0.1° and 45 ± 0.1°. The pH meter was standardized at each temperature with Beckman buffer solutions.

### Discussion

It was found that  $pK_1$  could not be calculated from the titration data as these concentrations did not make  $\bar{n}$  large enough. A separate titration was therefore performed in which the solution was made 0.005 *M* with  $\text{HNO}_3$  and 0.001 *M* with tetren  $\cdot 5\text{HNO}_3$ . This solution was then titrated with 0.05 *M* NaOH. A similar method was used for the chloride salt.  $pK_1$  could also be calculated only at 25°, as the accuracy of the pH meter did not permit any calculations at 35 and 45° because of the correction for  $[\text{H}^+]$  which must be applied to  $C_s$ .

Table I lists the value calculated for one of the five constants of tetren from the experiment data.

TABLE I

DETERMINATION OF  $pK_1$  DISSOCIATION CONSTANTS OF TETREN AT 25°

$$\Delta_1 = \log \left[ 1 + \frac{(1 - \bar{n})(\text{H}^+)}{\bar{n}K_1} \right]$$

$C_{\text{tetren}}$	$C_s$	$\bar{n}$	pH	$\frac{\log \bar{n}}{1 - \bar{n}}$	$\Delta_1$	$pK_1$
0.0009183	5723	0.62	9.81	+0.21	0.02	9.98
.0009166	4933	.54	9.89	+ .07	.02	9.94
.0009149	4218	.46	9.99	- .05	.02	9.92
.0009132	3534	.39	10.08	- .20	.01	9.87
.0009116	2871	.32	10.16	- .32	.01	9.83
						9.92

Where  $C_{\text{tetren}}$  = total concentration of tetren in solution

$$C_s = [\text{tetren H}^+] + 2[\text{tetren H}_2^{2+}] + 3[\text{tetren H}_3^{3+}] + 4[\text{tetren H}_4^{4+}] + 5[\text{tetren H}_5^{5+}]$$

Table II lists the values determined for the five constants at the three temperatures.

TABLE II

DISSOCIATION CONSTANTS AT 35 AND 45°

	25°	35°	45°
$pK_1$	2.65	2.43	
$pK_2$	4.25	3.99	3.74
$pK_3$	7.87	7.54	7.26
$pK_4$	9.08	8.81	8.53
$pK_5$	9.92	9.65	9.38

Further thermodynamic data calculated from them have no more accuracy than that to which the change in  $pK$  with temperature is shown; they are therefore not reported. The values so calculated, however, are in line with those expected from a comparison with the lower polyamines.

**Acknowledgment.**—The financial help of the Office of Ordnance Research, U. S. Army, is gratefully acknowledged in this and continuing investigations.

## THE DIFFERENTIAL THERMAL ANALYSIS OF PERCHLORATES

BY MEYER MELVIN MARKOWITZ

Department of Chemical Engineering, New York University, University Heights, New York City, N. Y.

Received November 10, 1956

The significance of differential thermal analysis (DTA) curves may often be increased when taken in conjunction with other studies. By supplementing observed DTA curves with information derived from chemical and X-ray analyses, kinetic mechanisms<sup>1,2</sup> and phase diagrams<sup>3,4</sup> have been determined. In a recent paper on DTA by Gordon and Campbell,<sup>5</sup> the consistent presence of an exothermic break in the DTA curves of the perchlorates of silver, the alkali metals and the alkaline earths is quite puzzling. Except with such substances as the hydrazine and ammonium nitrates and perchlorates which undergo vigorous oxidation reactions, and various azides, it is to be anticipated that the thermal decompositions of most inorganic materials which yield, at least in part, gaseous products are endothermic. From results reported in the literature concerning the pyrolysis of potassium perchlorate, it is believed that the endothermic nature of the decomposition of this salt can be adduced and that the general exothermic phenomena observed for the perchlorates<sup>6</sup> can be traced to the occurrence of reaction product crystallization.

It has been noted that in the heating of potassium perchlorate, there is at first the appearance of a

(1) R. K. Osterheld and L. F. Audrieth, *THIS JOURNAL*, **56**, 38 (1952).

(2) R. K. Osterheld and M. M. Markowitz, *ibid.*, **60**, 863 (1956).

(3) R. K. Osterheld and R. P. Langguth, *ibid.*, **69**, 76 (1955).

(4) E. P. Partridge, V. Hicks and G. W. Smith, *J. Am. Chem. Soc.*, **63**, 454 (1941).

(5) S. Gordon and C. Campbell, *Anal. Chem.*, **27**, 1102 (1955).

liquid, followed by complete solution, and finally the deposition of a solid until complete solidification occurs.<sup>6-8</sup> Decomposition proceeds partially through a chlorate intermediate, frequently found, although only in low concentrations. The first appearance of liquid in a heated sample is a function of both the temperature and the length of the heating period.<sup>7,8</sup> Chemical analyses of samples at the onset of liquefaction strongly suggest that melting ensues because of eutectic formation between the potassium perchlorate and its decomposition products, potassium chloride and potassium chlorate. Accordingly, the DTA curve will show a pair of endothermic breaks<sup>5</sup> which may correspond to rapid fusion plus slow concomitant thermal decomposition of the chlorate and perchlorate, then followed by the more rapid endothermic decompositions of the latter materials. As the potassium chloride concentration in the liquid phase increases with prolonged heating, the salt will start to be deposited from the melt. This latter effect will then result in an exothermic break corresponding to the evolution of the latent heat of crystallization of the metal chloride but moderated by the continuous endothermic decomposition of the perchlorate.

That a high concentration of potassium chloride may be formed during the relatively short interval from the first endothermic break (designated in Fig. 3, reference 5, as "fusion," 588°) to the exothermic break may be shown by assuming liquid phase decomposition of the potassium perchlorate while being maintained at an average temperature of 610° for four minutes. Using the rate equation,<sup>8</sup>  $k = 1.31 \times 10^{15} e^{-(70500/RT)}$ , at 610°, the calculated first-order rate constant is  $4.71 \times 10^{-3} \text{ sec.}^{-1}$ , which gives after the heating period, 67.7 mole % KCl and 32.3 mole % KClO<sub>4</sub>. The potassium chloride content is, of course, augmented during the period of the exotherm, so that at the end of the exotherm the residue is essentially pure solid potassium chloride.

Experimental proof for the validity of the aforementioned behavior may be found in the instances of rubidium, cesium, silver and magnesium perchlorates for which DTA's<sup>5</sup> had been carried out beyond the melting points of the respective chlorides (715, 646, 455 and 714°). Clearly indicated are endotherms, immediately following the exotherms, terminating at about 715, 647, 464 and 720°, respectively. The absence of an endotherm indicating the melting of lithium chloride (m.p. 614°) in the DTA for lithium perchlorate trihydrate is inexplicable.

Approximate thermodynamic calculations<sup>9</sup> (Table I) pertaining to the major reactions assigned to the breaks observed during the DTA of potassium perchlorate appear to substantiate an endothermic decomposition (reaction c), Table I. Negli-

gible heat capacity and solution effects were assumed over the temperature range involved (25-700°). The low heat of fusion ascribed to potassium perchlorate, 1.7-2.6 kcal./mole, is justified on the basis of the crystallographic transition occurring at 300°<sup>10</sup> which denotes the onset of rotation of the perchlorate groups in the solid state. Such rotation generally leads to low entropies of fusion, and consequently low heats of fusion.<sup>11-13</sup> In the computation of Table I, an entropy of fusion of 2-3 entropy units was assumed.

TABLE I

THE REACTION SEQUENCE OF POTASSIUM PERCHLORATE DURING DTA

	Obsd. DTA Temp., °C.	Equation <sup>a</sup>	Process	$\Delta H$ , kcal./mole
a	300	$\text{KClO}_4(\text{s, II}) \longrightarrow \text{KClO}_4(\text{s, I})$	Transition	3.29
b	588	$\text{KClO}_4(\text{s, I}) \longrightarrow \text{KClO}_4(\text{l})$	Fusion	1.7-2.6
c	610	$\text{KClO}_4(\text{l}) \longrightarrow \text{KCl}(\text{l}) + 2\text{O}_2(\text{g})$	Decompn.	1.7-0.8
d	660	$\text{KCl}(\text{l}) \longrightarrow \text{KCl}(\text{s})$	Crystn.	-6.1

<sup>a</sup> l = liquid, s = solid, g = gas.

The vigorous evolution of chlorous fumes found for the hydrated perchlorates of copper, zinc and mercury may be attributed to the hydrolysis of these salts of weak bases as previously reported for the cases of aluminum, magnesium and iron(III) hydrated perchlorates producing fumes of perchloric acid or chlorine oxides.<sup>14</sup>

The decomposition behavior of the perchlorates of strong bases is in distinction to that of the alkali metal nitrates,<sup>15,16</sup> where melting occurs at a temperature considerably below that of rapid decomposition to yield products of low melting points.

In conclusion, it may be said that the utility of DTA is enhanced when used with other analytical techniques, that there are no true melting points characterizing the metal perchlorates,<sup>17</sup> and that the general exothermic phenomena evidenced on the DTA curves of perchlorates<sup>5</sup> may be related to the deposition of high melting point solid decomposition products (*i.e.*, the metal chlorides) from the first-formed melts.

**Acknowledgment.**—Acknowledgment is made of the helpful discussions with Professor John E. Ricci, Department of Chemistry, New York University.

(10) C. Finbak and O. Hassel, *Z. physik. Chem.*, **B35**, 25 (1937).

(11) R. R. Wenner, "Thermochemical Calculations," McGraw-Hill Book Co., New York, N. Y., 1941, pp. 23-6.

(12) C. P. Smyth, *Chem. Revs.*, **19**, 329 (1936).

(13) S. Glasstone, "Textbook of Physical Chemistry," D. Van Nostrand Co., Inc., New York, N. Y., Second Edition, 1946, pp. 422-4, 462-3.

(14) G. G. Marvin and L. B. Woolaver, *Ind. Eng. Chem., Anal. Ed.*, **17**, 474 (1945).

(15) N. V. Sidgwick, "The Chemical Elements and Their Compounds," Vol. I, Oxford University Press, Oxford, 1951, pp. 700-1.

(16) M. Centnerszwer, *J. chim. phys.*, **27**, 9 (1930).

(17) A. E. Simchen, A. Glasner and B. Fraenkel, *Bull. Research Council Israel*, **2**, 70 (1952).

(6) A. Glasner and L. Weidenfeld, *J. Am. Chem. Soc.*, **74**, 2467 (1952).

(7) L. L. Bircumshaw and T. R. Phillips, *J. Chem. Soc.*, 703 (1953).

(8) A. E. Harvey, Jr., M. T. Edmison, E. D. Jones, R. A. Seybert and K. A. Catto, *J. Am. Chem. Soc.*, **76**, 3270 (1954).

(9) Data taken from F. D. Rossini, D. D. Wagman, W. H. Evans, S. Levine and I. Jaffe, "Selected Values of Chemical Thermodynamic Properties," National Bureau of Standards Circular 500, U. S. Government Printing Office, Washington, D. C., 1952.

## STUDIES ON THE LINEAR CRYSTALLIZATION OF NITROTOLUENE SYSTEMS<sup>1</sup>

By E. R. DALBEY AND W. A. GEY

Chemistry Division, U. S. Naval Ordnance Test Station, China Lake, California

Received December 1, 1956

Studies on the linear crystallization velocity (LCV) of 2,4,6-trinitrotoluene (TNT) have been reported in a recent paper from this Laboratory.<sup>2</sup> The effect of additives was shown to be fairly accurately related to the additive concentration by a modified Langmuir adsorption expression

$$R = R_0 C \frac{1}{1 + \alpha(1 - C) + \beta} \quad (1)$$

in which

$R$  = LCV of substrate + additive  
 $R_0$  = LCV of pure substrate  
 $C$  = mole fraction of substrate  
 $1 - C$  = mole fraction of additive  
 and  $\alpha$  and  $\beta$  are constants

Equation 1 was derived on the assumption that the effect of the additive is due to adsorption on the advancing crystal front. The Freundlich isotherm<sup>3</sup> was shown to be less exact than this modified Langmuir isotherm (1), for those additives which were highly growth active. Furthermore, extreme crystal-growth activity was found only in additives a part of whose molecule was similar in structure to the substrate molecule. Thus, 2,4,6-trinitrostilbene and its derivatives were found to be most effective in reducing the LCV of TNT.

In order to test further the applicability of equation 1 and the relation of molecular structure of the additive to crystal-growth activity, the effects of selected compounds on the LCV of a number of other simple nitroaromatic compounds have been investigated.

### Experimental

The equipment and procedures for determining the LCV were the same as those used in the previous study.<sup>2</sup> Some of the compounds used in this investigation were previously described; additional compounds were the following.

4-Nitrotoluene (Eastman Kodak Co., White Label) was crystallized twice from ethanol, using a Norite decolorization the first time, then dried *in vacuo* over sulfuric acid; m.p. 52.0–52.5°.

2,6-Dinitrotoluene.—2,6-Dinitro-4-aminotoluene was prepared as described by Parkes and Farthing.<sup>4</sup> Conversion of 2,6-dinitro-4-aminotoluene to 2,6-dinitrotoluene according to Holleman and Boeseken,<sup>5</sup> gave a very low yield. A procedure for the deamination was developed as follows: 9.2 g. (0.039 mole) of 2,6-dinitro-4-aminotoluene hydrochloride was dissolved in a mixture of 180 ml. of absolute ethanol and 46 ml. of concd. sulfuric acid and heated on a steam-bath. A solution of 27 g. (0.391 mole) of sodium nitrite in 40 ml. of water was added with stirring during 35 minutes. After stirring and heating for 20 minutes more, the mixture was poured on crushed ice, the alcohol evaporated at room temperature, and the 2,6-dinitrotoluene isolated by steam

(1) Abstracted, in part, from the thesis submitted by E. R. Dalbey in partial fulfillment of the requirements for the M.S. degree, University of Washington, August, 1953.

(2) W. A. Gey, *et al.*, *J. Am. Chem. Soc.*, **78**, 1803 (1956).

(3)  $\bar{R} = (R_0 - R)/R_0 = kC^{1/N}$ , in which  $R$  and  $R_0$  have the same designation as in equation 1, and  $C$  is moles of additive per 100 moles of substrate. H. Freundlich, "Colloid and Capillary Chemistry," Methuen and Co., Ltd., London, 1926.

(4) G. D. Parkes and A. C. Farthing, *J. Chem. Soc.*, 1275 (1948).

(5) A. F. Holleman and J. Boeseken, *Rec. trav. chim.*, **16**, 427 (1897).

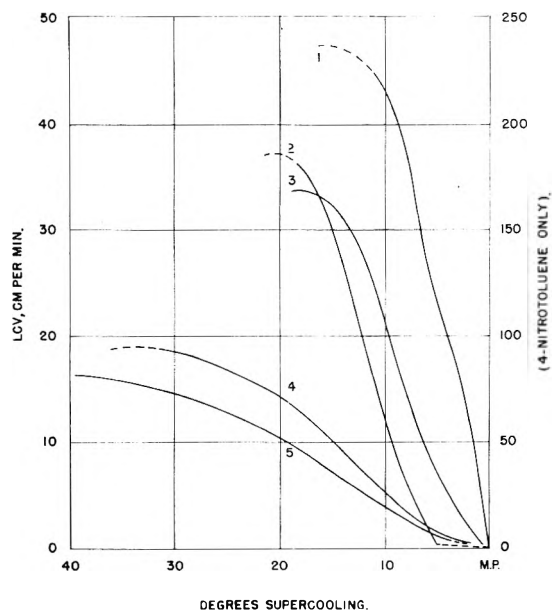


Fig. 1.—Linear crystallization velocities of various nitrotoluenes as related to temperature of supercooling (note different scale for 4-nitrotoluene): (1) dinitromesitylene; (2) 2,6-dinitrotoluene; (3) 4-nitrotoluene; (4) 2,4,6-trinitrotoluene; (5) 2,4-dinitrotoluene.

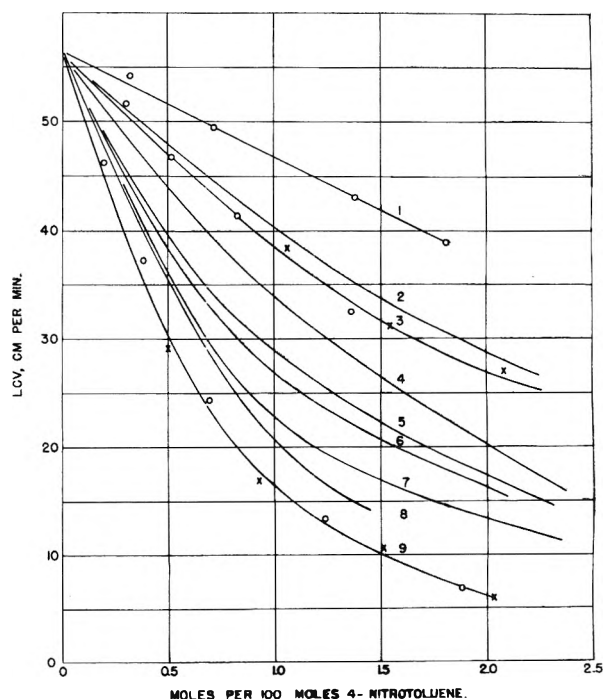


Fig. 2.—Linear crystallization velocity of 4-nitrotoluene as modified by various additives, 45.0°: (1) anthracene; (2) 2,4,6-trinitrostilbene; (3) 2,4-dinitrostilbene; (4) 4-nitrostilbene; (5) 2,4,4',6-tetranitrostilbene; (6) 2,3',4,6-tetranitrostilbene; (7) 2,3',4-trinitrostilbene; (8) 2,4,4'-trinitrostilbene; (9) 4,4'-dinitrodibenzyl.

distillation. The crude product was crystallized from Skellysolve-B and vacuum sublimed; m.p. 64.2–64.7°.

Anal. Calcd. for  $C_7H_6N_2O_4$ : C, 46.15; H, 3.32; N, 15.38. Found: C, 46.26; H, 3.51; N, 15.58.

The following nitroaromatics were prepared as described in the literature: 2,4-dinitromesitylene,<sup>6</sup> m.p. 86.0–86.5°;

(6) F. W. Kuster and B. Stallberg, *Ann.*, **278**, 213 (1894).

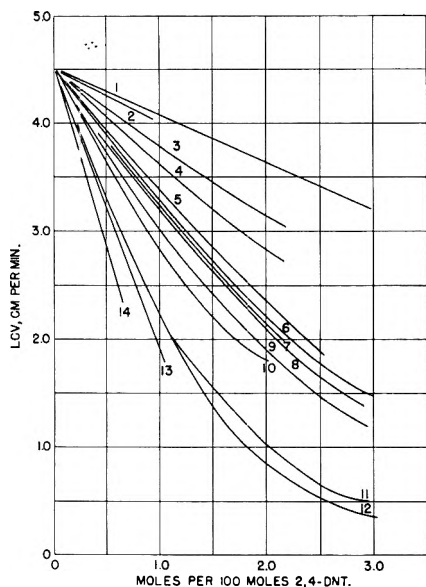


Fig. 3.—The linear crystallization velocity of 2,4-dinitrotoluene as modified by various additives, 60.0°: (1) anthracene; (2) 2,4,6-trinitrostilbene; (3) 3'-iodo-2,4,6-trinitrostilbene; (4) 2,2',4,4'-tetranitrodibenzyl; (5) 4'-isopropyl-2,4-dinitrostilbene; (6) 2,4-dinitrostilbene; (7) 2'-chloro-2,4-dinitrostilbene; (8) 3'-methyl-2,4-dinitrostilbene; (9) 4'-methyl-2,4-dinitrostilbene; (10) 2',4'-dichloro-2,4-dinitrostilbene; (11) 2,3',4-trinitrostilbene; (12) 2,4,4'-trinitrostilbene; (13) 2,4-dinitrophenylhydrazone of benzaldehyde; (14) 4'-dimethylamino-2,4-dinitrostilbene.

4,4'-dinitrostilbene,<sup>7</sup> m.p. 301–302°; 4,4'-dinitrodibenzyl,<sup>8</sup> m.p. 179.5–180.5°; 4-nitrostilbene,<sup>7</sup> m.p. 157–158°; 4'-methyl-2,4-dinitrostilbene,<sup>9</sup> m.p., softens to turbid liquid at 176–182°, becomes clear at 183–184°;

Anal. Calcc. for  $C_{15}H_{12}N_2O_2$ : C, 63.37; H, 4.26; N, 9.86. Found: C, 63.37; H, 4.39; N, 9.18.

2'-Chloro-2,4-dinitrostilbene,<sup>10</sup> m.p. 177.5–178°;

Anal. Calcc. for  $C_{14}H_8N_2O_2Cl$ : C, 55.18; H, 2.98; N, 9.20; Cl, 11.64. Found: C, 55.51; H, 2.93; N, 9.53; Cl, 11.62.

2,4,2',4'-Tetranitrodibenzyl,<sup>8</sup> m.p. 170–171°.

### Discussion

**LCV-Temperature Relationships.**—The effect of temperature on the LCV of the nitrotoluenes was determined and the results are shown in Fig. 1. In the region of maximum velocity each compound showed a threshold temperature, below which it appeared impossible to prevent spontaneous nucleation.

**LCV in the Presence of Additives. A. 4-Nitrotoluene.**—The average LCV of 4-nitrotoluene at 45° was 56.6 cm./min. The effects of the additives on LCV at this temperature are shown graphically in Fig. 2. Reproducibility of the data is shown in curves 3 and 9, Fig. 2, in which the crosses and open circles are the results of check experiments. As expected, additives containing a 4-nitrobenzal group brought about large changes in LCV. Anthracene shows a weak effect. 2,4,6-Trinitrostilbene and 2,4-dinitrostilbene show stronger effects but not nearly as large as the "opposite-ring" substituted 4-nitrostilbenes. The most effective addi-

(7) C. M. Anderson, *et al.*, *J. Am. Chem. Soc.*, **72**, 1263 (1950).

(8) W. H. Rinkenbach and H. A. Aaronson, *ibid.*, **52**, 5041 (1930).

(9) P. Pfeiffer, *Ann.*, **411**, 130 (1916), reported m.p. 197–198°.

(10) R. Robinson and A. Zaki, *J. Chem. Soc.*, 2485 (1927), reported m.p. 174°.

tive, up to its low limit of solubility, was 4,4'-dinitrostilbene; almost as effective was the more soluble 4,4'-dinitrodibenzyl. It is interesting that the order of effectiveness of the nitrostilbenes was dinitrostilbene > trinitrostilbene > tetranitrostilbene > mononitrostilbene. The fact that the 4,4'-dinitrodibenzyl is practically as effective as the corresponding dinitrostilbene shows that in this case the unsaturated bridge of the latter does not result in much stronger adsorption.

The data agree with the modified Langmuir relationship until the higher concentrations are reached where there are some deviations. With the two very strong inhibitors, 4,4'-dinitrostilbene and 4,4'-dinitrodibenzyl, the relationship is only followed for a very short range of concentration after which there is a great change of slope.

**B. 2,4-Dinitrotoluene.**—The 2,4-dinitrotoluene showed an average LCV at 60° of 4.53 cm./min. The data on the LCV of 2,4-dinitrotoluene with fourteen additives at 60° are plotted in Fig. 3.

As expected, the 2,4-dinitrostilbene compounds have a great inhibiting effect on 2,4-dinitrotoluene. The advantage of the 2,4-dinitrobenzal grouping is illustrated by comparison with the much weaker additives, anthracene, 2,4,6-trinitrostilbene and 3'-iodo-2,4,6-trinitrostilbene (the latter was one of the most powerful inhibitors for the 2,4,6-trinitrotoluene system). Substitution on the second ring of 2,4-dinitrostilbene in all cases enhanced crystal-growth activity with the exception of 4'-isopropyl-2,4-dinitrostilbene, which was slightly inferior to the unsubstituted compound. Substitution by 3'-nitro-, 4'-nitro- and 4'-phenyl- groups gave three additives of similar activity. 4'-Dimethylamino-2,4-dinitrostilbene, which is the most effective of the additives tried, could not be used in higher concentrations since the deep red color made it impossible to see the crystallization front. To its limit of solubility, the 2,4-dinitrophenylhydrazone of benzaldehyde is more active than any of the stilbenes except the dimethylaminodinitrostilbene. 2,2',4,4'-Tetranitrostilbene is not as effective as expected. 2,2',4,4'-Tetranitrodibenzyl was not nearly as effective as the tetranitrostilbene.

The data for the effect of additives on the LCV of 2,4-dinitrotoluene can be closely expressed by the Freundlich isotherm with values of  $k$  ranging from 0.725 for 4'-dimethylamino-2,4-dinitrostilbene to 0.098 for anthracene. The data do not fit the modified Langmuir adsorption isotherm.

**C. 2,6-Dinitrotoluene.**—The LCV determinations on 2,6-dinitrotoluene were made at 54.3°. It was not intended to study this system in detail, but merely to obtain a very brief insight into its LCV characteristics for comparison purposes. The effects of the three additives tried on the LCV are given in Table I. It may be noted that 2,4-dinitrophenylhydrazone benzaldehyde and 3',2,4-dinitrostilbene are about equally effective and both are somewhat better than 2,6-dinitrostilbene. All three are fairly effective LCV depressants.

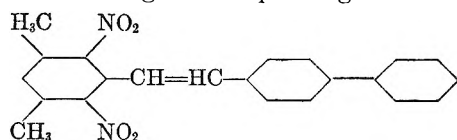
The 2,6-dinitrotoluene data were plotted according to the Langmuir and Freundlich relationships. The hydrazone follows the straight line of the modified Langmuir equation up to its limit of solu-

TABLE I  
LCV OF 2,6-DINITROTOLUENE IN THE PRESENCE OF  
ADDITIVES AT 54.3°

Concn. of additive (moles/100 moles substrate)	LCV, cm./min. in the presence of		
	2,6-Dinitro- stilbene	2,4- Dinitrophenyl- hydrazone benzaldehyde	2,3',4'-Trinitro- stilbene
0.0			13.7
0.5	10.8	9.9	9.9
1.0	8.2	7.1	7.0
1.5	6.1	5.3	5.1
2.0	4.5		3.55
2.5	3.35		2.45

bility, while the other two additives do not. The 2,6-dinitrostilbene follows the Freundlich relationship fairly well, while the 3',2,4-trinitrostilbene follows neither relationship well over the concentration range studied.

**D. 2,4-Dinitromesitylene.**—The effects of the three additives tested on the LCV at 74° are given in Table II. As expected, 2-naphthol showed a very weak effect, 2,4,6-trinitrostilbene a stronger one, and a resinous product prepared by refluxing an equimolar mixture of dinitromesitylene and 4-phenylbenzaldehyde (xylene solvent) in the presence of piperidine for several hours shows a strong effect. The resin was assumed to have a molecular structure and weight corresponding to



These additives to the dinitromesitylene system affect the crystallization according to the Langmuir-type isotherm.

TABLE II  
LCV OF DINITROMESITYLENE IN THE PRESENCE OF  
ADDITIVES AT 74.0°

Concn. of additive (moles/100 moles substrate)	LCV, cm./min. in the presence of		
	2- Naphthol	2,4,6- Trinitro- stilbene	Resin
0	45	45	45
0.5	41.7	37.6	19.7
1.0	39.3	33.4	13.0
1.5	37.0	30.4	10.3
2.0	34.9	27.4	8.4
2.5	32.7	24.5	7.2
3.5	29.4	20.3	...

**X-Ray Studies.**—In addition to merely slowing down the advancement of a single growing face of solid into the supercooled melt and thereby decreasing the LCV of a compound, it was thought that perhaps strongly absorbed additives might inhibit the LCV by changing the orientation of the crystals formed from the solidifying melt. To determine this effect, if any, rotation patterns were taken of 2,4-dinitrotoluene without additive and with 2% 2,4,4'-trinitrostilbene which had been crystallized at about 15° below the melting point in thin-walled glass capillaries (about 0.5 mm. i.d.). The additive was found to decrease the number of crystals and greatly increase the degree of orientation.

A similar experiment was made on the same samples contained in smaller (about 0.1–0.2 mm. i.d.) capillary tubes. Single crystals were not obtained, but it was even more apparent than in the previous case how much the orientation of solid was increased by the presence of additive. It appears that this greater orientation is related to the lower LCV of 2,4-dinitrotoluene in the presence of 2,4,4'-trinitrostilbene.

#### The Effects of Additives on the TNT System Compared with Effects on Other Nitro-aromatics.

—In general, conclusions from the study on the 2,4,6-trinitrotoluene system applied well to the compounds studied in this research. In all cases, the nitrostilbene additives gave much greater crystal growth activity than previous additives reported in the literature. The importance of having one end of the molecule similar to the molecule of the system being inhibited is well demonstrated.

Perhaps the greatest difference between TNT and the other systems is the extremely rapid decrease of LCV of TNT with very small concentrations of the stilbene additives, as demonstrated by the large "β" values obtained in the modified Langmuir equation for these additives. This great initial decrease is not observed with less powerful additives such as anthracene in TNT, nor with any additives in the other nitroaromatic compounds studied.

The modified Langmuir expression for the effect of additives on linear crystallization velocity, which was applicable to the TNT systems, was found to be not generally applicable to nitroaromatic systems.

The only conclusion reached from the data available is that the adsorption of the more powerful additives is a complicated phenomenon and like the adsorption of gases at higher pressures can follow various differing mechanisms. As the Freundlich and modified-Langmuir equations are both only approximate mathematical descriptions of the true phenomena, it is perhaps rather fortuitous when one law is followed over a large range of concentration.

**Acknowledgment.**—The authors wish to express their appreciation to E. C. Lingafelter and R. W. Van Dolah for encouragement and helpful discussions throughout the course of this work.

#### THERMODYNAMIC FUNCTIONS FOR THE ISOTOPIC HYDROGEN SELENIDES AND HYDROGEN TELLURIDE

By A. P. ALESHULLER

Received November 12, 1956

Although the thermodynamic functions for hydrogen and deuterium and tritium oxides and sulfides are well established,<sup>1–3</sup> no calculations of the thermodynamic functions of the hydrogen and deuterium selenides nor hydrogen telluride over a range of temperatures appears to be available.

While the vibrational frequencies of H<sub>2</sub>Se, HDSe and D<sub>2</sub>Se were obtained some years ago,<sup>4,5</sup>

- (1) F. D. Rossini, *et al.*, NBS Circular 500, 1952.
- (2) A. S. Friedman and L. Haar, *J. Chem. Phys.*, **22**, 2051 (1954).
- (3) L. Haar, J. C. Bradley and A. S. Friedman, *J. Research Natl. Bur. Standards*, **55**, 285 (1955).
- (4) A. Dadiou and W. Engler, *Wiener Anzeiger*, **128**, 13 (1935).
- (5) D. M. Cameron, W. C. Sears and H. H. Nielsen, *J. Chem. Phys.*, **7**, 994 (1939).

the molecular dimensions of these molecules have been determined only recently.<sup>6,7</sup> The vibrational frequencies used in calculating the thermodynamic functions are H<sub>2</sub>Se:  $\nu_1 = 2260$ ,  $\nu_2 = 1074$ ,  $\nu_3 = 2350$  cm.<sup>-1</sup>; HDSe:  $\nu_1 = 1691$ ,  $\nu_2 = 905$ ,  $\nu_3 = 2352$  cm.<sup>-1</sup>; D<sub>2</sub>Se:  $\nu_1 = 1630$ ,  $\nu_2 = 745$ ,  $\nu_3 = 1696$  cm.<sup>-1</sup>.<sup>4</sup> The molecular dimensions of hydrogen selenide are  $r(\text{Se-H}) = 1.460 \pm 0.013$  Å. and  $\langle \text{HSeH} \rangle = 91.0 \pm 0.6^\circ$ .<sup>7</sup> The moments of inertia for H<sub>2</sub>Se, HDSe and D<sub>2</sub>Se are as follows:  $I_1 = 3.42 \times 10^{-40}$ ,  $I_2 = 3.63 \times 10^{-40}$ ,  $I_3 = 7.05 \times 10^{-40}$ ;  $I_1 = 5.06 \times 10^{-40}$ ,  $I_2 = 5.44 \times 10^{-40}$ ,  $I_3 = 10.50 \times 10^{-40}$ ;  $I_1 = 6.67 \times 10^{-40}$ ,  $I_2 = 7.26 \times 10^{-40}$ ,  $I_3 = 13.93 \times 10^{-40}$  g.<sup>3</sup>-cm.<sup>6</sup> The moments of inertia of HDSe and D<sub>2</sub>Se are calculated on the assumption that  $r(\text{H-Se}) = r(\text{D-Se})$ . In the case of H<sub>2</sub>O, HDO and D<sub>2</sub>O the OH and OD distances are equal to at least the third decimal place and the valence angles are equal to at least a few hundredths of a degree.<sup>8</sup> Since the molecular dimensions of H<sub>2</sub>Se are uncertain to a far greater degree than the possible isotopic differences, the assumption of equal dimensions for H<sub>2</sub>Se, HDSe and D<sub>2</sub>Se will not cause a significant error in the thermodynamic functions. It is assumed also that  $I_1 + I_2 = I_3$ . For H<sub>2</sub>O, HDO and D<sub>2</sub>O the inertia defect is only  $-0.003 \times 10^{-40}$  g.-cm.<sup>2,8</sup> while in a highly refined calculation of the thermodynamic functions for the isotopic hydrogen sulfides  $I_1 + I_2$  is taken as equal to  $I_3$  to the third decimal place.<sup>3</sup>

The thermodynamic functions for H<sub>2</sub>Se, HDSe and D<sub>2</sub>Se to the rigid rotator-harmonic oscillator approximation are listed in Tables I, II and III for the ideal gas state at one atmosphere pressure.

TABLE I

THERMODYNAMIC FUNCTIONS FOR HYDROGEN SELENIDE IN THE IDEAL GAS STATE IN CAL./DEG./MOLE

T, °K.	C <sub>p</sub> <sup>o</sup>	$\frac{H^\circ - H_0^\circ}{T}$	$\frac{-F^\circ - H_0^\circ}{T}$	S <sup>o</sup>
100	7.95	7.95	35.61	43.56
200	8.00	7.96	41.12	49.08
250	8.11	7.97	42.90	50.87
275	8.18	7.99	43.66	51.65
298.16	8.26	8.01	44.30	52.31
300	8.27	8.01	44.35	52.36
325	8.36	8.03	45.00	53.03
350	8.47	8.07	45.59	53.66
400	8.67	8.12	46.67	54.79
500	9.13	8.28	48.50	56.78
600	9.61	8.46	50.02	58.48
700	10.09	8.66	51.34	60.00
800	10.54	8.87	52.51	61.38
900	10.94	9.07	53.57	62.64
1000	11.29	9.28	54.54	63.82

The only previous calculation of the thermodynamic functions of H<sub>2</sub>Se, HDSe and D<sub>2</sub>Se appears to be a computation of the entropies at 298.16°K.<sup>9</sup> These values are all about 0.5 e.u. higher than those given above. The difference is largely due to the use of the very approximate molecular dimen-

(6) E. Palik, *J. Chem. Phys.*, **23**, 980 (1955).

(7) A. W. Jache, P. W. Moser and W. Gordy, *ibid.*, **25**, 209 (1956).

(8) W. S. Benedict, N. Gailar and E. K. Plyler, *ibid.*, **24**, 1139 (1956).

(9) K. K. Kelly, U. S. Bureau of Mines Bulletin 477, 1948.

TABLE II

THERMODYNAMIC FUNCTIONS FOR HYDROGEN DEUTERIUM SELENIDE IN THE IDEAL GAS STATE IN CAL./DEG./MOLE

T, °K.	C <sub>p</sub> <sup>o</sup>	$\frac{H^\circ - H_0^\circ}{T}$	$\frac{-F^\circ - H_0^\circ}{T}$	S <sup>o</sup>
100	7.95	7.95	38.21	46.16
200	8.08	7.97	43.73	51.70
250	8.26	8.01	45.51	53.52
275	8.37	8.04	46.27	54.31
298.16	8.48	8.07	46.92	54.99
300	8.49	8.07	46.97	55.04
325	8.62	8.11	47.62	55.73
350	8.75	8.15	48.22	56.37
400	9.03	8.24	49.32	57.56
500	9.59	8.45	51.18	59.63
600	10.12	8.69	52.74	61.43
700	10.62	8.93	54.09	63.02
800	11.05	9.17	55.30	64.47
900	11.43	9.39	56.40	65.79
1000	11.75	9.61	57.40	67.01

TABLE III

THERMODYNAMIC FUNCTIONS FOR DEUTERIUM SELENIDE IN THE IDEAL GAS STATE IN CAL./DEG./MOLE

T, °K.	C <sub>p</sub> <sup>o</sup>	$\frac{H^\circ - H_0^\circ}{T}$	$\frac{-F^\circ - H_0^\circ}{T}$	S <sup>o</sup>
100	7.95	7.95	37.73	45.68
200	8.22	8.00	43.25	51.25
250	8.49	8.07	45.04	53.11
275	8.64	8.12	45.81	53.93
298.16	8.78	8.16	46.47	54.63
300	8.80	8.17	46.52	54.69
325	8.95	8.22	47.18	55.40
350	9.11	8.28	47.79	56.07
400	9.45	8.40	48.90	57.30
500	10.10	8.68	50.80	59.48
600	10.70	8.97	52.41	61.38
700	11.22	9.25	53.81	63.06
800	11.65	9.52	55.07	64.59
900	11.99	9.78	56.20	65.98
1000	12.28	10.01	57.25	67.26

sions estimated in the earlier work.<sup>5</sup> No calorimetric determination for H<sub>2</sub>Se is available.

A preliminary investigation of the infrared spectra of hydrogen telluride has been reported recently.<sup>10</sup> Since only a very rough estimate of the entropy of H<sub>2</sub>Te is given in the literature,<sup>9</sup> it appears worthwhile to calculate the thermodynamic functions for H<sub>2</sub>Te around room temperature. The bending fundamental  $\nu_2$  is at about 870 cm.<sup>-1</sup>. The stretching fundamentals  $\nu_1$  and  $\nu_3$  are located in the 1900 to 2200 cm.<sup>-1</sup> region. An overlap region may exist between 2120 to 2140 cm.<sup>-1</sup>.<sup>10</sup> Since  $\nu_1$  and  $\nu_3$  in H<sub>2</sub>Se are about 100 cm.<sup>-1</sup> apart and  $\nu_3$  is greater than  $\nu_1$  for H<sub>2</sub>O, H<sub>2</sub>S and H<sub>2</sub>Se,  $\nu_1$  is taken as  $\sim 2100$  cm.<sup>-1</sup> and  $\nu_3$  as  $\sim 2200$  cm.<sup>-1</sup>. Since  $\nu_1$  and  $\nu_3$  contribute less than 0.1 e.u. to C<sub>p</sub><sup>o</sup> and 0.01 e.u. to the other thermodynamic functions up to 400°K., these estimates should be good enough. An estimate of 1.7 Å. for  $r(\text{Te-H})$  and  $\langle \text{HTeH} \rangle = 89^\circ 30'$  has been given.<sup>10</sup> The calculation of  $r(\text{Te-H})$  from several empirical equations, which give excellent agreement with the experimental bond

(10) K. Rossmann and J. W. Straley, *J. Chem. Phys.*, **24**, 1276 (1956).

distances of  $\text{H}_2\text{O}$ ,  $\text{H}_2\text{S}$  and  $\text{H}_2\text{Se}$ , gives 1.69 Å.<sup>11,12</sup> Since the bond angles for  $\text{H}_2\text{S}$  and  $\text{H}_2\text{Se}$  are  $92.1^\circ$  and  $91.0 \pm 0.6^\circ$ , a bond angle for  $\text{H}_2\text{Te}$  should be about  $90 \pm 1^\circ$ . Using these data, the moments of inertia for hydrogen telluride are  $I_1 = 4.70 \times 10^{-40}$ ,  $I_2 = 4.78 \times 10^{-40}$ ,  $I_3 = 9.48 \times 10^{-40}$  g.cm.<sup>2</sup>.

The thermodynamic functions for  $\text{H}_2\text{Te}$  to the rigid rotator-harmonic oscillator approximation are listed in Table IV in the range from  $100^\circ$  to  $400^\circ\text{K}$ . for the ideal gas state at one atmosphere pressure.

Apparently the only datum in the literature on the thermodynamic functions for  $\text{H}_2\text{Te}$  is an estimate of the entropy at  $298.16^\circ$  of 56 e.u.,<sup>9</sup> compared with

(11) M. Huggins, *J. Am. Chem. Soc.*, **75**, 4126 (1953).

(12) W. Gordy, Smith and Trambarulo, "Microwave Spectroscopy," John Wiley and Sons, Inc., New York, N. Y., 1953.

the value of 54.7 e.u. calculated above.

TABLE IV

THERMODYNAMIC FUNCTIONS FOR HYDROGEN TELLURIDE IN THE IDEAL GAS STATE IN CAL./DEG./MOLE

$T, ^\circ\text{K.}$	$C_p^\circ$	$H^\circ - H_0^\circ$ $T$	$-F^\circ - H_0^\circ$ $T$	$S^\circ$
100	7.95	7.95	37.90	45.85
200	8.10	7.97	43.41	51.38
250	8.29	8.02	45.19	53.21
275	8.40	8.05	45.96	54.01
298.16	8.50	8.08	46.61	54.59
300	8.51	8.08	46.66	54.74
325	8.63	8.12	47.31	55.43
350	8.75	8.16	47.91	56.07
400	8.99	8.25	49.00	57.25

## COMMUNICATIONS TO THE EDITOR

### A REMARK ON SOME MEASUREMENTS OF TRANSFERENCE NUMBERS

Sir:

In view of a recent work on transference numbers by Kilpatrick and Lewis,<sup>1</sup> it would seem appropriate to recall the limitations of transference number measurements of a Hittorf type in a liquid.

Let us first consider the measurement of transference numbers of a sodium chloride solution in water. In the Hittorf type experiment, the change of the amount of sodium chloride in the cathode or anode compartment would be determined. The transference number which can be determined from this, refers to the center of gravity of the water as a reference frame. This is evident, since only the ratios of the amounts of water to salt are determined in the electrode compartments. Thus it is required that the water molecule do not take part in the electrical transport, but simply act as a neutral reference frame.

Without such a reference frame, transference numbers could not be determined by a Hittorf type method. In a fused salt a frame of reference is lacking. A transference number measurement in fused sodium chloride could seem to consist of an observation of a change of the amount of the salt in one of the electrode compartments, or in other words a displacement of the body of fused salt. But Sundheim<sup>2</sup> has shown recently that such an experiment is trivial. The results depend on the experimental arrangement without giving any information about intrinsic properties.

In a mixture of fused sodium chloride and potassium chloride only the ratio of the potassium transference number to the sodium transference number can be determined by measuring the

relative amounts of sodium and potassium in both electrode compartments

In some water solutions the assumption that water is a neutral particle which does not participate in the electrical transport, fails completely. Sodium hydroxide dissolved in water is such a case. This liquid should formally be regarded as consisting only of  $\text{Na}^+$ ,  $\text{H}^+$  and  $\text{OH}^-$  ions (or  $\text{Na}^+$ ,  $\text{H}^+$  and  $\text{O}^{2-}$  ions). It is of no consequence for our reasoning that the  $\text{H}^+$  ions and the  $\text{OH}^-$  ions most of the time are associated to  $\text{H}_2\text{O}$  molecules as long as these ions contribute significantly to the electrical transport. In this system, which is analogous to the mixture of fused sodium and potassium chloride, the Hittorf measurement will not tell how much of the electricity transport is carried by the cations ( $\text{Na}^+$  and  $\text{H}^+$ ) in relationship to what is carried by the anion ( $\text{OH}^-$  or  $\text{O}^{2-}$ ). A consistent treatment of the results of the transference number measurement will only reveal the ratio of the transference number of sodium to that of the proton. By arbitrarily implying that there is no electricity transport by the oxygens (for instance as  $\text{OH}^-$  ions) have absolute transference numbers been obtained for such systems. What has been reported as a high  $\text{OH}^-$  mobility in this case is more consistently described as a proton mobility.

The treatment of a system such as sodium fluoride dissolved in anhydrous hydrofluoric acid is identical with the treatment of the sodium hydroxide solution discussed above. Some difficulties encountered by Kilpatrick and Lewis in interpreting their experimental results on fluoride systems, would vanish if the points discussed in this note were taken into consideration.

THE PENNSYLVANIA STATE UNIVERSITY  
DEPARTMENT OF CERAMIC TECHNOLOGY  
COLLEGE OF MINERAL INDUSTRIES  
UNIVERSITY PARK, PENNSYLVANIA

T. FORLAND  
J. KROGH-MOE

(1) M. Kilpatrick and T. J. Lewis, *J. Am. Chem. Soc.*, **78**, 5186 (1956).

(2) B. R. Sundheim, *THIS JOURNAL*, **60**, 1381 (1956).

RECEIVED DECEMBER 12, 1956



*Collectors' Items*  
*Now Available at Special Reduced Rates*

**Chemistry—  
Key To Better Living**  
and  
**Seventy-Five Eventful Years**

*by Charles Edward Browne and Mary Elwira Weeks*

These two volumes—unique in their contribution to chemical literature—are now available for only \$7.50 when purchased together.

CHEMISTRY—KEY TO BETTER LIVING is a profusely illustrated history of chemical developments in the United States. It includes accounts of the activities of the Divisions of the Society and their influence on the progress of science and industry.

SEVENTY-FIVE EVENTFUL YEARS is the official history of the American Chemical Society. This book traces the growth of the Society, describes its manifold activities, relates the part it has played in affairs of national importance, and culminates with a description of the Diamond Jubilee.

Chemistry—Key To Better Living	\$4.00
Seventy-Five Eventful Years	5.00
Chemistry—Key To Better Living and Seventy-Five Eventful Years	\$7.50

*order from:*

Special Publications Department  
American Chemical Society

1155 Sixteenth Street, N.W.  
Washington 6, D.C.

**TWO CURRENT TITLES**  
in the  
**Advances In Chemistry Series**

**No. 10 LITERATURE RESOURCES FOR CHEMICAL PROCESS INDUSTRIES**

Discusses various information sources with 13 articles on market research, 7 on resins and plastics, 6 on textile chemistry, 10 on the food industry, 10 on petroleum, and 13 on general topics, plus 34 pages of index.

582 pages—paper bound—\$6.50 per copy

**No. 11 NATURAL PLANT HYDROCOLLOIDS**

Reviews materials usually used as protective colloids or “stabilizers” such as Calcium Pectinates, Agar, Gum Arabic, Gum Karaya, Tragacanth, Locust Bean Gum, Alginates and Red Seaweed Extracts.

103 pages—paper bound—\$2.50 per copy

also available: No. 4, Searching The Chemical Literature, \$2.00 . . . No. 5, Progress In Petroleum Technology, \$3.00 . . . No. 6, Azeotropic Data, \$4.00 . . . No. 7, Agricultural Applications of Petroleum Products, \$1.50 . . . No. 8, Chemical Nomenclature, \$2.50 . . . and No. 9, Fire Retardent Paints, \$2.50.

*order from:* Special Publications Department

American Chemical Society

1155 Sixteenth Street, N.W.

Washington 6, D. C.